

Modelling the exposure of engineered nanoparticles in urban aquatic systems

Prado Domercq

PhD

University of York

Environment and Geography

March 2019

Abstract

With the exponential growth of the nanotechnology industry in recent years, concerns about the exposure and potential environmental impacts of engineered nanoparticles (ENPs) have increased. Jointly, due to current increases in the size of urban populations, concerns are rising regarding the associated increase in product waste emission in cities, including novel potential, non-regulated contaminants such as ENPs.

Robust and sensitive analytical approaches for ENPs are still lacking, and therefore only a limited amount of experimental data are available on the ENP emissions and exposure in city environments. However, mathematical models provide a potentially powerful approach to understand the occurrence and fate of ENPs in city environments. While a number of these models already exist, these tend to operate at low temporal and spatial resolution required to fully understand exposure and risks in urban systems. This thesis aims to provide a new modelling approach that allows the estimation of ENPs exposure of urban surface waters at high spatial and temporal resolutions.

As a first step, the sources, release pathways and environmental fate processes of ENPs in urban aquatic systems were reviewed and the gained knowledge was used to design a new integrative modelling framework able to estimate the emissions and exposure of ENPs in surface waters of urban systems with high spatial and temporal resolution. This framework considers the different ENP-product that will be in use in urban systems and both point source and diffuse emission pathways into surface waters.

The proposed framework was then applied to model the spatial and temporal trends of ENP emissions in a case study city (York, UK). The main sources, drivers and activities causing the highest emissions in the city were identified, and emission hot spots and temporal emission trends were derived for the area and period simulated.

Exposure of the York river system to titanium dioxide ENPs (TiO₂ ENPs), which were estimated to be the highest emitted ENPs in York, was modelled to develop temporally and spatially resolved potential exposure concentrations in the York river system over time. The results were used alongside ecotoxicological species sensitivity distributions to assess the risk posed by TiO₂ ENPs in the York River system.

List of contents

Abstract	2
List of contents	3
List of tables.....	6
List of figures	8
Acknowledgements.....	12
Declaration	13
Chapter 1	14
Introduction.....	14
1.1 Engineered nanoparticles	14
1.2 Environmental concerns of ENPs.....	16
1.3 Urban contributions of ENPs	18
1.4 Environmental exposure modelling of ENPs	19
1.5 Aims and objectives.....	21
Chapter 2	23
Review of ENP uses, emission pathways and fate processes in the aquatic media	23
2.1 Introduction.....	23
2.2 Production and use of ENPs	23
2.3 Release mechanisms and emission pathways of ENPs	29
2.4 Fate processes of ENPs in the aquatic system	32
2.4.1 ENP chemical transformations	33
2.4.2 Physical transformations: ENPs aggregation processes.....	35
2.4.3 ENP interactions with macromolecules	36
2.4.4 ENPs biological transformations.....	37
2.5 Factors influencing ENP environmental fate processes.....	37
2.5.1 ENP aggregation.....	39
2.5.2 ENPs sedimentation/deposition	43
2.5.3 Dissolution	44
2.6 Conclusions.....	45
Chapter 3	47
Emission and fate modelling framework for engineered nanoparticles in urban aquatic systems at high spatial and temporal resolution	47
3.1 Introduction.....	47

3.2	Model framework for ENPs in urban environments.....	51
3.2.1	City analysis: urban zoning and river reach delimitation	53
3.2.2	Nano product inventory and classification of emission sources	56
3.2.3	Emissions estimation model	59
3.2.4	Surface water fate model	66
3.2.5	Challenges in model parametrization	68
3.3	Conclusions.....	71
Chapter 4.....		73
Modelling spatial and temporal trends of ENP emissions in York (UK)		73
4.1	Introduction.....	73
4.2	Methods	75
4.2.1	Description of the study area	75
4.2.2	York Hydrological zones and river sections	76
4.2.3	Definition of case studies	79
4.2.4	Emissions model framework	80
4.2.5	Model parametrization and assumptions	80
4.3	Results.....	92
4.3.1	Emission ranges of ENPs in York.....	92
4.3.2	Spatial variation of emissions	95
4.3.3	Temporal variation of emissions.....	97
4.4	Discussion.....	102
4.4.1	Emission ranges of ENPs in York.....	102
4.4.2	Spatial variation of emissions	104
4.4.3	Temporal variation of emissions.....	105
4.5	Conclusions.....	106
Chapter 5.....		108
Modelling exposure of the York River system to engineered nanoparticles at high temporal and spatial resolutions.....		108
5.1	Introduction.....	108
5.2	Methods	110
5.2.1	Modelling principles.....	110
5.2.2	Description of the river system.....	113
5.2.3	Model parametrization	115
5.3	Results and discussion	121
5.3.1	Measured physical and chemical characteristics.....	121
5.3.2	TiO ₂ ENP concentrations in York's river system.....	127

5.3.3	TiO ₂ ENPs distribution within the river.....	138
5.3.4	Risk assessment	140
5.4	Conclusions.....	143
Chapter 6		145
General discussion and recommendations		145
6.1	Summary and key findings	146
6.2	Research implications	149
6.3	Challenges, limitations and future work	150
6.4	Conclusions.....	153
Appendices		154
APPENDIX 1.....		154
A1. Supplementary information Chapter 4		154
A1.1	Study Area.....	154
A1.2	Emissions model parametrization.....	155
A1.3	Results of emission estimates.....	159
A1.4	Schematic representation of Emissions Model.....	161
APPENDIX 2.....		162
A2. Supplementary information Chapter 5		162
A2.1	River fate model parameterisation	162
A2.2	River fate model equations.....	167
A2.3	Monitoring data	169
A2.4	Exposure results	175
Abbreviations.....		179
References		182

List of tables

Table 2.1. Principal sectors of application of nanotechnology, ENP types and some of their improved properties	25
Table 2.2. Comparison of production amounts from six different sources scaled to the EU (according to GDP) in metric tons per year.	27
Table 2.3. Factors influencing the fate and behaviour of ENPs in the environment	37
Table 2.4. Level of relevance of fate processes in environmental fate modelling and for different types of ENPs	38
Table 2.5. General relevance of environmental transformation processes of ENPs in different environmental compartments	39
Table 2.6. Summary of experimental studies on the influence of environmental factor	41
Table 3.1. Summary of ENP-containing products available on the market and used in cities	58
Table 3.2. Examples of estimation of product usage (U_{prod}) and release rates (R_{Release}) for different ENP-containing product types	63
Table 3.3. Retention coefficients for the three ENP release pathways	66
Table 3.4. Summary of potential parametrization data and sources for the modelling framework	69
Table 4.1. List of studied ENPs, their investigated product applications, source and pathway of emission.	79
Table 4.2. Equations of product usage (U_{prod}) estimation for the different product types studied.	81
Table 4.3. Summary of selected values of model input parameters for the maximum (Max), minimum (Min) and average (Ave) scenarios.	82
Table 4.4. List of Bus companies operating in York, number of routes and their performances	83

Table 4.5. Number of buses circulating per HZ from Monday to Saturday (Week) and on Sundays and the corresponding fuel consumption (L).	85
Table 4.6. Datasets employed for the characterization of U_{prod} of the outdoor paints case studies.....	87
Table 4.7. Sample of building types of York picture in the performed survey.....	89
Table 4.8. Amount of outdoor paint used per HZ of York in Kg.....	90
Table 4.9. Estimated total mass of each ENP type studied available for loss and actual estimated mass loss in York during the period studied.....	93
Table 4.10. Estimated total mass of each ENP available for loss and actual estimated mass emitted in York during the period studied.	95
Table 5.1. List of RSs and their connexions to the York delimited HZs and serving WWTPs.	114
Table 5.2. List of monitoring sites along the rivers Ouse and Foss, their river section connetions (RS) and description.	118
Table 5.3. Assigned attachment efficiency (α_{hetero}) values according to the concentration of calcium ([Ca ²⁺]) and the dissolved organic carbon (DOC) in water.....	119
Table 5.4. Summary of predicted environmental concentrations (PEC) in surface water of TiO ₂ ENPs reported in the literature. Source: adapted from (Peters et al., 2018).	137
Table 5.5. Mean, lower and upper limit of estimated HC5 mg/L for TiO ₂ ENPs derived from SSD analysis performed by Chen et al. (2018).....	141

List of figures

Figure 1.1. Improved properties of engineered nanoparticles from their bulk material...	16
Figure 2.1. Major applications of nanoparticles.....	24
Figure 2.2. Production volumes of the top five most relevant ENPs	28
Figure 2.3. Possible pathways of occupational, environmental and human exposure to ENPs.....	29
Figure 2.4. Emissions pathways and environmental distribution of ENPs.....	31
Figure 2.5. Forms under which different types of ENPs are integrated in the registered consumer products of the Woodrow Wilson Inventory.	32
Figure 2.6. Environmental fate processes of ENPs.	33
Figure 2.7. Schematic representation of the role of Humic acids (HA), as a proxy of NOM on the aggregation and disaggregation processes of ENPs.....	42
Figure 3.1. Representation of the main factors influencing the emission of pollutants in urban environments.....	48
Figure 3.2. Urban modelling framework: source-pathway-receptor structure.....	51
Figure 3.3. Schematic representation of model framework	53
Figure 3.4. Subdivision of the York area of study into hydrological zones (HZs), river reaches (RSs) and localization of the local sewage treatment plants (WWTPs).....	55
Figure 3.5. Schematic representation of the ENP transport into, out of and throughout the defined river reaches and fate processes inside the river system..	67
Figure 4.1. Delimitation of HZs for York with a) delimited basins areas; b) WWTP catchment areas and c) drainage subnets allocated to the delimited river sections. d) Constitutes de final delimitation of the 12 HZ of York.....	78
Figure 4.2. Methodology of extraction of bus traffic information	84
Figure 4.3. Estimated total emissions of CeO ₂ , TiO ₂ and Ag ENPs to York's river system during the year 2016 for the maximum (MAX), average (AVE) and minimum (MIN)	92

Figure 4.5. Total estimated emissions in mg to York for the year 2016 per product type for the three ENPs studied, and for the maximum emitting scenario (MAX), the average emitting scenario (AVE) and minimum emitting scenario (MIN).	94
Figure 4.7. Median receiving CeO ₂ ENP emissions for the maximum (MAX), the average (Average) and minimum (MIN) emitting scenarios, per river section and maps of median CeO ₂ ENP emission values per day and per HZ.	95
Figure 4.8. Median receiving TiO ₂ ENP emissions for the maximum (MAX), the average (Average) and minimum (MIN) emitting scenarios, per river section and maps of median TiO ₂ ENP emission values per day and per HZ.	96
Figure 4.9. Median receiving Ag ENP emissions for the maximum (MAX), the average (Average) and minimum (MIN) emitting scenarios, per river section and maps of median Ag ENP emission values per day and per HZ.	96
Figure 4.10. Cumulative Distribution Functions (CDF) of the estimated total emissions to the York river system	98
Figure 4.11. Daily ENP emissions from TiO ₂ ENP-containing products and total amount emitted to the river sections OUSE2.....	99
Figure 4.12. Daily ENP emissions from TiO ₂ ENP-containing products emitted to the river sections OUSE3.....	100
Figure 4.13. Daily ENP emissions from Ag ENP-containing products and total amount emitted to the river sections OUSE2.....	100
Figure 4.14. Daily ENP emissions from Ag ENP-containing products emitted to the river sections OUSE3.....	101
Figure 4.15. CeO ₂ ENP estimated emissions for the RS OUSE2 and the average scenario	101
Figure 5.1. Schematic representation of the river model conformation, and fate processes inside the river system for TiO ₂ ENPs.....	111
Figure 5.2. Locations of York's two main rivers, the WWTPs serving the city, the delimited river sections and the established monitoring sites.	114
Figure 5.3. Ouse at Skelton catchment area extension.	116
Figure 5.4. Foss at Huntington catchment area extension	116

Figure 5.5. Arithmetic mean of the measured DOC concentrations for the Foss (F) and Ouse (O) sampling sites over the six months monitoring period	121
Figure 5.6. Arithmetic mean of the measured dissolved Calcium concentrations as (Ca^{2+}) for the Foss (F) and Ouse (O) sampling sites over the six month monitoring period ..	122
Figure 5.7. Arithmetic mean of the measured total suspended solids (TSS) concentrations for the Foss (F) and Ouse (O) sampling sites over the six month monitoring period	122
Figure 5.8. Daily discharge of the delimited RS of the river Ouse over the simulated period.	124
Figure 5.9. Daily discharge of the delimited RS of the river Foss over the simulated period	124
Figure 5.10. List of RSs and their corresponding runoff catchment areas.....	125
Figure 5.11. Daily TiO_2 ENP emissions to the delimited RSs of the river Ouse over the simulated period	126
Figure 5.12. Daily TiO_2 ENP emissions to the delimited RSs of the river Foss over the simulated period	127
Figure 5.13. Exposure profiles of freely dispersed TiO_2 ENPs (Free) in the flowing water of the modelled extension of the river Ouse over the simulated period	128
Figure 5.14. Exposure profiles of TiO_2 ENPs heteroaggregated with SPM (SPM-bound) in the flowing water of the modelled extension of the river Ouse over the simulated period	129
Figure 5.15. Exposure profiles of TiO_2 ENPs in the sediment compartments of the modelled extension of the river Ouse over the simulated period	130
Figure 5.16. Exposure profiles of freely dispersed TiO_2 ENPs (Free) in the flowing water of the modelled extension of the river Foss over the simulated period	131
Figure 5.17. Exposure profiles of TiO_2 ENPs heteroaggregated with SPM (SPM-bound) in the flowing water of the modelled extension of the river Foss over the simulated period	132
Figure 5.18. Exposure profiles of TiO_2 ENPs in the sediment compartments of the modelled extension of the river Foss over the simulated period	133

Figure 5.19. Box and whisker plots of the estimated ranges of TiO ₂ ENPs concentrations in the flowing water of all RSs of both rivers	134
Figure 5.20. Box and whisker plots of the estimated ranges of SPM-bound TiO ₂ ENPs concentrations in the flowing water compartment of all RSs of both rivers).	135
Figure 5.21. Box and whisker plots of the estimated ranges of TiO ₂ ENPs concentrations on the sediment compartment of all RSs of both rivers	135
Figure 5.22. Mass distribution of the different forms of TiO ₂ ENPs (i.e. Free and SPM-bound) in the three river compartments (flowing water, stagnant water and sediment) along the river Ouse.	138
Figure 5.23. Mass distribution of the different forms of TiO ₂ ENPs (i.e. Free and SPM-bound) in the three river compartments (flowing water, stagnant water and sediment) along the river Foss.	139
Figure 5.24. Generated SSD of TiO ₂ ENPs based on NOEC data from Chen et al. (2018).	141
Figure 5.25. Box and whisker plots of the estimated PECs of free TiO ₂ ENPs the water compartment and the estimated PNEC based on the HC5	142
Figure 5.26. Box and whisker plots of the estimated PECs of total TiO ₂ ENPs the water compartment of the RSs of the Ouse and the Foss and the estimated PNEC based on the HC5	143

Acknowledgements

I would like to express my gratitude to my supervisor Prof. Alistair Boxall for his patience and guidance throughout this journey and for the opportunity given to take part of the CAPACITIE team. I am deeply grateful for the experience and knowledge gained with him.

I am particularly grateful to Antonia Praetorius who has accompanied me through the process from all possible locations giving me advice, support and guidance. Thank you for all the shared hours of work and skype conferences, for being a great host in Vienna making me feel at home, for the shared meals, teas, cakes and confidences. Bust most importantly, thank you for sharing your passion for science and your great energy with me.

I am deeply thankful for the CAPACITIE project, and to the CAPACITIE team (Alistair, Lorraine, Elena, Xiu, Magda, Gabor, Emily, Fady, Mayank, Michelle, Xinwei, Rina, Kyle and Jen (honorary member)), for all the shared travels, conferences and adventures.

Special thanks to my office mates and now good friends Xui, Jen and Magda for all their support, and shared laughs and tears. I would also like to thank Samuel Thompson for his interest in my work and for taking the time to review my PhD thesis. And very special thanks to Jen and Sergio for their immense support during the last very intense days (even weeks) leading up to the submission of this work.

The biggest acknowledgements go to my family, my parents Arturo and Lourdes, my beloved sister Marta and her wife Vero, and my loving auntie Prado. Their unconditional love, support and guidance have been the fuel that pushed me through the challenging days.

Declaration

The content of this thesis is original work that I have conducted as a PhD student under the supervision of Professor Alistair Boxall and in collaboration with Dr Antonia Praetorius (April 2015 – March 2019).

The content of Chapter 3 and some parts of Chapter 1 (section 1.4) have previously been published in a peer reviewed journal article: Domercq, P., Praetorius, A. and Boxall, A.B., 2018. Emission and fate modelling framework for engineered nanoparticles in urban aquatic systems at high spatial and temporal resolution. *Environmental Science: Nano*, 5(2), pp.533-543. The content of this paper has been reworked, so that that it is presented in a consistent style and format in this thesis. The paper has been written by the candidate as leading author; however, it should be noted that the paper has gained in quality through suggestions, advice and editing from the co-authors.

The work presented in Chapter 5 was done in collaboration with Dr Antonia Praetorius whose contribution consisted in adapting and running the River Fate model based on discussions with and data collected by the candidate.

I hereby declare that this thesis is a presentation of original work undertaken by myself, except where otherwise acknowledged. This work has not previously been presented for an award at this, or any other, University. All sources are acknowledged as References.

This project has received funding from the European Union's Seventh Framework Programme for research, technological development and demonstration under grant agreement no 608014.

Chapter 1

Introduction

The expansion of the nanotechnology sector is leading to an increased availability and use of products containing engineered nanoparticles (ENPs) (HTF Market Report, 2018). Throughout their life cycle, ENP-containing products are subject to weathering and ageing and consequently, ENPs will be released from the products over time (Gottschalk and Nowack, 2011a). Therefore, in recent years, there has been growing concern about the exposure and potential environmental impacts of ENPs (Garner and Keller, 2014). More so in cities, where use, emission and exposure of these emerging pollutants is currently concentrated due to increasing urbanization and the steady growth of the urban population (United Nations, 2014). In this context, evaluating the risks of ENPs has become essential for regulatory purposes (Rauscher, Rasmussen and Sokull-Klüttgen, 2017). Therefore, this chapter firstly provides an introduction to ENPs (i.e. their definition and properties) to then discuss the concerns around the potential impacts of these materials in the natural environment. Later, it introduces the concept of cities as hot spots of ENP emissions and exposure. The chapter then reviews the models developed so far for estimating environmental exposure to ENPs, and finally provides the main aim and objectives of this thesis.

1.1 Engineered nanoparticles

There are several competing definitions for ENPs (Auffan *et al.*, 2009; Kreyling, Semmler-Behnke and Chaudhry, 2010; Boholm and Arvidsson, 2016). The EU Scientific Committee on Emerging and Newly Identified Health Risks (SCENIHR) defines engineered nanomaterials (ENMs) as “materials with one or more external dimensions, or an internal structure, at the nanoscale and which could exhibit novel characteristics compared to the same material at a larger scale” (European Commission, 2011). The International Standards Organization (ISO) defines nanoparticles as nano-objects with all three external dimensions in the nanoscale (Boholm and Arvidsson, 2016). But the most commonly used definition of ENPs and the one that will be used for the purposes of this

thesis, is the one that defines ENPs as “intentionally produced particles that have a characteristic dimension from 1 to 100nm and that have properties that are not shared by the non-nanoscale particles with the same chemical composition” (Auffan *et al.*, 2009).

ENPs are produced in different shapes (e.g. spheres, films, tubes, etc.) and compositions (i.e. organic nanoparticles such as dendrimers or liposomes, or inorganic nanoparticles such as metals (e.g. silver, copper, gold, etc.), metal oxides (zinc oxide, iron oxide, titanium dioxide and silicon dioxide) and carbon based ENPs (carbon nanotubes, and graphene)). However, their defining characteristic is their nano-dimensions that confers upon them their particular properties (Auffan *et al.*, 2009). These size-dependent properties include unique mechanical, electronic, photonic, and magnetic properties and are a consequence of quantum size effects that are not present in the bulk material (Uskoković, 2013) (Figure 1.1). Titanium dioxide (TiO_2) particles, for example, at the nano-scale exhibit more effective photocatalytic activity than bulk TiO_2 , a property which is now being exploited through their use in self-cleaning coatings (Parkin and Palgrave, 2005). Gold particles go from being naturally inert at the macroscopic scale to extremely effective oxidation catalysts when their size is reduced to a few nanometres (Auffan *et al.*, 2009). In addition, nanoparticles exhibit a particularly high surface reactivity, which is a consequence of the fact that a higher proportion of atoms at this small size scale are at the surface of the particle than in the interior (Uskoković, 2013).

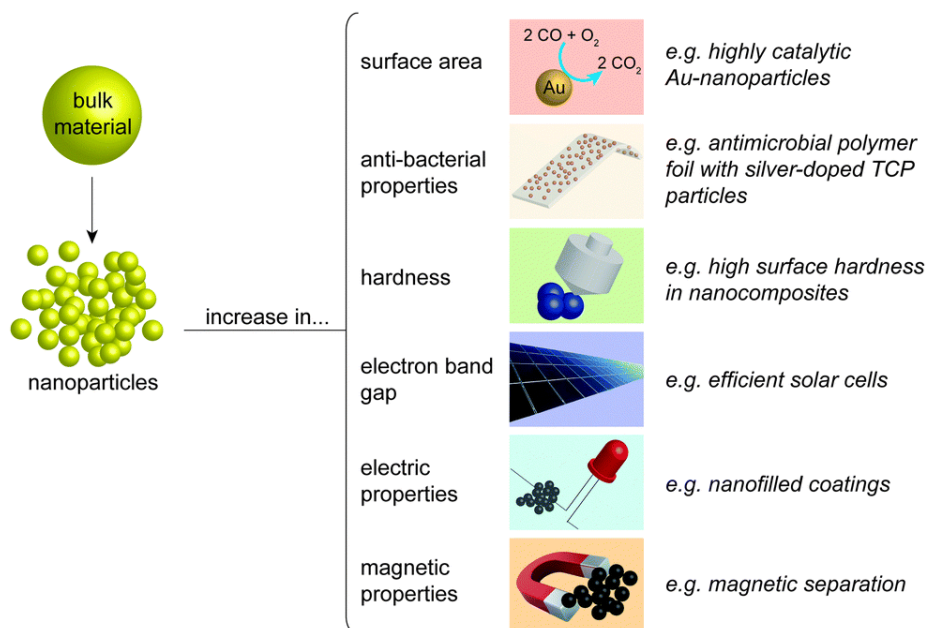


Figure 1.1. Improved properties of engineered nanoparticles from their bulk material. Source: image taken from (Stark *et al.*, 2015)

These improved properties and the commercial advantages of reducing the use of materials, makes them highly attractive for applications in almost every industrial sector, under what are usually called engineered nanomaterials (ENMs).

Since the late 1990's/early 2000's, when nano-enabled products first appeared in the marketplace, the nanotechnology sector has undergone continuous growth (Zhu *et al.*, 2017). Further expansion of the nanotechnology sector is forecast by the latest report published on Global Nanotechnology Outlook 2022 (Zhang *et al.*, 2013). Currently, evidence of release to the environment and consequent environmental exposure have been observed for some ENPs (Hennebert *et al.*, 2013; Gondikas *et al.*, 2014; Mitrano *et al.*, 2014). Therefore, as the nanotechnology field expands, emissions of ENPs to the biosphere during production, transport, use and disposal are expected to increase and the emissions will keep growing into the future (Giese, *et al.*, 2018).

1.2 Environmental concerns of ENPs

The expected increase in environmental exposure has raised concerns about consequent impacts on environmental health (Valsami-Jones and Lynch, 2015). This is because their unique nano-scale properties can also translate into new fate, transport and toxic qualities

(Warheit, 2018). For example, upon exposure (e.g. through inhalation, skin contact, ingestion, and injection), the very small size of ENPs allows them to pass more easily through cell membranes and other biological barriers, therefore, nanomaterials can be easily taken up into living organisms and cause cellular damage (Xia *et al.*, 2014). In this sense, one of the main toxicity concerns of ENPs is the so-called “Trojan Horse” effect, wherein compounds that might not normally enter a cell are internalized when associated with a ENP due to their small size and very reactive surface (Valsami-Jones and Lynch, 2015). Another toxic mechanism associated with some ENPs, is the enhanced production of reactive oxygen species (ROS) (Wiesner *et al.*, 2009). ROS are by-products of the cellular metabolism of oxygen, much of which occurs in the mitochondria. However, ROS can also be generated by other means such as by certain ENPs (Xia *et al.*, 2014). The overproduction of ROS can induce oxidative stress, resulting in cells failing to maintain normal physiological redox-regulated functions. This in turn can lead to DNA damage, unregulated cell signalling, changes in cell motility, cytotoxicity, apoptosis, and the initiation of cancers (Xia *et al.*, 2014).

Despite the fact that ENP toxicity has already been extensively studied in different biological systems and toxic effects have already been reported (Chen *et al.*, 2018; Wang *et al.*, 2014; Xia *et al.*, 2014; Oberdörster, 2004; Austin *et al.*, 2003), a debate on whether protocols used for ENP toxicity testing are adequate is still ongoing (Warheit, 2018). Furthermore, currently these toxic effects are not fully characterized for all types of ENPs or for their relevant exposure forms and under relevant environmental conditions (Warheit, 2018).

The novel properties of ENPs are also not yet accounted for in the current environmental risk assessment methods proposed by the Registration, Evaluation, Authorization, and Restriction of Chemicals (REACH) regulations. In fact, major deviations between the fate of ENPs and predicted fate by REACH have been found (Meesters *et al.*, 2013). For example, when evaluating the fate processes of ENPs in the environment, the conventionally used equilibrium partitioning coefficients for chemical substances (e.g., K_{ow}) cannot be applied to ENPs since ENPs (like colloids) are thermodynamically unstable suspensions and will never reach thermodynamic equilibrium (Praetorius *et al.*, 2014). Instead, the use of other fate parameters, such as attachment efficiencies, that take into consideration the ENPs and surrounding environment properties, would be more adequate (Praetorius *et al.*, 2014). Also, in the application of REACH, chemicals are

presumed to dissolve instantaneously into the environment once emitted whereas most ENPs won't dissolve but prevail in their particulate form in nanosized suspensions or aggregates (Meesters *et al.*, 2013). In terms of their toxicity, conventional dose response assessments (DRA) might not be adequate for ENPs either. DRA are usually reported in terms of mass, but for ENPs it has been suggested that their biological activity might not be mass-dependent but rather dependent on their physical or chemical properties (i.e. size, shape, agglomeration state and surface composition) (described in detail in section 2.4), which are not conventionally considered in toxicity studies (Garner and Keller, 2014; Hegde *et al.*, 2016). Overall the potential environmental risks associated to ENPs are not yet fully understood and to understand the risks posed by ENPs in the environment both, the exposure levels and the hazard potential need to be quantified (Caballero-Guzman and Nowack, 2016).

Currently, uncertainties at both levels, the exposure and the hazard level, still prevail (Garner and Keller, 2014) although evidence of release and consequent exposure have been found for some ENPs (Hennebert *et al.*, 2013; Mitrano *et al.*, 2014; Gondikas *et al.*, 2014) and warning of potential hazardous effects have been raised for others (García-Alonso *et al.*, 2014; Wang *et al.*, 2014).

1.3 Urban contributions of ENPs

Urban environments, being centres of human activities, have become hot spots of ENP emissions, and urban surface waters are one of their main sinks (Baalousha *et al.*, 2016). In the urban context, the use of ENPs is also increasing with the development of these new technologies. Current commercialised ENP-containing products include cosmetics, personal care products, food additives, paints and coatings (Keller *et al.*, 2013; Vance *et al.*, 2015a) which will be mostly used within cities. Also outdoor urban nanomaterials such as construction materials, outdoor paints and coatings and photocatalytic pavements, amongst others, emerge as potential sources of ENPs emissions into the urban environment (Baalousha *et al.*, 2016). The urban landscape is characterised by the prevalence of impervious cover and reduced green areas, this translates into reduced storm water infiltration rates and an increase in surface water runoff generation. The reported runoff coefficients, that measure the fraction of rainfall that is not infiltrated but prevails as runoff, for urbanised areas range between 0.70 and 0.95, while runoff coefficients for parks and gardens vary between 0.05 and 0.3) (Modaresi, Westerlund and

Viklander, 2010). Such structure enhances the transport of contaminants to the nearby surface waters and therefore exposure to mixtures of varying pollutants (de Zwart *et al.*, 2018). Therefore, urban environments must be targeted as relevant exposure environments of these emerging pollutants.

1.4 Environmental exposure modelling of ENPs

Appropriate analytical methods for the detection of ENPs in environmental matrices such as surface waters, are still under development, making large-scale monitoring campaigns currently impossible (Geissen *et al.*, 2015) and therefore, exposure levels for most ENPs are unknown. To address this challenge, mathematical models are powerful tools that can be used to estimate ENP emissions and environmental concentrations. These models provide an indication of the level of environmental exposure when experimental and monitoring data is unavailable (Sani-Kast *et al.*, 2015; Nowack, 2017). Furthermore, models enable a deeper understanding of the relative importance of different emission sources and pathways and, therefore, can serve as tools to support decision-making and support regulations. For example, insights from modelling efforts could be used to support selecting emission mitigation measures and developing more targeted monitoring campaigns. Models can also help inform the development of analytical methodologies for ENPs by helping to define which material types most need to be monitored and the required performance of the methods in terms of detection limits for particle number and particle size.

Over the last decade several different modelling approaches for deriving predicted environmental concentrations (PEC) of ENPs have been developed. These involve a wide variety of environmental exposure models with different applicability and objectives (Gottschalk *et al.*, 2013; Nowack, 2017). Some are focused on studying the mass flows of ENPs during their life cycle to the different technical (i.e. wastewater treatment plants and landfills) and environmental compartments (i.e. atmosphere, soil, sediment and water) (Keller *et al.*, 2013; Gottschalk *et al.*, 2015a; Liu *et al.*, 2015; Sun *et al.*, 2015). These are so-called material flow analysis (MFA) models and usually are classified as top-down models, in which the environmental compartment is typically treated as a black box and no specific information about the ENP fate processes is included. Others centre their attention on the study of the ENP-specific fate processes (i.e., environmental fate models (EFM)), in different environmental compartments: air (Kumar *et al.*, 2011), water

(Dale *et al.*, 2015) and soil (Goldberg *et al.*, 2014). These more mechanistic approaches are often called bottom up models and include relevant information on the ENP transport and fate processes such as advective transport, hetero-aggregation, dissolution, surface transformations, sedimentation and resuspension (Praetorius *et al.*, 2013) (these processes are described in detail in section 2.4). Since Boxall *et al.* (2007) provided the first approach and theoretical basis to quantitatively assess ENP concentrations in air, soil and water using a series of algorithms (Boxall *et al.*, 2007), these different kinds of models have been in constant evolution. The first approaches were based on hypothetical ENP production and use volumes, since no empirical studies had yet been performed at that time (Boxall *et al.*, 2007). Then, material flow analysis (MFA) (Mueller and Nowack, 2008) and particle flow analysis (PFA) (Arvidsson, Molander and Sanden, 2012) that rely on the use of market estimates of production volumes and average transfer coefficients between environmental compartments emerged. Finally, the incorporation of probabilistic elements using Monte Carlo simulations to MFA and PFA dominate the currently most used approaches (Gottschalk, Scholz and Nowack, 2010). A summary of the available models developed up to early 2013 for ENP predicted environmental concentration (PEC) assessment is presented by Gottschalk *et al.* (Gottschalk, Sun and Nowack, 2013).

Existing models vary in complexity depending on the number of uses targeted for a single ENP (from one single use to the consideration of the full product life cycle) and the incorporation of nanoparticle-specific environmental fate processes. They can cover different environmental (e.g. sediments, soils, atmosphere, surface water) and technical compartments (e.g. sewage treatment plant effluents and sewage treatment sludge), and different spatial scales have been explored (i.e. global, regional and local). More recent models can integrate various compartments (Meesters *et al.*, 2016) and spatial scales (Keller and Lazareva, 2014). However, such models generally assume average environmental characteristics and averaged constant use and release rates based on country wide averages (Keller and Lazareva, 2014) and spatial and temporal variations are overlooked. Environmental and geographical characteristics such as surface water chemistry and hydrology vary spatially and seasonally, and so do consumption patterns and population densities and distribution. These factors, amongst others (e.g. waste treatment technologies) have a direct effect on the use, emissions and fate of ENPs, causing variations of the final exposure concentrations that can go up to several orders of

magnitude (Grill *et al.*, 2016). Furthermore, within the complexity of urban systems, that integrate a wide variety of potential emission sources (i.e. point and diffuse), different types of land cover and changes in population density within short distances, exposure variations would be expected even higher and hot spots of exposure anticipated (Grill *et al.*, 2016).

While some local exposure models for ENPs at the watershed level have already been developed (Gottschalk *et al.*, 2011; Dale, Lowry and Casman, 2015a; Dumont *et al.*, 2015), ENP exposure models at the city level are not yet available with the required temporal and spatial resolution. This leads to the main aim of this thesis.

1.5 Aims and objectives

The primary aim of this thesis was to develop a new modelling framework that allows the estimation of ENP exposure in urban surface waters at high spatial and temporal resolutions. This aim was achieved using the following specific objectives:

- 1) To develop a modelling framework that accounts for the complexity of urban systems and allows the estimation of spatially and temporally resolved ENP emissions, as well as ENP exposure levels (Chapter 3).
- 2) To parameterise the framework locally for the characterization of the ENP emissions of a case study city (York) (Chapter 4).
- 3) To parameterise the framework with the obtained emission results and the most relevant water quality parameters of the study area obtained from a local monitoring campaign, in order to characterize the ENP exposure levels of the city and the potential risks posed (Chapter 5).

Work performed to address the aim and objectives described is presented in four different chapters:

Chapter 2 is a literature review of the main steps to be followed when performing the exposure assessment of engineered nanoparticles. We review the current knowledge on production and uses of ENPs and the approaches for their quantification, their identification and summarise information found on the different ENP release mechanisms and emission pathways along their life cycle. The current knowledge on fate processes of

ENPs in aquatic media is also reviewed, as well as the environmental factors influencing such processes.

Chapter 3 presents a newly designed urban framework for modelling ENP emissions and fate in urban aquatic systems. It outlines the main sources, pathways and emission mechanisms of ENPs to be expected in an urban context and proposes a series of steps and mathematical calculations to estimate urban ENP emission and exposure concentrations locally and with temporal resolution. It establishes a methodology for urban analysis to deliver the required spatial resolution and guides the user through the model parameterization by proposing sources and approaches for the data collection.

Chapter 4 presents the step by step application of the urban modelling framework to estimate emissions of various ENPs from a variety of sources in a case study city (York, UK). It describes the application of new approaches to derive key parameters of the model such as usage and release rates, and the main assumptions made. Finally predictions of spatial and temporal exposure by ENP type and source type are delivered, which serve identify the emission hot spots and main emission pathways of concern of the city of York.

Chapter 5 presents the application of the urban modelling framework for the estimation the levels of exposure of the case study city (York, UK) to a specific ENP type (TiO₂ ENPs). In this chapter, a description of the river fate model principles is presented, as well as full details of the model parametrization. The monitoring campaign performed for the parametrization of the area studied is described. Results of the monitoring campaign are presented and their influence on the exposure levels estimated discussed. Results of the spatial and temporal variations of the TiO₂ ENPs exposure concentrations in York's river system are presented and compared to a derived predicted no-effect concentration for risk assessment.

Chapter 6 summarizes the outcomes, discusses the limitations and provides an overall conclusion of this thesis and provides some recommendations for future research.

Chapter 2

Review of ENP uses, emission pathways and fate processes in the aquatic media

2.1 Introduction

In the context of evaluating the potential risks of ENPs, an assessment of their exposure in the environment is required (Gajewicz *et al.*, 2012). Any substance can become toxic at a certain exposure level. Therefore, before interpreting toxicological data it is essential to estimate the expected concentrations that organisms will encounter in the different environmental compartments (Colvin, 2003). To evaluate how and to what quantities of ENPs humans and ecosystems are exposed to, information on their production volumes, possible industrial applications, expected use of the derived products, pathways for disposal and/or recycling of such products and information on the pollutants behaviour, environmental transport, fate and distribution is needed (Gajewicz *et al.*, 2012). This chapter provides an overview of the knowledge gained so far on each of these points. Focusing on surface waters, the Chapter reviews ENP uses and applications, their potential release mechanisms and emission pathways, and the chemical and physical transformations and transport processes that they undergo once released into the environment. In addition, the investigation of the factors that influence such emissions and their behaviour and fate in the targeted environmental compartment (i.e. ambient conditions of exposure and surface water physical and chemical properties respectively) are discussed.

2.2 Production and use of ENPs

The new and improved properties that the use of ENPs provide, together with the commercial advantage of reducing the use of material makes them very popular on the global market. In fact, the integration of ENPs has expanded to nearly all sectors of the global economy (Mangematin and Walsh, 2012) (Figure 2.1). ENPs can now be found in agricultural applications (Khot *et al.*, 2012), automotive technologies (Coelho *et al.*, 2012), coatings, paints and pigments (Khanna, 2008), construction materials (Pacheco-

Torgal and Jalali, 2011), green energy technologies (Hussein, 2015), environmental remediation methods (Khin *et al.*, 2012), medical applications (Nikalje, 2015), food technology and packaging (Bradley, Castle and Chaudhry, 2011; Hannon *et al.*, 2015), textiles (Dastjerdi and Montazer, 2010), cosmetics and personal care products (Mihrianyan, Ferraz and Strømme, 2012), amongst many others (Keller *et al.*, 2013). The ENPs integrated in such technologies vary in composition, size and shape, as well as in the form in which they are integrated into the final product (surface bound, suspended in liquid, suspended in solid) (Hansen *et al.*, 2008). Table 2.1 summarizes some of the application areas of ENPs, some of the improved properties that they entail and the types of ENPs used.

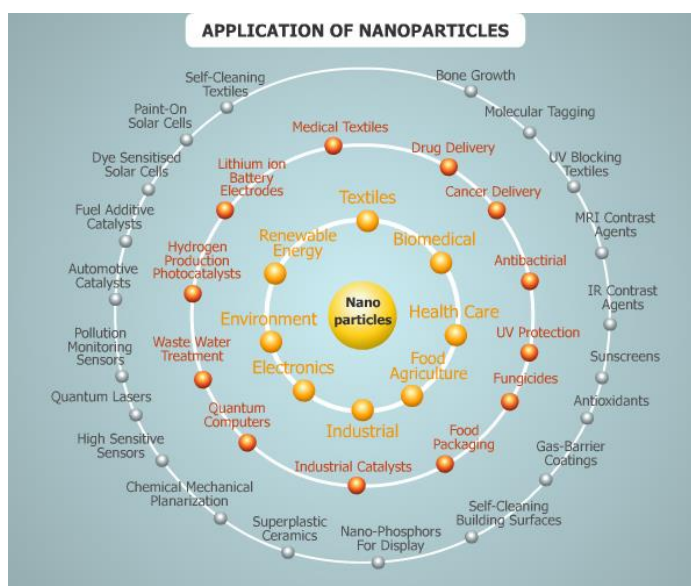


Figure 2.1. Major applications of nanoparticles. Source: taken from (Tsuzuki and Tsuzuki, 2009)

Table 2.1. Principal sectors of application of nanotechnology, ENP types and some of their improved properties

Application sector	ENP type	Improved properties	Ref
Agricultural sector	TiO ₂ , MWCNT, Pd, Au, SiO ₂ , Cu, CuO.	Increased growth rate, increased seed germination rate, smart agrochemical delivery system via plant roots	(Khot et al., 2012)
Automotive	MWCNT, TiO ₂ , CeO ₂	Lightweight construction, catalysts, scratch-resistant painting, lightweight and more resistant tires, sensors, windshield and body coatings	(Coelho et al., 2012) (Selvan, R B Anand and Udayakumar, 2009)
Coatings, paints and pigments	Al ₂ O ₃ , TiO ₂ , ZnO, SiO ₂ , Ag	Anti-fouling, Hydrophilic Surface, Self-Cleaning, UV resistance, anti-corrosive, scratch-resistant	(Khanna, 2008)
Construction materials	CNTs, carbon nanofibers, nanosilica or nanoclay, TiO ₂	Increase the strength and durability, increased thermal insulation, pollution protection, self-cleaning properties, self-repairing ability.	(Pacheco-Torgal and Jalali, 2011)
Green energy technologies	CNTs, TiO ₂ , MgO, Al ₂ O ₃ nanofluid, Ag/TiO ₂ nanocomposites	Increased efficiency of lighting and heating, increased electrical storage capacity.	(Hussein, 2015),
Environmental remediation	TiO ₂ , ZnO, zero valent iron (nZVI) nanoparticles	remediation of groundwater	(Khin et al., 2012)
Food technology and packaging	Ag, Au, Fe, Ir, ZnO, SiO ₂ , TiO ₂ , TiN, Al ₂ O ₃ , iron oxide (Fe ₃ O ₄ , Fe ₂ O ₃)	Improved physical performance, durability, barrier properties, biodegradation. Antimicrobial properties	(Hannon et al., 2015) (Bradley, Castle and Chaudhry, 2011)
Textiles	TiO ₂ , titania nanotubes (TNTs), Ag, Au, ZnO, Cu, CNTs, nano-clay and its modified forms, gallium, liposomes loaded nano-particles, metallic and inorganic dendrimers nano-composite, nano-capsules and cyclodextrins containing nano-particles.	Antimicrobial properties, improved physical resistance, anti-stains properties	(Dastjerdi and Montazer, 2010)
Cosmetics and personal care products	TiO ₂ , ZnO, fullerenes, liposomes, Ag, C, titanium/titania, silicon/silica, zinc/zinc oxide and gold.	Improve bioavailability (cosmetic nanocarriers), improved whitening agents, retain transparency while diffusing light	(Mihriyan, Ferraz and Strømme, 2012)

To assess the exposure of organisms of a certain region to ENPs, the quantification of their production volumes and the identification and quantification of use of their main applications is needed. Both steps have been identified as very challenging in the ENPs field and to carry a high level of uncertainty (Nowack *et al.*, 2015). This is because, to date (except some product-centric regulations for cosmetics, food and biocide products in EU (Rauscher, Rasmussen and Sokull-Klüttgen, 2017), there are no regulatory requirements that force producers to identify their materials by their nano-identity but only by their chemical identity and performance. Also, very few countries (i.e. France, Denmark, Belgium, Norway and Sweden), require their industries to report the nanomaterials produced or imported (<https://euon.echa.europa.eu/national-reporting-schemes>), contributing to the uncertainty.

With this lack of regulatory requirements, the general approach followed for the quantification of production amounts consists on company's consultation through surveys (Schmid and Riediker, 2008; Piccinno *et al.*, 2012; Keller *et al.*, 2013). However, this approach entails two main identified problems. Firstly, the inconsistencies that might be followed in the classification of a material as nano due to the lack of official ENP reporting guidelines. In this sense, different approaches from different companies might be taken when claiming nano-production amounts (e.g. when differently sized forms of the same material coexist some might label them as nano and some as the ordinary material). Secondly, the distinction between production, manufacturing and consumption volumes is frequently not made, and on many occasions they are used interchangeably due to lack of information, which will lead to over or under estimations (Nowack *et al.*, 2015).

Despite the uncertainty in the quantification of ENP production volumes, a general agreement on the most produced ENPs in terms of mass flow through the global economy is reported by Nowack *et al.* as a result of reviewing several studies investigating production and consumption volumes in different regions (Nowack *et al.*, 2015). These include titania (TiO₂), zinc oxide (ZnO), carbon nano-tubes (CNT), silver (Ag) and fullerenes (C₆₀). Other materials such as silica (SiO₂), alumina (Al₂O₃), iron oxides and cerium oxide (CeO₂) have a wide range of applications on the marketplace (Giese *et al.*, 2018) and are also reported, but large variability in the claimed production volumes was observed (mainly due to the previously mentioned problem associated with the

nanomaterial definition). Table 2.2 summarizes the values found from the different reviewed reports for some of the ENPs investigated.

Table 2.2. Comparison of production amounts from six different sources scaled to the EU (according to GDP) in metric tons per year. Source: table adapted from (Nowack *et al.*, 2015).

ENM	(Schmid and Riediker, 2008)	(Hendren <i>et al.</i> , 2011)	<i>et al.</i> (Piccinno <i>et al.</i> , 2012)	(Keller <i>et al.</i> , 2013)	(ANSES, 2013)	(Sun <i>et al.</i> , 2014)
TiO ₂	11500	8600-42000	550	20000	92000	10000
Ag	82	3-20	6	100	0.006	30
ZnO	1900	-	55	7900	1900	1600
CNT	26	60-1200	550	740	-	380
C60	-	2-90	0.6	-	<100	20
CeO ₂	-	40-770	55	2300	700	-
Al-ox	0.1	-	550	8100	15000	-
Fe-ox	9700	-	550	9700	6100	-
SiO ₂	2000	-	5500	22000	990000	-

Once the production amounts are established, product allocation and quantification of use should follow. Again, due to the already mentioned lack of regulation regarding product labelling (except the previously mentioned exceptions), this information is not easily accessible. In this case, the main sources of information available to generate the product allocation are online product inventories such as the Woodrow Wilson Inventory (Vance *et al.*, 2015a) or the Nanodatabase (Foss Hansen *et al.*, 2016). These are public inventories that have been created by the scientific community (i.e., The Woodrow Wilson Center and the Technical University of Denmark associated with further partners respectively) by collecting information on the nano-applications being introduced into the market. However, they are again encumbered by limitations associated with the ability to claim the presence of ENPs in the products and the frequent lack of proof when this is done (Nowack *et al.*, 2015). Furthermore, qualitative information is often given but accurate quantitative data are not provided. Another source of information for the product allocation is once more the use of surveys. An example is the research carried out by Keller *et al.* (Keller *et al.*, 2013), where they concluded from consultation with manufacturers that the dominant nano-enabled products in the market were at that time coatings/paints/pigments, electronics and optics, cosmetics, energy and environmental applications, and catalysts. Similarly, from the research performed by researchers from

the Netherlands National Institute for Public Health and the Environment (RIVM), using different available nano-databases, market reports and through consultation of expert groups, the high priority products for future exposure studies reported were identified as sun cosmetics, DIY coatings and adhesives as well as personal care and cleaning products (Wijnhoven *et al.*, 2009). Figure 2.2 summarizes the production amounts estimated by Sun *et al.* (2014) for the European Union (EU) for the top five most relevant ENPs, their volumes of application for specific product categories and the relative distribution of their volumes through different product categories (Mitrano *et al.*, 2015).

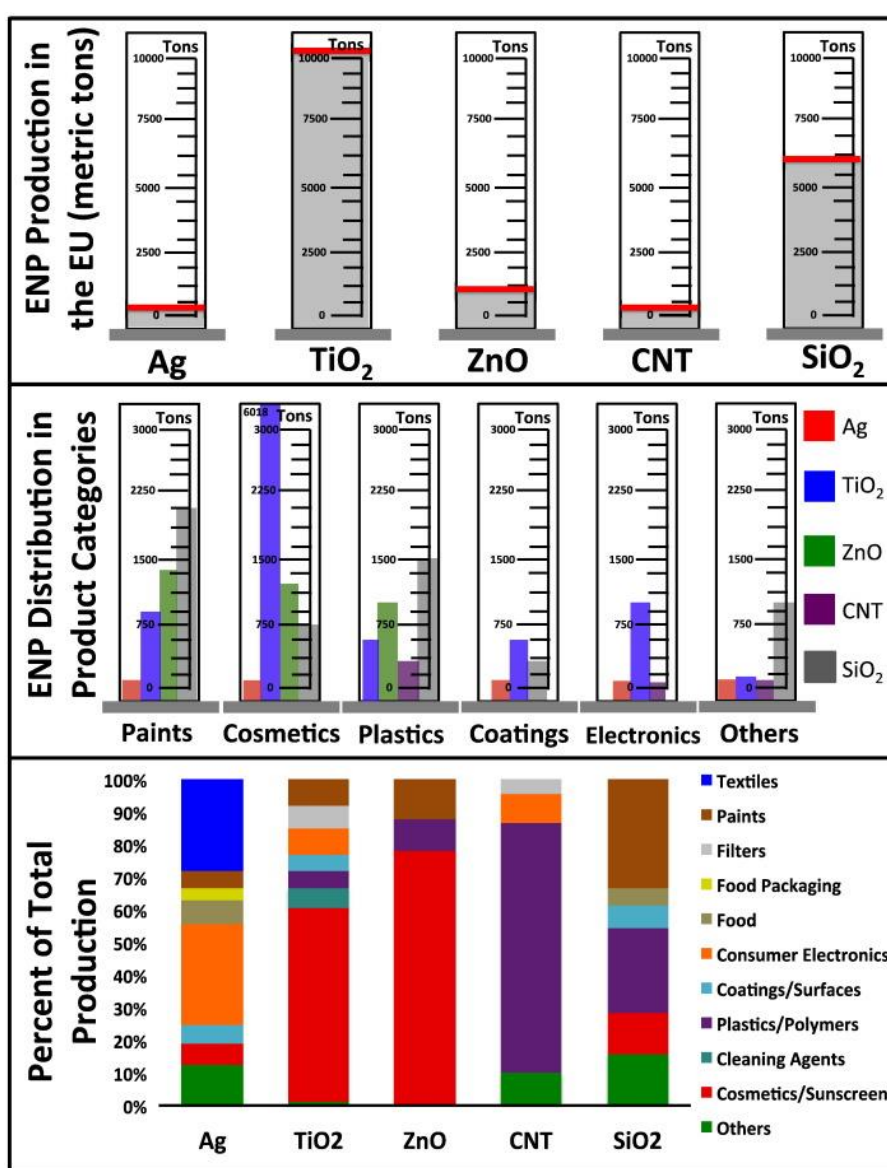


Figure 2.2. Production volumes of the top five most relevant ENPs estimated for the EU (top), the volumes estimated for a variety of their applications (middle) and their relative distribution into a selection of different product categories (bottom). Source: image taken from (Mitrano *et al.*, 2015).

2.3 Release mechanisms and emission pathways of ENPs

ENPs emissions can take place at any stage of their life cycle: during production (formulation and manufacturing), transport, use and after disposal (Klaine *et al.*, 2008). As shown in Figure 2.3, understanding the release mechanisms and emission pathways is key to properly estimating exposure. In addition, it would help to localize the most exposed areas within the environment studied (hot spots).

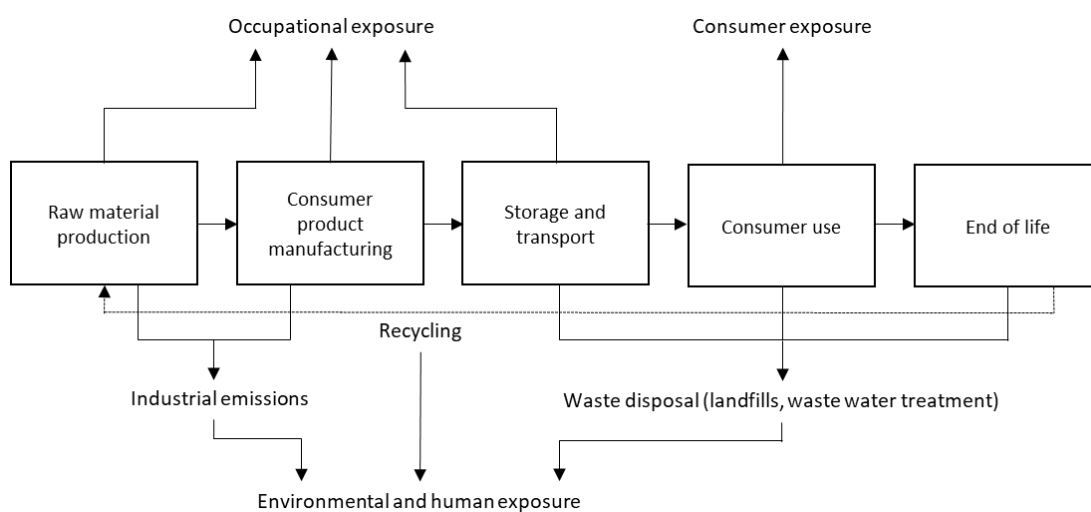


Figure 2.3. Possible pathways of occupational, environmental and human exposure to ENPs. Source: image adapted from (Hristozov *et al.*, 2009)

Different pathways of emissions will be followed by the ENPs depending on their life cycle stage, but also depending on the type of product they are integrated into, the form under which they are integrated in that product and the use given to it. During the production and transport stages, the main emission pathway consists of accidental spillages and minor emissions from solid waste disposal, wastewater or airborne emissions that may happen during manufacturing. During the use stage, ENPs can be released from applications through different pathways. For example, ENPs used in surface coatings or outdoor paints are emitted to surface waters due to weathering through runoff (Al-Kattan *et al.*, 2013). ENPs contained in textiles and personal care products are released down the drain from households during washing, and emitted to surface water after being treated in wastewater treatment plants (Keller *et al.*, 2014a; Mitrano *et al.*, 2014). Other ENPs can be directly emitted into surface water, such as those used in

sunscreens during bathing activities (Gondikas *et al.*, 2014), and to soils, when applied in agricultural fields such as nano-pesticides (Whiteley *et al.*, 2013). Atmospheric emissions of ENPs can also be expected during the use stage, for example from vehicle exhaust when using ENP-containing fuel additives (Johnson and Park, 2012). At the end of their product life, after disposal, ENPs would be emitted through leaching from landfills (Mitrano *et al.*, 2017), or where sewage sludge has been applied (Whiteley *et al.*, 2013). Atmospheric emissions of ENPs can also be expected from incineration of solid waste containing ENPs (Walser *et al.*, 2012).

According to the recent study by Giese *et al.*, on the assessment of emissions of ENPs through their whole life cycle into the environment, the overall material transfer is dominated by the flow into the technical compartments (i.e. landfills and incineration plants) at the end of life of the products. (Giese *et al.*, 2018). Landfills are considered as predominant sinks of ENPs, with an estimated 63–91 % of the global ENM production believed to end up in landfills (Keller *et al.*, 2013). Conversely, the release of ENPs into nature was found to be dominated by release during the use phase, emissions during the production and transport phases were estimated at only 1 to 5% of the total ENPs mass contained in most products (Giese *et al.*, 2018).

During each stage of the life cycle, ENPs may be emitted to the different environmental compartments (i.e., atmosphere, soil, water and sediment) (Figure 2.4). Once emitted, they will distribute throughout those different compartments through indirect pathways. For example, dry or wet deposition of ENPs emitted to the atmosphere (Kumar *et al.*, 2011), or leaching of ENPs to groundwater or surface water from land where ENPs-containing sewage sludge has been applied (Whiteley *et al.*, 2013).

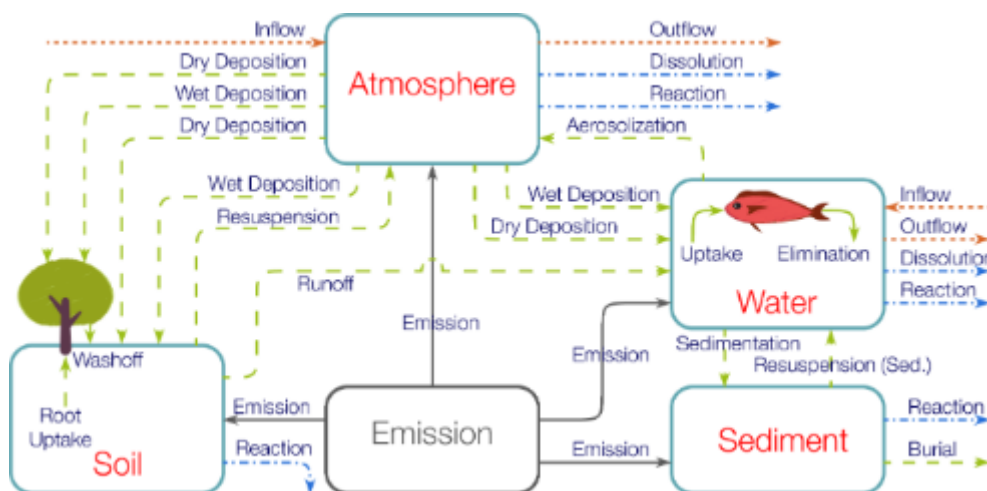


Figure 2.4. Emissions pathways and environmental distribution of ENPs. Source: image taken from Liu *et al.* (2015)

Different products have different release potential and this is mainly due to the way in which the ENPs are integrated in each type of product and the use given to that product. For example, ENPs can be strongly embedded within a solid material matrix, present in liquid form in emulsions or suspensions or even used as aerosols (Hansen *et al.*, 2009). Emissions from materials containing ENPs suspended in liquid or in aerosols are expected to be higher than those which have the ENPs bound to a solid matrix. The latter will need some kind of abrasion or degradation process to liberate the ENPs, but some products are more exposed to those conditions than others (i.e. outdoor coatings or textiles). Based on this concept a classification based on the release potential of the product was generated by Hansen *et al.* which consisted on three categories: (1) Expected to cause exposure; (2) May cause exposure; and (3) No expected exposure. Figure 2.5 shows the number of products containing ENPs in the different forms listed, from the registered products of the Woodrow Wilson Inventory (Vance *et al.*, 2015). From these results, it can be observed that most of the products containing metallic ENPs integrate them in liquid suspension or bound to their surface and therefore are likely to be released and cause exposure. Carbonaceous ENPs, on the other hand, are mainly embedded in the solid matrix and will pose lower exposure risk.

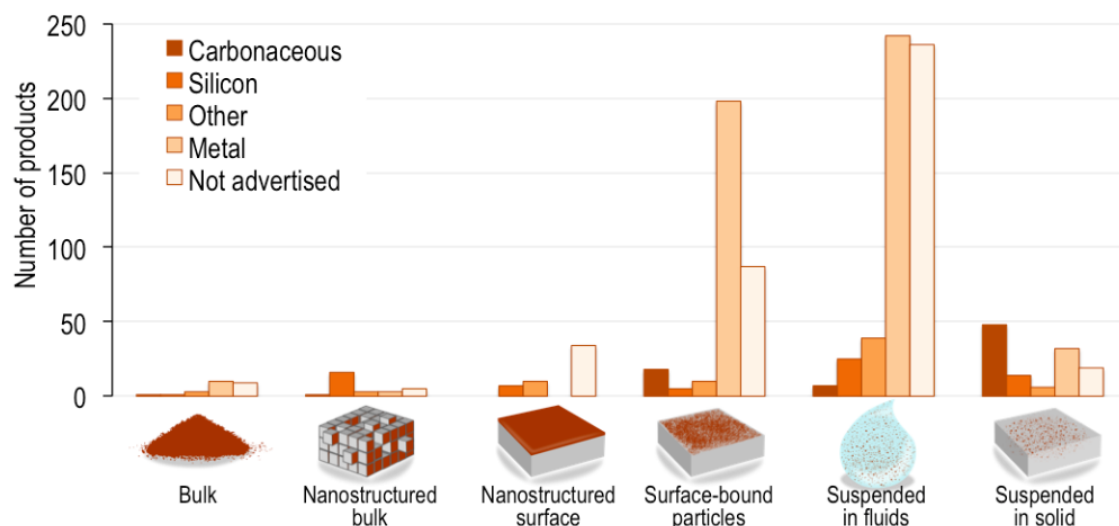


Figure 2.5. Forms under which different types of ENPs are integrated in the registered consumer products of the Woodrow Wilson Inventory. Source: image taken from (Vance et al., 2015).

During emission, ENPs are subject to alterations and transformations that will determine their properties and their behaviour and fate within the environment, and therefore determine their potential risks (Nowack *et al.*, 2016). For example, ENPs incorporated in textiles, cosmetics and sunscreens can be subject to a series of transformations during their use and washing processes. Those would include oxidation, reduction, dissolution and precipitation (Mitrano *et al.*, 2015). Similar effects were also observed for ENPs contained in outdoor paints and coatings, plastics and polymers (Mitrano *et al.*, 2015). Therefore, transformations during use would be a key aspect to consider when performing ENP exposure assessment studies. Finally, once emitted, the released ENPs will be subject to further transformations and transport processes along the different environmental compartments. These processes are discussed in the next section.

2.4 Fate processes of ENPs in the aquatic system

Engineered nanoparticles, once released into the environment (atmosphere, soil, sediment or aquatic systems), are subject to a series of physical, chemical and biological transformations that will influence their transport, fate and toxicity, and consequently their exposure levels and associated risks (Dwivedi *et al.*, 2015). As depicted in Figure 2.6, these include photochemical degradation, dissolution and chemical surface transformations such as sulfidation, oxidation and reduction. The physical transformations consist of aggregation processes between ENPs (homo-aggregation), or

with other suspended particulate matter (SPM) (hetero-aggregation), as well as interactions with macromolecules such as proteins or natural organic matter (NOM). Finally, biologically mediated transformations such as biological oxidation or biological degradation may also occur in natural systems (Lowry *et al.*, 2012).

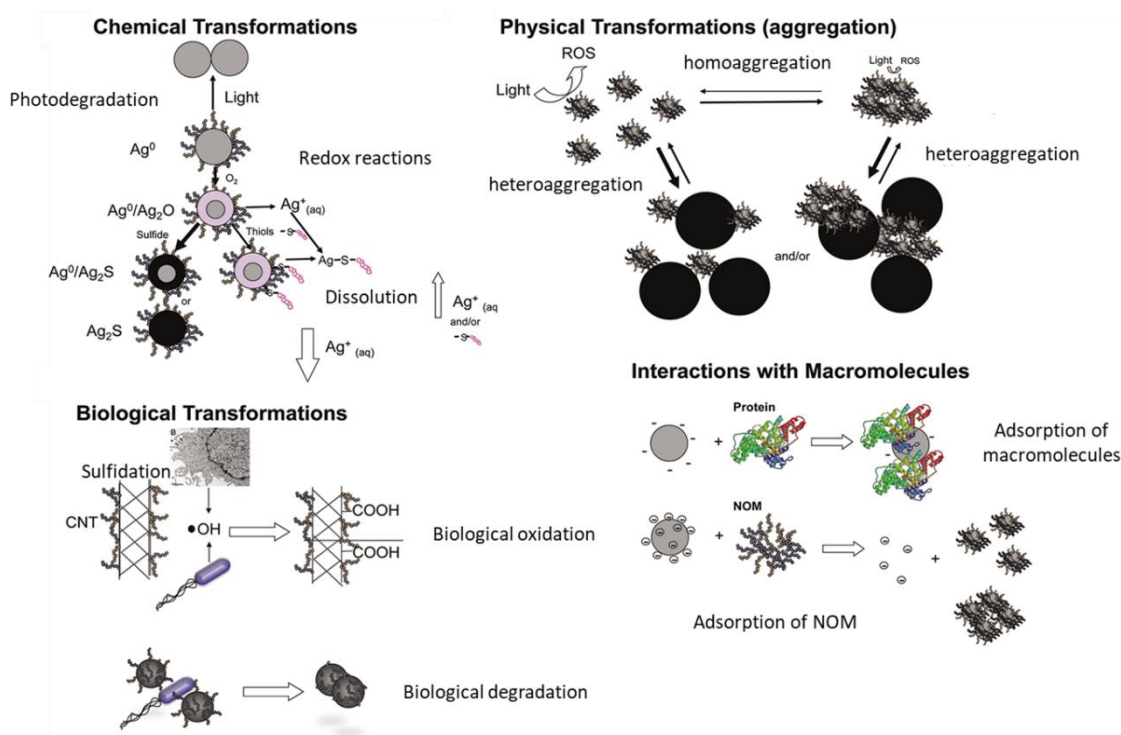


Figure 2.6. Environmental fate processes of ENPs. Source: image modified from (Lowry *et al.*, 2012).

These different environmental processes alter ENP size, surface composition and surface charge, which define their reactivity, their bioavailability, their toxicity and their persistence (Lowry *et al.*, 2012).

2.4.1 ENP chemical transformations

The main chemical reactions that ENPs are subject to in the environment include redox reactions, sulfidation, photochemical degradation and dissolution (Lowry *et al.*, 2012). The redox processes consist of the transfer of electrons between two chemical species and usually occurs at the ENP surface when in contact with organic or inorganic ligands present in both aquatic and terrestrial environments (Wagner *et al.*, 2014). ENPs susceptible to these reactions are metallic and metal oxides ENPs such as Ag, Cu, Zn, Fe

oxides or CeO₂ (Lowry *et al.*, 2012). These reactions will result in morphological changes of the ENPs such as dissolution, or surface coating formation and transformations, and therefore will contribute to changes in their persistence, bioavailability and toxicity to become more or less toxic upon transformation (Lowry *et al.*, 2012). For example, Ag ENPs are subject to dissolution through oxidation from Ag(0) to Ag(I), if this reaction occurs the toxicity increases due to the bactericidal properties of the silver ions (Lok *et al.*, 2007). CdSe/ZnS quantum dots are also susceptible to oxidation in marine environments and may release soluble toxic metal ions such as Cd (Zhang *et al.*, 2012). The oxidation of Fe oxides such as magnetite has also been observed to change their magnetic properties leading to an enhanced colloidal stability due to increased magnetic repulsion forces (Wagner *et al.*, 2014), thereby increasing their bioavailability.

The presence of light can also catalyse redox reactions that will change the ENP's oxidation state, charge and affect their surface coating, therefore again affecting their toxicity in one or the opposite direction (Lowry *et al.*, 2012). Some ENPs in the presence of light undergo a photodegradation process of their surface coating that might induce ENP aggregation and sedimentation from solution (Yin *et al.*, 2015). In this case, their potential toxicity will decrease due to the loss of their nano-size properties and bioavailability. On the other hand, sunlight can induce the generation of reactive oxygen species (ROS) from certain ENPs such as carbon nanotubes (CNT), and therefore enhancing their toxicity (Bennett *et al.*, 2013). ROS production has been reported for nanoparticles as diverse as C60 fullerenes (Oberdorster, 2004), single-walled carbon nanotubes (Shvedova *et al.*, 2004), quantum dots (Derfus *et al.*, 2004) and ultrafine particles (Brown *et al.*, 2001).

Sulfidation is a complexation process mediated by sulphide ligands. This process plays a major role in the toxicity of Ag ENPs in the environment and has been extensively studied (Levard *et al.*, 2013). It consists of the surface complexation of the Ag ENPs with sulphides to form Ag(0)/Ag₂S core-shell particles that results in the decrease of Ag⁺ species release due to a lower solubility of Ag₂S relative to Ag(0), and consequent decrease of Ag ENP toxicity.

During the dissolution process, as stated before, solid ENPs release individual ions or molecules into the water. This process would reduce the persistence of the ENPs in the aquatic compartment but also induces toxicity of some ENPs (García-Alonso *et al.*, 2014). For example, Ag ENPs show toxic effects as it releases silver ions (Tripathi *et al.*,

2017). Not all ENPs are susceptible to dissolution; in fact, this process is highly dependent on the material composition. The ENPs for which dissolution is considered relevant in the study of their environmental fate processes are: ZnO, Ag, Cu/CuO and quantum dots (QD) (depending on their chemical composition). On the contrary, dissolution is not usually considered for ENPs such as TiO₂, CeO₂ and CNT amongst others (Hartmann *et al.*, 2014).

2.4.2 Physical transformations: ENPs aggregation processes

Aggregation can be defined as the process in which primary particles interact through irreversible forces (chemical bonds or electrostatic interactions) to form larger particles (Jiang, Oberdörster and Biswas, 2009). In the agglomeration process however, weaker forces hold the particles together so this process is reversible (Jiang, Oberdörster and Biswas, 2009). Despite this distinction, these terms are often used interchangeably in the literature, with different conventions being used in different disciplines. Most of the literature on colloid science often uses the term aggregation to describe particle flocculation processes. Therefore, in this thesis, the term aggregation will be applied to describe these particle interaction processes irrespectively of their reversibility.

Due to their small size, ENPs present high surface energy and therefore a tendency to attach to surfaces and or to aggregate with other materials present in their dispersion media (e.g. SPM). In the aggregation process, ENP size increases and the “available” surface area of the particle is significantly reduced. This change in size and surface area will affect the ENPs transport and bioavailability, as well as their surface reactivity and toxicity (Lowry *et al.*, 2012). When the size of the particle increases, transport through porous media in soil and sediments may be restricted due to physical screening (Lin *et al.*, 2009). When ENPs are in suspension, the aggregation processes will dictate their dispersion stability and sedimentation rates (Petosa *et al.*, 2010). Generally, when ENP-ENP or ENP-SPM interactions succeed, larger ENPs aggregates form and quickly sediment out from the compartment they are dispersed in (i.e. atmosphere or water column) decreasing the exposure risk of their inhabiting organisms, and restricting their transport (Lin *et al.*, 2009). Smaller and well dispersed ENPs, on the other hand, will remain in suspension for longer times increasing exposure and potential risks (Lin *et al.*, 2009). When the “available” surface area of the ENPs is reduced due to homoaggregation or heteroaggregation with SPM, the surface energy and reactivity is also reduced

significantly due to this change in size. In this sense, surface mediated reactions such as dissolution or reactive oxygen species (ROS) generation would be reduced and therefore aggregation would increase the ENPs persistence in the environment and reduce their toxicity respectively (Lowry *et al.*, 2012).

The dispersion/sedimentation processes are highly influenced by the ambient conditions (i.e. pH, ionic strength, presence of NOM, ionic composition of the media, etc.), as well as by the ENP characteristics (i.e. chemical composition, surface coating, shape and size) (Dwivedi *et al.*, 2015) and these will be discussed in Section 2.5.

2.4.3 ENP interactions with macromolecules

Just as with the hetero-aggregation processes, due to their high surface reactivity, ENPs tend to interact with naturally occurring biomacromolecules or geomacromolecules including proteins, polysaccharides and natural organic matter (NOM), upon release into the environment (Lowry *et al.*, 2012). Adsorption of these macromolecules onto the ENPs surface would happen in all environments, for example, when ENPs are internalized by an organism they tend to develop a protein coating on their surface, often called the protein corona (Lynch and Dawson, 2008). This protein layer modifies the ENP properties within the medium (i.e., size, electrophoretic mobility and surface composition) and therefore, affects their subsequent behaviour and biological response (Walczyk *et al.*, 2010). In the natural environment (e.g. surface water), ENPs would interact in the same way with ubiquitous NOM present in the media and will as well affect the ENPs properties. Some studies show that humic substances (principal components of NOM) can sorb to different kinds of ENPs (zero-valent iron NPs, iron-oxide NPs, CNT and fullerenes, etc.) by forming nanoscale surface coatings and that such surface coatings can modify the nature of the ENPs in terms of surface charge and composition (Christian *et al.*, 2008). The effect of NOM on the aggregation and deposition behaviour of different types of ENP has been extensively studied (Baalousha, 2009; Quik *et al.*, 2010; Thio, Zhou and Keller, 2011) and will be discussed in Section 2.5. In addition, the influence of NOM over ENPs toxicity has also been demonstrated. For example, NOM was found to mitigate the bactericidal activity of zero valent iron (NZVI) (Chen *et al.*, 2011), also to mitigate quantum dots (QDs) (Lee *et al.*, 2011) and Ag ENPs toxicity (Gao *et al.*, 2012).

2.4.4 ENPs biological transformations

Biologically mediated transformations of ENPs by microorganisms and bacteria present in the environmental media (e.g. soil) are also expected. These mainly include biodegradation of ENP polymer coatings (Kirschling *et al.*, 2011) and biologically mediated degradation of carbon based ENPs (i.e. CNT) (Allen *et al.*, 2008). Again, these transformations will affect ENP behaviour and final fate through the modification of their surface charge, aggregation state and reactivity that influences their transport, bioavailability and toxicity (Lowry *et al.*, 2012).

2.5 Factors influencing ENP environmental fate processes

The environmental fate processes that ENPs are subject to vary according to the ENP's properties as well as the environmental media properties (Table 2.3), which control the extent of those processes (Dwivedi *et al.*, 2015). Dissolution rates, for example, are highly influenced by the characteristics of the aqueous medium. Particles such as ZnO and Ag dissolve in most aquatic media, with enhanced dissolution rates occurring at extreme pH values (particularly at low pH), while other metal and metal oxides such as CeO₂, Au and TiO₂ don't dissolve even over long periods of time (Garner and Keller, 2014).

Table 2.3. Factors influencing the fate and behaviour of ENPs in the environment

ENP properties	Environmental media properties
Chemical composition	pH
Size	Temperature (T)
Shape	Ionic strength (IS)
Surface charge	Ionic composition (Ca ²⁺ , K ⁺ , etc.)
Concentration	Natural organic matter concentration ([NOM])
Surface coating	UV light
	Suspended particulate matter concentration ([SPM])
	Dissolved oxygen (DO)
	System dimensions
	Flow rates

The chemical composition of ENPs defines how relevant the environmental fate processes will be. Table 2.4 shows a classification of the environmental fate processes according to their level of relevance (low, medium and high) for a selection of ENP types.

Table 2.4. Level of relevance of fate processes in environmental fate modelling and for Silver (Ag), Titanium dioxide (TiO₂), Zinc oxide (ZnO), Carbon nanotubes (CNTs), Copper oxide (CuO), Nano-scale zero valent iron (nZVI), Cerium oxide (CeO₂), Carbon black (CB) and Quantum dots (QDs). Source: adapted from (Hartmann et al., 2014).

Processes	Low	Medium	High
Photochemical	nZVI, CB	ZnO, CuO	Ag, CeO ₂ , TiO ₂ , CNT
Redox	TiO ₂ , CNT, CeO ₂ , CB	ZnO, CuO	Ag, nZVI
Dissolution	TiO ₂ , CNT, nZVI, CB	CeO ₂	Ag, ZnO
Aggregation/agglomeration			Ag, ZnO, TiO ₂ , CNT, CuO, nZVI, CeO ₂ , CB
Sedimentation			Ag, ZnO, TiO ₂ , CNT, CuO, nZVI, CeO ₂ , CB
NOM adsorption			Ag, TiO ₂ , ZnO, CuO, nZVI, CeO ₂ , CNT, CB
Sorption onto other surfaces/retention in soil			Ag, ZnO, CuO, TiO ₂ , CeO ₂ , CNT, nZVI, CB
Bio-degradation	Ag, TiO ₂ , ZnO, CuO, nZVI, CeO ₂ , CB	CNT	
Bio-modification		Ag, TiO ₂ , ZnO, CuO, nZVI, CeO ₂ , CB	CNT

The significance of these processes also vary depending on the environmental compartment studied. Table 2.5, presents the relevance of the fate processes according to the environmental compartment studied (air, soil, sediment and water).

Table 2.5. General relevance of environmental transformation processes of ENPs in different environmental compartments. Where: ++ means highly relevant for inclusion in ENPs fate modelling; + means relevant for inclusion in ENPs fate modelling; - means low/no relevance for inclusion in ENPs fate modelling; and * means highly dependent on the ENM chemical composition. Source: table taken from (Hartmann et al., 2014).

Processes	Compartments			
	Air	Water	Sediment	Soil
Photochemical reactions	++	+	-	-
Redox reactions	-	++*	++*	+
Dissolution/speciation	-	-/++*	-/++*	-/++*
Aggregation/ agglomeration	+	++	+	+
Sedimentation/ deposition	+	++	-	-
NOM adsorption	-	+	++	+
Sorption onto other surfaces	-	+	++	++
Bio-degradation	-	-/++*	-/++*	-/++*
Bio-modification	-	-/+	-/+	-/+

The factors influencing the most relevant aquatic ENPs fate processes (i.e. aggregation, sedimentation and dissolution) are further discussed below.

2.5.1 ENP aggregation

Under environmentally relevant conditions, homoaggregation processes are very unlikely to occur due to the very low expected ENP concentrations (i.e. ng per L to µg per L) (Gottschalk, Sun and Nowack, 2013). On the other hand, the presence of SPM in surface waters is ubiquitous and at much higher concentrations, consequently heteroaggregation processes will dominate ENP behaviour in aqueous suspension, becoming one of the main mechanisms that determines ENP transport, bioavailability and toxicity in surface waters (Clavier, Praetorius and Stoll, 2019).

The aggregation process of ENPs with SPM is best described by a pseudo-first order heteroaggregation rate constant ($k_{het-agg}$). This constant is considered to be dependent on SPM particle concentration (for which variation is assumed negligible), the collision rate (k_{coll}) between particles, and the surface interactions between the aggregating particles, which determine their so-called attachment efficiency ($\alpha_{het-agg}$) (Sani-Kast et al., 2015):

$$k_{het-agg} = k_{coll} \cdot \alpha_{het-agg} \cdot [SPM] \quad (2.1)$$

The collision rate is governed by the random movement of particles suspended in the fluid, also called “Brownian motion”, the fluid motion and by differential settling (gravitational forces) (Praetorius, Scheringer and Hungerbü, 2012). Brownian motion is considered the predominant factor that determines the ENP collision rate (Petosa *et al.*, 2010). The properties of the solution, such as temperature and the particle concentration, have some impact on the collision rate. For example, at higher temperature the particle motion increases and therefore a higher probability of particle collision is expected. Similarly, higher concentrations of particles will generate higher probability of collisions between them. However, these effects are not always described by a linear relationship and will depend on other solution and particles properties as well (Baalousha, 2009).

Upon collision, the particles might successfully attach to form aggregates or not. The probability of a successful attachment, commonly known as attachment efficiency ($\alpha_{het-agg}$), is determined by the sum of attractive and repulsive forces between the particles (Hartmann *et al.*, 2014). These include steric forces, electrical double layer forces (EDL), Van der Waals forces, hydration forces and hydrophobic forces which depend on the ENPs properties (size, surface charge, shape), SPM properties (composition, size, charge, etc.) and the solution properties (ionic strength, ionic composition and NOM concentration). The Derjaguin and Landau, and Verwey and Overbeck (DLVO) (Verwey and Overbeek, 1955; Derjaguin and Landau, 1993) theory explains how the combination of Van der Waals and EDL forces influences the particle-particle interactions as a function of the particles’ separation distance (Petosa *et al.*, 2010). However, it does not take into consideration other parameters in place (e.g., ENP type, SPM and some of the solution properties) and therefore, it is not sufficient to accurately predict the aggregation behaviour in the natural environment. Several experimental studies have investigated the influence of some of the solution properties on the ENPs aggregation behaviour (Table 2.6 summarizes some of them).

Table 2.6. Summary of experimental studies on the influence of environmental factors (i.e. concentration of ENPs (C_{ENP}), ionic strength (IS), natural organic matter concentration ([NOM])) and pH on the aggregation behaviour of different ENPs. If the aggregation is enhanced (+) or hindered (-).

ENP Type	Parameters studied	Influence on aggregation	Mechanism	Reference
Iron Oxide	C_{ENP}	+	Increase of collision frequency	(Baalousha, 2009)
	pH	According to PZC (higher aggregation closer to PZC)		
ZnO	[NOM]	-	Steric and electrostatic stabilization	(Bian <i>et al.</i> , 2011)
	IS	+		
	pH	According to PZC (higher aggregation closer to PZC)		
TiO ₂	[NOM]	-	Decreased electrostatic repulsions Steric and electrostatic stabilization	(Domingos, Tufenkji and Wilkinson, 2009)
	IS	+		
	pH	According to PZC (higher aggregation closer to PZC)		
CeO ₂	[NOM]	-	Steric and electrostatic stabilization	(Quik <i>et al.</i> , 2010)
Fe ₃ O ₄ (magnetite)	[NOM]	-	Steric and electrostatic stabilization	
SWCNT	IS	The aggregation of SWCNT was negligible in the presence of CaCl ₂ and AlCl ₃ Aggregation was not sensitive to pH		(Li and Huang, 2010)
	pH			
Ag	IS	+	Decreased electrostatic repulsions Enhance agglomeration through charge neutralization or bridging mechanisms caused by fibrillar attachment	(Akaighe <i>et al.</i> , 2012)
	[NOM]	+		

General trends in the roles played by the factors presented in Table 2.6 (ionic strength, pH and NOM concentration) can be extracted. While most ENPs present a specific surface charge (that defines their electrostatic forces), the pH, ionic strength, and NOM concentration of the media can modify this surface charge and influence the electrostatic interactions between them.

Generally, high ionic strength decreases electrostatic repulsions between particles and aggregation is enhanced. The pH of the surrounding media will also dictate the particles surface charge. For each particular system, the pH at which the surface charge becomes zero, as a consequence of charge neutralization, is called the point of zero charge (PZC), and as the surrounding pH moves towards this point the electric double layer (EDL) repulsion decreases and aggregation is promoted. NOM, on the other hand, can both, promote and decrease aggregation. NOM tends to adsorb to the ENPs surface and can in some cases provide steric and electrostatic stabilization promoting disaggregation (Loosli, Le Coustumer and Stoll, 2014), but in other instances NOM can enhance aggregation through charge neutralization or bridging mechanisms caused by fibrillar attachment (Jacques Buffle *et al.*, 1998) (Figure 2.7). For example, the presence of dissolved organic carbon (DOC), as a proxy for NOM, was found to reduce the attachment efficiency of ENPs resulting in a decrease in aggregation (Quik *et al.*, 2010; Li and Chen, 2012). However, NOM as also found to have the opposite effect when the natural colloids were large enough (Hotze, Phenrat and Lowry, 2010). In fact, several experimental studies also found exceptions to the ionic strength effect previously listed (Akaighe *et al.*, 2012; Chowdhury, Cwiertny and Walker, 2012; El Badawy *et al.*, 2012).

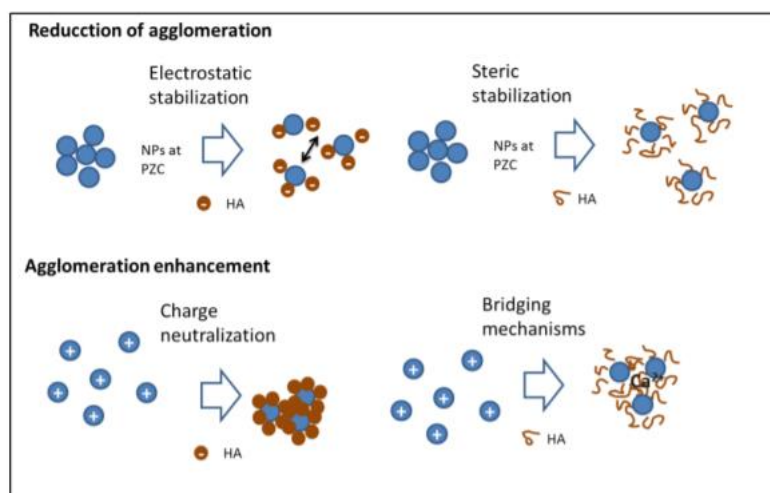


Figure 2.7. Schematic representation of the role of Humic acids (HA), as a proxy of NOM on the aggregation and disaggregation processes of ENPs.

Due to the complexity of factors influencing aggregation of ENPs, the calculation of $\alpha_{het-agg}$ is very challenging when looking into specific ENP-SPM combinations for distinct

solution conditions (Praetorius, *et al.*, 2014). However, experimental designs are available for their estimation as well as for the estimation of $k_{het-agg}$. They can be obtained for specific ENPs and under changing environmental conditions (pH, DOC (as a proxy for natural organic matter), ionic composition of the media, etc.) (Praetorius, Labille, *et al.*, 2014; Quik *et al.*, 2014).

2.5.2 ENPs sedimentation/deposition

Sedimentation is the process that describes the settling of the particles from the water column to the sediment due to gravitational settling forces, which influences the ENPs bioavailability. Stoke's law describes this process as follows:

$$v_{set}^{particle} = \frac{2}{9} \cdot \frac{\rho_{particle} - \rho_{water}}{\mu_{water}} \cdot g \cdot r_{particle}^2 \quad (2.2)$$

where $v_{set}^{particle}$ is the settling velocity of the particle or agglomerate studied, $\rho_{particle}$ its density, $r_{particle}$ its radius, μ_{water} is the dynamic viscosity of water and g is the acceleration due to gravity on earth (Praetorius, 2014). Sedimentation is, therefore, particle size and density dependent as well as a function of the viscosity and density of the fluid. Bigger particles, although they might diffuse more slowly, tend to settle more rapidly under gravity (Hartmann *et al.*, 2014). Consequently, this process is highly linked with the aggregation processes, since the aggregation rate becomes a limiting factor of sedimentation of ENPs in aquatic media (Hartmann *et al.*, 2014).

Again, the ENP characteristics (composition, size, shape and density) and the parameters of the aquatic media, such as the presence of NOM and its concentration, pH, and the ionic composition of the aquatic media have an effect on the sedimentation rates of the different ENPs (Quik *et al.*, 2014). Quik *et al.* estimated sedimentation and heteroaggregation rates by performing sedimentation studies for four different ENP types (C₆₀, CeO₂, SiO₂-Ag and PVP-Ag) and six different water types with varying characteristics (ionic content, DOC, EC, pH and NOM concentration). They found that the sedimentation rates were highest in seawater (highest ionic content) for all ENPs tested and that, even though the presence of NOM didn't seem to affect significantly their

sedimentation rates in any of the water types, the presence of NOM increased the fraction of ENPs in the sediment (bigger settling fractions found) (Quik *et al.*, 2014).

Other side-processes such as the so-called gravitational aggregation has also to be accounted for when studying ENP settling (Hartmann *et al.*, 2014). Gravitational aggregation happens when the slower-settling (smaller) particles/aggregates are captured by the more rapidly settling (larger) particles/aggregates. These side-process usually become relevant when aggregates become bigger. The study of sedimentation is considered key in ENP fate and toxicity research as it is a potential key removal mechanism for ENPs in the aquatic environmental compartments (Praetorius, Scheringer and Hungerbühler, 2012).

2.5.3 Dissolution

Besides the material composition, specific ENP characteristics such as size, agglomeration state, shape and surface coating, have an effect on the particle dissolution kinetics (dissolution rate) and the solubility equilibrium (Hartmann *et al.*, 2014). Size is a determining factor for dissolution to happen. For example, whereas bulk silver is considered insoluble in aqueous media, Ag ENPs releases free silver ions (Stone *et al.*, 2010). Additionally, many studies agree that the dissolution rate increases with decreasing particle size (Bian *et al.*, 2011; Dobias and Bernier-Latmani, 2013). This can be explained by the higher surface area of the material being exposed to the solvent as the size of the particle decreases. Dobias and Bernier (Dobias and Bernier-Latmani, 2013) found the important role of the surface area in the dissolution process while determining Ag loss from differently sized Ag ENPs. In their experiments, the surface area was normalized for all ENPs tested and the same trends found. According to this hypothesis, it is clear that aggregation will have a negative influence upon dissolution, aggregates having lower surface area than their constituent single ENPs (Dobias and Bernier-Latmani, 2013).

The influence of surface coatings and ENP shape on dissolution rates have also been investigated for different ENPs. In the same study by Dobias and Bernier, different rates of dissolution for Ag ENPs coated with different materials were found, and the mechanisms by which the surface coating impacts Ag ENP dissolution were proposed. However, no clear trend in the effect of surface coating dissolution was drawn in this study (Dobias and Bernier-Latmani, 2013). The study performed by Misra *et al.* on the

influence of CuO ENP shape on their dissolution rates and performance, showed that spherically shaped CuO ENPs dissolve to a greater extent and faster than the rod shaped ones (Misra *et al.*, 2012).

In addition, the aquatic media properties (pH, ionic strength, temperature, NOM concentration and dissolved oxygen) have been demonstrated to also influence the extent of the dissolution process (Bian *et al.*, 2011). For example, Gondikas *et al.* found that the presence of organic and/or inorganic components in the surrounding media could in some cases catalyse the dissolution of nanoparticles (Gondikas *et al.*, 2012). Misra *et al.* found that dissolution of ZnO ENPs was enhanced by humic acid (a proxy of NOM) at high pH (Misra *et al.*, 2012). Levard *et al.*, studied the role of the presence of oxygen on the dissolution of metallic ENPs through redox reactions and found that Ag ENPs would react with oxygen to form Ag₂O on the particle surface followed by subsequent Ag⁺ dissolution into the surrounding aqueous solution (Levard *et al.* 2012), while under anoxic conditions metallic silver is expected to react with sulphur altering the ENPs surface charge and affecting the dissolution rate (Levard *et al.*, 2012).

However, general trends for dissolution of all ENPs cannot be established since again, the combination of both, ENP characteristics and aquatic media properties, is what determines the extent of dissolution of a specific ENP (Misra *et al.*, 2012). In this sense, the best approach to describe dissolution is through the use of an experimentally obtained dissolution rate constant, k_{diss} , specific to the ENP and the characteristics of the environmental medium (Liu and Hurt, 2010).

2.6 Conclusions

In this chapter, we have reviewed the steps and considerations that have to be made to perform an exposure assessment of ENPs. Firstly, we reviewed the main commercial applications of ENPs and discussed the challenges, limitations and main approaches used to estimate their production and use volumes. Secondly, we described the main ENP emission pathways, suggested some ENP release mechanisms and reviewed the factors influencing their release potential. Finally, we provided a description of the main fate processes that ENPs might undergo once released into the environment, reviewed the influence of such processes on their final fate and potential toxicity, and summarized the main findings of the influence of the environmental and anthropogenic factors determining the extent of such processes.

Going back to the main aim of this thesis, which is focused on exploring tools for the assessment of ENP exposure in urban surface waters, in the next chapter we apply the gained knowledge to design a modelling framework that is able to tackle some of the challenges discussed here, such as the uncertainties surrounding usage volume quantification and ENP fate characterization (e.g. determination of ENP attachment efficiencies based on monitored surface water quality data). Furthermore, we suggest a new methodology where we integrate emissions and fate modelling at a high level of spatial and temporal resolution that has not been previously explored

Chapter 3

Emission and fate modelling framework for engineered nanoparticles in urban aquatic systems at high spatial and temporal resolution

3.1 Introduction

Cities are centres of human activity and consequently represent hot spots of pollutant emissions. With increasing urbanization and the steady growth of the urban population (United Nations, 2014), waste and pollution issues arising from cities are becoming more important (Pal *et al.*, 2014). For example, fresh water supply and wastewater management have become compromised in fast-growing, low-income urban areas where the existing infrastructures and the receiving waters cannot cope with the rise in fresh water demand and the generation of larger volumes of wastewater (Karn and Harada, 2001). At the same time, in developed countries, new technological developments and changes in consumer preferences (i.e. development and use of novel materials) together with demographic changes (e.g. ageing and consequent consumption of larger amounts of pharmaceuticals) have raised concerns over the impacts of the so-called emerging pollutants (EPs), which will be emitted to city environments in increasing amounts in the future (Geissen *et al.*, 2015). Furthermore, freshwater availability is set to decrease across many regions of the globe due to the effects of climate change (Gosling and Arnell, 2016), and with an increase of water scarcity, lower dilution and consequently higher concentrations of water pollutants, including EPs, can be expected.

EPs are novel pollutants that are not conventionally monitored and which have the potential to enter the environment and cause adverse effects on ecosystems and human health (Geissen *et al.*, 2015). Examples of EPs include pharmaceutical residues, personal care products (PCPs), ENPs and microplastics (MPs). The appearance of PCPs in surface waters (Peng *et al.*, 2008; Brausch and Rand, 2011) and of pharmaceutical residues in wastewater, surface, ground and drinking water in and around cities has already been proven (Heberer, Reddersen and Mechlinski, 2002), and signs of adverse ecological

effects have been observed (Tijani, Fatoba and Petrik, 2013). However, for certain EPs such as ENPs and MPs, appropriate analytical methods for their detection in environmental matrices are still under development, making large-scale monitoring campaigns currently difficult or impossible (Geissen et al., 2015).

With the current expansion of the nanomaterials market (HTF Market Report, 2018) and due to the fact that ENPs are already incorporated into a wide variety of products spanning various urban sectors (industry, households, buildings, traffic, leisure activities) and are likely emitted to urban surface waters through diffuse (runoff and leaching) and point sources (wastewater treatment plants, surface water overflows) (Baalousha *et al.*, 2016), approaches to quantify local ENP emissions and exposures are needed. Currently, acceptable exposure levels of ENPs in surface waters in terms of risk are under debate, while the overall picture of ENP emissions and fate in urban environments remains unclear (Baalousha et al., 2016; Duester et al., 2014).

The inherent characteristics of urban environments differ significantly from natural environments and they represent unique reactors that will influence ENP transformation and transport. An interplay of various natural and anthropogenic factors will affect ENP emissions and fate in cities (Figure 3.1).

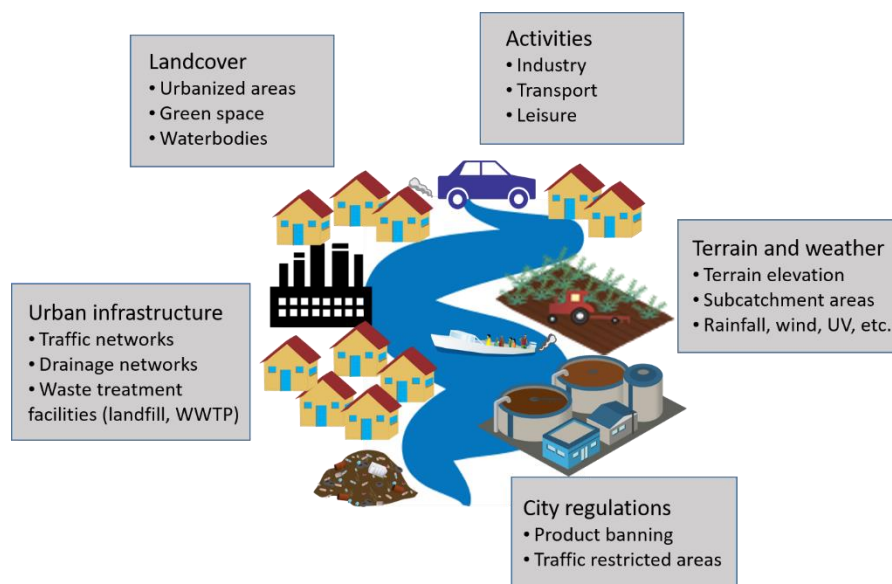


Figure 3.1. Representation of the main factors influencing the emission of pollutants, including ENPs, in urban environments

The complexity of sewage networks (with separated and combined systems), specific characteristics of wastewater treatment plants, geographical and meteorological conditions together with the variety of land cover types, predominant activities and specific regulations present in cities, need to be assessed. Temporal variations in the emissions of ENPs and exposure at the local scale are also expected due to dependencies on weather events and usage patterns; the same apply to the spatial variation of emissions and exposure. This was shown in the study carried out by Gottschalk et al.,(2011), who found high temporal and spatial variability in the local predicted environmental concentrations (PECs) determined for several ENPs and pointed out the location-time dependency for their risk assessment. More recent studies by Dumont et al., (2015) and Dale et al., (2015a) also emphasize the importance of understanding the spatial and temporal variations of ENP concentrations in surface waters.

Clearly, the estimation of ENP exposure in urban surface waters is a complex challenge and, in order to understand potential environmental impacts of ENPs in urban settings, exposure concentrations need to be assessed at high temporal and spatial resolution. To address this challenge, mathematical models emerge as powerful tools that can be used to estimate ENP emissions and environmental concentrations and provide an indication of what the environment is exposed to when experimental and monitoring data is missing (Nowack, 2017; Sani-Kast *et al.*, 2015; Duester *et al.*, 2014).

In the context of urban environments, no nanoparticle-specific models have yet been developed and several key factors are essential for performing a comprehensive urban exposure assessment. These factors need to be targeted within an integrated urban ENP model framework. Firstly, on the local scale of a city, high spatial and temporal resolution data on ENP emissions is required to account for all the source variabilities present in an urban environment (traffic, industry, leisure, etc.), as well as for the local temporal variations in emissions (weather influence, activity dynamics, etc.) and to ultimately provide highly resolved local exposure patterns. Most of the currently available ENP emission models base their emission estimations on global or regional production and usage rates (generally obtained from market reports and other peer-reviewed studies) (Keller *et al.*, 2013; Keller and Lazareva, 2014), and the dynamics of the emissions are only rarely considered (Praetorius *et al.*, 2013; Sun *et al.*, 2015). In terms of spatial resolution, the values of estimated emission volumes are usually provided as average figures per environmental compartment (natural: water, soil, air; or technical: sewage

sludge, landfill, etc.) rather than spatially resolved estimates. Secondly, the use of a bottom-up mechanistic approach for the ENP emissions is also missing as an input for existing ENPs environmental fate models. As described in Section 1.4, bottom-up models include nano-specific transport and fate process descriptors. However, they also usually rely on averaged production and emission volumes and transfer coefficients derived from MFA models (Keller *et al.*, 2013; Keller and Lazareva, 2014). In the urban context, we believe that very specific usage patterns of the ENP-containing products can be obtained and that these will influence the ENP release mechanisms and final exposure estimates. More detailed process descriptions are needed to replace the averaged transfer coefficients values used so far in MFA models. This can be achieved by developing release pathway-specific emission equations parametrized with product-specific release rates. Finally, since ENP behaviour is characterized by kinetically dominated transformation and transport processes (e.g. aggregation, sedimentation, dissolution, surface transformations) and is affected by the physical and chemical properties of the surrounding environment (surface water flow, pH, ionic content, UV exposure, etc.), a high spatial and temporal resolution of ENP fate processes is needed to account for the spatial and temporal variations in these parameters occurring within the urban environment.

In this chapter, a novel and comprehensive urban exposure modelling framework for assessing exposure to ENPs in urban aquatic environments based on a source-pathway-receptor structure is proposed (Figure 3.2). The framework uses a bottom up approach where PEC values can be derived from a detailed study of the emission, transport and fate mechanisms of ENPs contained in products used in cities. By considering all different ENP emission sources, all the identified release pathways, the temporal dynamics of those emissions, as well as the urban and environmental parameters influencing ENP fate processes, the framework presented here is able to estimate exposure at high spatial and temporal resolution. At this local scale, hot spots of emission and exposure across the city can be identified, as can the final speciation of the emitted ENPs (freely dispersed ENP aggregates or ENP attached to SPM) studied within different compartments of the aquatic environment (i.e. flowing water, stagnant water and sediment) over time.

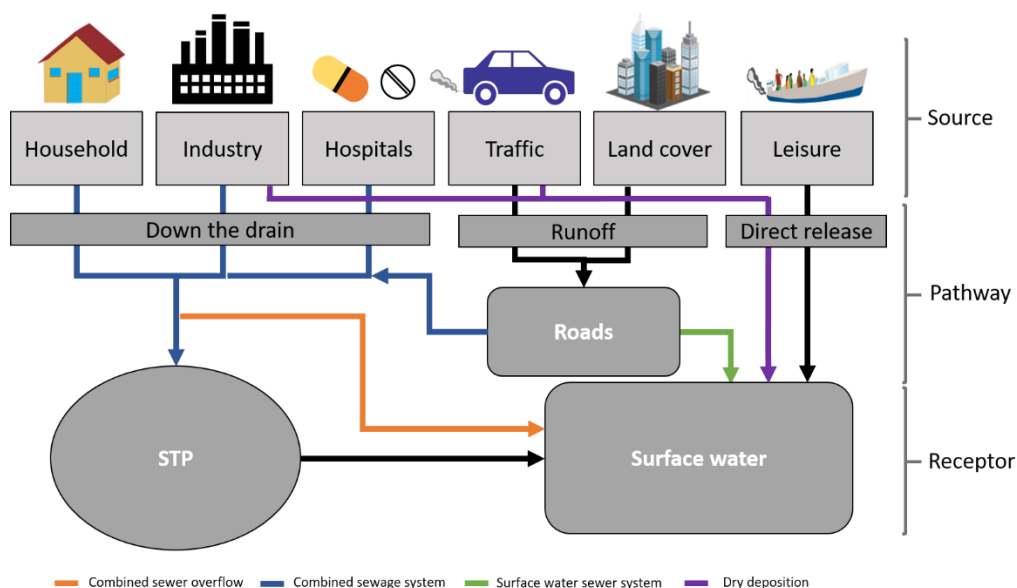


Figure 3.2. Urban modelling framework: source-pathway-receptor structure.

3.2 Model framework for ENPs in urban environments

The proposed modelling framework for estimating exposure to ENPs in urban environments brings together two separated but interconnected models:

- an **emission estimation model**, that estimates the emissions rates of specific ENP-containing products used in cities at high spatial and temporal resolution; and
- a **surface water fate model** that provides the final surface water concentrations (also in a spatially and temporally resolved way) for the parent ENPs and any transformation products (e.g. aggregates), taking into account the transport and fate processes that the ENPs undergo once released to the water compartment.

Both models employ a bottom up approach where emission equations and fate processes are based on the specific usage patterns, release pathways, transformation and transport behaviour of the ENP-containing products used within the city. The framework includes the use of monitored chemical and physical characteristics of the targeted surface water(s) in the city of interest to parametrize the fate processes. High spatial and temporal resolution is achieved using spatially resolved urban information within a geographical information

system (GIS) and local weather patterns. The proposed framework builds on four main steps (summarized in Figure 3.3) to obtain highly resolved predictions of exposure for ENPs in the urban surface water system:

1. City analysis - urban zoning and river reach delimitation: In order to obtain the required high local spatial resolution, we propose the delimitation of the surface water bodies into river reaches (or other surface water sections, e.g. for lakes) according to the location of established monitoring points, and a further subdivision of the urban area of study into sub-catchments, herecalled hydrological zones, following a similar approach as the one used by the SWAT model (Arnold *et al.*, 2012). ENP emission rates can then be obtained per hydrological zone and specific ENP exposure concentrations can be obtained for each of the connected river reaches.
2. Nano product inventory (NPI): An inventory of the currently used products containing ENPs in the studied urban area is developed and a preliminary classification is performed based on their probable sources of emission. A database with relevant information on these products (usage rates, market penetration, etc.) and the properties of the contained ENPs (size distribution, concentration, surface properties/coatings etc.) should be included in the inventory where available.
3. Emission estimation model (EEM): To obtain the ENP emission rates to each river reach, calculations based on the source of emission, release pathway and release dynamics are performed. For that purpose, the specific ENP release mechanisms from the specific product usage pattern (bottom up approach) and the emission pathway mechanisms are studied and the emission equation designed accordingly.
4. Surface water fate model (SWFM): Surface water exposure concentrations for specific ENPs in each river reach are obtained from a simulation of the fate processes that will occur for ENPs in the surface water system.

By employing this approach based on spatial information on usage and environmental parameters specific to a certain city it is possible to generate spatially and temporally explicit exposure estimations for ENPs in the studied

urban surface water system. In the next sections, the individual steps are described in more detail.

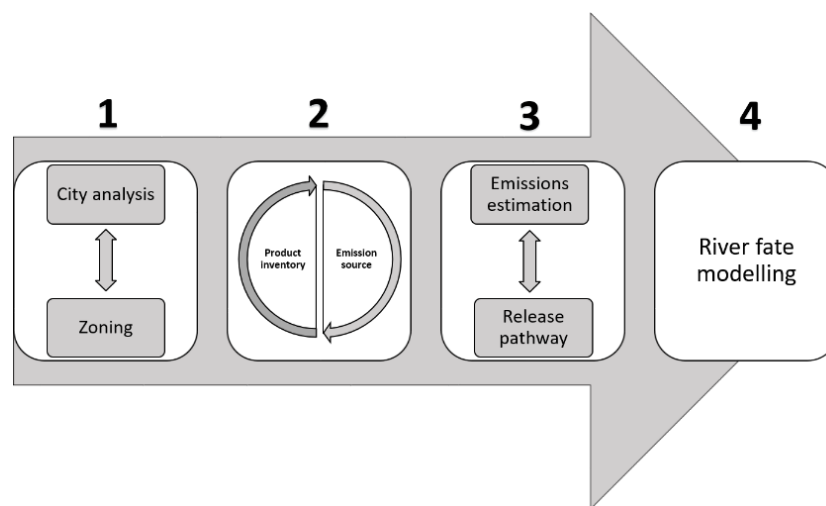


Figure 3.3. Schematic representation of model framework

3.2.1 City analysis: urban zoning and river reach delimitation

ENPs will be emitted to urban environments from point (wastewater generated in households, hospitals and industry) and diffuse sources (traffic emissions or weathering of urban land cover material, for example). By knowing the potential emission sources and their location within the studied city, and performing a spatial analysis of the area, a high spatial resolution of understanding of the emissions can be achieved and a map of estimated emissions across the city can be obtained.

We propose a subdivision of the studied urban area into so-called hydrological zones (HZs), a short of manually delimited sub-catchment areas similar to those proposed by Modaresi, Westerlund and Viklander, (2010), for the estimation of pollutants loads transport using GIS. These HZs will contain all the sections of the city's sewage network and small surface water bodies that flow into a previously defined common river reach. In this way, while ENP emissions are estimated per hydrological zone (enabling the identification of hot spots of emission within the city area), their distribution along the surface water system of the city can be modelled by indicating the specific hydrological zone-river reach connection.

The delimitation of river reaches is done based on the location of a number of monitoring stations established by the researcher's desired spatial resolution and urban characteristics. For example, in the case study presented in Chapter 4 for the city of York, monitoring stations were located upstream and downstream of each WWTP serving the city, as well as before and after the confluence of the two rivers flowing through the city (Figure 3.4). Each river reach covers a sufficient extension upstream and downstream of the monitoring station and for which homogeneous water characteristics can be assumed.

The manual subdivision of the city into hydrological zones is guided by the boundaries of determined sub-catchment areas and the extension of the drainage network covering these areas and discharging into their corresponding river reaches. Using GIS tools, by following a similar methodology as the one used by the SWAT model (Douglas-Mankin, Srinivasan and Arnold, 2010), two main data sets are analysed to provide this information: the digital elevation map (DEM) of the area (digital elevation data of the area derived from surveys carried out by remote sensing, LIDAR) and the city drainage network maps (sewage networks maps of the city containing the combined, surface and foul drainage networks, as well as combined sewer overflow (CSO) and storm water outlets (SWOs) locations). Information on the location of the waste water treatment plants (WWTPs) serving the area and their discharge points, as well as the localization of industrial activities will also guide the manual hydrological zone delimitation.

The DEM of the area provides information on the water flow directions and sub-catchment areas of the city based on the elevation of the terrain upon hydrological analysis (QGIS Grass package). This information guides the delimitation of areas of the city with confluent flows of runoff water and the identification of their discharge points (sub-catchment outlets) along the river. Additionally, since the runoff does not always follow the topography in a urban environment, but is instead redirected and transported through the man-made drainage networks (Modaresi, Westerlund and Viklander, 2010), the city drainage network maps provide further information on the connectivity of the different areas of the city to the local WWTPs and the location of CSO and SWO along the urban river system. Using both datasets, the path of the wastewater and collected runoff water can be fully tracked.

Further details of the methodology and its application to York are provided in Section 4.2.2 of Chapter 4. Figure 3.4 represents the generated subdivision for this city.

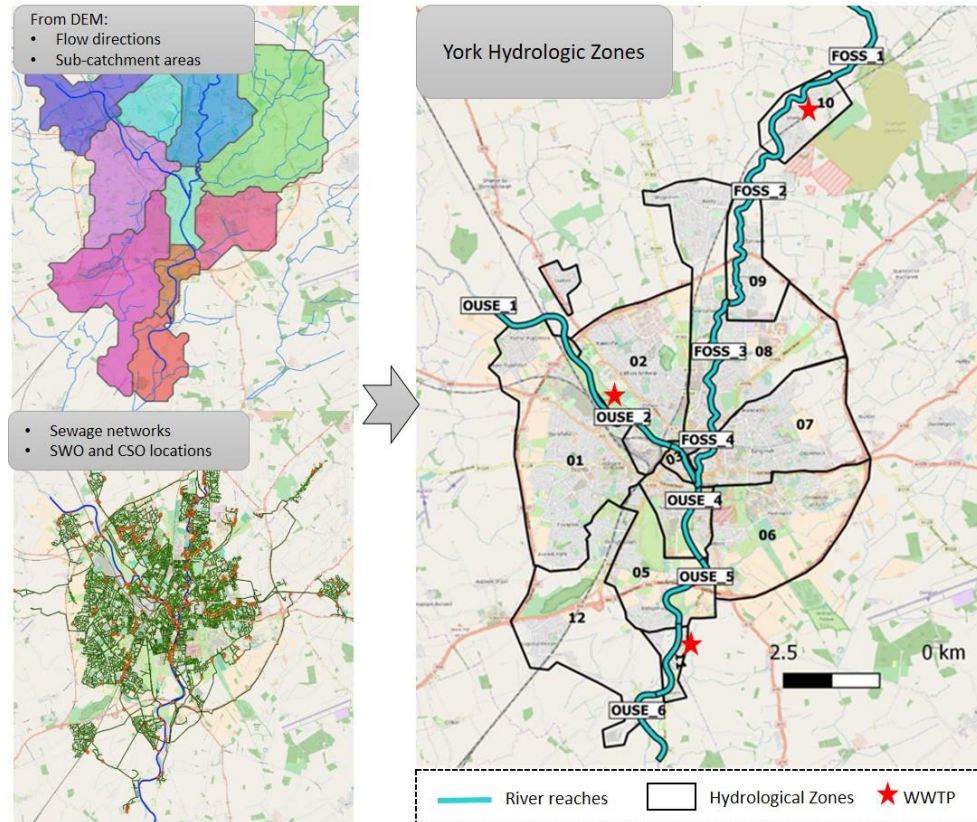


Figure 3.4. Subdivision of the York area of study into hydrological zones (HZs), delimitation of its rivers (Ouse and Foss) into river reaches (RSs) and location of the local waste water treatment plants (WWTPs)

Following this approach, ENP emission estimates can be obtained in a spatially resolved manner. For example, ENPs emitted from point sources can be tracked by knowing the specific location of the WWTP and CSO outlets (given by the water management local authorities). For the ENP emitted from diffuse sources and through runoff, the emissions' spatial distribution will depend on the terrain elevation (which determines runoff flow directions) as well as on sewer infrastructure (localization and sewer system type and capacity of the area studied).

3.2.2 Nano product inventory and classification of emission sources

In the urban context, nanotechnology is widely applied. ENPs are integrated into a wide variety of daily use products such as cosmetics, textiles, foods and paints and can be found in different outdoor urban materials such as building façade paints, wood coatings, self-cleaning glass, photocatalytic concrete pavements, and more (Baalousha *et al.*, 2016). Furthermore, urban nanotechnology is seen as a potential source of solutions for sustainable urban development: ranging from providing more resilient and durable construction materials with the potential of decreasing the urban heat-island effect (Santamouris, 2013), to contributing to the production of solar power generated by nano-photovoltaic systems (Micheli *et al.*, 2013), to improving water and air quality through the use of nano-based photocatalytic applications (Ibrahim *et al.*, 2016) or fuel combustion ENP-catalysts that reduce exhaust emissions (Selvan, R. B. Anand and Udayakumar, 2009; Wiek *et al.*, 2013).

To evaluate the urban ENP exposure, all the potential ENP emission sources must be identified. Therefore, all potential ENP-containing products commercialized and used in the targeted city need to be investigated and classified according to these emission sources. The main categories of ENP emission sources identified for urban environments are briefly presented in Figure 3.2 and explained in the following list:

- *Household*: this category includes all products used indoors that would be released down the drain together with normal wastewater. Product types within the household category include clothing, cosmetics, cleaning products and food additives.
- *Industry*: ENPs manufactured on site (depending on the industries present in the studied city) will be included in this category as well as other ENPs that might be used in industrial processes (catalysts, fuel additives, cleaning products, etc.).
- *Hospitals*: ENPs are currently used in medical applications and can consequently be released from hospitals or patients during a hospital stay or in their households.

- *Traffic*: ENP-containing products that might be released to streets and roads due to traffic (i.e. by exhaust emission and deposition) are included in this category. Examples include ENP-based fuel additives, ENPs generated due to tyre abrasion or ENP-containing products that are used for car maintenance such as car wax or car paint.
- *Land cover*: this category includes all ENP-containing products used outdoors and that will potentially release ENPs through weathering with rainfall. Examples of these products are paints and other outdoor urban coating products, ENP-containing construction materials (photocatalytic glass, solar panels, cement etc.) as well as ENPs used in novel nano-enabled agricultural technologies such as nano-pesticides and nano-fertilizers that can be used in urban gardens and road verges.
- *Leisure*: ENP-containing products that might be used during and for leisure activities such as sunscreens or boat paints fall under this category.

Table 3.1 provides a summary of the ENP-containing products most relevant to urban environments that will fall within the different emission source categories as well as the types of ENPs that can be integrated in the products. This list was developed by combining information gathered from the scientific literature and nano-product inventories such as the Nanotechnology Consumer products inventory (CPI), developed by the Woodrow Wilson International Centre for Scholars and the Project on Emerging nanotechnologies (Vance *et al.*, 2015a), and the most recent Nanodatabase (Foss Hansen *et al.*, 2016). It is worth noting that Table 3.1 not only contains products already on the market (and identifiable as containing ENPs by the Nanodatabase), but also covers potential future applications of ENPs in urban environments (e.g. within building material or in medical applications, marked in the table by *).

Table 3.1. Summary of ENP-containing products already available on the market and used in cities extracted from the Nanodatabase; and potential future applications of ENPs in urban environments identified by a literature review (*)

Emission Source	Product type	ENP
Household	Cosmetics (makeup and hair treatment)	SiO ₂ , TiO ₂ , ZnO, Carbon Black, Si, Cu
	Personal care products (toothpaste, deodorants and creams)	Ag, Au, TiO ₂ , ZnO
	Clothing	Ag, Si, ZnO
	Food additives	TiO ₂ , Cu, Zn, SiO ₂
	Sunscreens	TiO ₂ , ZnO
Industry	All product types and ENPs listed above and below	
Hospitals	Medical nanoformulations*	-
Traffic	Fuel additives	CeO ₂
	Cleaning agents	Ag, TiO ₂ , Au
	Maintenance products	SiO ₂ , Ti, Au, Ag
	Tyres (abrasion of tyres)	ZnO (Yang <i>et al.</i> , 2014), ZnS, Carbon Black (Kumar <i>et al.</i> , 2013)
Land cover	Construction materials*	carbon nanotubes, SiO ₂ , Ag,
	Paints and surface coatings	TiO ₂ , Al ₂ O ₃
	Nano-pesticides and nano-fertilizers*	TiO ₂ , Ag, SiO ₂ , Cu, ZnO
	Environmental remediation	Cu/CuO
Leisure	Sunscreens	Nano zero-valent iron (nZVI)
	Paints and surface coatings for boats	TiO ₂ , ZnO
		TiO ₂ , Ag, SiO ₂ , Cu

Once the emission sources have been identified, additional information is required for the evaluation of their relevance and quantification. Generally, the market penetration of the product (in terms of ratio of ENP-containing product available on the market vs non-nano options) and product type usage (amount of product used per capita in the selected time range) will be the two main factors to consider when estimating the relevance of various emissions in the city investigated. For example, in a southern European, coastal city, where the water leisure activities may be the main drivers of the economy, the market penetration and usage rates of products such as sunscreens will be higher than in cities with no seaside and colder weather. Therefore, for the first case the leisure source will be considered as one of the most relevant sources, while in the second city case it might not even be integrated into the emissions analysis. Other city characteristics, such as local or regional regulations regarding the specific use of certain products (i.e. banning of specific products or traffic restrictions in certain city zones), will influence the

relevance of studying certain types of ENP emissions for different cities. Also, the presence of industrial areas or urban agricultural areas (with consequent potential use of nano-pesticides or nano-fertilizers) in the city will influence the ENP emissions sources to be considered (industry or land cover sources respectively). Other information, relevant for the emission estimation calculations, such as ENP content of the product, composition and size distribution of the ENPs, will also be gathered. Some potential sources for gathering such information are discussed in the next section.

3.2.3 Emissions estimation model

Emissions of ENPs from ENP-containing products can occur during different stages of their life cycle (production, transport, use and disposal) (Keller *et al.*, 2013) and the extent of these emissions will be source and pathway dependent. A schematic representation of the emission sources and identified emission pathways to urban surface waters is summarised in Figure 3.2. The three most relevant release pathways for ENPs towards urban surface waters are i) down the drain, ii) runoff and iii) direct release.

Some experimental studies have already demonstrated ENP emissions from everyday products. For example, Benn *et al.* (2010) found that Ag ENPs integrated in toothpaste, shampoo, medical cloth and other household products were released to different extents down the drain after a 1 hour washing process in tap water. Also, in studies performed by Bossa *et al.* (2017) and Kägi *et al.* (2008), TiO₂ ENPs incorporated in building material (self-cleaning cement) and exterior paints respectively, were found in the leachate collected after simulated runoff events, leading, in the case of self-cleaning cement, to emission estimates of up to 33.5 mg of Ti/m² after 168 h of leaching. These released ENPs will be emitted to the aquatic environment (wastewater and/or surface waters) in different contexts (outdoors and indoors) depending not only on the specific usage and disposal pattern of the product, but also, in the case of outdoor use products (i.e. in traffic or land cover), on specific weather conditions (i.e. rainfall events leading to weathering of outdoor ENP-containing materials and transport of ENP deposited on the land cover of the city). At the same time, it has been demonstrated that a considerable portion of ENPs emitted with the wastewater (i.e. Ag and CeO₂ ENPs for the studies of Kägi

et al. 2011) and Limbach et al. (2008) respectively), is retained in the sludge of wastewater treatment plants. A similar process could occur for ENPs emitted with runoff, where ENPs could be retained to some extent in the impervious cover or in gully pots, through physical or chemical interactions (i.e. adsorption to concrete and/or adsorption to the retained sediment respectively). Therefore, to estimate ENP emissions to surface waters, it is not only important to consider the emissions of the ENPs from the source, but also the pathway that the ENPs follow once released from the product to the surface waters (that will determine the retention rates), and the weather conditions that trigger such emissions (in the case of runoff emissions). To estimate emissions of ENPs to surface water for each of the three identified release pathways we have developed the following generic equations as a function of time:

- Down the drain (wastewater) emissions:

$$WW_{Emiss}(t) = [P_{Emiss}(t) \cdot F_{WWTP}(t) \cdot (1 - c_{Ret}) + P_{Emiss}(t) \cdot (1 - F_{WWTP}(t))] \cdot T_{lag}(t) \quad (3.1)$$

- Runoff emissions:

$$RO_{Emiss}(t) = P_{Emiss}(t) \cdot (1 - c_{Ret}) \cdot T_{lag}(t) \quad (3.2)$$

- Direct release emissions:

$$D_{Emiss}(t) = P_{Emiss}(t) \cdot T_{lag}(t) \quad (3.3)$$

where P_{Emiss} represents the rate of emitted ENPs from the product for the time step simulated (t) (e.g. mg day^{-1}); F_{WWTP} is the fraction of the generated sewage that is directed to the corresponding WWTP on the day simulated, this factor can vary over time depending on the weather conditions (i.e. in days of heavy rainfall the sewage water network capacity might be surpassed and a fraction of the waste water will be discharged to the rivers through CSOs without treatment, being $F_{WWTP} < 1$); c_{Ret} is the ENP retention coefficient (or removal fraction in a WWTP) which the ENPs are subject to depending on the release pathway followed (down

the drain, runoff or direct release); and T_{lag} is a factor that considers the delay in the ENP emissions between the use of the product and ENPs release and their actual discharge into the surface waters. T_{lag} is measured in the same units as the time scale chosen for P_{Emiss} (e.g. days).

A more detailed explanation of the variables in equations 3.1, 3.2 and 3.3 is provided in the next sections.

3.2.3.1 Rate of ENP emissions from the product (P_{Emiss}).

The bottom up approach proposed for this modelling framework establishes a detailed quantification of the emissions of ENPs from products based on specific usage and disposal patterns. For this purpose, the following formula for the estimation of ENP emissions over time (t) was established:

$$P_{Emiss}(t) = C_{ENP} \cdot U_{prod}(t) \cdot F_{pen} \cdot R_{Release}(t) \quad (3.4)$$

where C_{ENP} is the concentration of the ENP in the product (i.e. $mg\ kg^{-1}$), U_{prod} is the amount of product used per capita (pc) on the simulated time step (t) of the model (e.g. $kg\ pc^{-1}\ day^{-1}$), F_{pen} is the market penetration of the ENP-containing product (estimated as the fraction of that product's market that contains ENPs), and $R_{release}$ is the product-specific release rate at time t (percentage of ENPs emitted from the total ENP content in the product).

The value of C_{ENP} can be obtained either from the product manufacturer (as done by Tiede et al. (2016) or from chemical analysis of a product (Tulve *et al.*, 2015); the value of F_{pen} can be obtained from sources such as consumer product surveys (such as surveys performed by Tiede et al. (2016) or Zhang et al. (2015)), manufacturer's surveys and market reports (e.g. Future Markets 2012 used by Keller and Lazareva (2014)). The values of U_{prod} can be estimated either by the use of technical guidance documents (such as the (TGD, 2003) used by Tiede et al. (2016)) or obtained through consumer surveys (Keller *et al.*, 2014a); or by the use of product-specific equations based on product usage patterns. Finally, $R_{release}$

can be obtained from experimental studies (Bossa *et al.*, 2017) or from manufacturers (i.e. ageing and end of life experiments). Some examples of equations for estimating the U_{prod} for a selection of product types and their corresponding R_{release} are presented in Table 3.2. The meaning and the units of these factors will vary depending on the product type and the information available.

Table 3.2. Examples of estimation of product usage (U_{prod}) and release rates ($R_{Release}$) for different ENP-containing product types. The meaning and the units of these factors will vary depending on the product type and the information available.

Product type	U_{prod} (mass or volume of product/time)	$R_{Release}$
Cosmetics and personal care products	$= U \cdot Pop$ U : usage per capita per day Pop : population of the area studied	=fraction of ENPs released from the specific product during usage. (i.e. as worst case scenario 100% of the contained ENPs would be released so $R_{Release} = 1$)
Fuel additives	$= F_j \cdot N_j$ F_j : fuel consumed (L) per vehicle type (j) per day, N_j : average number of vehicles of type j circulating in the area studied per day;	= fraction of ENPs released from the specific product during usage (in this case percentage of fuel additive that escapes from the exhaust)
Maintenance products	$= U \cdot SA_j \cdot N_j$ U : product usage per day per surface area of material exposed SA : surface area covered by the product per vehicle type (j) N_j : average number of vehicles of type j circulating in the area studied per day	= fraction of ENPs released from the product
Construction materials	$= U \cdot SA / \tau$ U : mass of product used per surface area of material exposed τ : number of days of exposure of the product, in this case lifetime of the construction material (i.e. 10 years, $\tau = 3650$ days) SA : building facades surface area exposed to weathering	= fraction of ENPs released from the product during its lifetime
Paints and surface coatings	$= U \cdot SA / \tau$ U : product usage (in mass or volume) per surface area of material exposed SA : building facades surface area exposed to weathering τ : number of days of exposure of the product, in this case frequency of facade painting (i.e. once every six months, the paint will be exposed and the ENPs released through 6 months, $\tau = 182$ days)	= fraction of ENPs released from the product during its lifetime

In the study performed by Tiede et al. (2016), data was available for 126 ENP-containing products commercialised in the UK., Quantitative information for C_{ENP} , U_{prod} and F_{pen} for 62 of them was found from similar information sources. For example, for cosmetics containing SiO_2 ENPs, the C_{ENP} value was found from the manufacturer's information (labelling) as 15% of the cosmetic composition. Usage was estimated as 0.8 g of product per capita per day by following the TGD (2003), and F_{pen} was estimated through the use of a local product survey where the number of nano-containing products was divided by the total amount of products (nano and non nano) available on the same market (0.5% of the skincare market).

3.2.3.2 Lag time (T_{lag}).

ENP emissions to surface waters do not always occur straight after product usage in terms of time, but instead they can be released over time or in specific moments over time (Sun *et al.*, 2017). Therefore, a factor that integrates this time dependency into the estimation of ENP emissions has to be adopted if temporal resolution in exposure is to be obtained.

In this modelling approach emission's variability over time is presented by factoring the time dependency of the ENPs usage, release and removal (i.e. through U_{prod} , R_{Release} and F_{WWTP}), and also by using a factor, here called lag time factor (T_{lag}), that indicates if the ENPs are emitted into the surface waters on the time step simulated and in which proportion. This factor is release-pathway dependent. For example, in emission processes that are triggered by rainfall (mainly the ones emitted through weathering of surfaces), during a dry day no emissions would happen and T_{lag} would have a value of 0, whereas on a rainy day T_{lag} would acquire the value of 1 to indicate that the emission is taking place. In the case of traffic emissions however, in a dry day, emissions still happen (mainly to the atmosphere) and ENPs are deposited (accumulated) on urban surfaces through dry deposition but not discharged in the surface waters until the actual runoff emission occurs during a rain event. In this case, T_{lag} would have a value of 0 on the dry day to indicate no discharge, but will be equal to 1 + the number of preceding dry days (accumulation days), on the day of the rain event. Furthermore, the determination of the T_{lag} factor in the case of atmospheric emissions could be refined by using atmospheric particle transport models. Kumar et al. (2011), present a review on the

different available dispersion models that address the dynamics of ENP dispersion in the atmosphere where lag time can be extrapolated from (Kumar *et al.*, 2011). Finally, for down the drain and direct release emissions, T_{lag} would again indicate if emissions happen ($T_{lag} = 1$) or not ($T_{lag} = 0$).

To quantify this second pathway explicitly, temporal variations can, therefore, be integrated within the model by means of T_{lag} , and the determination of its values will usually be weather-dependent. Local water management authorities would be therefore a key information source to establish T_{lag} values.

Alternatively, higher time resolution could be implemented if desired and if permitted by the computational power, depending on the data availability. For example, ENP emissions could be reported per hour if data on hourly usage and release is available (e.g. hourly traffic data can provide hourly emissions and hourly weather data provide T_{lag} in hours). Also, as mentioned in Section 3.2.3, ENP's WWTP removal can vary over time, also in association with the weather patterns (and reflected through the use of FWWTP), which can be also integrated if the information needed is available (i.e. sewage network capacity threshold and rainfall pattern).

3.2.3.3 Retention coefficient (c_{Ret}).

Once released, the pathways of ENPs towards the surface waters will determine the c_{Ret} to be applied in the emission estimation calculations. As pictured in Figure 3.2, ENPs emitted from point sources (households, industry and hospitals) will be discharged down the drain into surface waters via WWTPs. When ENPs follow this pathway a c_{Ret} factor must be applied based on the removal efficiency for the specific ENP and type of WWTP in place. Alternatively, whenever the sewage system in place is a combined system and a sewer overflow occurs, a fraction of sewage water ($1 - F_{WWTP}$) is directly discharged into the rivers via CSO without passing through the wastewater treatment facilities and consequently no c_{Ret} is applied. ENPs emitted from diffuse sources (traffic, land cover and leisure) will enter surface waters either via SWOs from separate surface water systems, and/or via CSO from combined sewer systems, or through direct release (in the case of leisure activities sources). As previously stated, the pathway of emission will

determine the c_{Ret} that applies to the ENPs as well as their spatial distribution. The c_{Ret} identified for the three established release pathways are summarised in Table 3.3.

Table 3.3. Retention coefficients for the three ENP release pathways

Pathway	c_{Ret}	Description
Down the drain	c_{stp}	The WWTP removal efficiency for the specific ENP and type of WWTP in place
Runoff	c_{road}	Road retention efficiency for the specific ENP
Direct release	-	No retention processes happen in this case

The values for each c_{Ret} will need to be obtained from experimental studies, if available, and will be ENP specific.

3.2.4 Surface water fate model

While the emission estimates serve to quantify ENP loads towards urban surface waters, environmental fate processes will determine the final concentration and distribution of ENPs within the water bodies (Figure 3.5). Furthermore, the environmental impact and health risks associated with exposure to ENPs will be strongly affected by the “form” in which the ENPs are present, i.e. whether they are freely dispersed, homo- and/or hetero-aggregated, dissolved or whether they have undergone transformations of their surface or surface coating. ENP concentration and form, as described in Section 2.4, will be determined by processes such as homo- and heteroaggregation, photochemical transformations, oxidation and reduction, dissolution, precipitation, adsorption/desorption of macromolecules, biotransformation among other biogeochemically driven processes (Nowack *et al.*, 2012). Many environmental factors, biotic and abiotic, play important roles in these transformation and transport processes: Ionic strength and composition, pH, water hardness and the presence of dissolved organic matter and suspended particulate matter (SPM) will alter aggregation and transformation processes and are expected to ultimately influence ENPs toxicity by altering their

availability for uptake and distribution within organisms, and via interactions with other pollutants (Handy, Owen and Valsami-Jones, 2008).

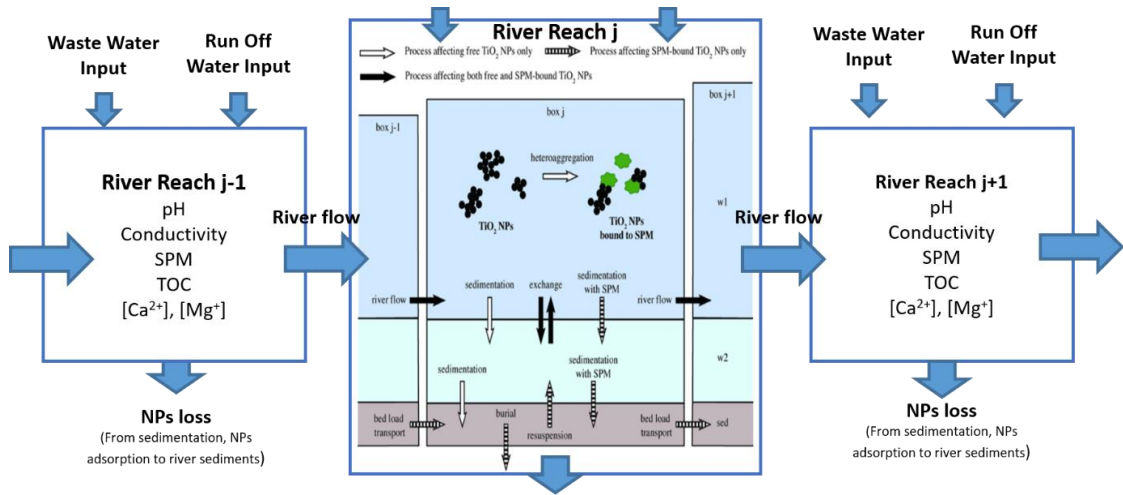


Figure 3.5. Schematic representation of the ENP transport into, out of and throughout the defined river reaches and fate processes inside the river system. Source: adapted from Praetorius, Scheringer and Hungerbühler (2012).

To account for the importance of environmental fate processes on the final exposure estimates of ENPs a comprehensive model framework for ENPs in surface waters needs to integrate a mechanistic river model where relevant transport and fate processes such as advective transport, sedimentation, resuspension, hetero-aggregation and dissolution of ENPs are simulated at high spatial and temporal resolution.

An approach to yield this level of temporal and spatial resolution in river basins was presented by Warren et al. (2005). They proposed a flexible approach for simulating the behaviour of chemicals in river basins based on the use of a connectivity matrix describing the river system. The connectivity matrix was built based on a number of segments in which the basin had been divided, and each of the matrix cells would be characterised with the properties of the corresponding segments (i.e. lengths, volumes and flow rates). Information on the connectivity between them was also provided. In this way a tailored spatial resolution was achieved (Warren et al., 2005).

A similar approach, based on a modular multimedia-box model, but that also includes nanoparticle-specific process descriptions for water and sediments, was developed by Praetorius et al. (2012). Here we proposed the use of such model to be directly linked to the emission estimation model. This river model can be easily adjusted and parameterised to represent the properties (e.g. dimensions and discharge) of the specific river(s) of a given city. In the model, spatial resolution is provided by the subdivision of the model into individual boxes, each of which is divided into three compartments (stagnant and flowing water compartments and sediment compartment). This model approach takes into account ENP-specific properties (composition, size, density, attachment efficiencies for aggregation etc.) to parametrise their fate processes in an aquatic medium. Variations in aquatic properties (discharge, water depth, pH, water composition etc.) can be included by subdividing the river model into individual sections of distinct conditions. For optimal parameterization of the model, we recommend to accompany the model development with local monitoring campaigns of surface waters to provide actual data on the key water parameters (e.g. pH, conductivity, ion concentration and concentrations of dissolved organics and suspended solids) which will affect the fate and distribution of ENPs around the surface water system of the city.

3.2.5 Challenges in model parametrization

As seen throughout the modelling framework description, a significant amount of data is required for full parametrization of the modelling approach. Table 3.4 summarises examples of data that could feed into each of the modelling framework steps, as well as some potential data sources.

Table 3.4. Summary of potential parametrization data and sources for the modelling framework

Framework steps	Related data	Sources
1. City analysis	Surface water distribution, flow directions, catchment areas (digital elevation maps, surface water maps)	Governmental geographical or environmental agencies (e.g. USGS, EEA, EPA, etc.). National or regional mapping agencies (i.e. Ordnance Survey)
	Urban waste water and surface water distribution and connections with surface water bodies (city drainage network maps, WWTP and CSO locations)	City council urban planning department or local water management companies (e.g. Yorkshire Water Ltd.)
	ENP emission source locations and distribution in the studied area (location of Industrial areas, WWTPs, traffic networks, leisure areas, etc.)	City council urban planning department, open source city council resources (e.g. YorkOpenData) and/or regional mapping agencies (e.g. Ordnance Survey)
2. NPI	List of commercialized ENP-containing products	Online nano-product inventories (i.e. CPI(Vance <i>et al.</i> , 2015a), Nanodatabase (Foss Hansen <i>et al.</i> , 2016)), commercial, consumer and industrial surveys (Dimitroulopoulou <i>et al.</i> , 2015) and market studies (i.e. Global Nanotechnology Market Outlook 2022 (Markets, 2015))
	ENP-containing products information (C_{ENP} , U_{prod} , F_{pen} , $R_{Release}$)	Manufacturer specifications, technical guidelines (TGD, 2003), consumer (Dimitroulopoulou <i>et al.</i> , 2015) and market surveys, market reports (Markets, 2015) When no data is available usage rates can be extrapolated from life cycle assessment studies (e.g. usage of ENP contained in fuel additives can be estimated from traffic data and vehicle performance as specified in Table 2)
	ENP characteristics (size distribution, surface/coating properties, etc.)	Manufacturer specifications, patent registry or in situ lab analysis of the product
3. EEM	Release rates from products or applications	Experimental studies (i.e. release of TiO ₂ ENPs from paints (Kaegi <i>et al.</i> , 2008), release of CeO ₂ ENPs from fuel additives application (Batley <i>et al.</i> , 2013))
	Sewage fraction to go to connected WWTP (F_{WWTP})	Local water management companies (e.g. Yorkshire Water Ltd.)

	Retention coefficient (C_{Ret})	Experimental studies (e.g. Kaegi et al. 2011(Kaegi <i>et al.</i> , 2011) and Limabch et al. 2008 (Limbach <i>et al.</i> , 2008))
	Lag time (T_{lag})	Local water management companies, local weather stations (e.g. Yorkshire Water Ltd.) and ENP dynamic atmospheric transport models (Kumar <i>et al.</i> , 2011)
4. SWFM	Water parameters (pH, flow, ionic strength, etc.)	Water quality monitoring campaigns (environmental agencies or performed independently)
	ENP characteristics (size distribution, composition, etc.)	Product specifications from manufacturers, or product analysis

The model parametrization is indeed one of the biggest challenges in exposure modelling (Nowack, 2017). This is because experimental data is often scarce or missing, especially in the case of emerging pollutants, such as ENPs, that are not conventionally monitored or regulated. To date, solely some nano-specific provisions in product-centric regulations (e.g. EU cosmetics, food information and biocide regulations) for products containing nanomaterials exist (Bowman, van Calster and Friedrichs, 2010; Amenta *et al.*, 2015). However, uniformity in ENP regulations in terms of product labelling and notification requirements is still lacking, which makes the estimation of ENP emissions, based on production and usage volumes, hard to perform.

New strategies, therefore, have to be found in order to bridge these data gaps. Some strategies are described within this modelling framework, where we propose the use of a bottom up approach for the determination of usage and release rates at the local level (Table 3.2). Local data, such as traffic patterns for the estimation of ENP-traffic related emissions, or local weather information for the estimation of local release rates of ENPs imbibed in materials exposed to weathering such as outdoor paints, are more easily accessible and accurate than using average ENP production estimates and steady-state release coefficients for example.

Additionally, it is worth noting that one of the advantages of modelling is its flexibility in terms of scenario analysis. In this sense, different tiers of assessment are always possible. For example, one could start with a rather rough estimation, using market data for consumption and averaged environmental conditions and later move to a more refined assessment (as data becomes available), using data collected specifically for the given city through the use of local consumption surveys and local water monitoring data. These different tiers can be assessed at different resolutions, both, in terms of space and time.

3.3 Conclusions

The modelling framework here presented has been designed to serve as a guide for estimating exposure of urban environments to ENPs. Taking into account the complexity of such systems and the level of local resolution targeted, it is worth pointing out that the precision of the PECs estimated will highly depend on the data availability and quality for the city studied. Our framework proposes an integrated

methodology to follow but has been designed in a highly flexible way so that it can be adapted to various types of cities and be workable for different levels of data availability. Furthermore, this urban modelling framework can be easily adjusted to other types of emerging pollutants, being particularly suited for other particulate contaminants such as microplastics. The modular nature of the framework makes it very versatile in terms of its inherent flexibility to integrate additional modules or release pathways that have not yet been identified but that could become relevant in the study of other emerging pollutants.

Chapter 4

Modelling spatial and temporal trends of ENP emissions in York (UK)

4.1 Introduction

As previously discussed in Chapter 3, there are many industrial and domestic applications of nanoparticles, many of which can result in emission to the environment. This chapter builds on this by presenting the application of the proposed modelling framework to predict the spatial and temporal trends of ENP emissions in a city case study (York, UK).

Within cities there are two types of emission sources (i.e. point source and diffuse source) that create spatial variability. Point sources are concentrated and have recognizable sources with specific locations from which pollutants are emitted. The main point source of emission in urban environments is the discharge of treated effluent from the WWTP, or untreated when coming from a sewer overflow (Taebi and Droste, 2004). Diffuse sources (also called non-point sources) on the other hand, don't have a concentrated localization within the city but allow particles to be deposited in such a way that rainfall induced runoff can carry them into natural surface water systems (Zoppou, 2001). Examples of diffuse emission sources are vehicle exhausts and vehicle wear, soil erosion, construction material and coatings erosion (Zoppou, 2001). The combination of these emission sources will result in unique spatial profiles for individual cities.

Additionally, the emissions generated from the aforementioned sources will vary over time due to their associated release pathways. Point sources usually follow a down the drain emission pathway (e.g. ENPs contained in personal care products, textiles, cleaning products, etc.), and can be either released continuously or with some sort of seasonal pattern with wastewater effluent. Diffuse emissions usually happen through a runoff pathway (i.e. emissions triggered by rainfall) and are highly time variable, causing repeated and intermittent pulses of pollutants reaching surface waters (Ashauer and Brown, 2013). Examples include the leaching of ENPs from ENP-containing outdoor coatings during rainfall (Zuin *et al.*, 2014), or the runoff of traffic-associated releases of

CeO₂ ENPs contained in fuel additives (Johnson and Park, 2012). Temporal and spatial resolution are therefore important aspects in the description of emissions in cities.

To cover these temporal and spatial aspects related to ENPs emissions and the complexity of the urban composition, a high-resolution approach, such as the one proposed in Chapter 3, is needed. With this approach, a full characterization of the city is performed from a bottom up perspective (from the source to the receptor) where natural and anthropogenic factors are accounted for when estimating ENP emissions. This approach recommends the evaluation and prioritization of the most relevant emission sources (i.e. ENP-containing products) within the targeted city. Thus, a local characterization of the chosen emission sources regarding their usage is proposed. Finally, an analysis of the release pathway is envisaged using the determination of relevant source characteristics (e.g. composition, market penetration, etc.). This would be augmented by accounting for the interplay of the various natural (weather patterns, land cover composition, etc.) and anthropogenic (drainage networks, waste water treatment facilities, etc.) aspects of the city influencing ENP discharge. For example, outdoor paints and coatings are exposed to variations in weather conditions (i.e. different intensities of rainfall, sunlight or changes in temperature), so weather factors will determine the extent of emissions and will have to be accounted for.

In this context, and with the objective of proving the usefulness of the proposed modelling approach in deciphering the temporal and spatial ENP emission trends in a city, the model was applied to characterize ENP emissions in the city of York. Temporal and spatial variations in emission sources and their contributions to total ENP loads in York's river system were investigated. This included identifying the main emitting areas (hot spots) and the conditions under which emissions are expected to be highest.

A variety of ENP types, emission sources, and different emission pathways have been covered. These included several personal care products (sunscreens, makeup and toothpaste), land cover material (outdoor paint) and a potential traffic emission source (fuel additives). The emission pathways studied were down the drain (for the personal care products) and run off (for the land cover and traffic sources) and three different ENP types were investigated (TiO₂, Ag and CeO₂ ENPs).

4.2 Methods

The calculations of ENP emissions in York were performed using a script written in Matlab software (MATLAB ver. R2018a), that integrates the spatial and temporal information on ENPs usage and release in York in form of excel spreadsheets. This script calls to each specific input to be loaded according to the case study and scenario chosen and performs the emission calculations in loop per day and HZ, according to the established emission-pathway equations (Figure A.1.1 of the Appendix).

4.2.1 Description of the study area

The area selected for this study was the urban area of the city of York, located in the northeast of England (latitude of 53°96'N and longitude of 1°09'W). York was chosen as it integrates the complexity of an urban system (with a network of bus lines, a train station, a central historical area, two universities and some industries), but is a manageable size for exposure analysis investigations where information such as traffic loads, sewage system networks or local weather, are needed. York covers an area of 271.9 km² and in 2016 had a population of 216721 inhabitants. York is located at the confluence of two rivers, the River Ouse and the River Foss, which run in a southerly direction and which are fed by a number of differently sized tributaries. Three WWTPs serve the area (Rawcliffe, Naburn and Walbutts). The area modelled in this study was bounded by the city's outer ring road which surrounds the main urbanised zones (where most of the bus lines and major traffic concentrates) but also includes the major adjacent municipalities of Strensall, Poppleton, Haxby, Bishopthorpe and Naburn, which fall outside the ring road. This selected area comprised approximately 40.7 km² of built surface (i.e. excluding the areas covered by gardens and other green extensions). The modelled area was chosen so that all population served by the three named WWTPs were included.

The WWTPs of Rawcliffe and Naburn emit treated effluent into the river Ouse to the Northwest and South of the city, respectively, and the WWTP of Walbutts discharges into the river Foss to the North East of the city (Figure 4.1). Information on the population served by each WWTP was obtained from Yorkshire Water Services Limited.

4.2.2 York Hydrological zones and river sections

The study area, following the city analysis method proposed in Section 3.2.1, was subdivided into 10 river reaches or river sections (RS) and 12 sub-catchment areas, the so-called hydrological zones (HZs), by using the Open Source Geographic Information System QGIS 2.18.13 with GRASS 7.2.1 software. The river sections were selected to include sections located upstream and downstream of the three WWTPs serving the city as well as before and after the confluence of the two rivers in the city centre (Figure 4.1) thus providing sufficient spatial resolution to account for potential water quality changes along the modelled area.

Three sets of information guided the manual delimitation of the HZs. Firstly, information on the extension and flow directions of the drainage networks of York and its outlets locations was obtained from Yorkshire Water Services Limited. Maps of the combined, surface and foul drainage networks serving the city, as well as the locations of the CSOs and SWOs were provided. The foul water network is designed to carry contaminated water from households to WWTPs whereas the surface water network carries streets runoff water to local streams, rivers or soakaways via SWOs. The combined network, which mainly exists in old parts of the city (city centre), takes both foul water and surface water to the WWTPs, but whenever there is an overflow it will discharge to the rivers directly via a CSO. Using the spatial analysis tool `v.net.alloc` from the Grass GIS package, which allocates subnets (i.e. sections) of a network to selected nearest centers, was used to identify the portions of the surface and combined drainage system (i.e. subnets) discharging into the SWOs and CSOs located in the previously established RSs of interest. In this way 10 subnets were distinguished along the study area of the city of York one per RS (Figure 4.1.c).

Secondly, Lidar Digital Terrain Model (DTM) data at 1 m spatial resolution was obtained for the York area from the online map and data delivery service Digimap (OS MasterMap. Accessed: Feb 2018). The DTM was analyzed using the QGIS Grass hydrologic modelling tools to obtain the dominant flow direction for each 1 m cell and to identify the drainage basins of the area. Firstly, the function `r.fill.dir` was used to remove all topographic depressions and flat areas. Then, the newly generated elevation raster map was analyzed with the watershed function (`r.watershed`) to generate an accumulation

raster map, a drainage direction raster map, a stream segments raster map and finally the basins raster map (Figure 4.1.a).

Finally, the map of the delimited WWTP catchment areas was also plotted (Figure 4.1.b) to visualize their extension over the area of interest. The results from these two analyses (the drainage basins map and the subnets map) and the extension of WWTP catchment areas, guided the manual delimitation of the 12 HZs. Each HZ was set to cover the area delimited by the boundaries of the obtained drainage basins, but that will, at the same time, coincide in some extent with each of the overlapping subnets extension (Figure 4.1). The new shape file of the HZs was created in QGIS with the manual editing tool Toggle Editing. Each HZ may be connected to more than one outlet that drains into a common RS. A total of 12 hydrological zones connected to the 10 established RS, were created (Figure 4.1). The list of connexions between HZs, RSs and WWTPs is presented in the Table A1.1 of the annexes.

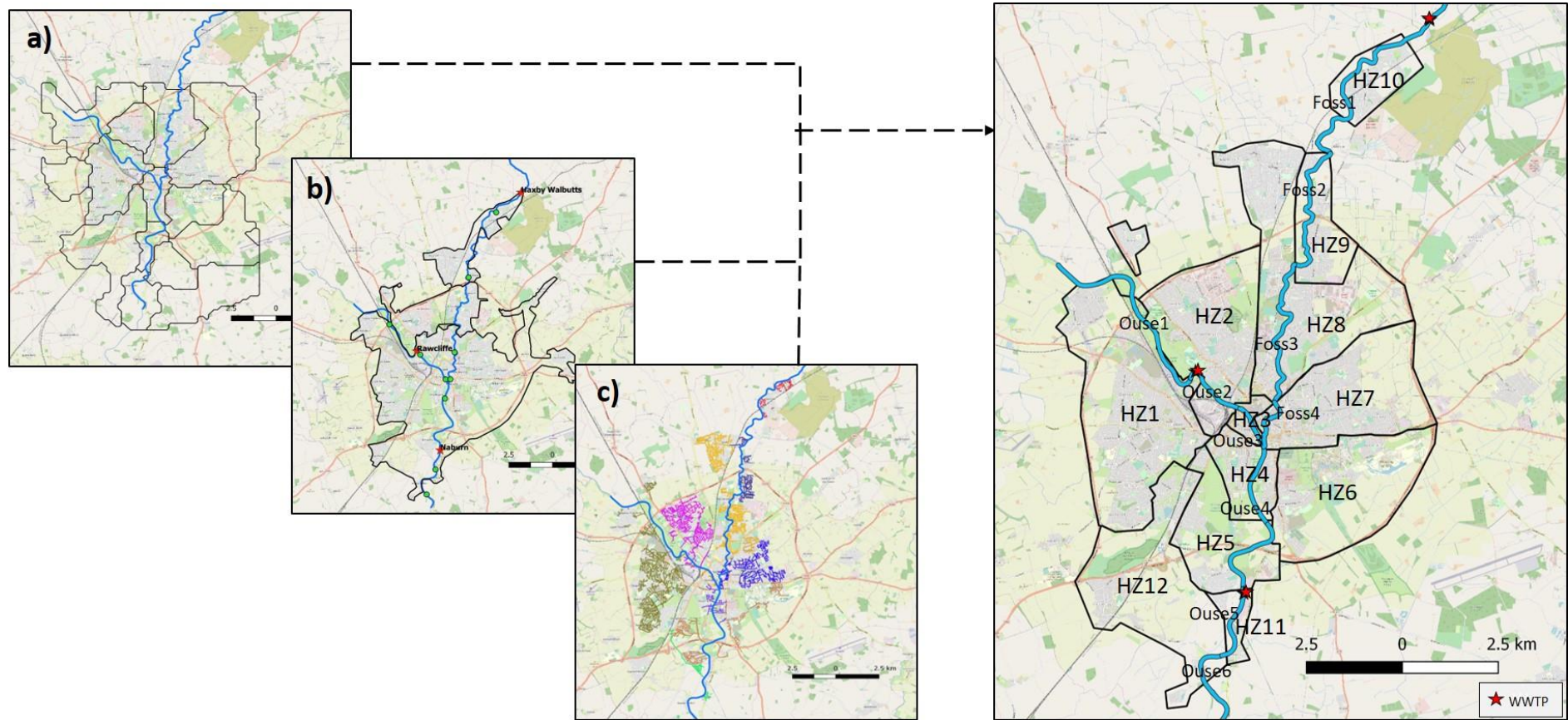


Figure 4.1. Delimitation of HZs for York with a) delimited basins areas; b) WWTP catchment areas and c) drainage subnets allocated to the delimited river sections. d) Constitutes de final delimitation of the 12 HZ of York with the WWTP located with the red star and the delimited RS in blue.

4.2.3 Definition of case studies

Several different ENP-containing product types were chosen as case studies, namely sunscreens, cosmetics (toothpaste and makeup), fuel additives, outdoor paint and textiles. These were selected to cover a variety of different city emission sources (i.e. vehicle emissions, paints and coatings, personal care products and clothing) and two different emission pathways (run off and down the drain). The case study products were selected based on the results of previous prioritisation exercises by Tiede et al. (2016) and RIVM (Wijnhoven, Dekkers and Hagens, 2009). Both exercises identified cosmetics and sunscreens to have a high potential to enter surface waters through down the drain emissions, due to the high usage rates and high market penetration of those products as well as the incorporation of the ENPs in liquid suspension. Also, coatings (e.g. exterior paints) and products labelled as automotive products (mainly fuel additives), were classified in the top of their rankings, having high probability of being released through run off processes to surface waters. In terms of the nanomaterials considered, nano-CeO₂, nano-TiO₂ and nano-Ag were chosen, as these materials are the most commonly present in the studied products. Table 1 summarizes the chosen case study by ENP type, and ENP product types, emission sources and pathways covered in this study.

Table 4.1. List of studied ENPs, their investigated product applications, source and pathway of emission.

ENP Type	Product (case study)	Source of emissions	Emission pathway
CeO ₂	Fuel additives	Traffic	Runoff
TiO ₂	Outdoor paint	Land cover	Runoff
	Makeup	Household	Down the drain
	Toothpaste		
	Sunscreen		
Ag	Outdoor paint	Land cover	Runoff
	Textiles	Household	Down the drain
	Toothpaste		

4.2.4 Emissions model framework

ENP emissions from the ENP-containing products studied were estimated using a model written in Matlab that integrates tailored emission estimation equations for the two urban emission pathways here explored (run off and down the drain) and for the different product types studied (cosmetics, fuel additives, paints and textiles). A detailed description of the emission pathways, the emission estimation equations and the required inputs is provided in Chapter 3. Those required inputs are case study and product type dependent, and in some cases (i.e. U_{prod}), can also vary spatially. They comprise the concentration the ENP in the product (C_{ENP}), the amount of product used per capita over the time step of the model (U_{prod}), the market penetration of the ENP-containing product (F_{pen}), the product-specific release rate ($R_{release}$), the ENP retention coefficient (C_{ret}), the corresponding lag-time factor (T_{lag}), and the fraction of the generated sewage that is directed to the corresponding WWTP (F_{WWTP}). The input information was integrated in a database in form of Microsoft Excel spreadsheets. This model was built to perform calculations of ENP emissions in loop for each day of an established calendar for the time period simulated and per HZ and RS, by following a series of commands structured as presented in Figure A4.1 of the Annexes.

4.2.5 Model parametrization and assumptions

To parameterise the model for the different case studies, input information was obtained from different sources such as published literature, technical guidelines, consumer surveys and local information of weather and traffic patterns of the city and the extension and composition of its urbanised areas (i.e. type of buildings, building dimensions, etc). The specific sources of information used to parametrise the different case studies are described in the following sections and listed in Table 4.2 as well as in the Appendix A1.2. From this information a maximum, minimum and an average emission scenario were generated and the summary of all inputs for all case studies and their three scenarios are summarized in Table 4.2. Full details on the criteria followed for the selection of these input values are presented in the Appendix A1.2 (Table 4.2, 4.3, 4.4 and 4.5 for C_{ENP} , F_{pen} , $R_{release}$ and Usage respectively). The approach followed for the estimation of U_{prod} for each case study is presented in Table 4.2.

Table 4.2. Equations of product usage (U_{prod}) estimation for the different product types studied.

Case study	U_{prod}
Fuel additive	$= \sum_{j=0}^j F_j \cdot N_j$ <p>F_j: fuel consumed (L) per vehicle type (j) per day, N_j: average number of vehicles of type j circulating in the area studied per day</p>
Outdoor paint	$= U \cdot SA$ <p>U: product usage (in mass or volume) per surface area of material exposed SA: building facades surface area exposed to weathering</p>
Sunscreen, makeup, toothpaste, textiles	$= U \cdot Pop$ <p>U: usage per capita (pc) per day Pop: population of the area studied</p>

Table 4.3. Summary of selected values of model input parameters (ENP concentration in the product (C_{ENP}), market penetration of the product (F_{pen}), ENP release rate from the product ($R_{release}$), ENPs retention coefficient (C_{ret}) and product usage (Usage)) for the maximum (Max), minimum (Min) and average (Ave) scenarios. The values for the parameters of the Ave scenario were estimated as the arithmetic mean of the Max and Min.

Case study		C_{ENP}	F_{pen} (market share) ^(g) (%)	$R_{release}$	C_{ret}	Usage
Fuel additive- CeO ₂	Max	7.5×10^{-6} kg/L ^(a)	100 ^(g)	5% ^(a)	0*	HZ specific U_{prod} (estimated based on performance and daily distance travelled) in L of total fuel combusted per day
	Ave	6.25×10^{-6} kg/L		3%		
	Min	5×10^{-6} kg g/L ^(a)		1% ^(a)		
Outdoor paint- TiO ₂	Max	6% wt ^(c)	1 ^(g)	$I_{rain}/3881^*$	0*	0.35kg/m ^{2(b)}
	Ave	4.5% wt				
	Min	3% wt ^(b)				
Outdoor paint- Ag	Max	0.1% wt ^(g)	1 ^(g)	$I_{rain} \times 0.3/554^*$	0*	0.248 kg/m ^{2(e)}
	Ave	0.05% wt ^(g)				
	Min	0.001% wt ^(g)				
Sunscreen- TiO ₂	Max	4.17% wt ^(f)	23.3 ^(f)	93% ^(f)	0.8 ⁽ⁱ⁾	1.9×10^{-3} kg/pc/d ^(k)
	Ave				0.895	0.97×10^{-3} kg/pc/d*
	Min				0.99 ⁽ⁱ⁾	0.04×10^{-3} kg/pc/d ^(k)
Makeup- TiO ₂	Max	3.24% wt ^(f)	52.3 ^(f)	72.7% wt ^(f)	0.8 ⁽ⁱ⁾	0.6×10^{-3} kg/pc/d ^(k)
	Ave				0.895	0.33×10^{-3} kg /pc/d
	Min				0.99 ⁽ⁱ⁾	0.06×10^{-3} kg /pc/d ^(k)
Toothpaste- TiO ₂	Max	0.003% wt ^(f)	50 ^(f)	100% wt ^(f)	0.8 ⁽ⁱ⁾	4.0×10^{-3} kg /pc/d ^(k)
	Ave				0.895	2.4×10^{-3} kg /pc/d
	Min				0.99 ⁽ⁱ⁾	0.8×10^{-3} kg /pc/d ^(k)
Textiles (clothing)- Ag	Max	0.27 % wt	<1 ^(g)	20% ^(h)	0.85 ⁽ⁱ⁾	89×10^{-3} kg /pc/d ^(g)
	Ave	0.14 % wt			0.92	
	Min	0.005 % wt			0.99 ⁽ⁱ⁾	
Toothpaste -Ag	Max	0.00032% wt ^(f)	0.1 ^(f)	100% wt ^(f)	0.85 ⁽ⁱ⁾	4.0×10^{-3} kg /pc/d ^(k)
	Ave				0.92	2.4×10^{-3} kg /pc/d
	Min				0.99 ⁽ⁱ⁾	0.8×10^{-3} kg/pc/d ^(k)

(a) Johnson, and Park, 2012.; (b) Hischier et al. 2015; (c) Al-Kattan et al. 2013; (d) rivm; (e) Kaegi, et al. 2010; (f) Keller et al. 2014a; (g) Tiede et al. 2016; (h) Lorenz et al. 2012; (i) Sun et al. 2016; (j) Dumont, et al. 2015. (k) Biesterbos et al. 2013. Values marked with * were assumed, being I_{rain} the daily rainfall intensity in mm. Further details on the assumptions in Table A1.4 of the Appendix.

Specific assumptions had to be made for the different case studies and are also specified in the following sections.

4.2.5.1 Fuel additives

In this study, we focused on the estimation of the potential emissions of ENPs generated by the bus fleet of the city when using CeO₂-ENP-containing fuel additives. The reason for this was to evaluate the use of such products in a relevant market. Since the product has been previously reported to have been used by bus companies in UK (Johnson and Park, 2012), but no information of other vehicles was available, we chose to work on this hypothetical scenario.

To parametrize this case study, a market penetration value of 1 was assumed in order to study the worst case scenario. Due to a lack of experimental data, a conservative value of zero was given to C_{Ret} . The values of C_{ENP} and $R_{release}$ were taken from Johnson, and Park, (2012) and used to build the max and min scenarios, as well as the average scenario by calculating the average of both parameters. In the case of U_{prod} , which will be the amount of fuel used per day and per HZ, specific values had to be estimated for each HZ. To do so, information on York's bus fleet such as the performance (M_j , in Km travelled per L of fuel used) of the different bus types (j) operating in York, their distance travelled per day (in Km per day), and the bus frequencies whiting each HZ (N_j , in number of buses per day), during weekdays and weekends, was collected from the local bus companies and York city council (Table 4.3).

Table 4.4. List of Bus companies operating in York, number of routes and their performances

Bus company	Number of bus routes	Vehicle performance (K mL ⁻¹) (average)
First	19	2.39
Arriva	4	3.98
Connexions	3	3.20
Transdev	8	2.10
EYMs	5	2.01
Utopia	2	2.73*
Stephenson's	2	2.73*
Reliance	3	2.73*

*Value taken from the average of the other five companies since data was not available from the companies

Then, with the use of the geoprocessing QGIS tools (toggle editing), the bus lines were mapped with allocated information of the bus types used, their performance and

frequency. Then, with the use of the vector clip tool, the needed information of distance travelled (L_j in km) per HZ was extracted as shown in Figure 4.2.

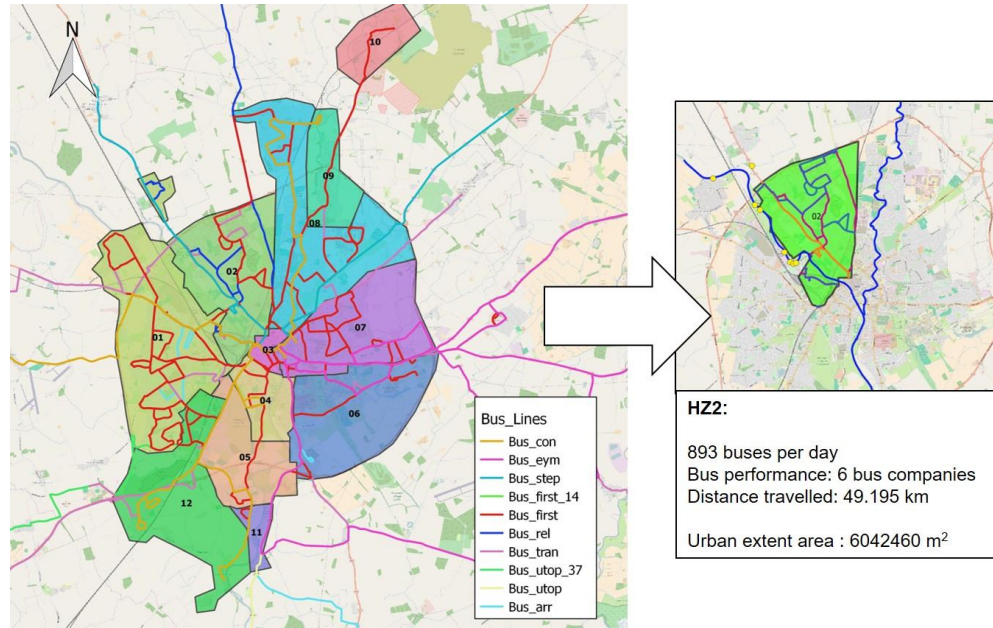


Figure 4.2. Methodology of extraction of bus traffic information (i.e. bus daily frequencies, distance travelled and bus company)

This information was then used for the estimation of U_{prod} as follows:

$$U_{prod,HZ} = \sum_{j=0}^n F_{j,HZ} \times N_{j,HZ} \quad (4.1)$$

$$F_{j,HZ} = \frac{L_{j,HZ}}{M_j} \quad (4.2)$$

Where $F_{j,HZ}$ is the amount of fuel used per vehicle type (j) and per day in the HZ studied ($L \text{ d}^{-1}$), $N_{j,HZ}$ the number of buses of each type travelling in the HZ per day, $L_{j,HZ}$ is the distance travelled (in km d^{-1}) by each bus type in the selected HZ per day and M_j the performance of the bus type (in km L^{-1}). Table 4.4 presents the full list of number of buses circulating per HZ from Monday to Saturday (Week) and on Sundays and the corresponding distance travelled and fuel consumption.

Table 4.5. Number of buses circulating per HZ from Monday to Saturday (Week) and on Sundays and the corresponding fuel consumption (L).

HZ	N° buses per day on week days	Total fuel Usage (L d⁻¹) on week days	N° buses per day on Sundays	Total fuel Usage (L d⁻¹) on Sundays	Distance travelled (km)
HZ1	1044	1768	511	802.5	86.4
HZ2	1038	942.6	504	440	49.2
HZ3	4909	1397.4	2328	717.4	47.6
HZ4	1724	712.7	811	276.6	31.4
HZ5	999	583.5	469	237.5	30.2
HZ6	1100	1062.4	541	513.3	48.9
HZ7	2092	1818.1	991	827	79.5
HZ8	836	1809.3	342	644.7	75.7
HZ9	224	165.4	59	60	8.4
HZ10	105	97.8	51	47.5	4.5
HZ11	196	98.2	54	29.5	7.4
HZ12	588	549.9	255	199.1	30.2

Finally, based on experimental research findings (Batley *et al.*, 2013), it was hypothesized that ENPs are emitted with exhaust and directly deposited onto the road surfaces. ENPs are assumed to accumulate on the road surface during dry periods with emission only occurring once a rainfall event happens. No atmospheric transport of the ENPs was considered, as this was kept out of the scope of the study. However, future consideration of such processes is envisaged. In this case study, as explained in Section 3.2.3.2, T_{lag} was therefore set as 0 on the dry days (indicating no ENPs discharge to the rivers), and on rainy days to be equal to 1 + the number of preceding dry days (accumulation days), to account for the ENPs build up.

4.2.5.2 Outdoor paints

For the estimation of the amount of ENPs released from outdoor paints in the delimited HZs of York F_{pen} , C_{ENP} , $R_{release}$, C_{ret} , U_{prod} and T_{lag} , had to be calculated or assumed. The F_{pen} of paints was established as 1%, reported by Tiede *et al.* (2016) as the corresponding market share extracted from the Observatorynano EU project (<https://www.safenano.org/research/observatorynano/>). C_{ENP} values were found in two different experimental studies (Al-Kattan *et al.*, 2013; Hischer *et al.*, 2015) for TiO₂ ENP-containing outdoor paints and in the case of Ag ENP-containing outdoor paints, these values were taken from the ENP exposure study performed by Tiede *et al.* (2016). In both cases the two different C_{ENP} values were used to build the max and min scenarios

and to estimate the average for the average scenario (as indicated in Table 4.3). To estimate $R_{release}$ it was assumed that, for TiO₂ ENP-containing paints, all ENPs contained in the applied paint were emitted during an established usage duration of 7 years (from Sun et al., 2016) in a proportional manner according to the rainfall intensity of the simulated day (I_{rain}) and the total rainfall over that period. In this sense, $R_{release}$ was calculated as the rainfall intensity of the studied day (in mm) divided by the total rainfall generated in York over the previous seven years (from 2009 until 2016 the total depth of rainfall was 3881 mm (*Weather Pages, Department of Electronics, University of York*, access date: 02/2018); $R_{release} = I_{rain} \text{ (mm)} / 3881 \text{ (mm)}$). For Ag ENP-containing paints, however, it was assumed that only the 30% of the contained ENPs were released over one year period, as estimated by Kaegi et al., (2010), and also proportionally to the rainfall intensity. Therefore, $R_{release} = I_{rain} \text{ (mm)} / 3881 \text{ (mm)}/7$). U_{prod} was calculated for each HZ, according to the approach proposed in Table 4.2. To estimate the amount of paint used for outdoor facades in each HZ of the city, the following information was needed:

1. Extension of surface area (SA) of the building facades exposed to weathering (m²)
2. The ratio of houses using outdoor paint in the city
3. Rate of SA painted vs non-painted
4. Amount of paint used per unit area (kg/m²)

The information used for to estimate each of the points listed is presented in Table 4.6.

Table 4.6. Datasets employed for the characterization of U_{prod} of the outdoor paints case studies

Dataset	Description	Source
Building composition	York buildings stock profile, categorised in 5 main categories: flats, terraced, detached, semidetached houses and others.	London data store (Dwellings by Property Build Period and Type, LSOA and MSOA). https://data.london.gov.uk/dataset/property-build-period-lsoa
Surface area (SA) of building facades	Mapped polygons of the buildings in the city and their heights, from which the surface area of their facades are obtained.	OS MasterMap Building Heights Layer [Shape geospatial data], Tile(s): SE55, SE65, SE54, SE64 , Updated: October 2017 , Ordnance Survey, Using: EDINA Digimap Ordnance Survey Service, https://digimap.edina.ac.uk/roam/download/os , Downloaded: February 2018
Rates of SA painted per building type	Ratios of painted area of the façade surface per building type were obtained for the city of York	On site survey and image processing
Frequency of outdoor paint use in the different HZ of the city	The frequency of use of outdoor paint was estimated via building survey of one representative street per HZ of the city. Frequency of paint use was estimated per street and assumed as the representative frequency of the specific HZ where the street is located.	On site survey
Amount of paint used per surface area	0.35 kg/m ² for TiO ₂ ENPs 0.248 kg/m ² for Ag ENPs	From (Hischier <i>et al.</i> , 2015) and (Kaegi <i>et al.</i> , 2010)

1. Extension of surface area (SA) of the building facades exposed to weathering

The mapped polygons of the city buildings with allocated information on their heights was obtained from Ordnance Survey Mastermap (OS MasterMap Topography Layer – Building Height Attribute). This dataset was projected in QGIS interface and, using geoprocessing tools, the building polygons were extracted per HZ and projected in new layers. For each HZ layer, the building polygons were dissolved into single polygons when sharing walls (i.e. mainly terraced and semidetached houses) and then the perimeter of the facades exposed to weathering were calculated. Using the perimeter information and the building heights (AbsH2 from OS MasterMap Topography Layer –Building Height Attribute), the SA extension of each building façade was obtained and could be added per HZ.

2. The ratio of houses using outdoor paint in the city

A building survey was carried out along the city to determine the percentage of houses using outdoor paint in York. A sample of 10 streets from different neighbourhoods representing the HZs around the city were chosen and an average ratio of painted buildings of 37% was obtained. This ratio was then applied to the building facades SA of all HZs except the city center (old town, HZ3) where almost all of the buildings have some sort of outdoor paint.





3. Rate of SA painted vs non-painted

The façade paint ratio per building type was also estimated to account for the areas of the façade that are not covered in paint (i.e. doors, windows and other building artefacts). For that, thirty pictures of buildings representing the four main building types in York (terraced, detached, semidetached and flats represented in Table 4.6) were analysed using the image processor software Image J (Schneider, Rasband and Eliceiri, 2012).

Firstly, the images were calibrated (Analyze → set scale) by using an average standard UK door measure (800 mm width (Department for Communities and Local Government, 2013)). Then, with the area selection tools, sections of the images were created so that the total façade surface area and the surface area of the non-painted artefacts could be measured (Analyze → measure). With this information, paint usage ratios were obtained as area painted divided by total façade SA area. Finally, the obtained building type paint usage ratios were applied to each HZ based on the building type. Information on property type (terraced, detached, semidetached and flats) for the city of York was obtained from

LONDON DATA STORE (<https://data.london.gov.uk/dataset/property-build-period-lsoa>) and extracted per HZ using QGIS software.

Table 4.7. Sample of building types of York picture in the performed survey

Building type	Picture sample
Detached house	
Semidetached house	
Block of Flats	
Terraced House	

The SA painted, building composition and paint use frequencies obtained for each HZ of the city of York are presented in Table A1.7 of the Appendix.

4. Amount of paint used per unit area (kg/m^2)

To estimate the final SA painted per HZ we applied the paint use frequency of each HZ and an average ratio of SA painted of 0.2 estimated from the image processing survey. A factor of $0.35 \text{ kg}/\text{m}^2$ and $0.248 \text{ kg}/\text{m}^2$ of paint application for TiO_2 and Ag ENP-containing outdoor paints were used as stated in Table 4.8. The final values of kg of paint used per HZ (U_{prod}) are presented in the following table.

Table 4.8. Amount of outdoor paint used per HZ of York in Kg

HZ	U_{prod} Ag-Outdoor paint (kg)	U_{prod} TiO_2-Outdoor paint (kg)
HZ1	40932	57766
HZ2	16471	23245
HZ3	17975	25368
HZ4	10318	14562
HZ5	5980	8440
HZ6	6163	8698
HZ7	36033	50854
HZ8	23463	33113
HZ9	7981	11263
HZ10	8950	12631
HZ11	618	871
HZ12	11855	16731

For T_{lag} , in the case of land cover ENP-containing products, such as construction materials and outdoor surface paints and coatings, it was assumed that ENPs release is triggered by rainfall and happen through weathering over time and proportionally to the rainfall intensity. According to Al Kattan et al. (2014), the exposure to variable weather conditions enhances the ageing of paints and triggers the release of the ENPs contained in their matrices along with rainfall water. Therefore, in this case study it is assumed that during dry days no emissions happen and then the T_{lag} factor would adopt a value of 0, whereas on rainy days T_{lag} would acquire the value of 1 to indicate that the emission is taking place. Again, a conservative value of zero was given to C_{ret} .

4.2.5.3 Household products

Sunscreens, makeup, toothpaste, and textiles are products that are used and released from households. The ENP release mechanism consists of emissions down the drain after washing-off of the ENP from the product (Keller *et al.*, 2014a). For the parametrization of these case studies, F_{pen} and $R_{release}$ values for sunscreen, toothpaste and makeup (foundation), were taken from the study on release of engineered nanomaterials from personal care products (PCP) performed by Keller *et al.* (2014). Their estimated fractions of product on the market that contains ENPs were taken to parametrise the F_{pen} of each of the product types, and the transfer factors to WWTPs reported from their survey on PCP disposal in the U.S were used as $R_{release}$. In addition, the information given on the ingredient concentration and the fraction of ingredient that is 100 nm or less was combined to generate C_{ENP} values for these products. Information on maximum and minimum usage per capita per day was found in Biesterbos *et al.* (2013) report for the cosmetics (toothpaste, sunscreen and makeup) and used to build the max, min and average scenarios. For textiles F_{pen} , C_{ENP} and usage values were taken from Tiede *et al.* (2016). When more than one value was found (C_{ENP} in this case), the maximum and minimum values were taken to build the max, min and average scenarios. The population served per WWTP reported by Yorkshire Water Ltd was used to estimate total product usage for the city (Table S1). For the toothpaste, textiles, and sunscreens case studies, it was assumed that U_{prod} was proportional and even for all of York population (and given in mg per capita per day), with no gender or age differences. However, for the makeup (foundation) case study, it was assumed that the female population between 15 and 75 years old (the 80% of the York's 51% female population according to 2011 census) were the only users (<https://www.yorkopendata.org/yceo/>). Also, a maximum and minimum value of wastewater retention efficiency for TiO_2 and Ag ENPs were found in Biesterbos *et al.* (2013) and used for the three scenarios. Finally, it was assumed that all of the generated sewage was directed to the corresponding WWTP ($F_{WWTP} = 1$) and that the emissions happened constantly with no delay between release and discharge ($T_{lag} = 1$).

All the input parameters established per product type and scenario (summarized in Table 4.3) were then fed into the emissions model and emissions were calculated per day for the year of 2016. Results of emission in mass of ENPs per day of the simulated year were obtained for each of the HZs and by product type. The final discharged emissions to each RS were estimated as well per product type as the cumulative of the emissions received

per HZ connected. Total emissions of each ENP type to the RSs were estimated as the total contribution per day from each of the ENP-containing products considered.

4.3 Results

4.3.1 Emission ranges of ENPs in York

The total amount of the three different ENP types studied (i.e. CeO₂, TiO₂ and Ag ENPs) discharged from all the product types considered (i.e. fuel additives, outdoor paints and cosmetics) to York's river system over the simulated year and for the three simulated scenarios of maximum (MAX), average (AVE) and minimum (MIN) emissions, is presented in Figure 4.3.

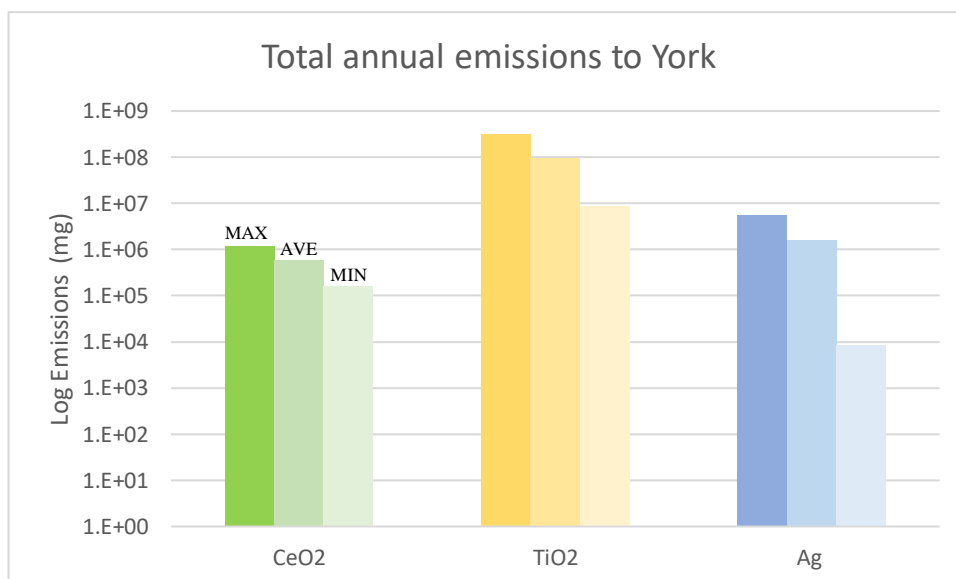


Figure 4.3. Estimated total emissions of CeO₂, TiO₂ and Ag ENPs to York's river system during the year 2016 for the maximum (MAX), average (AVE) and minimum (MIN) emitting scenarios from darker to lighter tones in the bar chart.

Over the three scenarios, TiO₂ ENPs present the highest emission values from the three ENPs studied. The estimated total amount of ENPs discharged to York's river system over the simulated year is presented in Table 4.4 together with the estimated amount of ENPs used (i.e. available for loss) in the city (only from the considered most relevant products: outdoor paints, toothpaste, makeup, textiles and fuel additives) during that period. It can be observed that TiO₂ ENPs are the highest in usage and also lead to the highest emissions, followed by Ag and CeO₂ ENPs. In terms of loss rates, TiO₂ ENPs have the highest for the three scenarios, and in this case, CeO₂ ENPs loss rates are highest

than those associated to Ag ENPs. Emissions were estimated in a daily basis and per RS and then added for the whole year and the whole river system.

Table 4.9. Estimated total mass of each ENP type studied available for loss and actual estimated mass loss in York during the period studied (from the 1st of January until the 15th of December of 2016).

ENP type	Scenario	Mass of available ENPs for loss in York during 2016 in Kg	Estimated cumulative total predicted emissions in York during 2016 in Kg	% Loss
CeO₂	MAX	27	1.2	4.5%
	AVE	22	0.6	2.7%
	MIN	18	0.16	0.9%
TiO₂	MAX	1878	323	17.2%
	AVE	1009	95.4	9.4%
	MIN	141	8.57	6.1%
Ag	MAX	184	5.67	3.1%
	AVE	95.4	1.61	1.7%
	MIN	3.39	0.01	0.3%

When comparing the median values of daily emissions found for the average scenario of the three ENPs, we can see that TiO₂ ENPs daily emissions are two orders of magnitude higher than those of CeO₂ and Ag ENP emissions, being these two last ones within the same order of magnitude (although Ag ENP emissions being two times higher), (244 g/day, 2 g/day and 4 g/day respectively). Variability in the total mass emitted between scenarios is observed for the three ENP types, being more pronounced for Ag, and TiO₂ than for CeO₂ ENPs. This variability represents the uncertainty associated with the model inputs. In some cases the values found for certain inputs, such as C_{ENP} for Ag ENP-containing products (e.g. textiles or outdoor paints) were quite different (within three orders of magnitude), while in the case of TiO₂ ENP-containing products, the information found was more consistent (within the same order of magnitude). The median values of daily ENP emissions obtained for the MIN and MAX scenarios of Ag and CeO₂ ENPs differ in three and one orders of magnitude respectively (0.02 g/day and 16 g/day, 0.5 g/day and 3.7 g/day), while for TiO₂ the median values of the two scenarios differ in two orders of magnitude (i.e. 5.8 g/day and 886 g/day respectively).

The total emission generated per case study (ENP type-product type) during the simulated year and for the whole river system of York for the three simulated scenarios is presented

in Figure 4.4. In this figure and in Table 4.10, it can be observed the different contributions of each product type to the total ENP emissions. These contributions vary depending on the scenario simulated. For the worst case scenario (i.e. MAX) and average scenario (i.e. AVE), the highest emissions are associated with the products emitted down the drain (i.e. for TiO₂ ENPs, sunscreen and makeup emit more than the outdoor paints; for Ag ENPs, textiles are highest contributors of Ag emissions). However, for the best case scenario (i.e. MIN), total ENP emissions are dominated by the products emitted through run off (i.e. CO₂ ENP-containing fuel additives and TiO₂ ENP-containing outdoor paints).

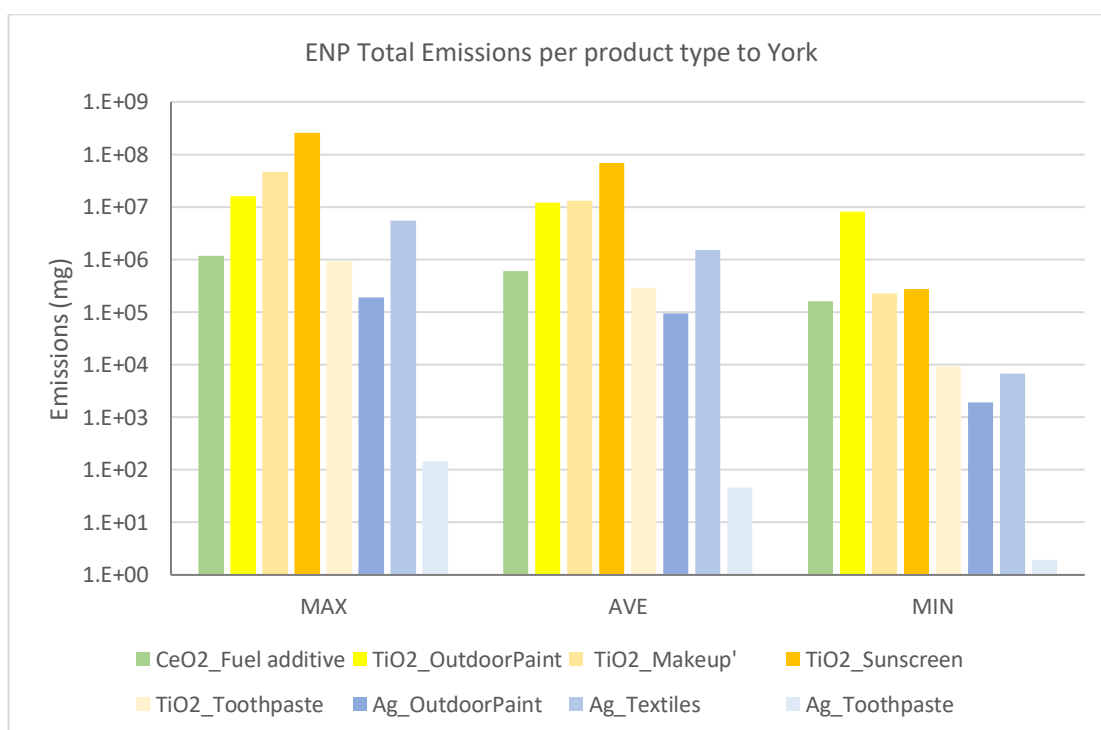


Figure 4.4. Total estimated emissions in mg to York for the year 2016 per product type (fuel additive, outdoor paint, makeup, sunscreen, toothpaste and textiles) for the three ENPs studied (CeO₂, TiO₂ and Ag ENPs), and for the maximum emitting scenario (MAX), the average emitting scenario (AVE) and minimum emitting scenario (MIN).

Table 4.10 also presents the estimated total amount of ENPs available for loss to York's river system over the simulated year for each product type, for the worst-case scenario (i.e. MAX), and the estimated amount of ENPs emitted and their corresponding loss rates. The contributions of the product types for the MIN and AVE scenarios can be found in tables A.1.8 and A.1.9 of the Appendix.

Table 4.10. Estimated total mass of each ENP available for loss and actual estimated mass emitted in York during the period studied (from the 1st of January until the 15th of December of 2016) for the MAX scenario per case study (ENP type-Product type).

ENP type	Product Type	Mass of available ENPs for Loss in York during 2016 in Kg	Cumulative total predicted losses in Kg	% Loss	% contribution to total emission
CeO ₂	Fuel Additive	27	1.2	4.5	100
TiO ₂	Outdoor paint	158	16	10	4.9
	Sunscreen	1400	261	19	80.6
	Makeup	315	45.9	15	14.2
	Toothpaste	5	0.9	20	0.3
Ag	Outdoor paint	1.87	0.19	10	3.354
	Textile	182	5.5	3.0	96.643
	Toothpaste	1x10 ⁻³	1.4x10 ⁻⁴	15	0.003

4.3.2 Spatial variation of emissions

The spatial variability of the mass of ENPs discharged over the different RSs of York per day is presented in Figures 4.5, 4.6 and 4.7 for CeO₂, TiO₂ and Ag ENPs respectively. These figures represent the median emission values of the three scenarios (MAX, Average and MIN) for each RS. To visualize the spatial variation of ENP emissions along the delimited HZs of the city, median daily emission values of the average scenario per HZ are mapped next to each plot presented on the figures.

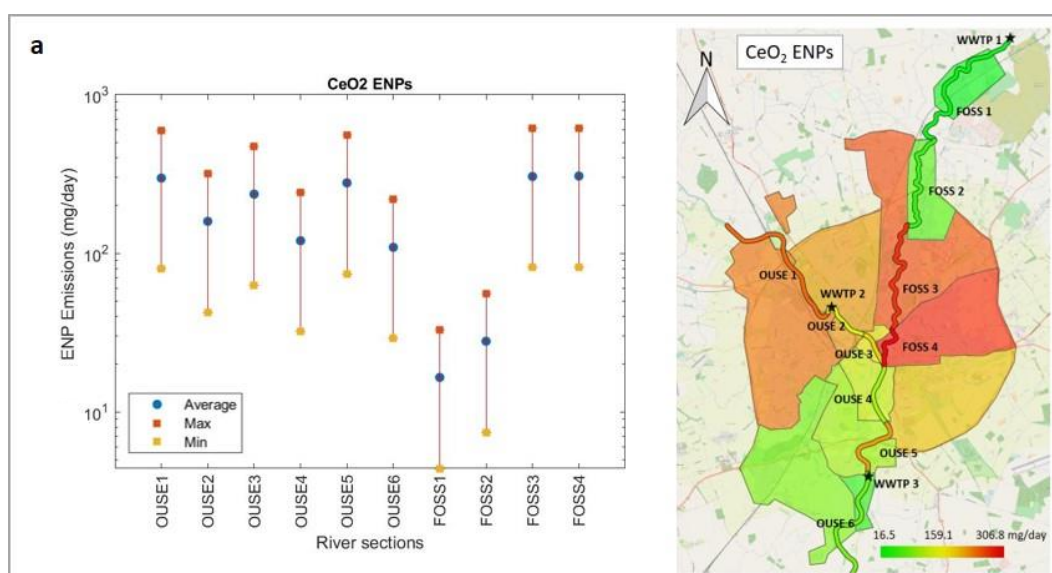


Figure 4.5. Median receiving CeO₂ ENP emissions (in log scale) for the maximum (MAX), the average (Average) and minimum (MIN) emitting scenarios, per river section (OUSE1, OUSE2, OUSE3, OUSE4, OUSE5, OUSE6, FOSS1, FOSS2, FOSS3 and FOSS4) and maps of median CeO₂ ENP emission values per day and per HZ.

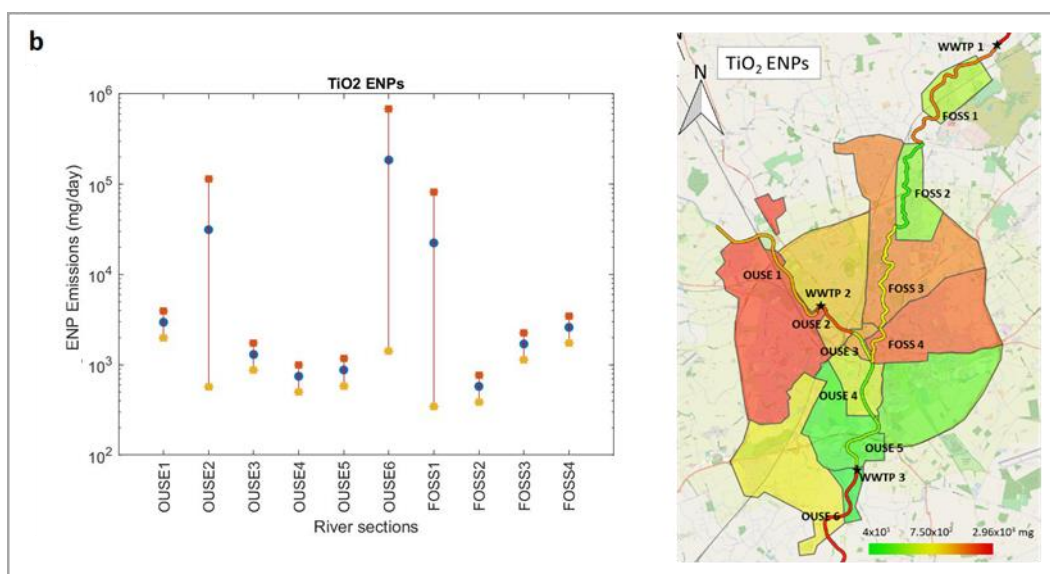


Figure 4.6. Median receiving TiO₂ ENP emissions (in log scale) for the maximum (MAX), the average (Average) and minimum (MIN) emitting scenarios, per river section (OUSE1, OUSE2, OUSE3, OUSE4, OUSE5, OUSE6, FOSS1, FOSS2, FOSS3 and FOSS4) and maps of median TiO₂ ENP emission values per day and per HZ.

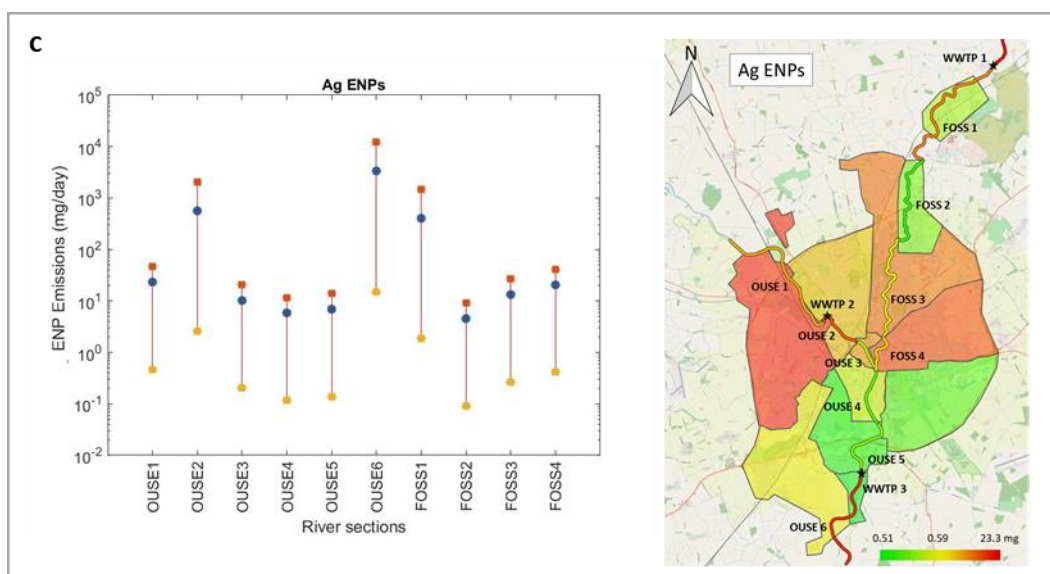


Figure 4.7. Median receiving Ag ENP emissions (in log scale) for the maximum (MAX), the average (Average) and minimum (MIN) emitting scenarios, per river section (OUSE1, OUSE2, OUSE3, OUSE4, OUSE5, OUSE6, FOSS1, FOSS2, FOSS3 and FOSS4) and maps of median Ag ENP emission values per day and per HZ.

Differences in ENP emission patterns in the HZs of the city (which only reflect the runoff emissions) and their receiving RSs (which reflect the total emissions from WWTP and runoff), are observed between CeO₂ ENPs and TiO₂ and Ag ENPs. For the CeO₂ ENPs

traffic related emissions, the highest emissions concentrate in the East and Northeast of the city (hydrozones HZ7 and HZ8 respectively) with also high contributions from the West and Northwest (HZ2 and HZ1 respectively). TiO_2 and Ag ENP emissions follow the same spatial pattern in HZ emissions distribution, with the highest runoff emitting area located in the West of the city (HZ1) followed by the East (HZ7) Northeast (HZ8) and the city center (HZ3). These areas emit runoff to five main RS out of the ten delimited in this study, these are Foss3, Foss4, Ouse1, Ouse5 and Ouse3. Only three river sections receive direct down the drain emissions from the city, being these the ones where the outfalls of the local WWTPs are located (i.e. Ouse2, Ouse6 and Foss1), and the ones receiving the highest emissions of Ag and TiO_2 ENPs. Generally, the river sections receiving the lowest runoff emissions (e.g. CeO_2 ENPs) are Foss1 and Foss2.

4.3.3 Temporal variation of emissions

The temporal variability of the total ENP emissions along the year 2016 for York's river system is shown in Figure 4.8 as cumulative distribution functions (CDF). Each curve per ENP type represents the probability of a certain mass to be emitted over the year for three simulated scenarios (i.e. MIN, AVE and MAX).

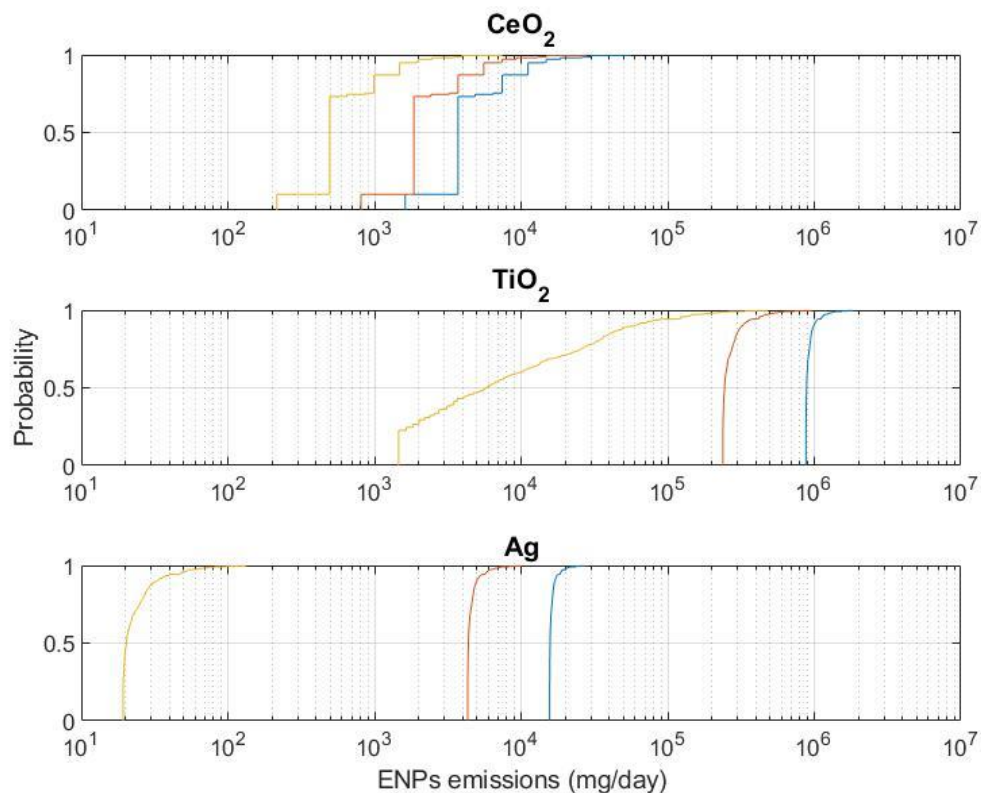


Figure 4.8. Cumulative Distribution Functions (CDF) of the estimated total emissions (mg in log scale) to the York river system for each day from the first of January until the 15th of December of 2016 in which emissions happen (350 days for TiO_2 and Ag ENPs, and 216 rain days for CeO_2 ENPs), for max (blue), average (orange) and min (yellow) scenarios for the 3 ENP Types.

High temporal variability in the ranges of ENP emissions along the year is observed for CeO_2 ENPs and for TiO_2 ENP in the best-case scenario (i.e. MIN), represented as the steepness of each CDF (i.e. the steeper the gradient the less variability). The variability of CeO_2 ENP emissions within each single scenario represents a variation of two orders of magnitude, while for TiO_2 and Ag ENPs emissions are always within the same order of magnitude (except from TiO_2 ENPs at the MIN scenario, where the variability is of three orders of magnitude). This is due to the composition of such emissions. In this study only runoff emissions (i.e. fuel additives and outdoor paints) have been considered as temporary variable (associated to rainfall variability). On the other hand, down the drain emissions were assumed to be homogenous over time (i.e. constant rates of emission along the year). In this sense, because CeO_2 ENP are here considered to only be emitted through runoff, temporal variations in CeO_2 ENP emissions are expected. For TiO_2 and Ag ENPs however, emissions come from both pathways, runoff and down the drain,

therefore, a contribution of both patterns is expected. For example, for the MAX and AVE scenarios the down the drain emissions dominate the total ENP emissions, being in this case the temporal variations predicted not as pronounced as for CeO₂ ENPs. On the other hand, for the MIN scenario of emission of TiO₂ ENPs, outdoor paints (runoff emitting products) dominate the contributions to total TiO₂ ENPs emissions (Figure 4.5 and Table A.1.9) and hence the big temporal variability observed in the CDF.

Further details of the temporal variations of the ENP emissions are presented in Figures 4.9 to 4.13. Figures 4.9 and 4.10 present the total daily emissions over the year 2016 of TiO₂ ENPs and the contribution from their different products (i.e. toothpaste, makeup, sunscreen and outdoor paint) to a RS with WWTP discharge (Ouse2) (Figure 4.9), and to a RS without WWTP discharge (Ouse3) (Figure 4.10). Figures 4.11 and 4.12 represent the temporal variations of receiving total emissions in the same two RSs respectively but of the emitted Ag ENPs, and the contributions from textiles, outdoor paints and toothpaste. In Figures 4.10 and 4.12, the rainfall pattern of the year 2016 is also plotted in blue against the runoff emissions. Figure 4.13 presents the daily CeO₂ ENP emissions to OUSE2 along the year 2016 against rainfall.

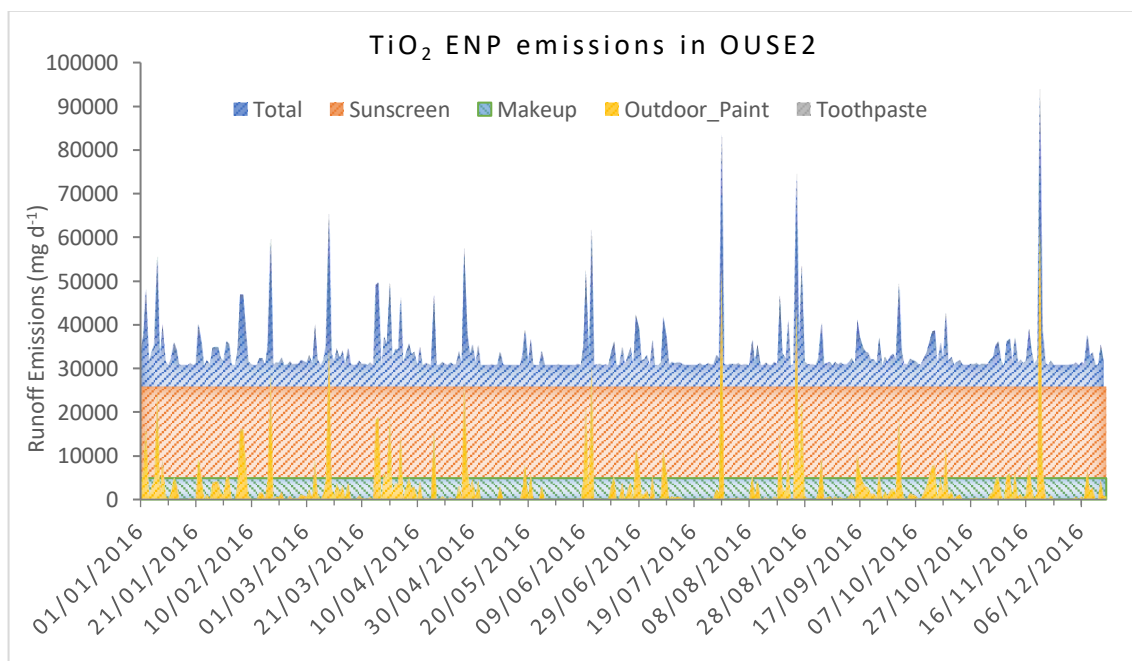


Figure 4.9. Daily ENP emissions from TiO₂ ENP-containing products and total amount emitted to the river sections OUSE2 (i.e. Outdoor paint, makeup, sunscreen and toothpaste) during 2016 for the average scenario

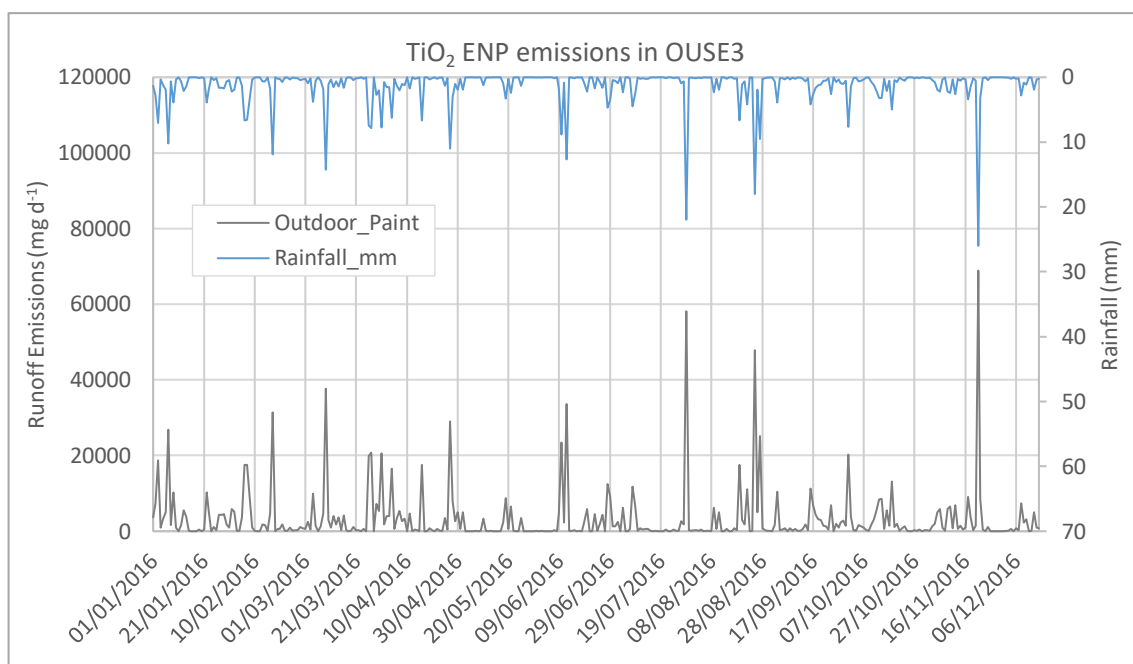


Figure 4.10. Daily ENP emissions from TiO_2 ENP-containing products emitted to the river sections OUSE3 (i.e. Outdoor paint) during 2016 for the average scenario against the rainfall pattern for the same year (plotted in blue in the secondary axis).

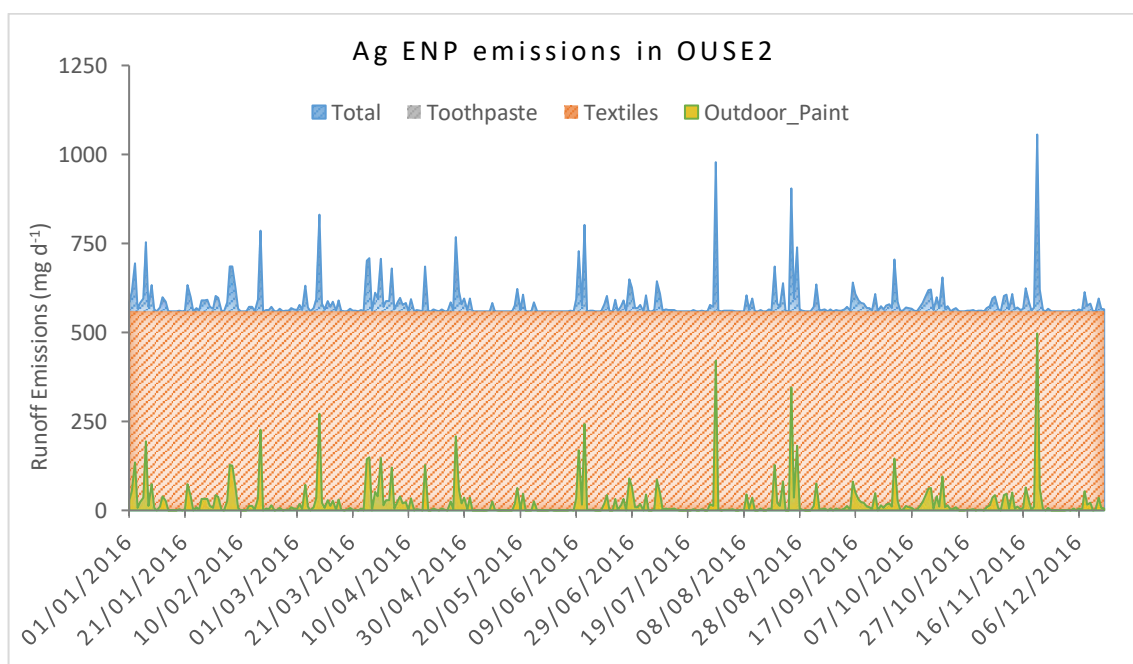


Figure 4.11. Daily ENP emissions from Ag ENP-containing products and total amount emitted to the river sections OUSE2 (i.e. Outdoor paint, textiles and toothpaste) during 2016 for the average scenario.

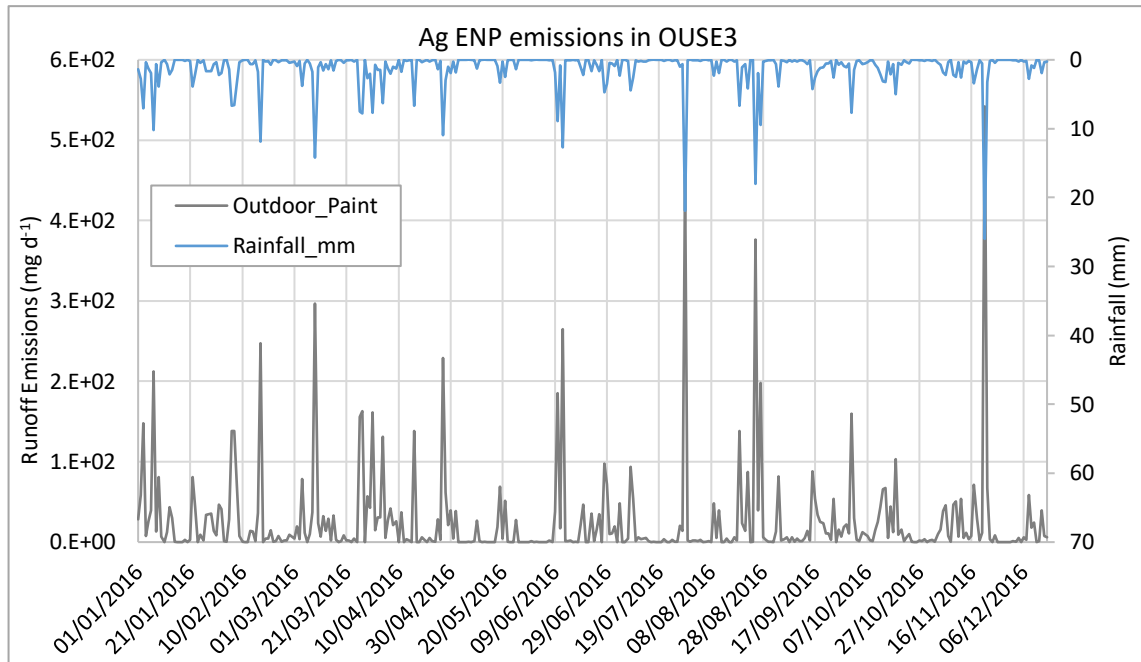


Figure 4.12. Daily ENP emissions from Ag ENP-containing products emitted to the river sections OUSE3 (i.e. Outdoor paint) during 2016 for the average scenario against the rainfall pattern for the same year (plotted in blue in the secondary axis).

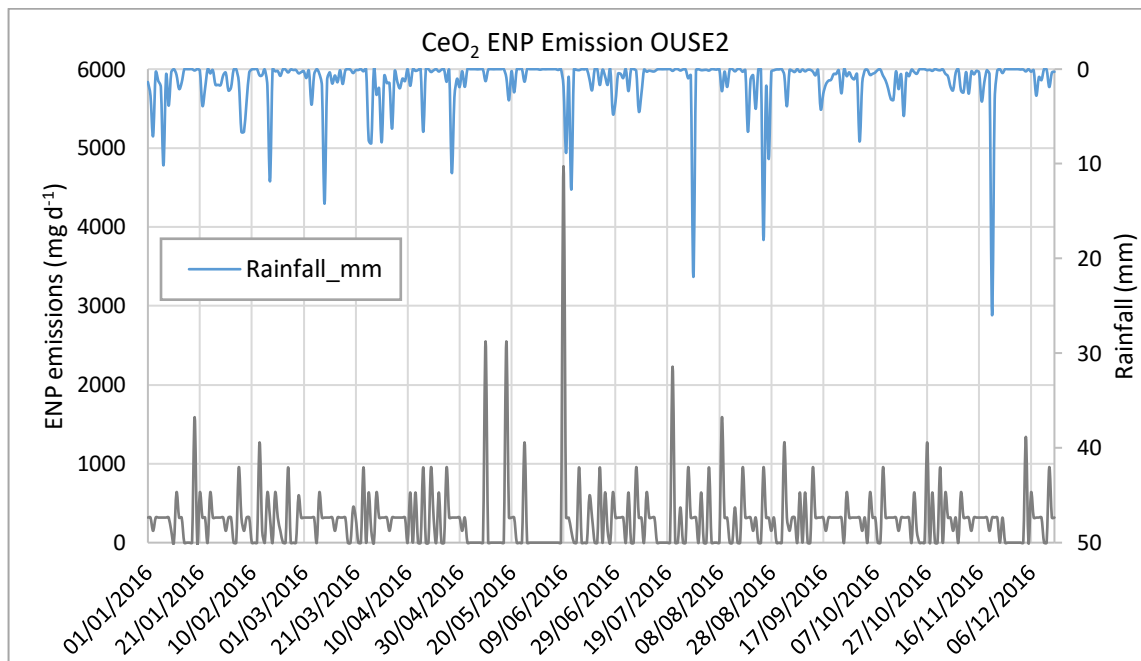


Figure 4.13. CeO₂ ENP estimated emissions for the RS OUSE2 and the average scenario over the year 2016 in mg (in grey).

The river section OUSE2 only receives runoff emissions (from outdoor paints or traffic), while OUSE3 receives emissions also from the products released down the drain due to the location of the WWTP outflow. The down the drain emissions are constant over the

year and their emissions range from a few micrograms per day (i.e. Ag ENP-containing toothpaste), to tenths of grams per day (i.e. TiO₂ ENP-containing sunscreens). The emissions coming from products releasing through runoff vary throughout the year from a few grams to tens of grams per day. Run off emissions vary proportionally to the rainfall intensity for outdoor paints (Figure 4.10 and 4.12), and proportionally to the rainfall frequency for traffic emissions (Figure 4.13). On dry days, no emissions from runoff emitting products are predicted and therefore ENP emissions are dominated by the down the drain emitting products. On the rain days, the influence of the runoff pattern is predicted and peaks of higher emissions are expected.

4.4 Discussion

The applicability of the proposed spatially and temporally resolved ENP emissions model was explored for the city of York in order to characterize the city emissions. With the results obtained, the expected ENP emission ranges for the city for a maximum (MAX), average (AVE) and minimum emitting scenario (MIN) were estimated. In addition, the sources contributing the most to such emissions, the most runoff emitting areas of the city specific to the ENP type and the conditions under which highest emissions would happen were identified. All these findings are further discussed below.

4.4.1 Emission ranges of ENPs in York

Ranges of TiO₂, Ag and CeO₂ ENP emissions were estimated for York based on the city's characteristics (urban building structure, water collection and treatment systems, weather patterns, population, etc.) and activities (e.g. traffic dynamics) from the proposed bottom up perspective. The main products containing the targeted ENPs in York were identified and their emissions to each RS of York estimated to then obtain the total city ENP emissions.

Results showed that TiO₂ ENPs are the most emitted ENPs of the three studied in York, which correlates with several published global ENP emission studies where TiO₂ ENPs are considered to dominate ENPs emissions to the environment, and specifically to surface waters (Keller *et al.*, 2013; Keller and Lazareva, 2014; Sun *et al.*, 2014). The estimated total ENP emissions to York's river system for the simulated year varied from 9 to 323 kg for TiO₂ ENPs, from 0.16 to 1.20 kg for CeO₂ ENPs and from 0.01 to 5.7 kg for Ag ENPs. When comparing our results with emission estimates from an alternative

study performed for Germany (Giese *et al.*, 2018), we found that our estimates fall within the same emission ranges after scaling their results by population (Germany 81197500 against York 206207). The projected estimates for York obtained from their data would vary between 1.6 and 4 kg of CeO₂ ENPs, and from 0.18 and 0.27 kg of Ag ENPs. Their CeO₂ ENPs emission estimates fall within the upper level of our estimated range, which is expected due to the fact that in their study they took account of a wider list of CeO₂ ENP-emitting products. For Ag ENPs, we obtain a wider emission range but that would include their predictions. This suggests that despite the use of a different approach, and the fact that our model was specifically parametrized for a limited amount of ENP applications (although the identified as most relevant) and for a very specific urban scenario (the city of York), the overall approach and initial assumptions followed are probably reasonable. Furthermore, we provide many more insights into the composition of the final emissions by performing a product specific characterisation of the emissions with spatial and temporal resolution.

For York, we were able to identify the main emitting sources from the list considered in our study. From our findings, down the drain emitting products (mainly sunscreen, makeup and textiles) result higher ENP emissions than the runoff emitting products considered (outdoor paints and fuel additives). Again, this is in accordance with previously performed modelling studies such as the one carried by Gottschalk *et al.* on the TiO₂ ENPs-containing products contributions to final emitted concentration (Gottschalk *et al.*, 2015). Gottschalk *et al.* reported a higher contribution of TiO₂ ENP emissions from cosmetics than from outdoor paints due to their relative application (according Sun *et al.* (2014) the main applications of the produced TiO₂ ENPs are cosmetics (59.4% of the nano-TiO₂ produced while paints was estimated as 8.9%). However, in our study, under certain circumstances, such as the higher retention rates (C_{Ret}) and lower ENP content in household products (C_{ENP}) of the simulated MIN scenario of TiO₂ ENP, the opposite tendency was predicted. This difference results from the chosen top down calculations usually followed by MFAs, against the bottom up approach followed in our study. Traditionally MFA base their emission calculations in global production volumes of ENPs and scaling factors (relative application factor) per product type, without considering other relevant factors in the ENP emissions such as actual usage volumes or experimentally obtained release rates. However, our model does not consider production volumes but characterised product-specific usage and release rates (Usage,

R_{release}) specific to the studied area (through population or extension of the area considered), as well as release pathways characteristics (C_{ret} and T_{lag}). We argue that at the local level, this type of detail becomes essential since from the global mass flow perspective certain sources (such as diffuse sources) could be underestimated.

Furthermore, usage in this case seems to be a determining factor, since it varies extensively between the product types (i.e. personal care products and outdoor paints). When considering household products (makeup, toothpaste, etc.), usage rates are estimated at few grams per capita per day, but when looking at land cover products (such as outdoor paints or fuel additives) usage is estimated in kg per meter square of the city buildings surface area. In our opinion, these input parameters, chosen case-by-case and according to the emission source and pathway, provide a more refined approach compared to MFA for the characterisation of ENP emissions that proves useful at the urban level.

4.4.2 Spatial variation of emissions

It was observed that significant spatial variability in the ENP emissions within the city exist as well as an associated spatial variation of receiving emissions along York's river system. This is due to the nature of the emitting areas (HZ) connected to them as well as due to the location of the WWTP outlets. Differences between the HZ's building composition (types of buildings on that area) and extension (Table A1.7), and traffic load (indicated as fuel consumption) (Table 4.6), were identified as the main drivers that lead to the runoff emission differences. Usage rates (reflected in Tables 4.7 and 4.6 for paints and fuel additives respectively) vary according to those factors and influence emissions accordingly which is reflected in Figures 4.7 to 4.9. For example, the spatial emission pattern found for the CeO_2 ENP traffic emissions in York correlates with the fuel consumption of each area, which depends in turn on the traffic load and distance travelled within it (e.g. HZ7, which corresponds to the East of York, is the area of the city with the highest volume of fuel consumed and therefore generates the highest emissions). In the case of TiO_2 and Ag ENPs, the spatial trend correlates with the usage rates of outdoor paint of each HZ. The estimated paint usage per HZ is summarized in Table 4.8 and it can be observed that the highest emitting areas (HZ1 and HZ7) are those with higher paint usage due to their building extension and composition. Similarly, it is intuitive to understand that the RSs receiving the lowest CeO_2 ENP runoff emissions (Foss1 and 2) are those that receive runoff water from the smallest areas and that also have lower traffic

loads in the city, in this case HZ9 and HZ10. Finally, the RS predicted to receive the highest emissions, as expected according to the model set up, are those where the WWTPs outfalls are located (Ouse2, Ouse6 and Foss1). However, it is worth noting that the spatial emission pattern will exhibit temporal variation, which is discussed in the next section.

4.4.3 Temporal variation of emissions

Temporal variations of the ENP emissions throughout the year were simulated for the three ENP types studied in York by integrating the influence of the weather conditions. Overall, higher emissions were predicted on rainy days of the simulated year (78% of the time), while on the dry days total emissions are sometimes expected two or three times lower. The emission sources and emitted particles over time are associated with the emission pathway and therefore, in the case of runoff, also with the weather conditions. Weather patterns influence emission ranges through the release pathway mechanism. On dry days, only point source emissions are assumed to occur (e.g. personal care products and textiles released via WWTP effluent). On rainy days, diffuse emissions triggered by rainfall (i.e. outdoor paints and fuel additives) dominate the temporal variation.

Time variable emission patterns were also predicted per product type. ENPs released down the drain were simulated as a constant emission over the year, since there were no time related factors to their usage nor to their ENP release mechanism (although some temporal emissions trends can be expected for specific products such as sunscreens). On the other hand, the diffuse emissions varied over time and proportionally to rainfall intensity (for outdoor coatings and paints), or to the duration of dry (accumulation) periods. For traffic emissions, it was assumed that during dry days ENP emissions were still happening although no runoff emission into the river takes place on those days (no emissions to RS). Therefore, dry days were taken as accumulation days where ENPs accumulate on the surface of the city and when the rainfall event happen the ENP emission to the RS is multiplied by a factor proportional to the number of preceding ENP accumulation days (dry days).

Therefore, once more the bottom up approach used here, which includes weather factors such as rainfall frequency or intensity, proves essential in local exposure assessments.

4.5 Conclusions

In this chapter, the proposed ENP emissions model presented in Chapter 3 was applied for the first time to a small case study city. New approaches for integrating urban relevant available data were explored and integrated to develop a thorough assessment of urban ENP emissions. The emission ranges from specific sources according to the city's activity and from the estimated usage trends of ENP-containing products were determined. The main sources, drivers and activities causing such emissions were identified and localized within the city. Finally, the temporal trends of such emissions were studied and the main factors of influence identified.

These results show that temporal and spatial variations in the emissions of emerging pollutants at a local scale can be expected and could, in turn, influence risk assessment outputs. Therefore, this level of detail should be taken into account when performing urban exposure assessments, rather than the predominant spatially averaged and steady state models currently available (Keller *et al.*, 2013b; Gottschalk *et al.*, 2015a; Sun *et al.*, 2016b).

The relative influence of specific emission sources or pathways in the determination of the emissions of specific ENPs and their temporal and spatial patterns can be also derived from this approach due to the bottom up method followed. Here emissions are parametrised in a case by case basis, and emission estimates are derived from pathway-specific equations. The results for the case studies presented here show that the integration of run off emissions must be considered alongside down the drain emissions, especially under certain weather conditions, if urban exposure is to be evaluated accurately.

However, due to the nature of modelling, limitations do exist and have to be accounted for when performing this kind of exposure assessments. They consist mainly of the uncertainties attached to the use of assumptions and extrapolations. For example, data on experimental parameters such as ENP's release rates from specific products are not often available (i.e. outdoor paints), which leads to making conservative assumptions such as the one made in this study where all ENPs contained in paints are assumed to be released over the use period of the product. At the same time, potential bias of the results might be caused by the number and types of products considered in the study and their allocated market penetration factors. In this sense, it is very important to carry out a thorough

analysis of the study area so that the bias is reduced or at least the results are put in context for their interpretation.

In order to identify and quantify the uncertainties in the model outputs, the use of sensitivity and uncertainty analysis (e.g. using Monte Carlo Simulation) is envisaged. A formal uncertainty analysis will provide information on all the potential values that the outputs can take, with their associated probability distribution. Jointly, a sensitivity analysis would determine the influence of each input parameter on the model output values, therefore indicating which are the inputs that will need to be further refined in order to get the most accurate results.

We believe that with local scale modelling (such as urban modelling), such uncertainty is reduced, since more detail and control over the main uncertainty contributing factors is present (through the use of case by case input parameters).

Chapter 5

Modelling exposure of the York River system to engineered nanoparticles at high temporal and spatial resolutions

5.1 Introduction

As discussed in the previous chapter, ENP emissions to urban surface waters vary over time and space. Following emission to aquatic environments, ENPs can undergo a series of physical and chemical transformations (characterised by specific fate processes) that will determine their final “form”, concentration and their distribution within the water bodies. These final exposure levels and the “form” in which they are exposed in the different surface water compartments (i.e. sediment, flowing water and stagnant water) will be key factors in determining their environmental and health risks (Levard *et al.*, 2012; Mitrano *et al.*, 2015). In this chapter, the transport and fate process that ENPs undergo in rivers are modelled following the proposed urban model framework presented in Chapter 3 and using the ENP emissions results obtained in Chapter 4 (specifically those obtained for TiO₂ ENPs). Temporally and spatially resolved potential exposure concentrations over time are generated and the potential risk posed by TiO₂ ENPs in the river Ouse and Foss assessed.

As presented in Section 2.4, most relevant fate processes that ENPs will undergo in surface waters are aggregation, sedimentation, dissolution, redox and bio-transformations (Hartmann *et al.*, 2014). As a consequence of these processes ENPs can be transformed into dissolved, homo- and/or heteroaggregated forms, undergo bio or redox transformations at their surface or at surface coating, remain freely dispersed in their pristine form or settle (as homo- or heteroaggregates) into the sediment layer. These different forms may have different toxicity levels or be differently bioavailable, and therefore pose different levels of environmental risks (Garner and Keller, 2014). Additionally, these different forms will distribute differently along the various compartments of the surface water body (Dale, Lowry and Casman, 2015a), becoming

more or less bioavailable for the specific species inhabiting each compartment (e.g., water column or sediment). The importance of these different ENP fate and transformation processes will be dictated by the ENPs physical and chemical characteristics (Dwivedi *et al.*, 2015), and by environmental factors such as pH, ionic strength and composition, water hardness and the presence of dissolved organic matter and suspended particulate matter (SPM) (Sani-Kast *et al.*, 2015a).

Spatial and temporal variations in the water quality factors affecting ENP fate and behaviour are expected along the river courses due to natural (e.g. river geomorphology) and anthropogenic sources (e.g. wastewater discharge areas from WWTP or runoff), especially in local urban contexts where they are expected to vary over short times and distances (Sani-Kast *et al.*, 2015a). Similarly, as demonstrated in the previous Chapter, spatial and temporal variations in the ENP emissions over short distances will occur in city systems. Both, the spatial and temporal variability of the water quality factors and of the emissions, will provoke temporal and spatial variations in exposure and therefore in the risk levels.

In this context, to fully characterize ENP risks at the local level in urban systems, spatial and temporal exposure variations must be investigated. As discussed in Chapter 1, analytical limitations for the study of ENP occurrence in the environment still prevail, and the evaluation of the risks posed by ENPs has, therefore, been so far approached through the use of modelling tools that calculate predicted environmental concentrations (PEC) in specific environmental compartments (Bundschuh *et al.*, 2018). However, these models often lack spatial and temporal resolution. The most commonly used modelling approaches, material flow analysis models (MFA) (Mueller and Nowack, 2008; Keller *et al.*, 2013; Meesters *et al.*, 2014; Sun *et al.*, 2014, 2016b; Gottschalk *et al.*, 2015c), give average exposure concentrations per environmental compartment that can potentially underestimate or overestimate risks at certain locations such as emission hot spots (e.g. WWTP effluents) or areas of low population density. The few studies that attempt to give some sort of spatial resolution have highlighted the importance of such considerations (Dale, Lowry and Casman, 2015a; Dumont *et al.*, 2015), but they often also fail at integrating the spatial and temporal variability of emissions (i.e. by using average ENP loads), as well as the heterogeneity of environmental conditions (i.e. varying pH, water hardness or SPM concentration along the water body). Furthermore, to date very few modelling studies have linked spatially explicit emission estimates with spatially

parameterised ENP fate models driven by experimental data (Dale, Lowry and Casman, 2015a; Dumont *et al.*, 2015). By linking these, more realistic exposure scenarios can be built locally and local and temporal exposure trends can be identified. Having this kind of information would help setting-up measures to reduce exposure and the associated risks.

In this Chapter the applicability and usefulness of the developed model framework presented in Chapter 3 for a detailed local exposure assessment is explored by studying the exposure concentrations of TiO₂ ENPs along York's river system at high temporal and spatial resolution. To achieve this, the spatially resolved daily emissions of TiO₂ ENPs obtained for York (Chapter 4), were integrated together with locally monitored water quality parameters into a modified version of an ENP multimedia river fate model developed by Praetorius *et al.* (2012).

Spatial and temporal trends of exposure along both of the rivers flowing through York are reported with collated information on the distribution of the ENPs in the river compartments (i.e. flowing water, stagnant water and sediment).

5.2 Methods

5.2.1 Modelling principles

A modified version of the river multimedia box model developed by Praetorius *et al.* (2012), written in Matlab code, was used to simulate the fate and transport of the TiO₂ ENPs released into York's river system.

This model framework was developed to investigate the transport and fate of ENPs in surface waters by including for the first time process descriptors specific to ENPs (Praetorius, Scheringer and Hungerbü, 2012). The main advantage of this model is its flexibility. While models such as NanoDUFLOW (Quik, de Klein and Koelmans, 2015) or the model developed by Dale, Lowry and Casman (2015), are specifically designed for the water bodies studied (i.e. River Dommel and the James River Basin, respectively), Praetorius *et al.*'s model can be easily adapted to York's river system. This model framework has been previously applied to study the fate of TiO₂ ENPs in the Rhine River (Praetorius, Scheringer and Hungerbü, 2012), as well as to investigate the key environmental features (mainly SPM concentration and size distribution) affecting the overall TiO₂ ENPs fate in the Lower Rhône River, France (Sani-Kast *et al.*, 2015b). In

this study, we have adapted the multimedia box model to York's river system and we have integrated temporal and spatial resolution to the emission loads and surface water parameters.

The model represents the target river system of study (described in Section 5.2.2) as a set of horizontally connected boxes, each of which is further subdivided into a number of consecutive boxes of equal length (here: around 750 m) to create a spatial distribution for the simulation of the particles' transport. Each box is subdivided into three different compartments representing a moving water (w1), a stagnant water (w2) and a sediment layer (sed). In the adaptation to York's river system, the horizontally connected boxes were established as the 10 river sections delimited for the city (described in Section 4.2.3). Figure 5.1. presents a schematic representation of the river model, the transport into, out of and throughout the defined river sections and river compartments and fate processes inside the river system for TiO₂ ENPs.

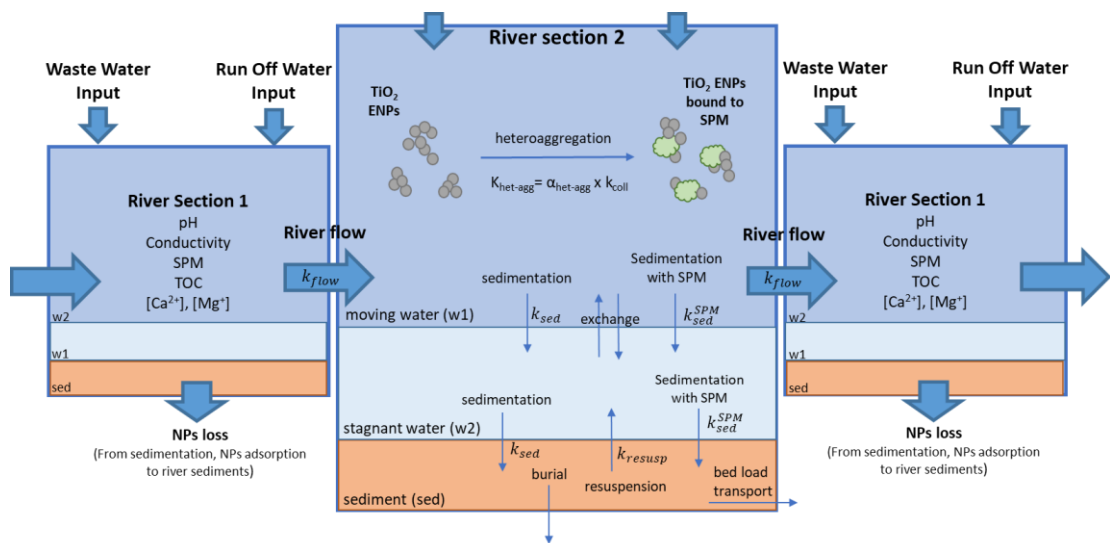


Figure 5.1. Schematic representation of the river model conformation, the transport into, out of and throughout the defined river sections and river compartments (i.e., moving water, stagnant water and sediment) and fate processes inside the river system for TiO₂ ENPs. Source: Adapted from Praetorius et al. (2012).

ENP transport between boxes (i.e. advective transport with moving water and sediment bed load transport) and between compartments (i.e. sedimentation, sediment resuspension, and burial in the deep sediment), as well as the relevant processes influencing the environmental behaviour and transport of the TiO₂ ENPs (i.e.

heteroaggregation with suspended particulate matter (SPM)) were simulated as described in Praetorius et al. (2012).

For the simulation of the processes all the compartments within each box are assumed to be well-mixed. Water is exchanged between the moving water compartment (w1) and the stagnant water compartment (w2) and vice versa at a rate of $k_{exch,12}$ and of $k_{exch,21}$ (in s^{-1}) respectively. Transport of water from the moving water compartment of one box to the next occurs at the river flow velocity and with a transport rate constant of $k_{river,flow}$ (in s^{-1}). River velocities (in m/s) varied daily and were estimated by dividing the daily discharge (m^3/s) (from the National River Flow Archive (NRFA) (<https://nrfa.ceh.ac.uk/>)) by the river cross section (Section 5.2.2). The maximum velocity was set to 2 m/s (i.e. if the estimated velocity was larger than 2 it was set to 2 m/s). Sediment resuspension into the stagnant water compartment occurs at a rate constant of k_{resusp} (in s^{-1}) and at an average velocity (v_{resusp}) of $1.0 \times 10^{-6} m s^{-1}$ (Praetorius, Scheringer and Hungerb , 2012), and is buried in the deep sediment at rate constant of k_{burial} (in s^{-1}) and at a velocity (v_{burial}) of $3.42 \times 10^{-8} m s^{-1}$. Horizontal sediment transport at the surface of the sediment compartment takes place at an average rate, $v_{sed,transfer}$, of $3.0 kg s^{-1}$ and with a rate constant of $k_{sed-transfer}$ (Praetorius, Scheringer and Hungerb , 2012). Table A2.2 to A2.5 summarizes all the inputs needed for the model and how the model rate constants are estimated.

The heteroaggregation of ENPs with the naturally occurring SPM takes place at a heteroaggregation rate constant, $k_{het-agg}$, obtained by multiplying the collision frequency, k_{coll} , of the particles by the attachment coefficient (α_{hetero}). It was assumed that the overall SPM concentration in the river does not change significantly as a result of heteroaggregation, so the process is expressed with a pseudo-first-order rate constant by multiplication by the SPM particle concentration, as described in Section 2.5.1 Equation 2.1.

By using time and spatially resolved information on water quality parameters (obtained from a local monitoring campaign conducted during the first year of this project) and on ENP emissions (results obtained in the previous Chapter), the system fate and transport equations were parametrised. Coupled mass-balance equations integrating all the processes acting on the TiO_2 ENPs in each river compartment (i.e. w1, w2 and sed) were then solved numerically through discretisation by applying Euler's method to estimate the concentration of both free TiO_2 ENPs and TiO_2 ENPs bound to SPM along the rivers

and as a function of time. These equations are provided in the Appendix 2 (River model equations A2.1 to A2.10). The model was run dynamically for four types of TiO₂ ENPs (further described in section 5.2.3) and for the period from July 1st to December 14th with an integrating time step of 2 minutes.

5.2.2 Description of the river system

The river fate model was set up for the two rivers comprising York's river system (i.e. the Ouse and the Foss) (described in Section 4.2.1). The river Ouse, with a catchment area of 3315 km² (Figure 5.3), reaches the city from the north-west, joins the Foss downstream of the city centre and then flows southwards to leave the city. This river passes through the main urbanised areas receiving runoff water from the surrounding HZs and effluent from two wastewater treatment plants (WWTPs): Rawcliffe WWTP, located upstream of the city centre that serves a population of 27 900, and Naburn WWTP, located downstream of the city and serving a population of 180 500. The total modelled Ouse extension was 22.7 km long and it was subdivided in six river sections of varying lengths. The river Foss, which has a catchment area of 118 km² (Figure 5.4), flows from the north of the city, mainly through rural areas, until it joins the Ouse. It is smaller in size and receives water from the surrounding HZs and effluent from the Walbutts WWTP which is located upstream of York and serves a population of 18 600 people. The modelled length of the Foss was 15.9 km long and was subdivided into four river sections of varying lengths. Figure 5.2 pictures the study area and the RSs delimited. The list of connecting HZ and RS are provided in Table 5.2.



Figure 5.2. Locations of York's two main rivers, the WWTPs serving the city, the delimited river sections (Ouse 1 to 6 and Foss 1 to 4) and the established monitoring sites.

Table 5.1. List of RSs and their connexions to the York delimited HZs and serving WWTPs.

River Section	HZ	WWTP (population served)
Ouse 1	HZ1	-
Ouse 2	HZ2	Rawcliffe (28022)
Ouse 3	HZ3	-
Ouse 4	HZ4	-
Ouse 5	HZ5+HZ6	-
Ouse 6	HZ11+HZ12	Naburn (168594)
Foss 1	HZ10	Haxby (20105)
Foss 2	HZ9	-
Foss 3	HZ8	-
Foss 4	HZ7	-

In order to adjust the fate model to the river system, the physical characteristics (e.g. length, width, depth and flow velocity) and water quality characteristics (i.e. temperature, pH, dissolved oxygen, electrical conductivity, total suspended solids, dissolved organic carbon and ionic content) of each river section were gathered from a variety of

information sources and a local monitoring campaign (described in Section 5.2.3.1). This information was later transformed into the required input parameters needed. A full description of the model parametrization is provided in the next section.

5.2.3 Model parametrization

5.2.3.1 *River system physical parametrization*

The width and length of all RSs was needed to parametrize each model box. These parameters were determined using georeferenced data of York's hydrological network obtained from EDINA Digimap Ordnance Survey Service (Ordnance Survey (GB)). Using QGIS software the georeferenced data was manipulated to measure the length of the RSs, and width was provided in the dataset. The river's depth was assumed to be 3 m and 2 m for the Ouse and the Foss respectively, based on the navigation information provided by the Canal and River Trust (<https://canalrivertrust.org.uk/>). The RSs dimensions and their segmentation are summarized in Table A2.1 of the Appendix. The daily discharge of both rivers in the simulated year (2016) was obtained from the National River Flow Archive (NRFA) (<https://nrfa.ceh.ac.uk/>) as gauged daily flow (GDF) in m³. Both values were obtained from the closest monitoring stations to the upstream Ouse and Foss delimited RSs (i.e. Ouse at Skelton station and Foss at Huntington Station respectively, shown in Figures 5.3 and 5.4). The mean flow for the Ouse, as reported by the NRFA, is 51.406 m³/s, the 95% Exceedance (Q95) 7.756 m³/s and has a base flow index (BFI) of 0.45. The mean flow of the Foss is 0.875 m³/s and has a Q95 of 0.072 m³/s and a BFI of 0.43.

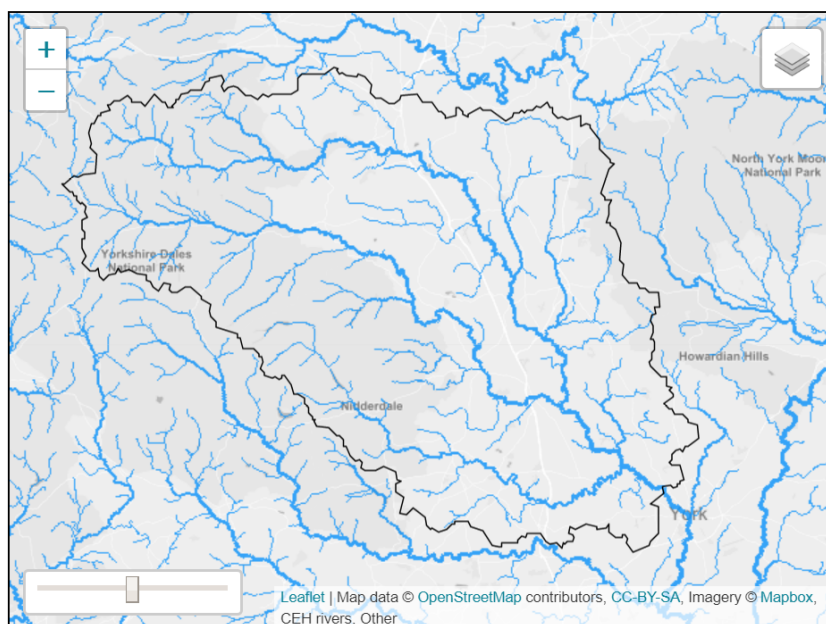


Figure 5.3. Ouse at Skelton catchment area extension. Image from © NERC (CEH) 2019. For Great Britain: Contains Ordnance Survey data © Crown copyright and database right 2019.

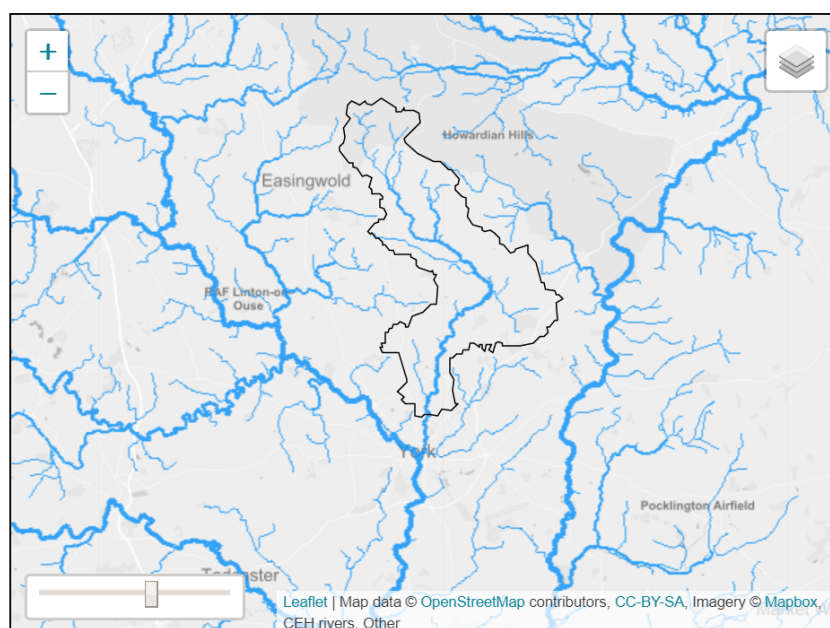


Figure 5.4. Foss at Huntington catchment area extension. Image from © NERC (CEH) 2019. For Great Britain: Contains Ordnance Survey data © Crown copyright and database right 2019.

The discharge of each RS was estimated as the addition of the receiving flow from the previous river/s section/s, from the runoff generated in their surrounding areas and from the WWTP discharge points (as indicate in Table 5.1). Runoff discharge was estimated

daily by multiplying the surface area extension of the RS's corresponding HZ by the daily rainfall of the year 2016 acquired from the University of York Department of Electronics weather station (<https://weather.elec.york.ac.uk/archive.html>). Some values of infiltration of annual precipitation (%) can be found for urban areas of different characteristics in the literature (e.g. multistore blocs, detached houses or semidetached houses, ranging between 11, 17 and 24 respectively, as per Pauleit and Duhme, (2000)). However, urban surfaces are very complex and runoff coefficients for different surface types are very different (Li *et al.*, 2018), therefore, in this study the very conservative assumption, where all rainfall is translated into runoff, was made based on the indications that runoff increases with increasing impervious cover (Li *et al.*, 2018). A potential analysis of the land cover composition to include different infiltration rates is envisaged.

The WWTP discharge was estimated by using an average wastewater production per capita per day of 135 L (estimate provided by Yorkshire Water Ltd) and multiplied by the population number served by each WWTP (Table 5.1).

5.2.3.2 River system monitoring campaign

Because ENP behaviour in aqueous suspension is heavily influenced by the physicochemical characteristics of the medium (Domingos, Tufenkji and Wilkinson, 2009; Zhang *et al.*, 2012; Quik *et al.*, 2014; Sharma *et al.*, 2014; Sani-Kast *et al.*, 2015a), the water body of each RS was parameterized with information gathered from a water quality monitoring campaign. The monitoring campaign was designed to provide data on the spatial and temporal variation in key water quality parameters. This was done by taking measurements once a month over a 6 months period (from the 1st of July until the 15th of December of 2016) over nine established monitoring sites (approximately one per RS). Initially, a full year monitoring campaign was planned but logistical problems shortened the campaign to six months. This campaign was designed with higher spatial resolution than the available information on water quality parameters published at the Environmental Agency's archive (<https://environment.data.gov.uk/water-quality/>).

The monitoring sites were strategically chosen based on their ease of access and position in relation to the three WWTP serving the city. They were located upstream and downstream of the WWTPs, before and after the two rivers join in the city centre, and at further locations to give sufficient spatial resolution to build water quality parameters and exposure concentration profiles. Table 5.1 lists the monitoring sites established, their

description and the RS in which they are located. Figure 5.2 indicates the locations of the sampling sites.

Table 5.2. List of monitoring sites along the rivers Ouse and Foss, their river section connections (RS) and description.

Monitoring site	River section	Description
F1. Strensall	Foss 1	Downstream of Wallbuts WWTP
F2. Earswick	Foss 2	Further downstream of Wallbuts WWTP
F3. Heworth	Foss 3	River Foss before passing the city centre
F4. Tower	Foss 4	Upstream of River Foss and Ouse junction
O1. A1237	Ouse 1	River Ouse upstream of Rawcliffe WWTP.
O2. Rawcliffe	Ouse 2	Downstream of Rawcliffe WWTP
O3. Skeldergate	Ouse 3	Upstream of River Foss and Ouse junction
O4. Millenium	Ouse 4	Downstream where the Foss joins the Ouse, upstream of Naburn WWTP
O5. Naburn	Ouse 5 Ouse 6	Downstream of Naburn WWTP

The parameters monitored were temperature (T), pH, dissolved oxygen (DO), electrical conductivity (EC), total suspended solids (TSS), dissolved organic carbon (DOC) and ionic content (Ca^{2+}). These parameters were chosen based on the identified parameters to have bigger influence on the ENPs fate and transport processes in surface waters (i.e. heteroaggregation, sedimentation and convective flow) (Praetorius, Scheringer and Hungerbühler, 2012; Clavier, Praetorius and Stoll, 2019).

Measurements of T, pH, DO and EC were taken directly at the monitoring sites using an Aquaread Probe (Aquaprobe® AP-2000). Where the sampling point could be easily accessed, the probe was directly submerged in the water body and three measurements taken. When no easy access to the water body was possible for direct measurement, grab water samples were collected in triplicate and measurements done in the sample container after thorough mixing. At each monitoring site, three 1 L samples replicates were collected and stored in PVC bottles for a later TSS analysis. In addition, at each site three 50 mL samples replicates were drawn into a 50 mL disposable syringe and filtered through a 0.45 μm glass-fibre syringe filters (Whatman®) into 250 ml conical

polypropylene centrifuge tubes (Falcon™) previously washed with a Nitric acid solution (10%), and stored in the cold (4°C) for DOC and ionic content analysis.

On arrival in the laboratory, the 1 L samples were filtered through a Buchner filtration system with 0.7 µm glass-fibre filter (GF/F) (Whatman®) (pre-combusted, 450 °C, 4 h). The filters with the remaining filtrate were then combusted overnight at 103-105°C for later estimation of the total suspended solid weight. Aliquots of the 50 ml samples were analysed for DOC on the following day using an Elementar Vario Toc total organic carbon analyser. The remaining sample volumes were acidified to 5% by volume with HNO₃ and stored at 4°C for a later analysis of cations using a Thermo iCAP 7000 ICP-OES.

Statistical analysis of the monitoring data was conducted in R (R Core Team, 2014). To determine whether significant spatial differences of the measurements taken (i.e. [Ca²⁺], DOC and TSS) existed between the two rivers and during the different months, two way ANOVA tests were conducted (Tables A2.9 to A2.14 of the Appendix).

The concentration of DOC together with dissolved calcium concentration ([Ca²⁺]) were used as indicators for the determination of heteroaggregation attachment coefficient (α_{hetero}) (Praetorius et al., 2014) as described in Table 5.1.

Table 5.3. Assigned attachment efficiency (α_{hetero}) values according to the concentration of calcium ([Ca²⁺]) and the dissolved organic carbon (DOC) in water.

[Ca ²⁺] (mg/L)	[DOC] (mg/L)	α_{hetero}
<35	-	0.001
35-50	≥3	0.001
35-50	<3	0.01
50-65	≥2.5	0.01
50-65	<2.5	0.1
65-80	≥2.0	0.1
65-80	<2	1
≥80	-	1

Temperature and SPM concentration affect the collision rate within the heteroaggregation equations (as described in section 2.5.1).

5.2.3.3 Nanoparticle characteristics

The TiO₂ ENPs considered in this study were assumed to be released from four different product types: sunscreens, makeup, toothpaste and outdoor paint. During their use phase and along the release pathway until they enter the river waters, the ENPs likely undergo a series of transformations, mainly involving aggregation processes; therefore, it was assumed that rather than being discharged in their freely dispersed form, the ENPs enter the river sections in a homo-aggregated state. It was also assumed that the primary TiO₂ NPs are uncoated and spherical. Information on the sizes expected for these aggregates was obtained from several experimental studies where ENP leachates from such products have been analysed to characterize the ENP sizes (Keller et al., 2014a; Kaegi et al., 2008; Weir et al., 2012; Lewicka et al., 2011). The initial size of the aggregated TiO₂ ENPs was set to be 25 nm (particle diameter) for the ENPs released from makeup and sunscreen (Keller *et al.*, 2014a), 450 nm for those released from toothpaste (Kaegi et al., 2008; Weir et al., 2012), and 150 nm for those released from outdoor paints (Kaegi *et al.*, 2008). The shape of the aggregated TiO₂ NPs (and the SPM) is approximated by spherical particles. More details on the TiO₂ ENP assumed properties are provided in the Appendix (Table A2.4).

The mass flux of TiO₂ ENPs emitted was input for each day of the six month simulation period as mass per product type (mg day⁻¹). Of the products studied, makeup, toothpaste and sunscreen were considered to be emitted with the wastewater effluent from the three WWTPs serving York and, therefore, only discharged into the RSs in which the WWTP discharge points are located (i.e. Ouse 2, Ouse 6 and Foss 1). The TiO₂ ENP contained in the outdoor paints on the other hand, are considered to be released with runoff and discharged at the beginning of each RS.

The emission values were derived from the results obtained in the previous chapter through the application of the urban ENP emissions model. We assumed negligible upstream ENP loads for both rivers (Ouse1 and Foss1), and the incoming TiO₂ ENP mass flow was transformed to a particle flow. All model calculations were performed on the basis of particle numbers, both for the TiO₂ NPs and the SPM.

5.3 Results and discussion

5.3.1 Measured physical and chemical characteristics

Measured values of the most relevant parameters affecting the fate and transport processes of TiO₂ ENPs (i.e. DOC, calcium ([Ca²⁺]) and SPM concentration, here measured as total suspended solids (TSS)), over the monitored period and along the monitoring sites, are summarized in Figures 5.5, 5.6 and 5.7 (and in Appendix 2, Tables A2.6 to A2.8).

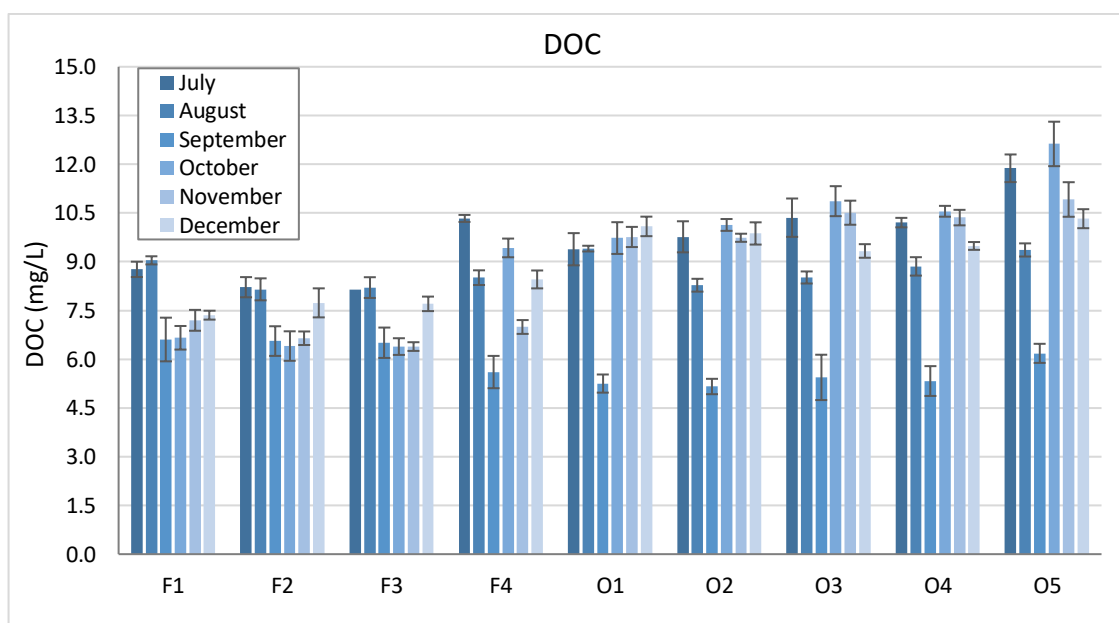


Figure 5.5. Arithmetic mean of the measured DOC concentrations for the Foss (F) and Ouse (O) sampling sites over the six months monitoring period (July to December 2016), with their corresponding standard deviations estimated from the three measured replicates.

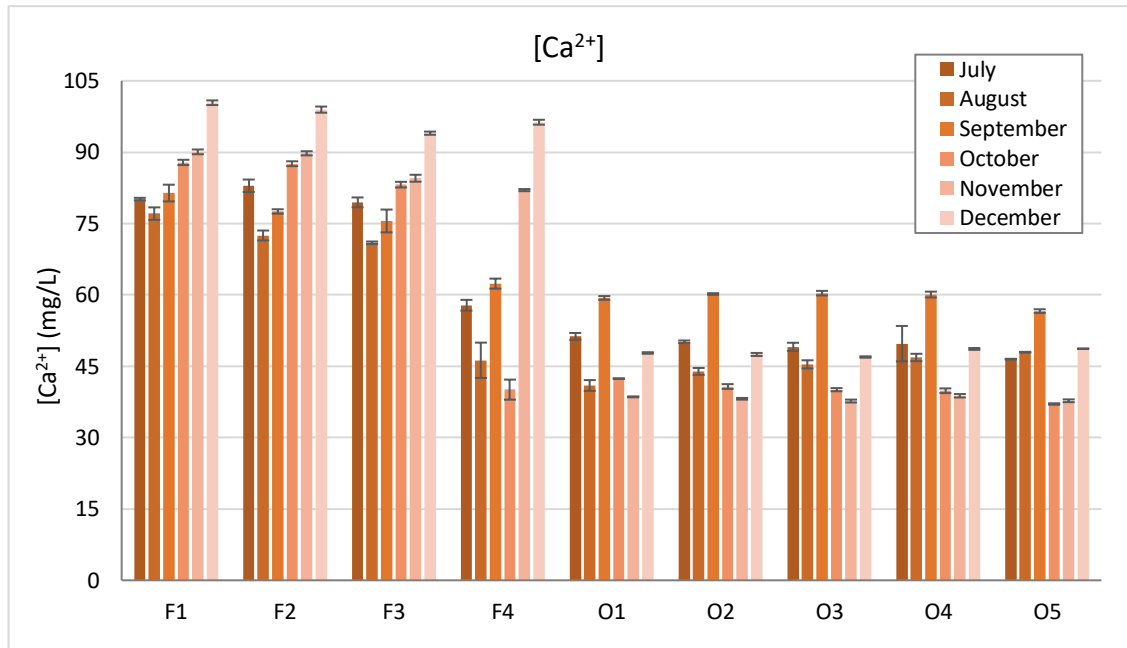


Figure 5.6. Arithmetic mean of the measured dissolved Calcium concentrations as (Ca^{2+}) for the Foss (F) and Ouse (O) sampling sites over the six month monitoring period (July to December 2016), with their corresponding standard deviations estimated from the three measured replicates.

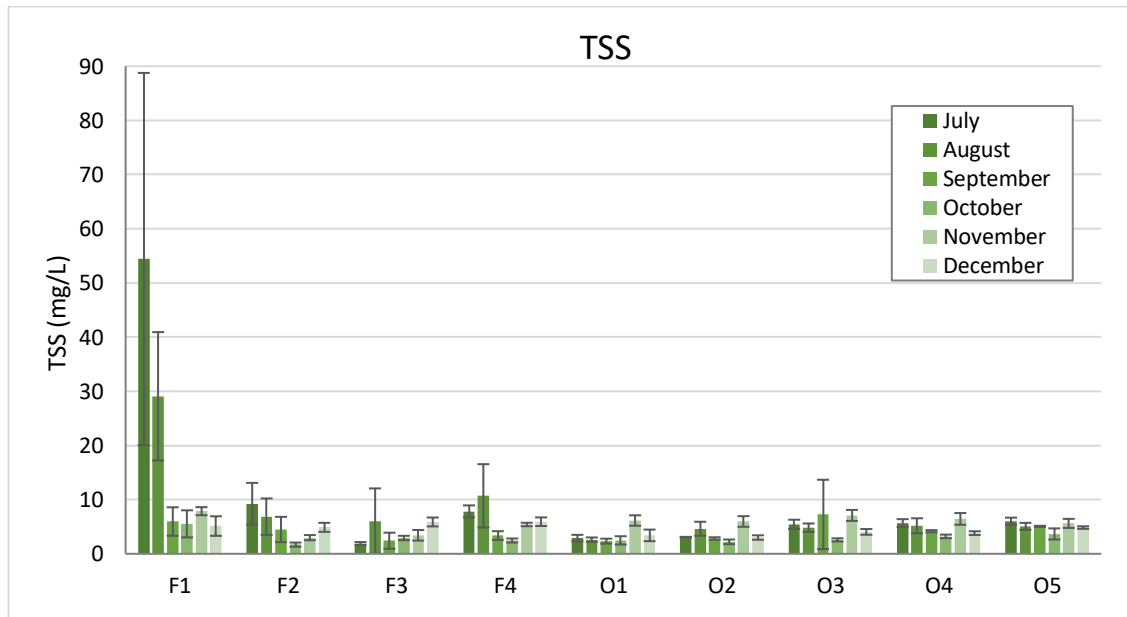


Figure 5.7. Arithmetic mean of the measured total suspended solids (TSS) concentrations for the Foss (F) and Ouse (O) sampling sites over the six month monitoring period (July to December 2016), with their corresponding standard deviations estimated from the three measured replicates.

The spatial and temporal variations of these parameters will influence the final exposure levels estimated by the model by affecting the extent of specific fate processes such as the ones simulated here (i.e. heteroaggregation and sedimentation).

Firstly, statistically significant differences ($p < 0.05$) in DOC and calcium concentrations between both rivers (Ouse sites (O) and Foss sites (F)) were observed, these variables also varied over time. For SPM levels (estimated as total suspended solids (TSS)), no significant differences between the two rivers were found. Generally, higher DOC concentration values were found in the Ouse compared to the Foss (except for the month of August, where Ouse DOC levels were lower than in the Foss). The opposite trend was found for the calcium concentrations: calcium concentrations in the Foss were significantly higher than in the Ouse. Since DOC and calcium concentration levels have an influence on the attachment efficiency (α_{hetero}) of the ENPs (see Table 5.3), different heteroaggregation and sedimentation rates would be expected in both rivers. Generally, while the threshold of influence of DOC is surpassed in both rivers (DOC is $> 3\text{mg/l}$ for most of the months and monitoring sites), the Foss has higher calcium concentrations, and , thus, would be expected to have higher heteroaggregation rates ($\alpha_{hetero} = 1 / 0.001$) compared to the Ouse ($\alpha_{hetero} = 0.001 / 0.01$).

Secondly, in terms of differences between monitoring sites within each river, a Tukey HSD test with sampling site as factor for the three parameters was performed. The results showed that for the Ouse no significant differences between sampling sites were found for the Calcium and DOC concentrations ($p > 0.05$), but that for the Foss the Calcium levels of the different sampling sites were significantly different ($p\text{-value} < 0.05$) (Section 2.3 of the Appendix 2).

Finally, in terms of temporal variation, a seasonal trend in the values was found for the three variable, mainly observed between the warmer months (i.e. July and August) and the colder months (i.e. November and December). Generally, July and August have higher TSS and DOC concentrations than November and December, and the opposite situation is found for calcium concentrations. However, these trends and their level of significance is river and parameter dependent. According to these monthly variations, higher heteroaggregation and potential sedimentation would be expected for the months of November and December for the river Foss ($\alpha_{hetero} = 1$) and for the month of September in the case of the river Ouse ($\alpha_{hetero} = 0.01$).

Further parameters, such as discharge and ENPs emission loads, will also influence the estimation of concentrations and their temporal and spatial variation are presented in Figures 5.8, 5.9 and 5.10.

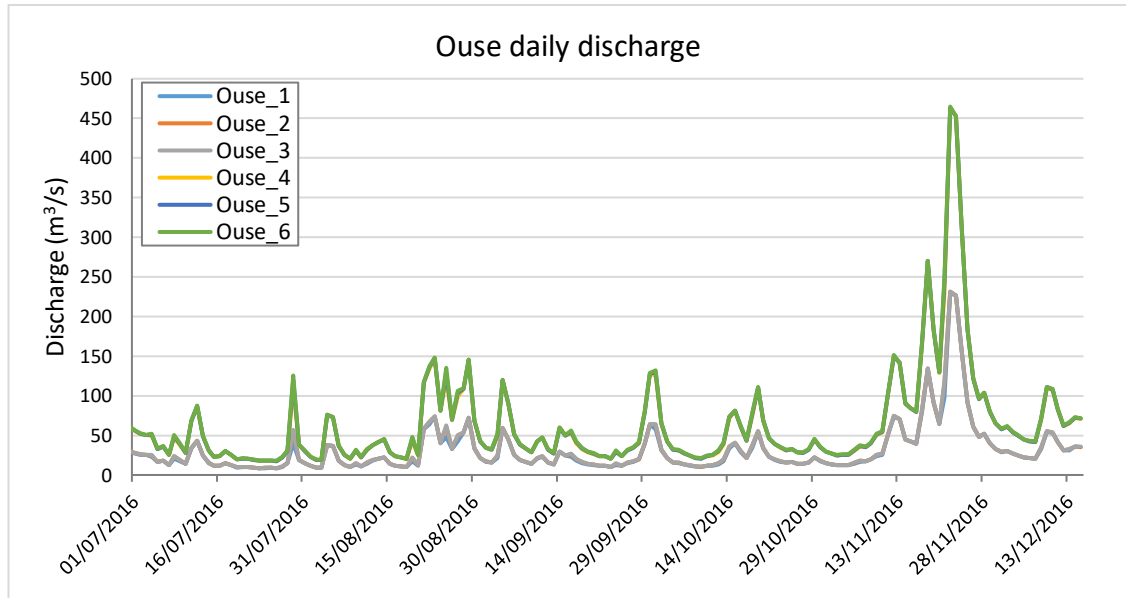


Figure 5.8. Daily discharge of the delimited RS of the river Ouse over the simulated period (1st July to 15th December 2016) obtained as described in Section 5.2.3.1 using data from NRFA (<https://nrfa.ceh.ac.uk/>).

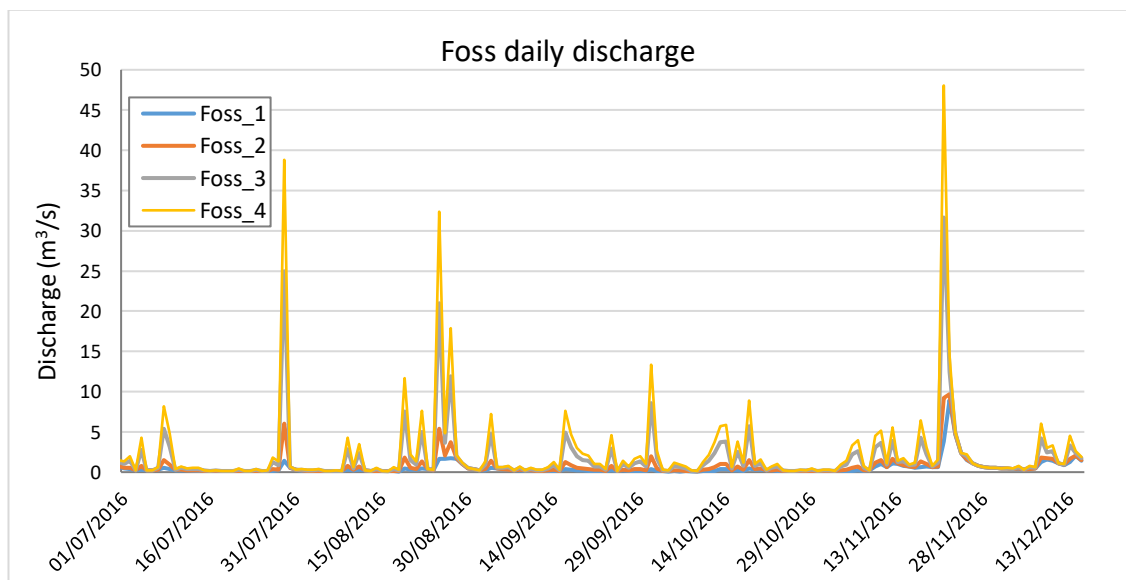


Figure 5.9. Daily discharge of the delimited RS of the river Foss over the simulated period (1st July to 15th December 2016) obtained as described in Section 5.2.3.1 using data from NRFA (<https://nrfa.ceh.ac.uk/>).

The discharge in the river Ouse is around ten times higher than in the river Foss, and the river Ouse is generally wider and deeper than the Foss, meaning that higher dilution factors of the emitted particles will be expected for the Ouse. Within the Ouse, discharge increases with distanced downstream (from Ouse 1 to 6). The discharge at the start of RS Ouse 1 is approximately half of that in Ouse 6. The highest discharge in 2016 in the river Ouse was recorded in November followed by August. For the Foss, the discharge also increases with distance downstream by approximately a factor of five from upstream to downstream. This effect would be explained by the very conservative assumption made in this model, which translates all rainfall into runoff. A comparison of the runoff catchment areas of each RS is presented in Table 5.10, giving an indication of how much discharge should increase by in these rivers. The highest discharge in the river Foss was measured in the month of November, followed by July and August.

River Section	HZ	Surface area runoff catchment (Km ²)
Ouse 1	HZ1	10.26
Ouse 2	HZ2	6.04
Ouse 3	HZ3	0.82
Ouse 4	HZ4	2.18
Ouse 5	HZ5+HZ6	4.03
Ouse 6	HZ11+HZ12	2.37
Foss 1	HZ10	0.28
Foss 2	HZ9	1.80
Foss 3	HZ8	7.46
Foss 4	HZ7	5.45

Figure 5.10. List of RSs and their corresponding runoff catchment areas (connecting delimited HZs).

The emissions of TiO₂ ENP to York's river system considered in this study are the estimated product-specific TiO₂ ENP loads of the average simulated scenario described in Chapter 4. As discussed in Chapter 3, the dominant source of TiO₂ emissions from the ones considered in the York study (i.e. sunscreen, toothpaste, makeup and outdoor paint), is the use of sunscreen in the worst and average scenarios, but the temporal variation of their emissions is assumed to be dominated by the runoff emissions coming from outdoor paints, and therefore, controlled by the weather. In Figures 5.11 and 5.12 we present the profiles of predicted total ENP emissions (considering the contributions from all products), for both rivers (Ouse and Foss respectively) and each of their RSs over time.

As already shown in Chapter 4, the runoff related ENP loads are rainfall intensity dependent and will only happen on rainy days, on the other hand, WWTP emissions are constant. This effect can be observed in Figures 5.11 and 5.12, on the dry days a constant emission level is estimated, while on rainy days peaks of emission appear and are proportional to the intensity of the rainfall event.

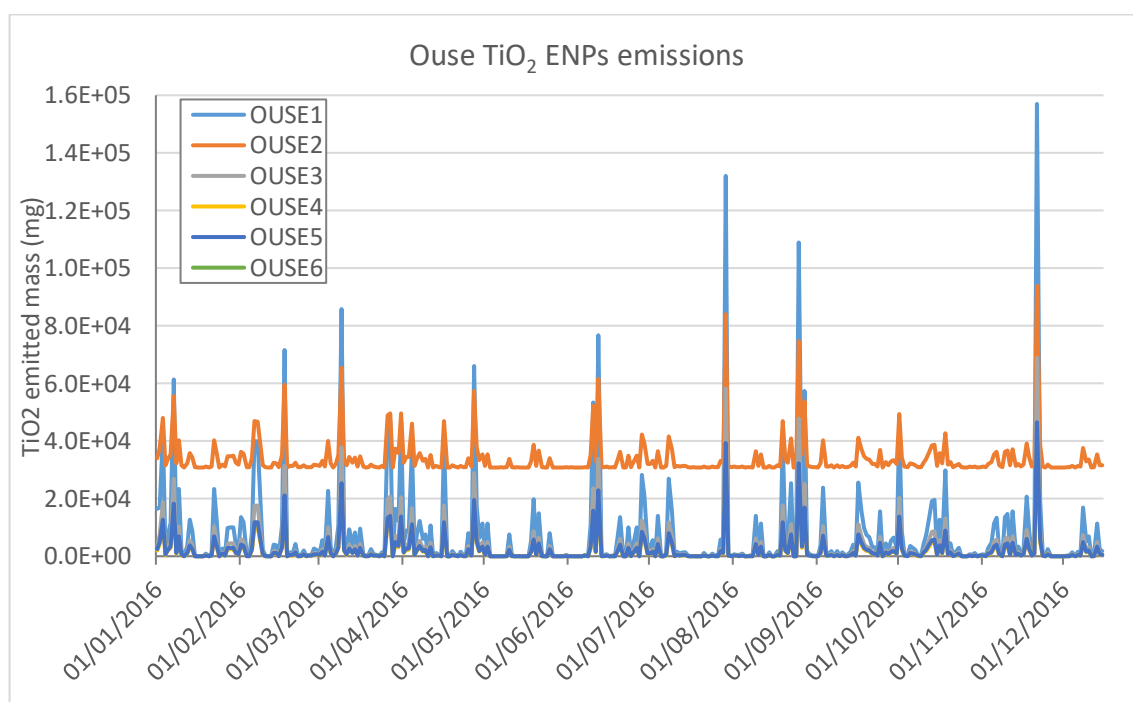


Figure 5.11. Daily TiO₂ ENP emissions to the delimited RSs of the river Ouse over the simulated period (1st of July to 15th of December 2016)

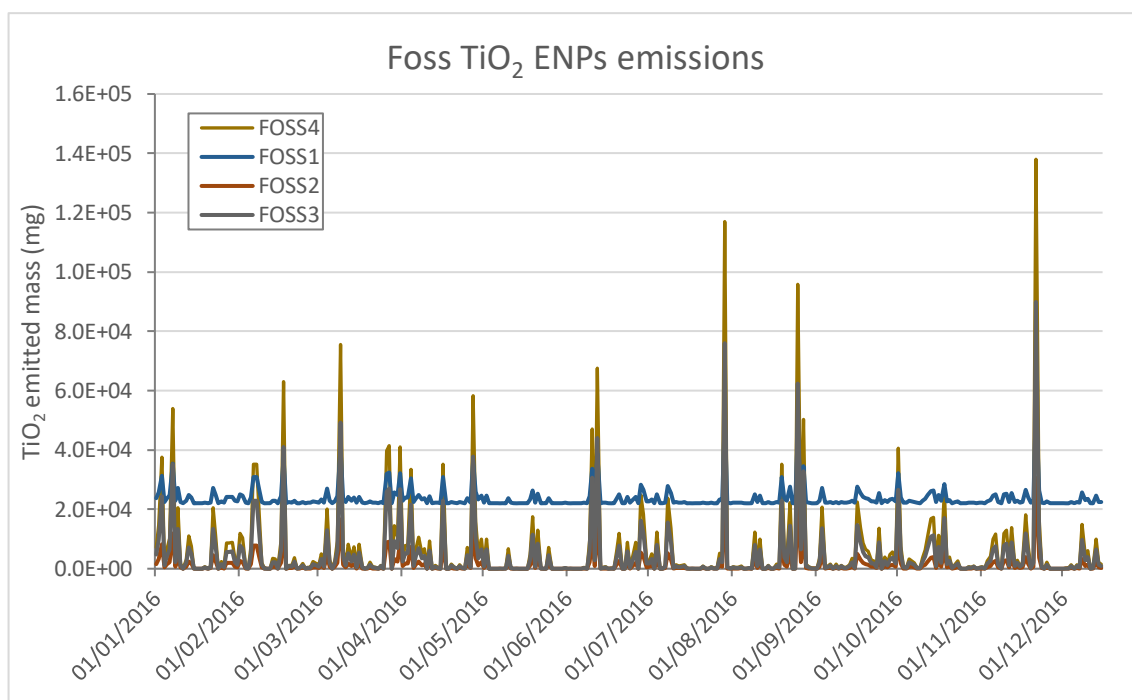


Figure 5.12. Daily TiO₂ ENP emissions to the delimited RSs of the river Foss over the simulated period (1st of July to 15th of December 2016)

As shown in Figures 5.11 and 5.12, the rivers Ouse and Foss receive emissions of the same order of magnitude, although the emissions to the river Ouse are slightly higher than those of the river Foss. The highest emissions were estimated for the rainiest dates of the studied period (i.e. 21st of November, 29th of July and 25th of August).

5.3.2 TiO₂ ENP concentrations in York's river system

The concentrations of TiO₂ ENPs estimated over the selected time period (i.e. from the 1st of July until the 14th of December of 2016) and in the rivers Ouse and Foss, are presented in Figures 5.13 to 5.14 and 5.15 to 5.16, respectively. In these figures, the concentrations of the freely dispersed and SPM-bound TiO₂ ENPs are also plotted for the flowing water compartment and the concentration of total TiO₂ ENPs are shown for the sediment compartment. Calculations were performed with a time resolution of 2 minutes and a spatial resolution of 750 m.

Free TiO₂ ENPs in flowing water in river Ouse

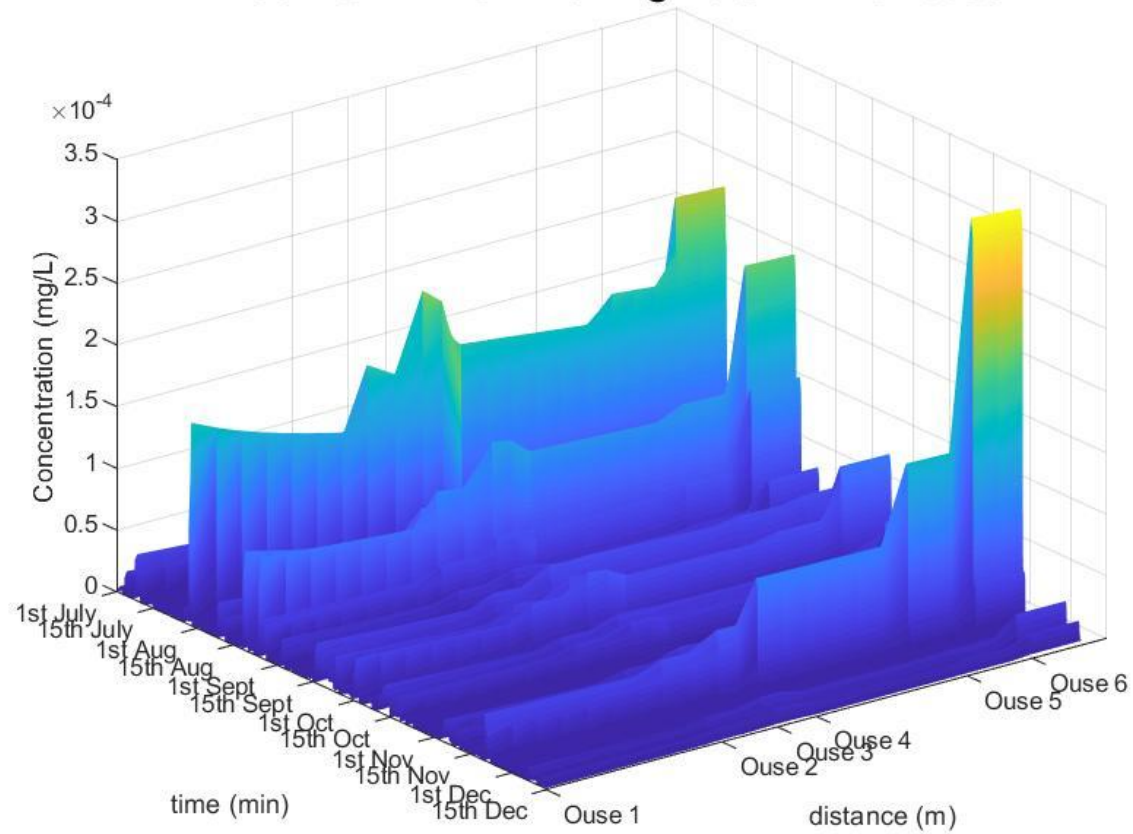


Figure 5.13. Exposure profiles of freely dispersed TiO₂ ENPs (Free) in the flowing water of the modelled extension of the river Ouse over the simulated period (from the 1st of July until the 15th of December of 2016)

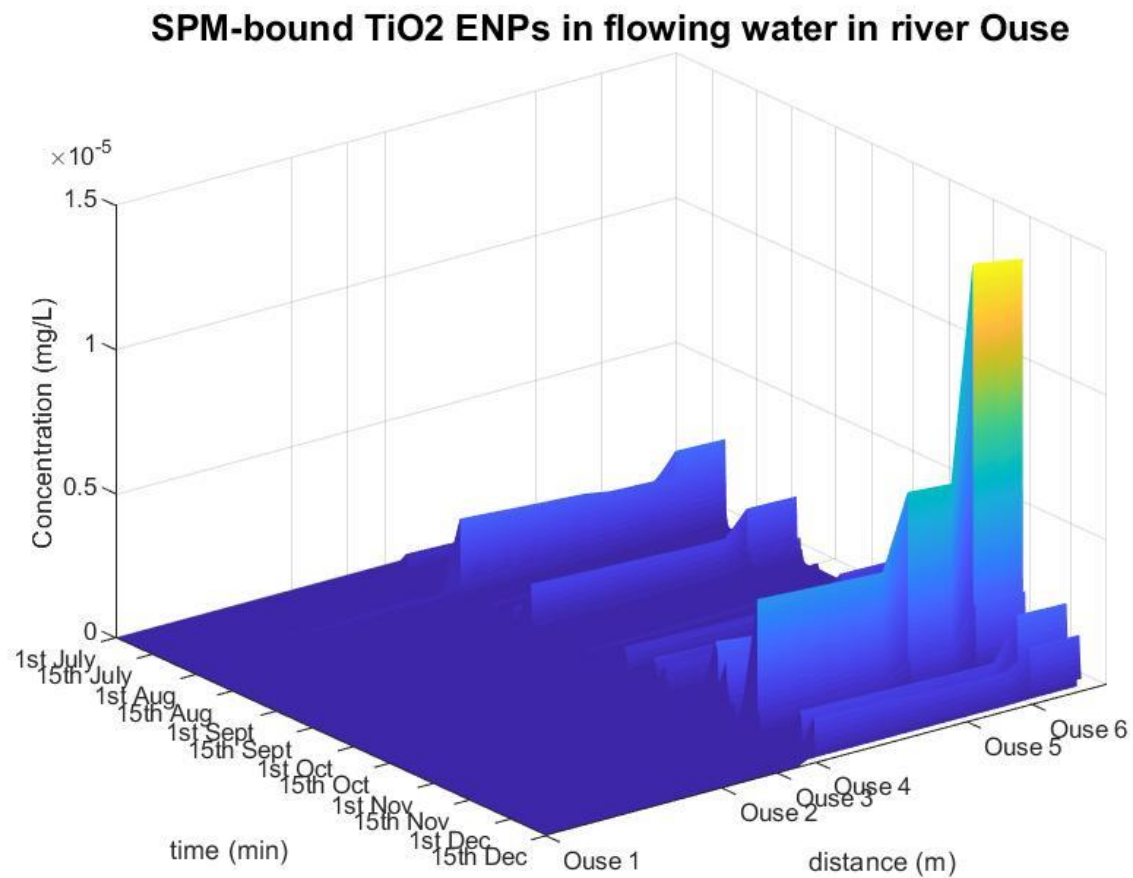


Figure 5.14. Exposure profiles of TiO₂ ENPs heteroaggregated with SPM (SPM-bound) in the flowing water of the modelled extension of the river Ouse over the simulated period (from the 1st of July until the 15th of December of 2016)

TiO₂ ENPs in sediment in river Ouse

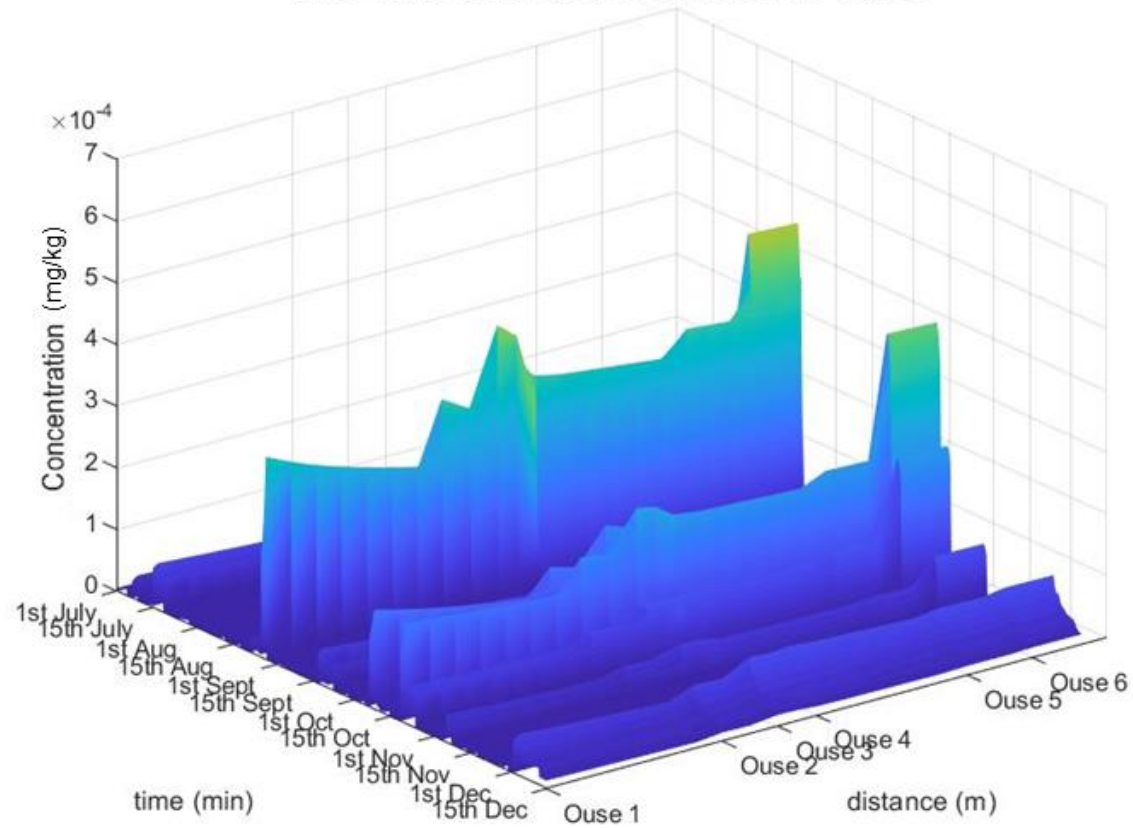


Figure 5.15. Exposure profiles of TiO₂ ENPs in the sediment compartments of the modelled extension of the river Ouse over the simulated period (from the 1st of July until the 15th of December of 2016)

Free TiO₂ ENPs in flowing water in river Foss

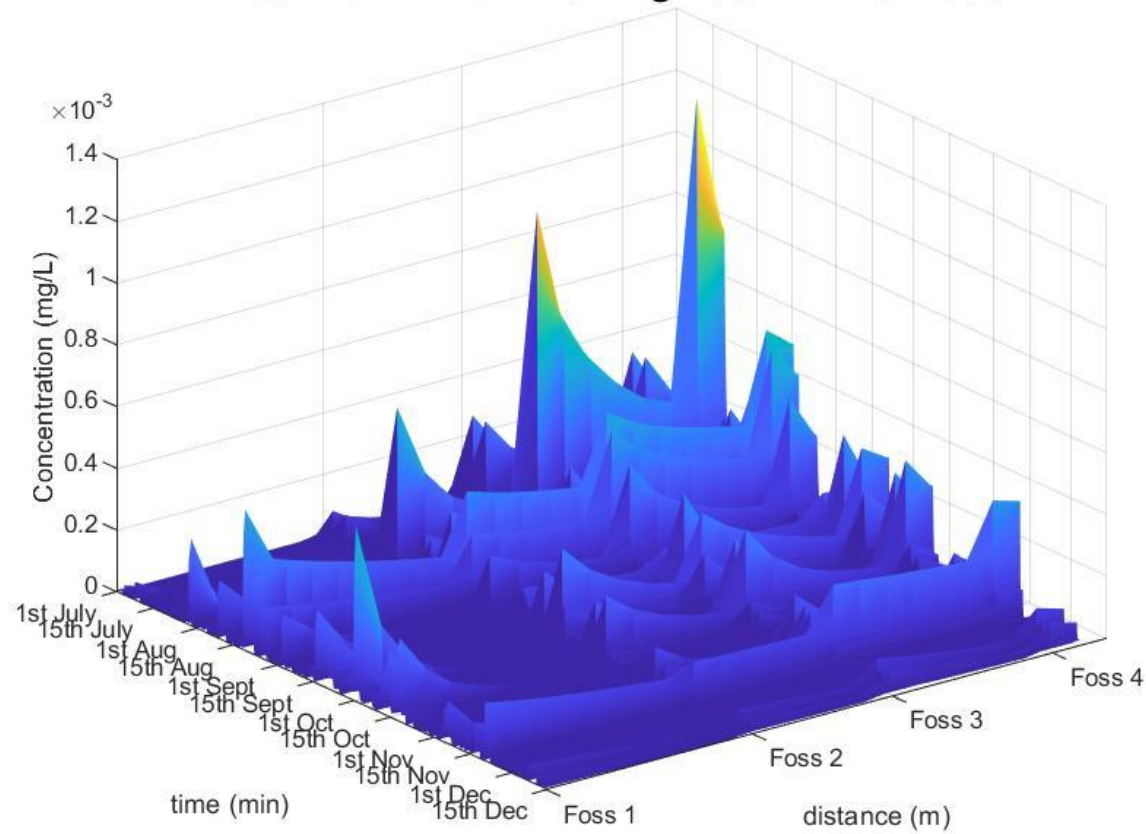


Figure 5.16. Exposure profiles of freely dispersed TiO₂ ENPs (Free) in the flowing water of the modelled extension of the river Foss over the simulated period (from the 1st of July until the 15th of December of 2016)

SPM-bound TiO₂ ENPs in flowing water in river Foss

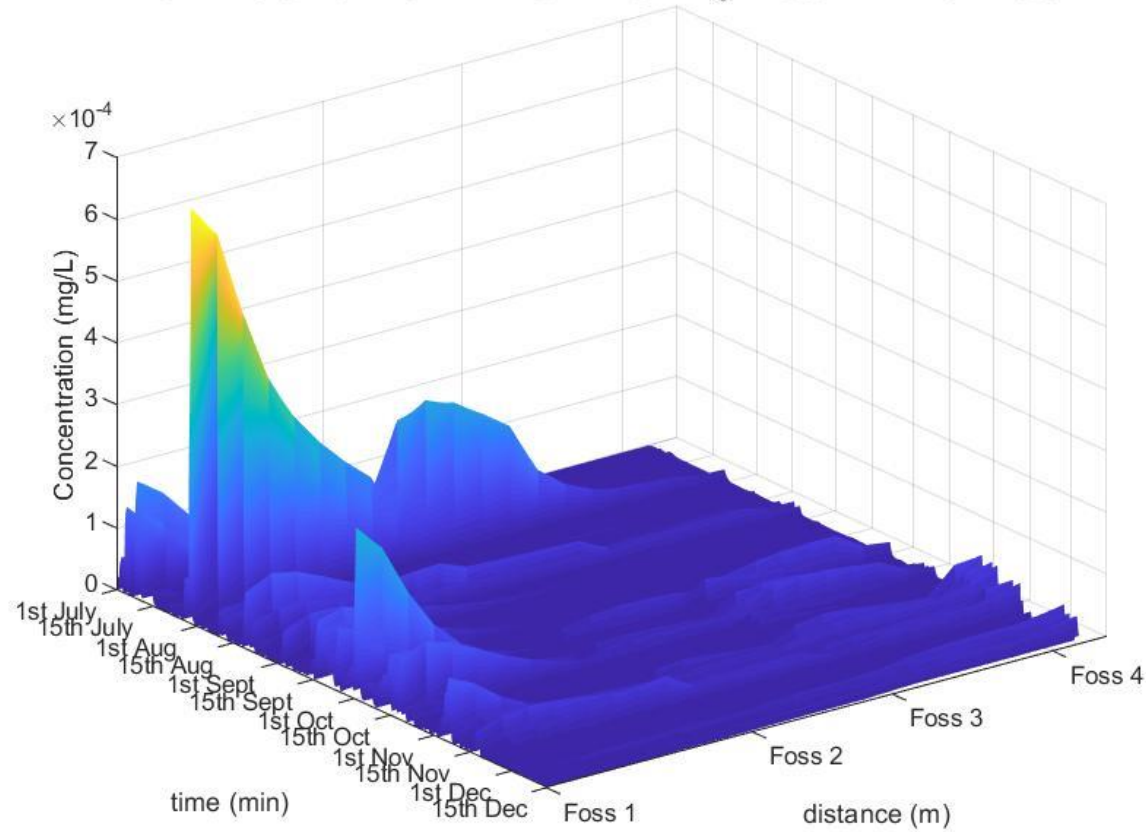


Figure 5.17. Exposure profiles of TiO₂ ENPs heteroaggregated with SPM (SPM-bound) in the flowing water of the modelled extension of the river Foss over the simulated period (from the 1st of July until the 15th of December of 2016)

TiO₂ ENPs in sediment in river Foss

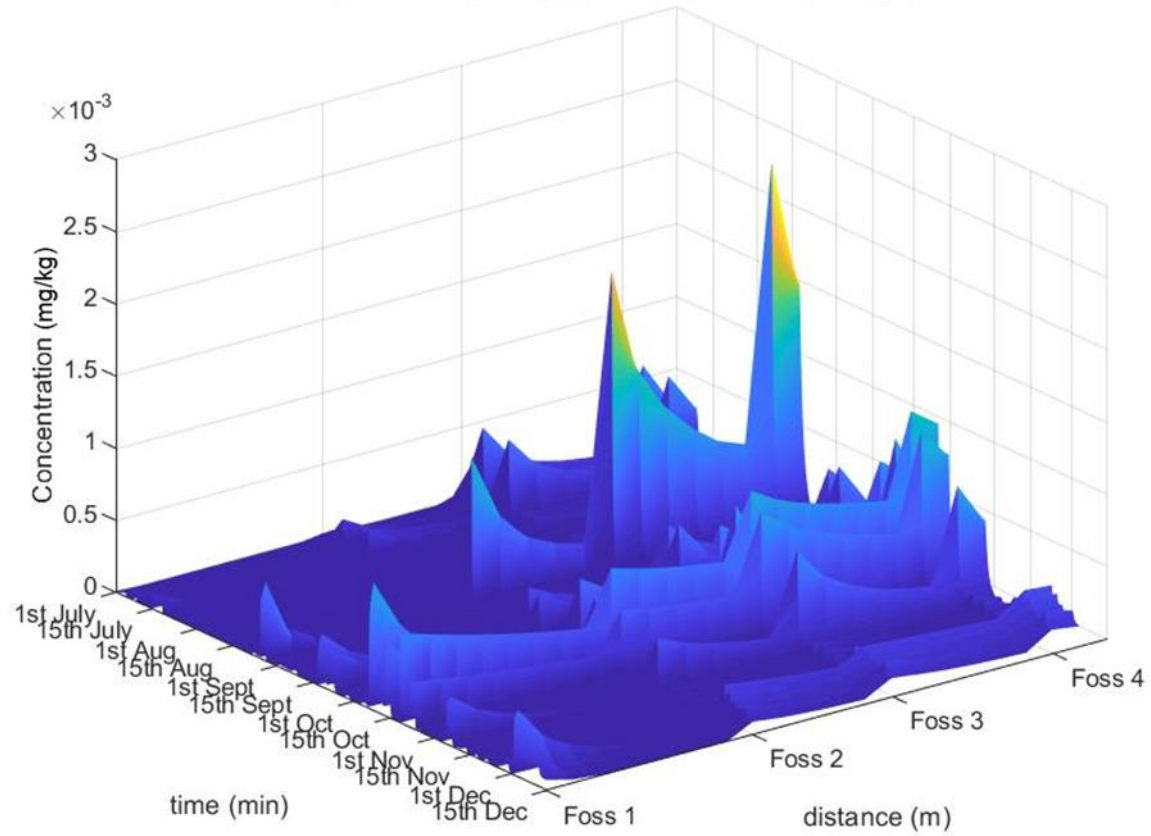


Figure 5.18. Exposure profiles of TiO₂ ENPs in the sediment compartments of the modelled extension of the river Foss over the simulated period (from the 1st of July until the 15th of December of 2016)

Figures 5.16 to 5.18 present the total distribution of the estimated exposure concentrations of freely dispersed and SPM-bound TiO_2 ENPs in flowing water and total TiO_2 ENPs in sediment along each river section over the simulated period. The monthly maximum (Max), median, 95th and 5th percentile of the exposure concentrations (mg/L) for each RS is provided in the Appendix 2 (Tables A2.9 to 2.11).

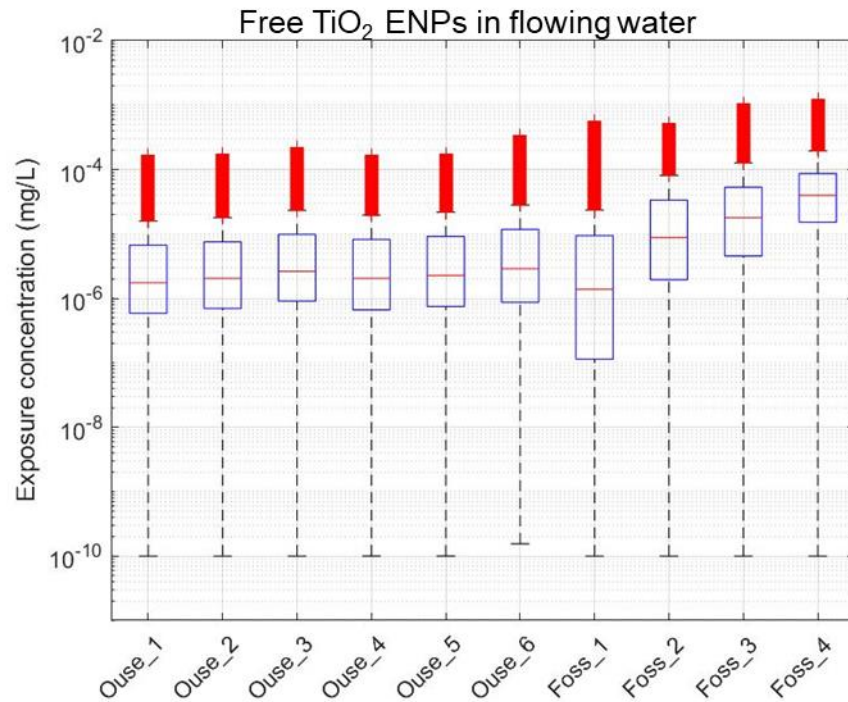


Figure 5.19. Box and whisker plots of the estimated ranges of TiO_2 ENPs concentrations in the flowing water of all RSs of both rivers (i.e. Ouse 1 to 6 and Foss 1 to 4). On each box, the central mark indicates the median, and the bottom and top edges of the box indicate the 25th and 75th percentiles, respectively. The whiskers extend to the most extreme data points not considered outliers, and the outliers are plotted individually using the '+' symbol.

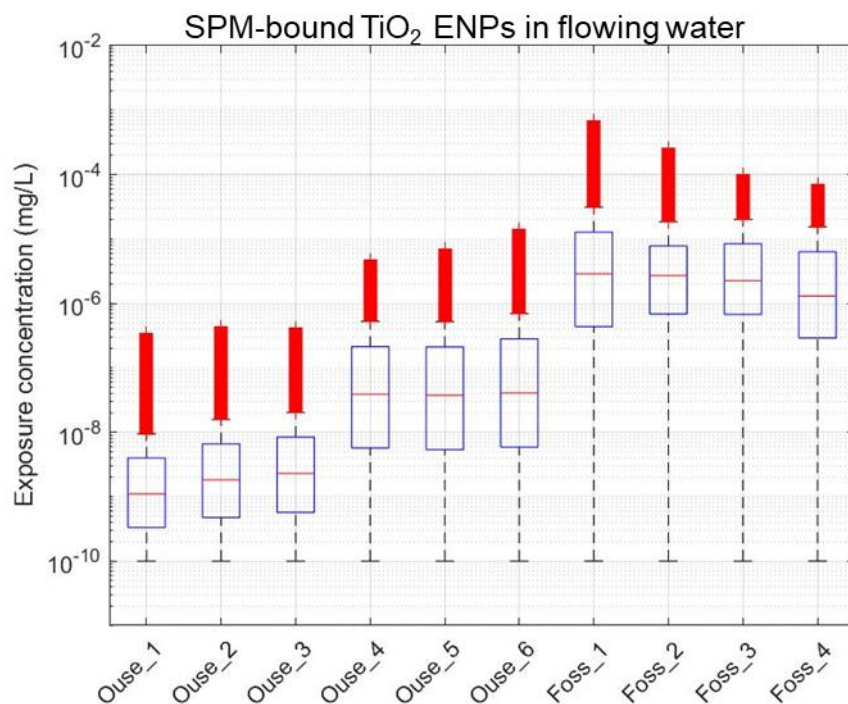


Figure 5.20. Box and whisker plots of the estimated ranges of SPM-bound TiO₂ ENPs concentrations in the flowing water compartment of all RSs of both rivers (i.e. Ouse 1 to 6 and Foss 1 to 4).

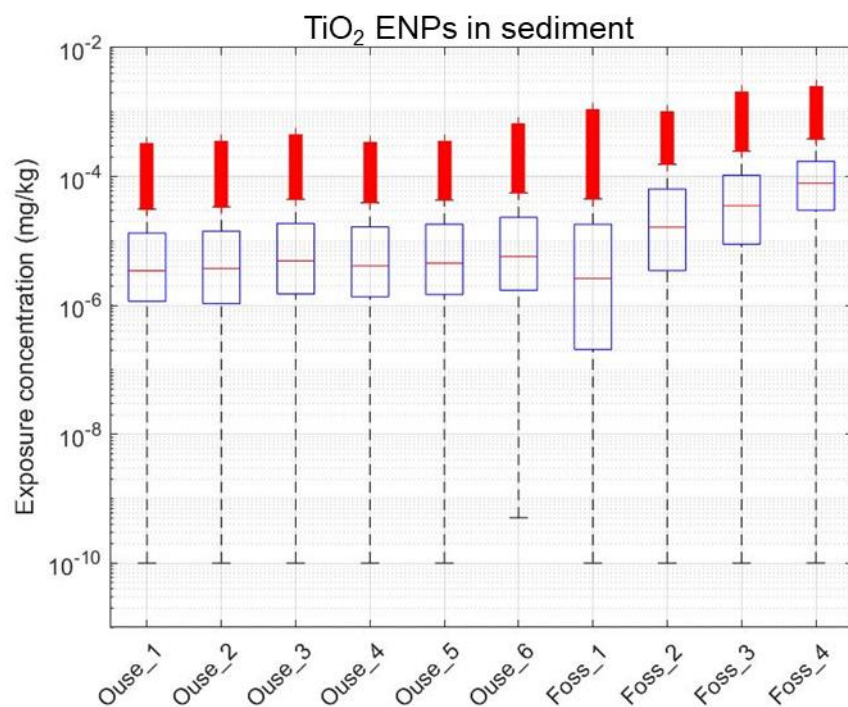


Figure 5.21. Box and whisker plots of the estimated ranges of TiO₂ ENPs concentrations on the sediment compartment of all RSs of both rivers (i.e. Ouse 1 to 6 and Foss 1 to 4).

The estimated concentrations were highly variable. In the river Ouse, concentrations ranged from $1.81 \cdot 10^{-14}$ ng/L to $3.33 \cdot 10^2$ ng/L, while in the Foss varied from $5.8 \cdot 10^{-10}$ ng/L to $1.27 \cdot 10^3$ ng/L. Generally, the median concentrations of freely dispersed TiO₂ ENPs in flowing water range between 0.93 ng/L and 5.14 ng/L for the Ouse and $2.21 \cdot 10^{-4}$ ng/L and 65 ng/L for the Foss.

The estimated median concentrations of the TiO₂ ENPs attached to SPM (SPM-bound ENPs) in flowing water were up to four orders of magnitude lower than the freely dispersed ENPs in the Ouse RSs. In the RSs of the river Foss, however, similar concentrations of the freely dispersed and SPM-bound ENPs in flowing water were predicted. This suggests that in the river Ouse the probabilities of SPM-ENP interactions were lower or that less effective interactions occur there compared to the river Foss. It can be explained by the described heteroaggregation trends predicted in Section 5.3.1 from the monitoring data. The attachment efficiency values (α_{hetero}) assigned for the Ouse are lower than for the Foss due to the lower calcium concentration levels measured in the Ouse (In the Foss α_{hetero} ranges between 1 and 0.001, while in the Ouse α_{hetero} goes from 0.001 up to 0.01). Residence times of ENPs in the Foss are also higher than in the Ouse, therefore increasing the probability of ENP-SPM interactions in the Foss.

From the estimated data, and as observed in Figure 5.16, maximum exposure levels (hot spots) for the Foss are observed in the downstream river sections (i.e. Foss 3 and Foss4) and during the month of July, going up three orders of magnitude from the median exposure concentrations of the river ($\mu\text{g/L}$). This spatial distribution of exposure is due to spatial trends of emissions along the river Foss, since Foss 3 and Foss 4 receive the highest levels of runoff emissions (Figure 5.12). Temporally, the highest exposure levels along the period studied coincide with the days where emissions were estimated to reach peak levels (i.e. 21st of November, 29th of July and 25th of August).

For the river Ouse (Figure 5.13), exposure hot spots were also observed for the downstream RSs, which in this case are the RSs receiving lower ENPs emissions. Therefore, the Ouse's exposure profile suggests that in this river, the effect of advective flow transport dominates ENPs fate, smooths the incoming emissions and promotes ENPs accumulation downstream (i.e. residence times are much lower than in the Foss), which again can be explained by the higher discharge volumes causing faster flows and lower residence times.

The estimated concentrations of free TiO₂ ENPs in flowing water predicted here fall within the same ranges of PECs estimated by other modelling approaches performed for other rivers (Table 5.4). The differences between models reflect the underlying assumptions about the considered ENP sources, release amounts, pathways, and time periods. Although the comparison does not serve as a model validation, it suggests that the modelling approach used here predicts average concentrations within a reasonable range. Furthermore, while we are able to predict similar PEC values, this model provides a much wider perspective into the ENPs emissions, providing information about the ENPs fate, transport and distribution between sub compartments of the river over time.

Table 5.4. Summary of predicted environmental concentrations (PEC) in surface water of TiO₂ ENPs reported in the literature. Source: adapted from (Peters et al., 2018).

TiO₂ ENPs (µg/L)	Method	Matrix	Year and reference
0.7–16	Model	Surface water	(Nicole C. Mueller and Nowack, 2008)
0.012–0.057	Model	Surface water EU	(Gottschalk <i>et al.</i> , 2009)
0.002–0.010	Model	Surface water US	(Gottschalk <i>et al.</i> , 2009)
0.016–0.085	Model	Surface water CH	(Gottschalk <i>et al.</i> , 2009)
1.45	Model	Surface water	(O’Brien and Cummins, 2010)
0.0027–0.27	Model	Surface water	(Musee, 2011)
8.8	Model	Surface water	(Johnson <i>et al.</i> , 2011)
0.01–1.6	Model	Surface water	(Gottschalk and Nowack, 2011b)
0.55–6.48	Analytical	Surface water	(Neal <i>et al.</i> , 2011)
0.7–24.5	Model	Surface water	(Silva <i>et al.</i> , 2011)
0.4–1.4	Model	Surface water EU	(Sun <i>et al.</i> , 2014)
0.54–3.0	Model	Surface water CH	(Sun <i>et al.</i> , 2014)
0.0006–0.1	Model	Surface water	(Gottschalk <i>et al.</i> , 2015)
0.0002–5	Model	Surface water	(Good <i>et al.</i> , 2016)
2.2	Analytical	Surface water	(Donovan <i>et al.</i> , 2016)
0.19–4.4	Model	Surface water	(Sun <i>et al.</i> , 2016b)

5.3.3 TiO₂ ENPs distribution within the river

As shown in the previous section, once ENPs enter the river system, they will distribute between the different surface water compartments (i.e. flowing water, stagnant water and sediment).

Figure 5.22 and 5.23 summarizes the distribution of the ENPs concentration through the river compartment as percentage of the total exposure along the rivers Ouse and Foss, respectively. The maximum concentrations for the six-month period simulated were used to construct these profiles.

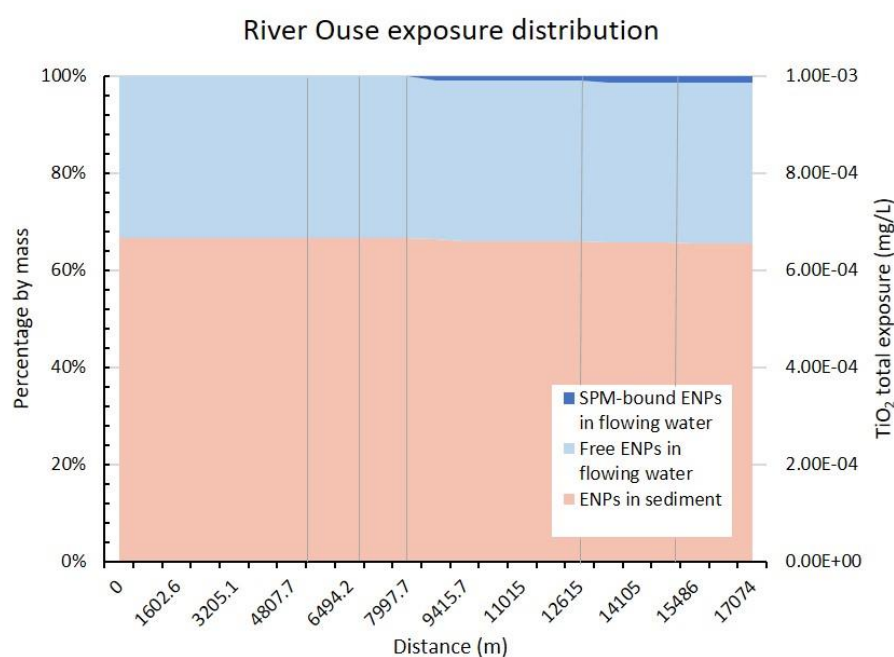


Figure 5.22. Mass distribution of the different forms of TiO₂ ENPs (i.e. Free and SPM-bound) in the three river compartments (flowing water, stagnant water and sediment) along the river Ouse.

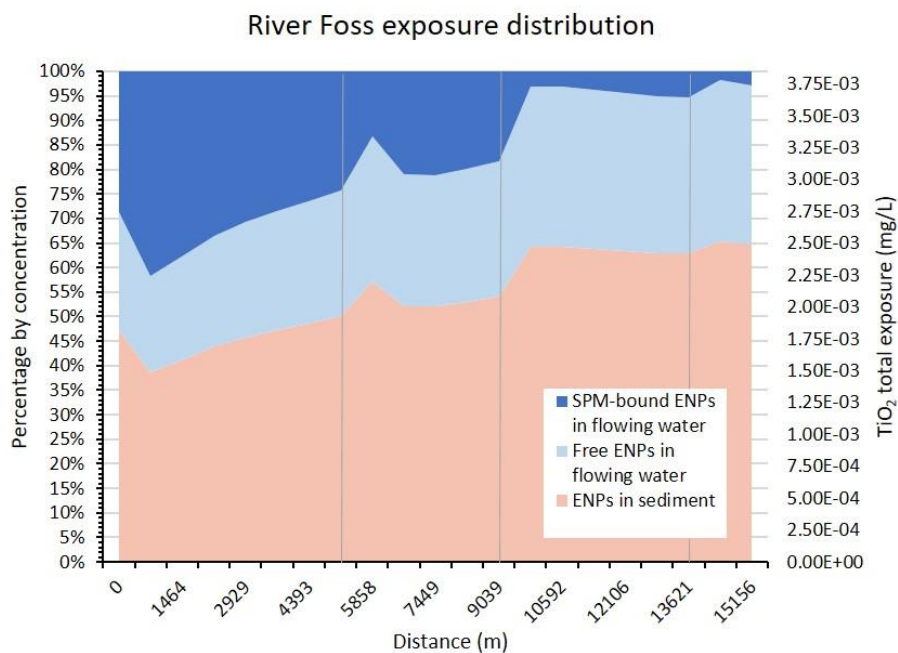


Figure 5.23. Mass distribution of the different forms of TiO_2 ENPs (i.e. Free and SPM-bound) in the three river compartments (flowing water, stagnant water and sediment) along the river Foss.

Different distribution patterns were observed for both rivers. As pictured in Figure 5.23 a third of the ENPs in the river Ouse are transported into the sediment upon emission (67%) and the fraction of ENPs bound to SPM in the flowing water is almost negligible. For the Foss, 47% of the TiO_2 ENPs are predicted to be transported in the most upstream reach into the sediment and from the particles remaining in the water column (flowing water), 25% to remain freely dispersed in the flowing water while 28% are predicted to be attached to SPM. Along the river Ouse, the predicted ENP distribution profile remains almost unchanged from upstream to downstream. However, in the Foss, a decrease of the fraction of SPM-bound ENPs in flowing water is predicted along the river from upstream to downstream. This is due to sedimentation processes. In the applied fate model, ENP distribution rates between compartments are a function of the spatiotemporal variability of the river flow velocity, and therefore, vary with discharge (Praetorius, Scheringer and Hungerbü, 2012). The river Foss, due to its smaller dimension, is more sensitive to discharge fluctuations and the spatiotemporal variability of its stream flow becomes more affected than the streamflow of the Ouse, which translates into bigger influence on the sedimentation process.

5.3.4 Risk assessment

To put our predictions of exposure into a risk context, we compared our findings with the results of a species sensitivity distribution analysis (SSD). The SSD is a well established approach that can guide the assessment of the environmental risks posed by ENPs (Gottschalk and Nowack, 2013; Garner *et al.*, 2015; Jacobs *et al.*, 2016; Chen *et al.*, 2018). This method consists of ranking different species among a group according to their sensitivity to a certain ENP (Garner *et al.*, 2015). The different species sensitivities can be quantified by different concentrations end points such as the so called no-observed-effect concentration (NOEC), the 10% lethal concentration (LC10), the 50% lethal concentration (LC50), the 10% effect concentration (EC10), and the 50% effect concentration (EC50) (Jacobs *et al.*, 2016). Once the ranking is developed with the chosen end point for the group of species, a statistical distribution of these different sensitivities is built into the so-called SSD curve (Jacobs *et al.*, 2016). From the SSD curve the potentially affected fraction of species for a particular concentration of interest can be extracted (Garner *et al.*, 2015). A commonly used effect fraction in the risk assessment of chemicals (TGD, 2003) is the 5th percentile of the fitted distribution (HC5). This concentration is then divided by an extra safety factor, also called an assessment factor (AF) that can vary between 1 and 5 (TGD, 2003), to obtain a predicted no effect concentration (PNEC) that is assumed to be sufficiently protective for the ecosystem. Finally, to quantify the risk, a Risk quotient (RQ) is determined by dividing the predicted environmental concentration (PEC) by the PNEC (Chen *et al.*, 2018). When the RQ is greater than or equal to 1, a potential unacceptable risk of the ENP is assumed and further assessment would be required or controls put in place to minimise risks. When the RQ is less than 1, the risk of the ENP is considered acceptable (European Chemicals Agency, 2008).

PNEC values for TiO₂ ENPs in surface water were generated here from the SSD analysis performed by Chen *et al.* (2018). In their study, Chen *et al.* gathered toxicity records from more than 300 published laboratory toxicological studies for several types of metallic ENPs (i.e. Ag, TiO₂, CeO₂, CuO and ZnO), including LC50, EC50 and NOEC values for crustacea, fish, algae, nematodes and bacteria. The derived HC5 values for TiO₂ ENPs from their study are presented in Table 5.5.

Table 5.5. Mean, lower and upper limit of estimated HC5 mg/L for TiO₂ ENPs derived from SSD analysis performed by Chen *et al.* (2018).

Endpoint	Mean of HC5 (mg/L)	Lower limit (mg/L)	Higher limit (mg/L)
LC50 Ag ≤ 20 nm	5.8	1.6	38
EC50	0.57	0.16	2.8
NOEC	0.19	0.04	1.3

According to the data presented in Table 5.5, the SSDs fitted to the NOEC is the most protective of the presented endpoints. Therefore, PNECs were generated from the NOEC SSD analysis. The provided data from Chen *et al.* (2018) for the construction of the TiO₂ ENPs SSD consists in NOEC values for 17 different species. The “SSD generatorV1” (EPA, 2018) was here used to generate the SSD distribution presented in Figure 5.24. PNEC values were obtained by dividing the mean HC5 by an assessment factor of 5 (i.e. PNEC = HC5/5) in accordance with the technical guidance (TGD, 2003).

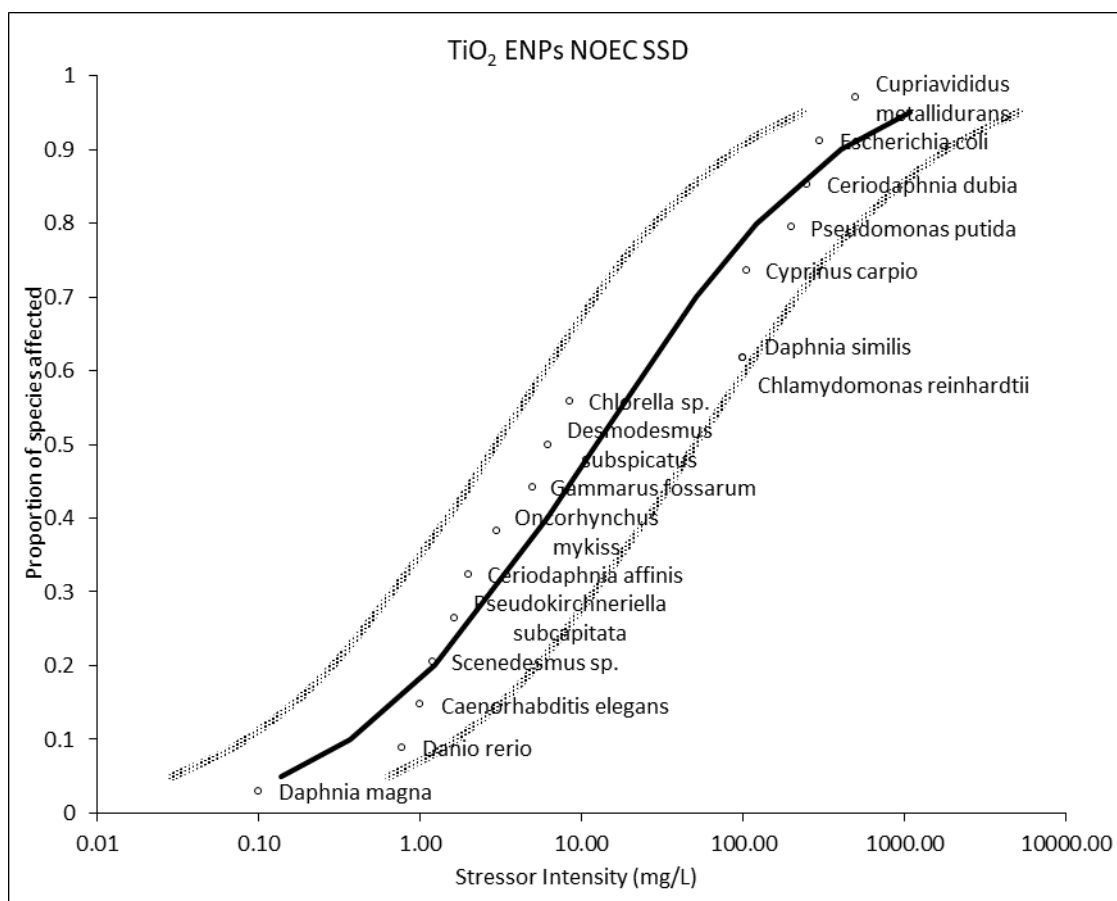


Figure 5.24. Generated SSD of TiO₂ ENPs based on NOEC data from Chen *et al.* (2018). The dotted lines depicts the 95% confidence interval.

Figures 5.25 and 5.26 present the distributions of estimated PECs of free (considered the bioavailable fraction) and total (free and SPM-bound together) TiO₂ ENPs in flowing water for the rivers Ouse and Foss, respectively including the derived PNEC, i.e. 380 µg/L (confidence interval 0.08-0.26 mg/L).

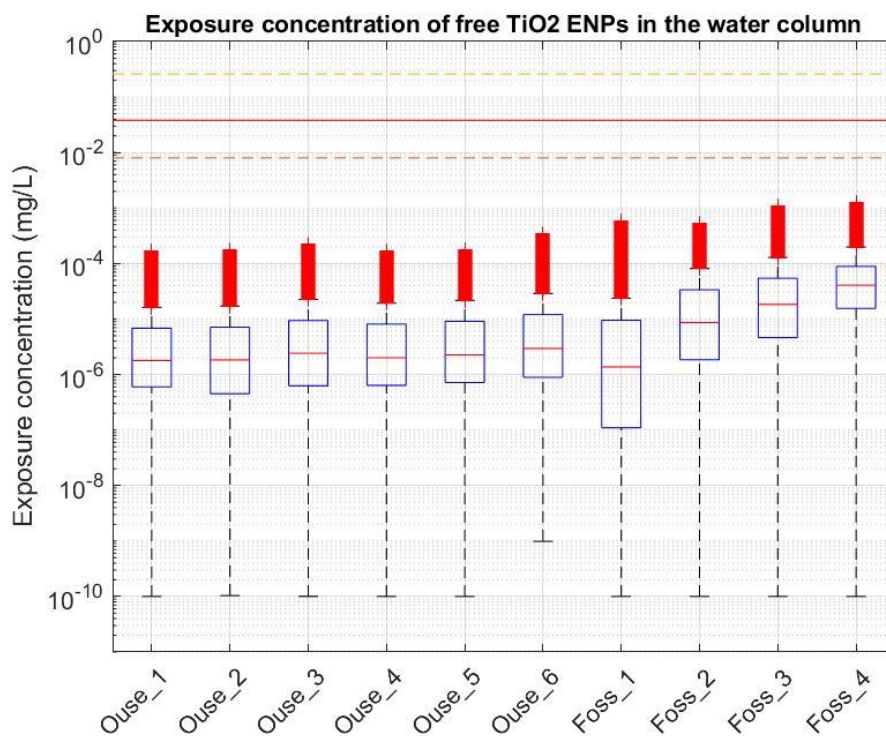


Figure 5.25. Box and whisker plots of the estimated PECs of free TiO₂ ENPs the water compartment (flowing + stagnant water) of the RSs of the Ouse and the Foss (i.e. Ouse 1 to 6 and Foss 1 to 4). In red the estimated PNEC based on the HC5 and confidence interval in dashed lines).

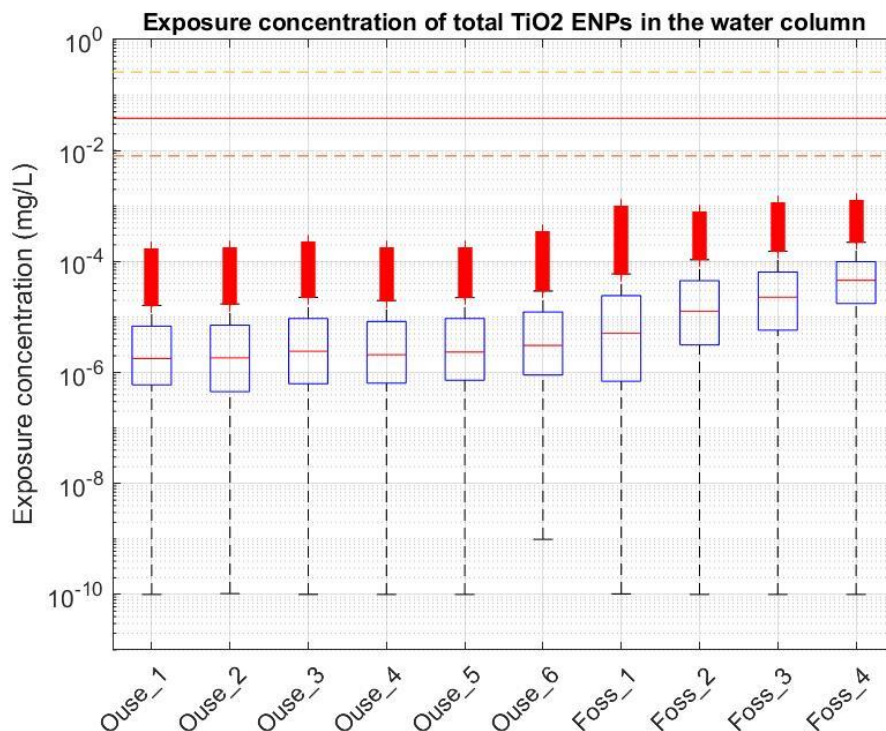


Figure 5.26. Box and whisker plots of the estimated PECs of total TiO_2 ENPs the water compartment (freely dispersed and SPM-bound ENPs in flowing and stagnant water) of the RSs of the Ouse and the Foss (i.e. Ouse 1 to 6 and Foss 1 to 4). In red the estimated PNEC based on the HC5 and confidence interval in dashed lines).

According to the plotted results, RQs are always below 1 and the derived risk of TiO_2 ENPs in York river system can be considered acceptable.

5.4 Conclusions

In this chapter, we have parameterized, for the first time, the proposed ENP fate model at the urban level by estimating spatial and temporal variations of key input parameters influencing ENP fate and final exposure. The concentration variations over time and space of two different ENP forms (i.e. free ENPs and ENPs attached to SPM) were predicted for the modelled river system, with specifications of their distribution along three RS compartments (i.e. flowing water, stagnant water and sediment). The obtained results, suggest that, at the local level, high variability of PEC are expected within short times and distances. This stresses the need for high resolution local modelling tools to inform local authorities. However, for the case study presented here (York's river system exposure to TiO_2 ENPs), the risk assessment suggests no potential risk since the concentrations predicted lie well below the estimated PNEC value and its confidence interval.

A fundamental issue with the work presented here, is the lack of calibration and validation of the estimated ENP concentrations. Calibration and validation of fate models are hindered at present by the lack of field data due to the current analytical limitations in the detection of ENPs in complex environmental samples (Howard *et al.*, 2010; Dale, Lowry and Casman, 2015a; Gondikas *et al.*, 2018). However, the principal objective of this Chapter was not to predict ENPs concentrations with certainty, but rather to illustrate the use of the proposed modelling framework of Chapter 3 and to stress on the need of exposure assessments at higher spatial and temporal resolution for the study of potential environmental risks in urban environments.

As discussed in Chapter 4, the uncertainties attached to the use of assumptions and extrapolations are inherent to the use of modelling tools and have to be accounted for when evaluating the obtained results. For example, in the presented study, a very conservative assumption was made in which all rainfall is translated into runoff, ignoring any potential infiltration. This assumption would influence the final concentration obtained for the different river compartments, since the ENP partition processes (i.e. sedimentation, hetero-aggregation and advective transport) are discharge-dependent. In order to evaluate the influence of such assumption as well as other parameters, sensitivity and uncertainty analysis emerge as very helpful tools. A formal uncertainty analysis will provide information on all the potential values that the outputs can take, with their associated probability distribution. Jointly, a sensitivity analysis would determine the influence of each input parameter (and attached assumption) on the model output values, therefore indicating which are the inputs/assumptions that will need to be further refined in order to get the most accurate results.

Chapter 6

General discussion and recommendations

The commercialisation of new technologies such as engineered nanomaterials often occurs ahead of the development of sufficient and adequate information about the potential environmental and health risks that they may cause. Recently, new regulations such as REACH and Classification, Labelling and Packaging (CLP) have been introduced with the aim of deriving better and earlier identification of the intrinsic properties and hazardous potential of new substances before their commercialization (Schwirn, Tietjen and Beer, 2014). However, for emerging pollutants such as ENPs these regulatory systems still need specific technical adaptations that will account for non-conventional parameters describing the fate and hazardous potential (e.g. size, shape, surface coating, etc) of these materials (Meesters *et al.*, 2013). To help develop such adaptations, mathematical modelling tools have been proposed to gain a deeper understanding on the sources of ENPs and their emissions, fate and effects (Mueller and Nowack, 2008; Nowack *et al.*, 2012; Keller *et al.*, 2013; Duester *et al.*, 2014). Predictions of average environmental exposure concentrations have already been derived from modelling approaches by studying their emission and fate processes in different settings (Gottschalk and Nowack, 2011a; Dale *et al.*, 2015; Klein *et al.*, 2016; Meesters *et al.*, 2016; Nowack, 2017; Williams *et al.*, 2019). However assessments at high spatial and temporal resolutions have not previously been performed.

This PhD therefore focused on assessing the exposure to ENPs in urban surface waters at high spatial and temporal resolutions. Urban waters are potential hot spots of use, release and exposure of these materials and are likely to show large variability in exposure over time and space. To date, no nanoparticle-specific models of this sort, at the urban scale, have been developed. Therefore, the main aim of this project was to design and apply a new modelling framework to estimate ENP exposure in urban surface water systems at high spatial and temporal resolution. Due to the complex composition of cities with expected spatial and temporal variations of activity, population density and land cover

types, the integration of high spatial and temporal resolution to the framework was considered essential for urban modelling. The different steps followed to fulfil this aim are described in the next section with the key derived findings.

6.1 Summary and key findings

In order to begin to design the modelling framework, the key aspects affecting the emissions and exposure of ENPs in urban river systems were reviewed in Chapter 2. The chapter included a review of the main ENP uses, emission pathways and fate processes in aquatic media. Firstly, the most produced ENPs and their main commercial applications were identified from the literature, and the challenges and limitations for the estimation of their production and use volumes discussed. It was found that the main ENPs of concern regarding production and use volumes are TiO₂, ZnO, CNT, Ag and SiO₂ ENPs, and that the main applications of these ENPs include paints, cosmetics and personal care products. However, a high level of uncertainty in the quantification of production and use volumes for these materials was identified from all reviewed materials (e.g. use of market reports, manufacture and consumer consultations and online databases) which can be attributed to the lack of regulation regarding labelling and claims of the ENPs content by industry. Secondly, information on the ENPs emission pathways and release mechanisms along the different stages of the ENPs life cycle were identified and the factors influencing their release potential reviewed. From the reviewed information, it was concluded that emissions during the use phase of the ENP-containing product probably dominate the release of ENPs into nature. It was also highlighted that the way in which ENPs are integrated into a product, and the use given to it, are the most relevant parameters that will determine their release potential. ENPs in aerosols and liquid suspensions were identified as the most likely to be emitted, followed by ENPs bound to surfaces of the materials such as paints and coatings. Finally, the main fate processes that different ENPs undergo once released into the environment were reviewed as well as the influence of such processes on their final fate and their potential toxicity. The main environmental and anthropogenic factors determining the extent of such processes were also reviewed, highlighting the complexity of the interactions between particle properties and environmental factors and the importance of a detailed parametrization when performing ENP fate modelling.

Chapter 3 built on the information gathered in Chapter 2 and proposed a novel modelling approach for estimating the exposure of ENPs in urban surface waters. It discussed the complex nature of cities and argued the need for an assessment of the spatial and temporal variability of ENP emissions and exposure. The proposed modelling framework combines an emission and a fate model for ENPs and integrates a four steps strategy that provides high spatial and temporal resolution. Firstly, it recommends a methodology for performing a spatial analysis of the modelled city using GIS tools. Secondly, recommendations on information sources needed for performing an urban ENP-product inventory are made and a classification strategy delivered. In the third step, three ENP release pathways linked to the previously categorized sources were identified (i.e. runoff, down the drain and direct release emissions) and equations for the estimation of the mass of ENPs emitted through each of them proposed. Again, data sources and strategies for the parametrization of these equations are listed. Finally, an ENP fate model that can account for the spatial and temporal variations of the ENPs emissions and of the environmental parameters was proposed (based on the model of Praetorius, Scheringer and Hungerbühler, 2012). The handling of knowledge gaps was also discussed together with alternative information sources and the use of assumptions, which will be further discussed in the next section. The proposed framework should be capable of identifying local emission hot spots and predicting exposure across a city, while generating information on the final speciation of the emitted ENPs (i.e. nano form, aggregates and other transformation products) within the studied environmental compartments over time.

The application of the modelling framework for modelling spatial and temporal trends of ENP emissions in a case study city (York, UK) was presented in Chapter 4. Here several ENPs types (i.e. TiO_2 , Ag and CeO_2) and a variety of emission sources (representing both point and diffuse emissions) of priority concern were studied. First, the spatial analysis strategy was successfully applied for York proving its potential for application to other urban systems when readily available data are available (i.e. DTM and urban drainage network information). Secondly, new strategies for local parametrization of product type specific usage and release rates were presented, and finally spatially and temporally resolved emissions were estimated per product type and ENP type. The use of this novel approach allowed the identification of the main sources, drivers and activities causing the highest emissions in the city. Furthermore, hot spots of emission were identified in the

city and temporal emission trends derived for the period simulated. The results showed that TiO₂ was likely to be the highest contributor to ENPs emissions in York. This agrees with results obtained from other studies (e.g. Giese, Klaessig, Park, Kaegi, Steinfeldt, Wigger, Von Gleich, *et al.*, 2018). In addition, and in agreement with the previously cited studies, the so-called down the drain emission pathway was identified as the main contributor for such emissions. However, temporal variations were led by the runoff emission pathway, and therefore, by weather conditions. This shows that priority should be placed on further studying run off emissions when looking at short-term temporal exposure trends (instead of average yearly exposure). It is worth noting, however, that some highly conservative assumptions were made in this study and would need further refining when information becomes available. For example, the assumption made on all rainfall translated into runoff when estimating emissions through weathering, comes useful when applying the precautionary principle, but could be refined when data on infiltration rates for the studied terrain becomes available. Finally, the areas producing the highest emissions were identified. These were areas where higher human activity was localized (i.e. most constructed, populated and busier areas), and the higher emitting dates correlated with the days of higher rainfall intensity following long dry periods. Estimated emissions on wet days sometimes doubled and even triplicated the estimated emissions of dry days. Spatial differences between areas were smaller but still significant (up to one order of magnitude), confirming the spatial and temporal variability of ENP emissions at the local scale.

Finally, the estimated total emissions of TiO₂ ENPs in the city of York were used in conjunction with gathered water quality information from a six month local monitoring campaign to model the exposure of York river system to TiO₂ (Chapter 5). The proposed river fate model (Praetorius, Scheringer and Hungerbühler, 2012) was adapted temporally to run in dynamic mode and spatially to the area of study through the use of the delimited river sections. Parameterisation was done daily or monthly, depending on the required parameter (i.e. daily ENPs emissions, daily water discharge and monthly surface water parameters per river section) and spatially (per RS). The spatial-temporal variations of the input parameters were analysed and concentrations over time and space for the modelled river system were obtained for three RS compartments (i.e. flowing water, stagnant water and sediment), and for two different ENP forms (i.e. free ENPs and ENPs attached to SPM). Finally,

preliminary conclusions about the influence of the selected model parameters on the ENPs exposure trends were derived for the York river system, and a first assessment of the risk posed by the obtained exposures was performed. The results demonstrated highly variable concentrations over time and space. Generally, for the two rivers in York, estimated median exposure concentrations were in the ng per litre range, and maximum exposure values never exceeded the estimated PNEC (380 µg/L). Therefore, RQs were always below 1 so the derived risk of TiO₂ ENPs in these rivers was considered acceptable. The obtained results were consistent with other model predictions (Musee, 2011; Sun *et al.*, 2014; Gottschalk *et al.*, 2015a) and recent measured values (Peters *et al.*, 2018) of TiO₂ exposure in surface water. The influence of the river water quality properties (e.g. calcium and dissolved organic carbon concentrations) on ENP fate, as well as the dominance of the transport and fate processes on the final exposure trends in both rivers was as well investigated. This suggests that performing a higher resolution parametrization of the the model in an urban context could benefit predicting spatiotemporal exposure trends. However, the validation of these results is still missing, as well as the performance of a sensitivity analysis that would help evaluate the influence of the cited environmental parameters to determine whether they have more or less influence in these complex systems.

6.2 Research implications

Environmental risk assessment (ERA) requires the integration of exposure and ecological effect assessment, and the use of modelling tools for both purposes is a current common practice (Jager and Ashauer, 2018). Furthermore, in the context of emerging pollutants such as ENPs, exposure modelling has become an essential tool for their risk assessment since they can provide information on PEC values in the absence of analytical data (Nowack, 2017).

To perform an ERA, the comparison between an exposure indicator (e.g. PEC) and an effect indicator (e.g. PNEC) is common practice in order to derive a risk quotient (RQ). Current regulatory practice typically uses averaged PECs for each environmental compartment (i.e. water, sediment, air, soil and biota) generally estimated for standardized environmental scenarios (Scientific Committee on Emerging and Newly Identified Health Risks *et al.*, 2013). However, this procedure is currently under revision due to claims of lack of realism (Franco *et al.*, 2017).

Its relatively simple strategy overlooks the complexity of environmental conditions, ecosystems and biological communities and therefore these predictions have high levels of uncertainty and are often precautionary. Furthermore, the integration of the complexity of spatially and temporally varying environmental scenarios and discharges is considered one of the key deficiencies of current ERA practices (Scientific Committee on Emerging and Newly Identified Health Risks et al., 2013). One of the proposed revisions of ERA is the use of mechanistic effects assessment approaches such as toxicokinetic-toxicodynamic (TKTD) models coupled to mechanistic fate models that would produce time-varying exposure and effects.

In this context, the proposed modelling tool presented in this thesis fits perfectly in the transition into a more refined ERAs (Jager, 2016). The integrated methodology for the assessment of ENPs urban emissions and surface water exposure presented here can be adapted to other types of pollutants of urban systems by means of adaptation of its fate and transport equations. Therefore, it provides a potential mechanistic fate modelling approach that could feed TKTD models in the new ERA paradigm proposed by Jager (2016).

6.3 Challenges, limitations and future work

In this project, we have proposed an integrated methodology for the assessment of ENPs urban emissions and surface water exposure. This methodology brings together, for the first time, a spatially and temporally resolved emissions estimation model and a spatially and temporally resolved ENP fate model. This new framework is able to predict local emission and exposure variations over time and space, and is capable of identifying hot spots of emission and exposure as well as temporal variation trends. It also provides insights into the main sources, pathways and drivers of ENPs emissions. However, the proposed framework is subject to a series of limitations that are discussed here.

The main limitation of the model resides in its dependency on the input data quality and availability and the need for some assumptions. This will influence the quality of the results obtained and the uncertainty associated with them. Also, the selection of input parameters can translate into bias of the model results.

The quality of the model results are subject to the quality and precision of the model parametrization. The framework proposed and its integrated methodology have been designed in a highly flexible way so that it can be adapted to various types of cities and be workable for different levels of data availability. However, the degree of uncertainty associated with the model calculations is highly dependent on the specific city under consideration and its data availability. For example, if a remote city is chosen, limited information availability may be encountered leading to increased uncertainty. On the other hand, if for larger cities, the complexity of its structure, including more complex traffic and sewage networks, might challenge the spatial analysis of the city and integration of further parameters not previously considered for the analysis might be needed. Both, a lack or even excess of information can lead to high degree of uncertainty due to, on the one side, a lack of knowledge, and, on the other, the cumulative effect of uncertainty in many parameters and their interactions. Monte-Carlo (MC) simulation based techniques for the estimation of uncertainties, together with the use of sensitivity analysis to better understand the influence of each input in the uncertainty associated to the final results, is here proposed for future work.

Potential bias is another limitation of the proposed framework associated with parametrization. It has been argued that modelling results could vary extensively due to the chosen source of information for the model parametrisation. According to Bundschuh *et al.* (2018), the available data on production volumes can differ greatly depending on the method of data collection (Bundschuh *et al.*, 2018) and thus lead to very different results. In this sense, it is very important to carry out a thorough analysis of the input data so that the bias is eliminated or at least the results are put into context for their interpretation. In addition, the use of certain assumptions can lead to under or overestimation of emission and exposure. Generally, in our proposed framework we employed conservative approaches when assumptions are to be made. Such conservative assumptions applied here include:

1. The retention of ENPs by urban surfaces (C_{ret}) when emitted via runoff, was assumed to be zero. However, runoff ratios for urban environments have been reported to range between 11 and 24 (Pauleit and Duhme, (2000). This information, based on the land cover type (e.g. green areas, paved areas, etc.), could be used to improve C_{ret} for different areas of the city.

2. The atmospheric transport of certain ENPs, such as the ones emitted with exhaust, was also assumed to be zero. However, currently available atmospheric transport models could be integrated to generate more accurate predictions of the transport of these ENPs through urban environments. In fact, the modular nature of the framework makes it very versatile in terms of its inherent flexibility to integrate additional modules or release pathways that have not yet been identified but that could become relevant in certain types of cities or other emerging pollutants.
3. Improvements in the monitoring campaign could also be made by increasing the length as well as its spatial and temporal resolution. Also, some improvements in the spatial analysis are previewed as future work. For example, specific location of drainage system outlets were readily available and their integration in the river model for a more accurate estimation of the emission profiles is recommended.
4. Release rates from outdoor paints were established based on the assumption that all ENPs contained in the product would be released during a established usage duration period. However, less conservative values of $R_{release}$ could be derived from outdoor paints weathering experimental studies such as the ones performed by Al-Kattan et al. (2013), or Zuin *et al.*, (2014).

While the use of assumptions and extrapolations is characteristic of mathematical modelling, with local scale modelling (such as the urban modelling depicted here) the associated uncertainty can be reduced, since more detail and control over the main uncertainty contributing factors is achieved.

Finally, analytical methods such as Single particle inductively coupled plasma–mass spectrometry (spICP-MS) and multi-element detection (time-of-flight) spICP-TOFMS are becoming available as emerging techniques capable of simultaneously measuring nanoparticle size and number concentration of metal-containing nanoparticles at environmental levels (Gondikas *et al.*, 2018; Montoro Bustos *et al.*, 2018). Therefore, future work could use these techniques to validate the proposed model by carrying sampling campaigns in the modelled area. Meanwhile, measurement of total Ti concentration in surface waters could as well be used as upper limit on the estimated TiO₂ ENPs concentrations.

6.4 Conclusions

In the introduction of this thesis, three main objectives were established and within this PhD, each of them has been addressed. The three objectives were:

- 4) To develop a modelling framework that accounts for the complexity of urban systems and allows the estimation of spatially and temporally resolved ENP emissions, as well as ENP exposure levels.
- 5) To parameterise this framework locally for the characterization of the ENP emissions of a case study city.
- 6) To parameterise the framework with the obtained emission results and the most relevant water quality parameters of the study area obtained from a local monitoring campaign, in order to characterize the ENP exposure levels of the city and the potential risks posed.

The main contribution of the research performed in this PhD has been to shift from national/regional scale assessment of ENP emissions and fate modelling to the urban local scale, providing emission and exposure estimates at high levels of spatial and temporal resolution. For the first time a spatially and temporally resolved ENP emission model has been integrated with a spatially resolved dynamic fate model, providing a high level of detail about the sources, pathways and main drivers of emissions and associated exposure of ENPs in cities. The presented modelling framework has the potential to be adapted to other urban contaminants, becoming a potential enabler of more refined ERAs that are able to account for the spatial and temporal variations of pollutant exposure. The presented novel approach highlights the significance of providing higher spatio-temporal resolution of emission and exposure estimates for a more comprehensive ENPs risk assessment. This approach could contribute to a full probabilistic risk assessment (e.g. expected total risk) by integrating the distribution of environmental exposure and the SSD to give a different measure of risk. This could provide more meaningful insights to the ERA, although might be contested as less pragmatic in regulatory risk assessment schemes.

Appendices

APPENDIX 1

A1. Supplementary information Chapter 4

A1.1 Study Area

Table A1.1. Connections between hydrological zones (HZ), river sections (RS) and Sewage treatment plants (STP) serving the city of York. Population served by each STP according to Yorkshire Water Limited in parenthesis.

River Section	HZ connection	STP connection (pop served)
OUSE_1	HZ1	-
OUSE_2	HZ2	Rawcliffe (28022)
OUSE_3	HZ3	-
OUSE_4	HZ4	-
OUSE_5	HZ5+HZ6	-
OUSE_6	HZ11+HZ12	Naburn (168594)
FOSS_1	HZ10	Haxby (20105)
FOSS_2	HZ9	-
FOSS_3	HZ8	-
FOSS_4	HZ7	-

A1.2 Emissions model parametrization

Table A1.2. Selection criteria of the values of the maximum (Max), minimum (Min) and average (Ave) scenarios of ENPs concentration in the product (C_{ENP}) per case study.

Case study	C _{ENP}	Estimation
Fuel additive- CeO ₂	Min= 5mg/L Ave=6.25 mg/L* Max=7.5 mg/L	From Johnson and Park, (2012). Min and Max values are the ones claimed by the two producers (Rhodia and Envirox)
Outdoor paint- TiO ₂	Min=3 % wt Ave= 4.5 % wt* Max= 6% wt	Min value taken from Hischier et al. (2015) and max from Al-Kattan et al. (2013)
Outdoor paint- Ag	Min= 0.001% wt Ave= 0.05% wt* Max= 0.1% wt	Min and max values taken from (Tiede <i>et al.</i> , 2016)
Sunscreen- TiO ₂	6.95% wt x 60% = 0.0417	From the consumer survey performed (Keller <i>et al.</i> , 2014a) (US). C _{ENP} is estimated as by multiplying the ingredient concentration by the fraction of ingredient that is <100 nm or less.
Makeup- TiO ₂	5.4% wt x 60% = 0.0324	From the consumer survey performed by (Keller <i>et al.</i> , 2014a) (US). C _{ENP} is estimated as by multiplying the ingredient concentration by the fraction of ingredient that is <100 nm or less.
Toothpaste- TiO ₂	0.5% wt x 0.6% = 0.00003	From the consumer survey performed by (Keller <i>et al.</i> , 2014a) (US). C _{ENP} is estimated as by multiplying the ingredient concentration by the fraction of ingredient that is <100 nm or less.
Textiles (clothing)- Ag	Min=0.005% wt Ave=0.1375%* Max=0.27 % wt	From (Tiede <i>et al.</i> , 2016)
Toothpaste -Ag	0.0008% wt x 39.7% = 0.000003176	From the consumer survey performed by (Keller <i>et al.</i> , 2014a) (US). C _{ENP} is estimated as by multiplying the ingredient concentration by the fraction of ingredient that is <100 nm or less.

Values marked with * were estimated as the average.

Table A1.3. Selection criteria of the values of the maximum (Max), minimum (Min) and average (Ave) scenarios of the market penetration of the product (F_{pen}), per case study.

Case study	F_{pen} (%)	Estimation
Fuel additive- CeO_2	100*	Values couldn't be found in the literature and the conservative approach taken
Outdoor paint- TiO_2	1%	From (Tiede <i>et al.</i> , 2016). Reported value of market share by the observatory nano EU project: "Today approximately 1% of the construction related products on the market have nanoenhanced features"
Outdoor paint- Ag	1%	From (Tiede <i>et al.</i> , 2016). Reported value of market share by the observatory nano EU project: "Today approximately 1% of the construction related products on the market have nanoenhanced features"
Sunscreen- TiO_2	23.30%	Average value is taken from (Keller <i>et al.</i> , 2014a) estimated fraction of product on the market that contains ENM
Makeup- TiO_2	52.3%	Average value is taken from (Keller <i>et al.</i> , 2014a) estimated fraction of product on the market that contains ENM
Toothpaste- TiO_2	50%	Average value is taken from (Keller <i>et al.</i> , 2014a) estimated fraction of product on the market that contains ENM
Textiles (clothing)- Ag	1%	From (Tiede <i>et al.</i> , 2016). 1% corresponding market share extracted from the Observatory nano EU project
Toothpaste -Ag	0.10%	Average value is taken from (Keller <i>et al.</i> , 2014a) estimated fraction of product on the market that contains ENM

Table A1.4. Selection criteria of the values of the maximum (Max), minimum (Min) and average (Ave) scenarios of the ENPs release rate (R_{release}), per case study.

Case study	R _{release}	Estimation
Fuel additive- CeO ₂	Min=1% Ave=3%* Max=5%	From (Johnson and Park, 2012). Min and Max values from independent tests based on 2,000 miles of driving indicate that modern diesel particulate filters are capable of removing between 95 and 99% of 10- to500-nm particles.
Outdoor paint- TiO ₂	$I_{rain} / 3881$	R _{release} was estimated as the rainfall intensity of the day (I_{rain}) divided by the rainfall generated during the use release duration of the product (assuming all ENPs are emitted during this period of time). From (Sun <i>et al.</i> , 2016a) use release duration is 7 years. For York 3881mm of rainfall generated in the last 7 years
Outdoor paint- Ag	$I_{rain} \times 0.3/554$	From the experimental study of (Kaegi <i>et al.</i> , 2010), 30% of paint was released over 1 year period. R _{release} = 0.3/rainfall of 1 year. (average yearly rainfall York = 3881mm/7= 554 mm)
Sunscreen- TiO ₂	93%	From (Keller <i>et al.</i> , 2014a) transfer factor to WWTPs reported from the survey on PCP disposal in the US.
Makeup- TiO ₂	73% wt	From (Keller <i>et al.</i> , 2014a) transfer factor to WWTPs reported from the survey on PCP disposal in the U.S
Toothpaste- TiO ₂	100%	From (Keller <i>et al.</i> , 2014a) transfer factor to WWTPs reported from the survey on PCP disposal in the US.
Textiles (clothing)- Ag	20%	From (Lorenz <i>et al.</i> , 2012), the fraction of Ag released in one washing/rinsing cycle compared to the initial amount was 20%, 14.8%, 23.5% and 17.6% for textiles 4–7.
Toothpaste -Ag	100%	From (Keller <i>et al.</i> , 2014a), transfer factor to WWTPs reported from the survey on PCP disposal in the US.

Values marked with * were estimated as the average.

Table A1.5. Selection criteria of the values of the maximum (Max), minimum (Min) and average (Ave) scenarios of the product usage (Usage), per case study.

Case study	Usage	Estimation
Fuel additive- CeO ₂	HZ specific	-
Outdoor paint- TiO ₂	0.35kg/m ²	From (Hischier <i>et al.</i> , 2015)
Outdoor paint- Ag	0.248 kg/m ²	From (Kaegi <i>et al.</i> , 2010)
Sunscreen- TiO ₂	Max = 1.9 g/pc/d Ave = 0.97 g/pc/d Min = 0.04 g/pc/d	From (Biesterbos <i>et al.</i> , 2013)
Makeup- TiO ₂	Max = 0.6 g/pc/d Ave = 0.33 g/pc/d Min = 0.06 g/pc/d	From (Biesterbos <i>et al.</i> , 2013)
Toothpaste- TiO ₂	Max = 4 g/pc/d Ave = 2.4 g/pc/d Min = 0.8 g/pc/d	From (Biesterbos <i>et al.</i> , 2013)
Textiles (clothing)- Ag	89g/pc/d	Assumption made by (Tiede <i>et al.</i> , 2016), based on the UK consumptions of textiles (2M t per year)
Toothpaste -Ag	Max = 4 g/pc/d Ave = 2.4 g/pc/d Min = 0.8 g/pc/d	From (Biesterbos <i>et al.</i> , 2013)

Values marked with * were estimated as the average.

Table A1.6. Number of buses circulating per HZ from Monday to Friday (Week) and on Sundays and the corresponding fuel consumption (L)

HZ	N° buses Week days	Fuel Usage (L) Week days	N° buses Sundays	Fuel Usage (L) Sundays	Distance travelled (km)
HZ1	1044	1768	511	802.5	86.421
HZ2	1038	942.6	504	440	49.195
HZ3	4909	1397.4	2328	717.4	47.576
HZ4	1724	712.7	811	276.6	31.411
HZ5	999	583.5	469	237.5	30.194
HZ6	1100	1062.4	541	513.3	48.896
HZ7	2092	1818.1	991	827	79.55
HZ8	836	1809.3	342	644.7	75.725
HZ9	224	165.4	59	60	8.452
HZ10	105	97.8	51	47.5	4.463
HZ11	196	98.2	54	29.5	7.415
HZ12	588	549.9	255	199.1	30.246

Table A1.7. Building composition by building type percentage (i.e. Detached, semidetached, terraced and flats) and paint use frequencies obtained for each HZ of the city of York.

HZ	%Detached	%Semidetached	%Terraced	%Flats	Paint use frequency	SA painted (m ²)
HZ1	26.9	24.6	25	23.5	34.7	2283982.4
HZ2	33.1	36.6	16.5	13.8	21.8	1494383.1
HZ3	19	28.5	33.2	19.4	100.0	345820.9
HZ4	7.5	23	46.4	23.1	31.1	626170.3
HZ5	11.2	21.7	36.4	30.6	26.8	417796.0
HZ6	12.4	21.2	36.5	29.9	16.7	707299.4
HZ7	26.3	34.8	22.5	16.4	49.2	1436482.3
HZ8	11.9	27	36.2	25	24.0	1878420.8
HZ9	13.6	22.1	40.8	23.5	41.2	367528.8
HZ10	37.7	15.9	31.3	15.1	52.5	321102.8
HZ11	22.4	17.7	43.7	16.2	14.7	78350.9
HZ12	13.9	20.9	42.7	22.6	37.2	601220.6

A1.3 Results of emission estimates

Table A1.8. Estimated total mass of each ENP available for loss and actual estimated mass emitted in York during the period studied (from the 1st of January until the 15th of December of 2016) for the AVE scenario per case study (ENP type-Product type).

ENP type	Product Type	Mass of available ENPs for Loss in York during 2016 in Kg	Cumulative total predicted losses in Kg	% Loss	% contribution to total emission
CeO₂	Fuel Additive	22.1	0.60	2.7	100
TiO₂	Outdoor paint	118.6	12	10.2	12.7
	Sunscreen	714.9	70	9.8	73.2
	Makeup	173.1	13	7.6	13.9
	Toothpaste	2.73	0.29	10.5	0.3
Ag	Outdoor paint	0.93	0.10	10.2	5.921
	Textile	94.5	1.51	1.6	94.076
	Toothpaste	5.8x10 ⁻⁴	4.6x10 ⁻⁵	7.9	0.003

Table A1.9. Estimated total mass of each ENP available for loss and actual estimated mass emitted in York during the period studied (from the 1st of January until the 15th of December of 2016) for the MIN scenario per case study (ENP type-Product type).

ENP type	Product Type	Mass of available ENPs for Loss in York during 2016 in Kg	Cumulative total predicted losses in Kg	% Loss	% contribution to total emission
CeO₂	Fuel Additive	17.7	0.16	0.9	100
TiO₂	Outdoor paint	79.1	8.06	10.2	94
	Sunscreen	29.5	0.27	0.9	3.2
	Makeup	31.5	0.23	0.7	2.7
	Toothpaste	0.91	9.1x10 ⁻³	1.0	0.1
Ag	Outdoor paint	0.02	1.9x10 ⁻³	10.2	22
	Textile	3.4	6.7x10 ⁻³	0.2	77.98
	Toothpaste	1.9x10 ⁻⁴	1.9x10 ⁻⁶	1.0	0.02

A1.4 Schematic representation of Emissions Model

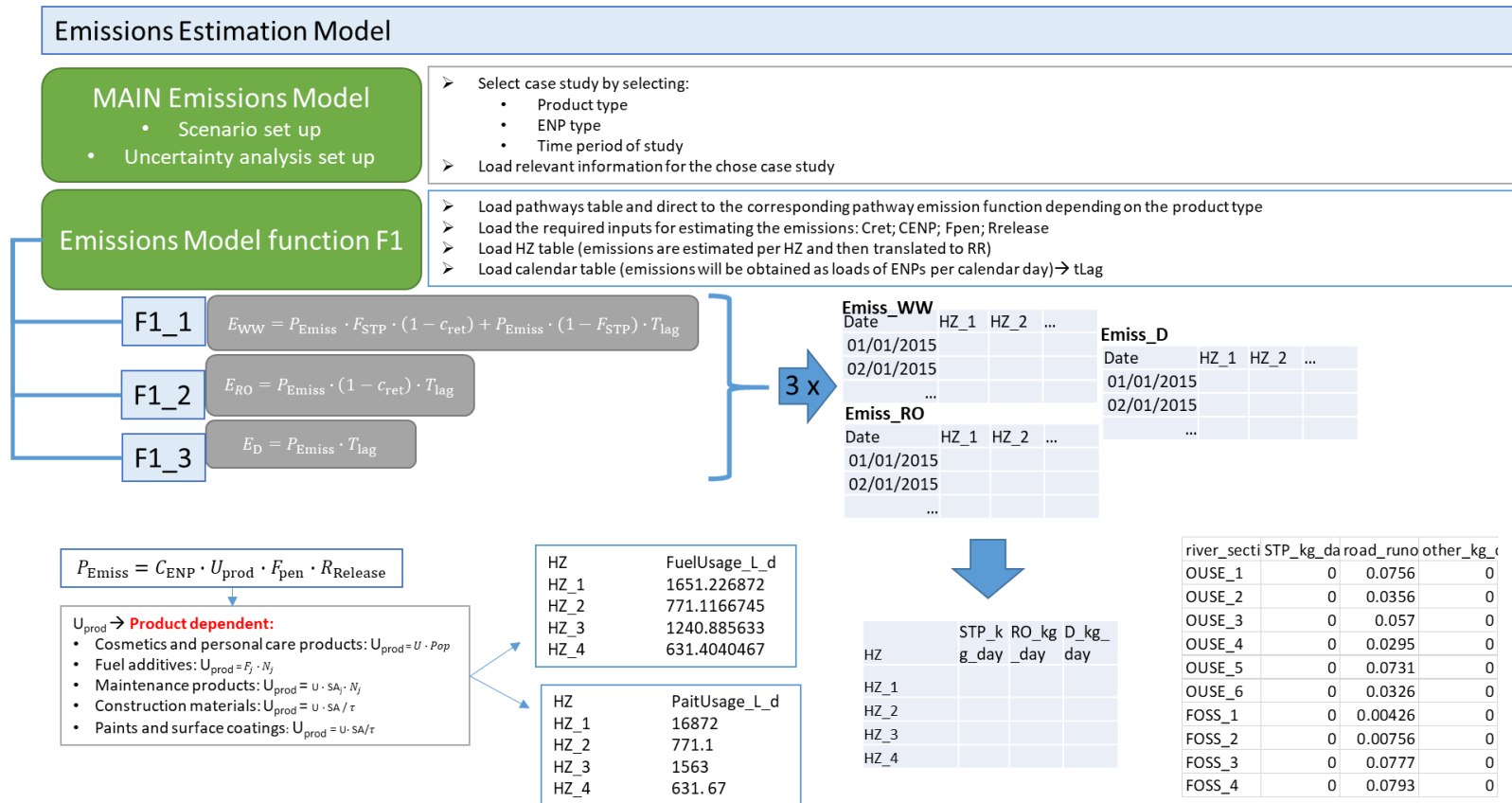


Figure A.1 1. Schematic representation of Emissions Model

APPENDIX 2

A2. Supplementary information Chapter 5

A2.1 River fate model parameterisation

Table A2.1. River sections connectivity, dimensions and segmentation

RS	Flow into	Length (m)	Width (m)	Depth (m)	N° of boxes
Ouse_1	Ouse_2	5609	38.5	3	7
Ouse_2	Ouse_3	1770	43.6	3	2
Ouse_3	Ouse_4	1236	45.5	3	2
Ouse_4	Ouse_5	4799	44.8	3	6
Ouse_5	Ouse_6	2071	28.3	3	3
Ouse_6	-	2383	13.5	3	3
Foss_1	Foss_2	5858	6.9	2	8
Foss_2	Foss_3	3977	6.5	2	5
Foss_3	Foss_4	4544	11.8	2	6
Foss_4	Ouse_4	1555	17.6	2	2

Table A2.2. River parameters. Source: adapted from (Praetorius, Scheringer and Hungerbühler, 2012)

Parameter	Symbol	Value	Unit
Depth of moving water (w1)	h_{w1}	3 (Ouse), 2 (Foss)	m
Depth of stagnant water (w2)	h_{w2}	0.4	m
Depth of the sediment (sed)	h_{sed}	0.02	m
Cross sectional area of first box of moving water	$A_{w1,1}$	$h_{w1} \times \text{width}_{w1}$	m ²
Cross sectional area of last box of moving water	$A_{w1,n_{boxes}+1}$	$4 \cdot A_{w1,1}$	m ²
Volume of box n of moving water (w1)	$V_{w1,n}$	$\frac{A_{w1,n} + A_{w1,n+1}}{2} \cdot l_{box,n}$	m ³
Volume of box n of stagnant water (w2)	$V_{w2,n}$	12% of $V_{w1,n}$	m ³
Volume of box n of sediment (sed)	$V_{sed,n}$	5% of $V_{w1,n}$	m ³
Sediment density	ρ_{sed}	2.5	g cm ⁻³
Porosity of sediment	Φ_{sed}	0.85	-
Mass of sediment in box n of river sediment	$m_{sed,n}$	$(1 - \Phi_{sed}) \cdot \rho_{sed} \cdot V_{sed,n}$	kg
River flow velocity	$v_{river,flow}$	Estimated per RS	m s ⁻¹
Velocity of sediment transfer (bed load shift)	$v_{sed,transf}$	3.0	kg s ⁻¹
Sediment resuspension velocity	v_{resusp}	1.0×10^{-6}	m s ⁻¹
Sediment burial velocity to deep sediment	v_{burial}	3.42×10^{-8}	m s ⁻¹

Table A2.3. Rate constant of processes in the river model. Source: adapted from (Praetorius, Scheringer and Hungerbühler, 2012) $i = 1 \dots r_{sized}^{TiO_2 \text{ products}}$

Parameter	Symbol	Value	Unit
Water exchange rate constant between moving water and stagnant water	$k_{exch,12}$	1×10^{-5}	s^{-1}
Water exchange rate constant between stagnant water and moving water	$k_{exch,21}$	$k_{exch,12} \cdot \frac{V_{w1}}{V_{w2}}$	s^{-1}
River flow rate constant of box n	$k_{river,flow,n}$	$v_{riv,flow} \cdot \frac{A_{w1,n}}{V_{w1,n}}$	s^{-1}
Heteroaggregation rate constant between TiO_2 and SPM	$k_{het-agg}$	$\alpha_{het-agg} \cdot k_{coll} \cdot C_{particle}^{SPM}$	s^{-1}
Settling velocity of TiO_2 ENPs	$v_{set}^{TiO_2}$	$\frac{2}{9} \cdot \frac{\rho_{TiO_2} - \rho_{water}}{\mu_{water}} \cdot g \cdot r_{TiO_2,i}^2$	s^{-1}
Settling velocity of SPM	v_{set}^{SPM}	$\frac{2}{9} \cdot \frac{\rho_{SPM} - \rho_{water}}{\mu_{water}} \cdot g \cdot r_{SPM}^2$	s^{-1}
Sedimentation rate constant of TiO_2 ENPs in moving water	$k_{sed,w1}^{TiO_2}$	$\frac{v_{set}^{TiO_2}}{h_{w1}}$	s^{-1}
Sedimentation rate constant of TiO_2 ENPs in stagnant water	$k_{sed,w2}^{TiO_2}$	$\frac{v_{set}^{TiO_2}}{h_{w2}}$	s^{-1}
Sedimentation rate constant of SPM in moving water	$k_{sed,w1}^{SPM}$	$\frac{v_{set}^{SPM}}{h_{w1}}$	s^{-1}
Sedimentation rate constant of SPM in stagnant water	$k_{sed,w2}^{SPM}$	$\frac{v_{set}^{SPM}}{h_{w2}}$	s^{-1}
Sediment resuspension rate constant	k_{resusp}	$\frac{h_{w2}}{v_{resusp}}$	s^{-1}
Sediment burial rate constant to the deep sediment	k_{burial}	$\frac{h_{sed}}{v_{burial}}$	s^{-1}
Rate constant of horizontal sediment transfer (bed load shift) of box n	$k_{sed-transfer,n}$	$\frac{h_{sed}}{v_{sed,transf} \cdot m_{sed,n}}$	s^{-1}

Table A2.4. ENP and SPM parameters. Source: adapted from (Praetorius, Scheringer and Hungerbühler, 2012)

Parameter	Symbol	Value	Unit
radius TiO ₂ ENPs makeup	$r_{TiO_2,makeup}$	25/2=12.5 ^a	nm
radius TiO ₂ ENPs sunscreen	$r_{TiO_2,sunscreen}$	25/2=12.5 ^a	nm
radius TiO ₂ ENPs toothpaste	$r_{TiO_2,toothpaste}$	450 ^b	nm
radius TiO ₂ ENPs paint	$r_{TiO_2,paint}$	150 ^c	nm
Diameter of TiO ₂ ENPs	$d_{TiO_2}^{primary}$	$r_{TiO_2} \cdot 2$	nm
Fractal dimensions of TiO ₂ ENP aggregates	D_f	2	-
Density of bulk TiO ₂	ρ_{TiO_2}	4.23	g cm ⁻³
Density of aggregated TiO ₂ ENPs	$\rho_{TiO_2}^*$	$\frac{\rho_{TiO_2} \cdot V_{TiO_2}^{solid} + \rho_{water} \cdot (V_{TiO_2}^{total} - V_{TiO_2}^{solid})}{V_{TiO_2}^{total}}$	g cm ⁻³
Vector with input TiO ₂ ENPs flow for each box	$q_{TiO_2}^{input}$	Specific to the day	m ⁻³ s ⁻¹
Radius of SPM	r_{SPM}	8500	nm
Average density of SPM	ρ_{SPM}	2	g cm ⁻³
Solid volume in the fractal aggregate filled with primary TiO ₂ ENPs	$V_{TiO_2}^{solid}$	$\frac{4}{3} \cdot \pi \cdot \left(\frac{d_{TiO_2}^{primary}}{2}\right)^{3-D_f} \cdot \left(\frac{d_{TiO_2}}{2}\right)^{D_f}$	m ³
Total volume in the fractal aggregate	$V_{TiO_2}^{total}$	$\frac{2}{9} \cdot \frac{\rho_{TiO_2}^* - \rho_{water}}{\mu_{water}} \cdot g \cdot r_{TiO_2}^2$	m ³

a.(Keller *et al.*, 2014a); b. (Kaegi *et al.*, 2008; Weir *et al.*, 2012);c. (Kaegi *et al.*, 2008)

Table A2.5. Table of constants needed for the river model. Source: adapted from Praetorius, Scheringer and Hungerbühler(2012)

Parameter	Symbol	Value	Unit
Shear rate	G	10	s^{-1}
Dynamic viscosity of water	μ_{water}	1.002	mPa s
Water density	ρ_{water}	1000	$kg\ m^{-3}$
Boltzmann constant	k_B	1.38×10^{-23}	$J\ K^{-1}$
Gravitational acceleration on earth	g	9.81	$m\ s^{-2}$

A2.2 River fate model equations

From Praetorius et al (2012), the first order differential equations to express the concentration changes per river compartment are listed here:

- Free TiO₂ ENPs in the first box of moving water

$$\frac{dc_{w1,1}^{TiO_2}}{dt} = -(k_{exch,12} + k_{river,flow,1} + k_{dep,w1}^{TiO_2} + k_{het-agg}) \cdot c_{w1,1}^{TiO_2}(t) + k_{exch,21} \cdot \frac{V_{w2,1}}{V_{w1,1}} \cdot c_{w2,1}^{TiO_2}(t) + q_{TiO_2}^{input} \quad (A2.1)$$

- Free TiO₂ ENPs in boxes 2 to n_{boxes} of moving water:

$$\frac{dc_{w1,n}^{TiO_2}}{dt} = -(k_{exch,12} + k_{river,flow,n} + k_{dep,w1}^{TiO_2} + k_{het-agg}) \cdot c_{w1,n}^{TiO_2}(t) + k_{exch,21} \cdot \frac{V_{w2,n}}{V_{w1,n}} \cdot c_{w2,n}^{TiO_2}(t) + k_{river,flow,n-1} \cdot \frac{V_{w1,n-1}}{V_{w1,n}} \cdot c_{w1,n-1}^{TiO_2}(t) \quad (A2.2)$$

For n= 2, . . . , n_{boxes}

- Free TiO₂ ENPs in stagnant water:

$$\frac{dc_{w2,n}^{TiO_2}}{dt} = -(k_{exch,12} + k_{dep,w2}^{TiO_2} + k_{het-agg}) \cdot c_{w2,n}^{TiO_2}(t) + (k_{exch,21} + k_{dep,w1}^{TiO_2}) \cdot \frac{V_{w1,n}}{V_{w2,n}} \cdot c_{w1,n}^{TiO_2}(t) \quad (A2.3)$$

For n= 1, . . . , n_{boxes}

- Free TiO₂ ENPs in the first box of sediment:

$$\frac{dc_{sed,1}^{TiO_2}}{dt} = -(k_{resusp} + k_{burial} + k_{sed-transfer,1}) \cdot c_{sed,1}^{TiO_2}(t) + k_{dep,w2}^{TiO_2} \cdot \frac{V_{w2,1}}{V_{sed,1}} \cdot c_{w2,1}^{TiO_2}(t) \quad (A2.4)$$

- Free TiO₂ ENPs in boxes 2 to n_{boxes} of sediment:

$$\begin{aligned} \frac{dc_{sed,n}^{TiO_2}}{dt} = & -(k_{resusp} + k_{burial} + k_{sed-transfer,n}) \cdot c_{sed,n}^{TiO_2}(t) + k_{dep,w2} \cdot \\ & \frac{V_{w2,n}}{V_{sed,n}} \cdot c_{w2,n}^{TiO_2}(t) + k_{sed-transfer,n-1} \cdot \frac{V_{sed,n-1}}{V_{sed,n}} \cdot c_{sed,n-1}^{TiO_2}(t) \end{aligned} \quad (A2.5)$$

For n= 2, . . . , n_{boxes}

- TiO₂ ENPs bound to SPM in the first box of moving water:

$$\begin{aligned} \frac{dc_{w1,1}^{TiO_2+SPM}}{dt} = & -(k_{exch,12} + k_{river,flow,1} + k_{dep,w1}^{SPM}) \cdot c_{w1,1}^{TiO_2+SPM}(t) + \\ & k_{het-agg} \cdot c_{w1,1}^{TiO_2}(t) + k_{exch,21} \cdot \frac{V_{w2,1}}{V_{w1,1}} \cdot c_{w2,1}^{TiO_2+SPM}(t) \end{aligned} \quad (A2.6)$$

- TiO₂ ENPs bound to SPM in boxes 2 to n_{boxes} of moving water:

$$\begin{aligned} \frac{dc_{w1,n}^{TiO_2+SPM}}{dt} = & -(k_{exch,12} + k_{river,flow,n} + k_{dep,w1}^{SPM}) \cdot c_{w1,n}^{TiO_2+SPM}(t) + \\ & k_{het-agg} \cdot c_{w1,n}^{TiO_2}(t) + k_{exch,21} \cdot \frac{V_{w2,n}}{V_{w1,n}} \cdot c_{w2,n}^{TiO_2+SPM}(t) + k_{river,flow,n-1} \cdot \\ & \frac{V_{w1,n-1}}{V_{w1,n}} \cdot c_{w1,n-1}^{TiO_2+SPM}(t) \end{aligned} \quad (A2.7)$$

For n= 2, . . . , n_{boxes}

- TiO₂ ENPs bound to SPM in the stagnant water:

$$\begin{aligned} \frac{dc_{w2,n}^{TiO_2+SPM}}{dt} = & -(k_{exch,12} + k_{dep,w2}^{SPM}) \cdot c_{w2,n}^{TiO_2+SPM}(t) + k_{het-agg} \cdot \\ & c_{w2,n}^{TiO_2}(t) + (k_{exch,21} + k_{dep,w1}^{SPM}) \cdot \frac{V_{w1,n}}{V_{w2,n}} \cdot c_{w1,n}^{TiO_2+SPM}(t) + k_{resusp} \cdot \frac{V_{sed,n}}{V_{w2,n}} \cdot \\ & c_{sed,n}^{TiO_2+SPM} \end{aligned} \quad (A2.8)$$

For n= 1, . . . , n_{boxes}

- TiO₂ ENPs bound to SPM in the first box of sediment:

$$\frac{dc_{sed,1}^{TiO_2+SPM}}{dt} = -(k_{resusp} + k_{burial} + k_{sed-transfer,1}) \cdot c_{sed,1}^{TiO_2+SPM}(t) + k_{dep,w2}^{SPM} \cdot \frac{V_{w2,1}}{V_{sed,1}} \cdot c_{w2,1}^{TiO_2+SPM}(t) \quad (A2.9)$$

- TiO₂ ENPs bound to SPM in boxes 2 to n_{boxes} of sediment:

$$\frac{dc_{sed,n}^{TiO_2+SPM}}{dt} = -(k_{resusp} + k_{burial} + k_{sed-transfer,n}) \cdot c_{sed,n}^{TiO_2+SPM}(t) + k_{dep,w2}^{SPM} \cdot \frac{V_{w2,n}}{V_{sed,n}} \cdot c_{w2,n}^{TiO_2+SPM}(t) + k_{sed-transfer,n-1} \cdot \frac{V_{sed,n-1}}{V_{sed,n}} \cdot c_{sed,n-1}^{TiO_2+SPM}(t) \quad (A2.10)$$

For n= 2, . . . , n_{boxes}

A2.3 Monitoring data

Table A2.6. Arithmetic mean and standard deviations (std) of the monthly measured Total Suspended Solid (TSS) concentrations in mg/L per monitoring site along the river Foss (F1 to F4) and the river Ouse (O1 to O5).

TSS (mg/L)		July	August	September	October	November	December
Strensall	Mean	54.42	29.07	5.96	5.53	7.87	5.12
	std	34.35	11.85	2.63	2.50	0.75	1.80
F1	Mean	9.23	6.86	4.48	1.69	2.98	4.89
	std	3.85	3.36	2.34	0.38	0.48	0.83
Earswick	Mean	1.90	6.04	2.41	2.92	3.41	5.88
	std	0.26	6.03	1.48	0.40	0.98	0.82
Tower	Mean	7.83	10.70	3.37	2.46	5.41	5.92
	std	1.10	5.84	0.80	0.37	0.32	0.79
A1237	Mean	2.90	2.62	2.33	2.48	6.14	3.40
	std	0.60	0.40	0.46	0.77	0.96	1.07
O1	Mean	3.07	4.62	2.82	2.21	5.96	3.00
	std	0.06	1.29	0.24	0.43	0.98	0.41
Skeldergate	Mean	5.45	4.83	7.26	2.57	7.09	4.04
	std	0.84	0.77	6.41	0.30	1.01	0.52
Millenium	Mean	5.68	5.17	4.17	3.21	6.44	3.81
	std	0.72	1.39	0.20	0.33	1.09	0.34
Naburn	Mean	6.02	5.07	5.06	3.67	5.61	4.84
	std	0.65	0.64	0.11	1.02	0.84	0.23
O5	Mean						
	std						

Table A2.7. Arithmetic mean and standard deviations (std) of the monthly measured dissolved calcium concentration ($[Ca^{2+}]$) in mg/L per monitoring site along the river Foss (F1 to F4) and the river Ouse (O1 to O5).

$[Ca^{2+}]$ (mg/L)		July	August	September	October	November	December
<i>Strensall</i>	Mean	80.14	77.09	81.41	87.84	90.07	100.40
<i>F1</i>	std	1.31	1.76	0.55	0.50	0.49	0.57
<i>Earswick</i>	Mean	82.94	72.49	77.54	87.57	89.76	98.95
<i>F2</i>	std	1.04	0.46	0.51	0.44	0.65	0.64
<i>Heworth</i>	Mean	79.44	70.95	75.54	83.18	84.52	93.99
<i>F3</i>	std	0.27	2.39	0.60	0.73	0.34	0.35
<i>Tower</i>	Mean	57.82	46.25	62.37	40.08	82.02	96.30
<i>F4</i>	std	3.72	1.05	2.11	0.23	0.52	0.71
<i>A1237</i>	Mean	51.27	40.96	59.36	42.40	38.57	47.79
<i>O1</i>	std	1.13	0.39	0.05	0.09	0.16	0.16
<i>Rawcliffe</i>	Mean	50.14	43.91	60.18	40.73	38.16	47.48
<i>O2</i>	std	0.72	0.17	0.50	0.18	0.32	0.21
<i>Skeldergate</i>	Mean	49.08	45.40	60.36	40.07	37.68	46.94
<i>O3</i>	std	0.86	0.48	0.33	0.31	0.14	0.19
<i>Millenium</i>	Mean	49.75	46.84	60.07	39.85	38.79	48.64
<i>O4</i>	std	0.78	0.61	0.49	0.36	0.19	0.30
<i>Naburn</i>	Mean	46.48	47.95	56.59	37.06	37.74	48.69
<i>O5</i>	std	0.08	0.38	0.16	0.30	0.01	0.26

Table A2.8. Arithmetic mean and standard deviations (std) of the monthly measured Dissolved Organic Carbon concentration (DOC) in mg/L per monitoring site along the river Foss (F1 to F4) and the river Ouse (O1 to O5).

DOC (mg/L)		July	August	September	October	November	December
<i>Strensall</i>	Mean	8.77	9.04	6.61	6.66	7.20	7.36
<i>F1</i>	std	0.24	0.13	0.67	0.36	0.32	0.14
<i>Earswick</i>	Mean	8.22	8.15	6.56	6.41	6.65	7.73
<i>F2</i>	std	0.31	0.34	0.46	0.45	0.21	0.45
<i>Heworth</i>	Mean	8.14	8.20	6.51	6.39	6.39	7.70
<i>F3</i>	std		0.32	0.47	0.26	0.13	0.22
<i>Tower</i>	Mean	10.33	8.51	5.60	9.43	6.99	8.46
<i>F4</i>	std	0.11	0.23	0.50	0.29	0.21	0.28
<i>A1237</i>	Mean	9.39	9.40	5.25	9.73	9.76	10.09
<i>O1</i>	std	0.50	0.09	0.28	0.49	0.31	0.30
<i>Rawcliffe</i>	Mean	9.77	8.28	5.16	10.13	9.74	9.87
<i>O2</i>	std	0.48	0.20	0.24	0.18	0.12	0.34
<i>Skeldergate</i>	Mean	10.36	8.52	5.44	10.86	10.51	9.33
<i>O3</i>	std	0.59	0.19	0.70	0.46	0.37	0.21
<i>Millenium</i>	Mean	10.20	8.86	5.33	10.55	10.36	9.49
<i>O4</i>	std	0.15	0.28	0.46	0.17	0.24	0.12
<i>Naburn</i>	Mean	11.88	9.36	6.18	12.63	10.92	10.32
<i>O5</i>	std	0.42	0.20	0.29	0.68	0.53	0.29

Statistical analysis of the three monitored parameters ([Ca²⁺], DOC and TSS) was performed. Firstly, a Shapiro-Wilk's method was applied to test for normality by using the R function `shapiro.test()` (Royston, 1982). Secondly a two way ANOVA analysis was performed in R using the `aov()` function, and finally, a Tukey HSD tests (Tukey, 1949), that calculates post hoc comparisons on each factor in the model was carried out.

1.- Normality

The distribution of the measured values of the three parameters were found to follow a normal distribution (p-value > 0.05).

Table A2.9. Results of Shapiro-Wilk's normality test for the measured values of [Ca²⁺], DOC and TSS, during the monitoring campaign of York rivers.

Parameter	p-value
[Ca ²⁺]	1.35x10 ⁻⁹
DOC	0.00409
TSS	1.87x10 ⁻⁸

2.- Two way ANOVA

Differences between the variance in the obtained values for the three monitored parameters ([Ca²⁺], [DOC] and TSS) were tested between sampling sites and months.

-Calcium concentration ([Ca²⁺])

Table A2.10. Summary of results obtained from the two way ANOVA of the Calcium concentrations measured in York's monitoring campaign as a function of sampling site and month.

	Df	Sum	Mean	F	Pr(>F)
As factor Sampling Site	8	47505	5938	6992.6	<2e-16 ***
As factor Month	5	4775	955	1124.5	<2e-16 ***
As factor of Sampling Site and month	40	9938	248	292.6	<2e-16 ***
Residuals	107	91	1		

According to the results of the two way ANOVA, the calcium concentrations measured for the different sampling sites and months are significantly different, but it exists an interaction between the factors (sampling sites and months).

When looking into the Tukey HSD test as factor of sampling site, we observed that there is no significant differences between sampling sites in the Ouse's calcium concentrations ($p > 0.05$), but that in the Foss the calcium levels of the different sampling sites were significantly different (p -value < 0.05).

For both rivers the calcium measured concentrations were significantly different between months ($p < 0.05$), however depending on the sampling sites that are compared. An interaction of months and sampling sites was found ($p < 0.05$).

-Dissolved organic carbon concentration ([DOC])

Table A2.11. Summary of results obtained from the two way ANOVA of the DOC concentrations measured in York's monitoring campaign as a function of sampling site and month.

	Df	Sum Sq	Mean Sq	F value	Pr(>F)
As factor Sampling Site	8	145.35	18.17	119.91	$< 2e-16$
As factor Month	5	246.58	49.32	325.48	$< 2e-16$
As factor of Sampling Site and month	40	136.74	3.42	22.56	$< 2e-16$
Residuals	108	16.36	0.15		

According to the results of the two way ANOVA, DOC concentrations measured for the different sampling sites and months are significantly different, but it exists an interaction between the factors (sampling sites and months).

When looking into the Tukey HSD test as factor of sampling sites it was found that DOC levels were significantly different ($p < 0.05$) between the Foss and the Ouse. Whiting the same river, DOC concentrations measured for the different sampling sites were found to be significantly different ($p < 0.05$) except from those shown in Table A2.12.

Table A2.12. List of pairwise comparisons between sampling sites that present non significantly different DOC concentrations.

	diff	lwr	upr	p adj
F2-F1	-0.32111	-0.73185	0.089629	0.256002
F3-F1	-0.38222	-0.79296	0.028518	0.089372
F3-F2	-0.06111	-0.47185	0.349629	0.999931
O2-O1	-0.10556	-0.5163	0.305185	0.996248
O3-O1	0.229444	-0.1813	0.640185	0.702552
O4-O1	0.195	-0.21574	0.605741	0.85189
O3-O2	0.335	-0.07574	0.745741	0.20658
O4-O2	0.300556	-0.11019	0.711296	0.341761
O4-O3	-0.03444	-0.44519	0.376296	0.999999

For both rivers, the DOC measured concentrations were significantly different between months ($p < 0.05$), but with the exception of the ones listed in the following table:

Table A2.13. List of pairwise comparisons between months that present non significantly different DOC concentrations.

	diff	lwr	upr	p adj
December-August	0.225926	-0.081462884	0.533315	0.278646
November-August	0.020741	-0.286648069	0.32813	0.999959
November-December	-0.20519	-0.512573995	0.102204	0.385741
October-December	0.27037	-0.037018439	0.577759	0.118498

An interaction of months and sampling sites was found ($p < 0.05$) also for DOC. The list of interactions can be obtained from Tukey HSD tests, which calculates post hoc comparisons on each factor in the model (1431 interactions).

-Total suspended solids

Table A2.14. Summary of results obtained from the two way ANOVA of the TSS concentrations measured in York's monitoring campaign as a function of sampling site and month.

	Df	Sum Sq	Mean Sq	F value	Pr(>F)
As factor Sampling Site	8	133.98	16.748	17.128	1.65e-15 ***
As factor Month	5	145	29	29.659	< 2e-16 ***
As factor of Sampling Site and month	36	263.76	7.327	7.493	1.91e-15 ***
Residuals	95	92.89	0.978		

According to the results of the two way ANOVA, TSS concentrations found for the different sampling sites and months are significantly different, but it exists an interaction between the factors (sampling sites and months).

A2.4 Exposure results

Table A2.15. Summary of predicted concentrations (mg/L) of the freely dispersed TiO₂ ENPs in the flowing water per month (from July to December 2016) and per RS. The monthly maximum (Max), median, 95th and 5th percentile for each RS are reported.

Month		Ouse_1	Ouse_2	Ouse_3	Ouse_4	Ouse_5	Ouse_6	Foss_1	Foss_2	Foss_3	Foss_4
Jul-16	Max	1.65E-04	1.73E-04	2.21E-04	1.69E-04	1.77E-04	2.40E-04	2.84E-04	5.28E-04	1.04E-03	1.27E-03
	95 th percentile	3.25E-05	3.74E-05	4.89E-05	4.68E-05	4.71E-05	5.00E-05	6.30E-06	7.25E-05	1.61E-04	2.66E-04
	Median	9.31E-07	1.34E-06	1.78E-06	1.36E-06	1.45E-06	1.80E-06	2.21E-10	1.03E-06	1.41E-05	3.39E-05
	5 th percentile	1.53E-19	1.24E-10	1.65E-10	5.94E-09	6.42E-09	6.77E-09	5.80E-16	1.11E-11	1.88E-07	7.37E-07
Aug-16	Max	8.17E-05	9.64E-05	1.24E-04	1.09E-04	1.13E-04	2.11E-04	4.58E-04	3.60E-04	4.95E-04	6.19E-04
	95 th percentile	5.47E-05	5.78E-05	7.06E-05	6.95E-05	7.10E-05	1.08E-04	1.63E-04	1.53E-04	1.86E-04	2.82E-04
	Median	7.32E-07	1.04E-06	1.38E-06	1.44E-06	1.53E-06	1.71E-06	2.69E-06	7.88E-06	1.85E-05	4.12E-05
	5 th percentile	1.81E-20	5.51E-11	6.64E-11	1.02E-07	1.10E-07	1.09E-07	1.35E-08	3.82E-07	1.03E-06	3.28E-06
Sep-16	Max	3.35E-05	3.54E-05	4.57E-05	4.50E-05	4.38E-05	4.62E-05	2.40E-04	2.17E-04	3.60E-04	4.31E-04
	95 th percentile	2.42E-05	2.68E-05	3.40E-05	3.01E-05	3.05E-05	3.77E-05	6.71E-05	9.33E-05	1.12E-04	1.77E-04
	Median	2.53E-06	3.34E-06	4.52E-06	3.90E-06	4.31E-06	5.10E-06	1.37E-06	1.93E-05	3.35E-05	6.50E-05
	5 th percentile	1.83E-09	1.36E-07	2.18E-07	2.44E-07	2.64E-07	2.92E-07	2.43E-08	1.37E-06	2.96E-06	7.30E-06
Oct-16	Max	3.57E-05	4.15E-05	5.38E-05	4.33E-05	4.55E-05	8.34E-05	5.71E-04	3.17E-04	3.22E-04	4.04E-04
	95 th percentile	1.92E-05	2.25E-05	2.93E-05	2.62E-05	2.74E-05	5.04E-05	9.25E-05	1.09E-04	1.12E-04	1.99E-04
	Median	2.35E-06	3.26E-06	4.26E-06	3.47E-06	3.90E-06	5.14E-06	1.60E-06	1.52E-05	1.71E-05	5.51E-05
	5 th percentile	2.47E-12	1.53E-09	6.01E-09	1.07E-07	1.12E-07	1.14E-07	3.80E-09	4.41E-07	2.43E-07	7.96E-06
Nov-16	Max	3.84E-05	4.35E-05	5.54E-05	8.91E-05	1.49E-04	3.33E-04	1.91E-04	1.43E-04	2.73E-04	4.05E-04
	95 th percentile	1.76E-05	2.09E-05	2.71E-05	2.03E-05	2.12E-05	3.79E-05	6.90E-05	7.19E-05	9.86E-05	1.36E-04
	Median	9.88E-07	1.30E-06	1.71E-06	1.42E-06	1.85E-06	3.78E-06	2.08E-06	7.64E-06	1.30E-05	2.13E-05
	5 th percentile	2.30E-95	2.06E-11	2.28E-11	2.43E-11	2.61E-11	1.77E-10	3.54E-10	1.06E-10	1.39E-10	1.22E-09
Dec-16	Max	1.20E-05	1.40E-05	1.80E-05	1.44E-05	1.51E-05	2.91E-05	5.95E-05	5.62E-05	9.88E-05	1.21E-04
	95 th percentile	8.38E-06	1.07E-05	1.39E-05	1.08E-05	1.21E-05	2.49E-05	2.79E-05	3.38E-05	5.24E-05	8.14E-05

	Median	6.40E-07	8.74E-07	1.22E-06	8.83E-07	9.65E-07	1.26E-06	1.25E-06	2.23E-06	2.73E-06	7.71E-06
	5 th percentile	1.25E-161	3.56E-11	4.08E-11	2.39E-11	2.66E-11	1.59E-10	3.38E-10	5.03E-11	6.33E-12	9.46E-13

Table A2.16. Summary of predicted concentration (mg/L) of the SPM-bound TiO₂ ENPs in the flowing water per month (from July to December 2016) and per RS. The monthly maximum (Max), median, 95th and 5th percentile for each RS are reported

Month		Ouse_1	Ouse_2	Ouse_3	Ouse_4	Ouse_5	Ouse_6	Foss_1	Foss_2	Foss_3	Foss_4
Jul-16	Max	3.48E-07	4.34E-07	4.16E-07	2.77E-06	2.31E-06	3.09E-06	6.74E-04	2.61E-04	9.89E-05	1.92E-05
	95 th percentile	6.29E-08	1.04E-07	1.06E-07	5.67E-07	5.04E-07	4.84E-07	1.31E-04	5.31E-05	1.57E-05	8.25E-06
	Median	1.47E-09	3.81E-09	4.05E-09	9.21E-09	8.15E-09	8.33E-09	1.58E-06	2.75E-06	6.85E-07	4.87E-07
	5 th percentile	1.56E-21	2.06E-13	5.41E-13	9.94E-11	8.79E-11	8.82E-11	4.25E-09	3.77E-09	1.06E-08	1.55E-08
Aug-16	Max	2.05E-08	3.11E-08	4.22E-08	1.63E-06	1.42E-06	2.23E-06	1.12E-04	5.48E-05	2.78E-05	1.84E-05
	95 th percentile	6.05E-09	1.24E-08	1.72E-08	4.86E-07	4.17E-07	7.66E-07	4.72E-05	2.41E-05	1.58E-05	9.01E-06
	Median	1.17E-10	3.51E-10	4.99E-10	8.95E-09	8.54E-09	1.13E-08	1.93E-06	1.39E-06	1.76E-06	8.40E-07
	5 th percentile	1.37E-23	9.38E-15	2.42E-14	2.25E-10	2.23E-10	2.28E-10	6.62E-08	1.41E-07	1.76E-07	4.41E-08
Sep-16	Max	7.89E-08	1.09E-07	2.17E-07	3.04E-07	3.08E-07	3.08E-07	1.11E-04	1.69E-05	8.05E-06	3.05E-06
	95 th percentile	3.95E-08	6.77E-08	1.24E-07	2.30E-07	2.39E-07	2.42E-07	5.79E-05	6.57E-06	4.38E-06	1.96E-06
	Median	2.78E-09	6.63E-09	1.23E-08	2.90E-08	3.06E-08	4.00E-08	4.07E-06	1.67E-06	1.35E-06	7.24E-07
	5 th percentile	6.46E-12	7.43E-11	1.18E-10	1.53E-09	1.44E-09	1.42E-09	1.77E-07	2.29E-07	2.78E-07	1.09E-07
Oct-16	Max	5.12E-09	5.87E-09	7.47E-09	1.04E-06	8.44E-07	1.46E-06	2.80E-04	3.79E-05	5.96E-05	2.88E-05
	95 th percentile	2.65E-09	4.30E-09	5.50E-09	8.10E-07	7.17E-07	8.88E-07	7.19E-05	2.23E-05	3.56E-05	1.67E-05
	Median	3.05E-10	7.46E-10	1.01E-09	2.68E-08	2.36E-08	2.31E-08	5.07E-06	4.74E-06	7.83E-06	1.74E-06
	5 th percentile	1.41E-15	7.93E-13	3.17E-12	2.56E-10	2.39E-10	2.38E-10	3.98E-08	2.49E-07	3.13E-07	3.00E-08
Nov-16	Max	1.10E-08	1.36E-08	1.79E-08	4.72E-06	7.03E-06	1.43E-05	1.05E-04	3.39E-05	4.50E-05	7.02E-05
	95 th percentile	5.46E-09	1.11E-08	1.41E-08	2.25E-06	1.89E-06	2.69E-06	3.86E-05	2.36E-05	2.94E-05	4.81E-05
	Median	1.44E-10	3.08E-10	4.41E-10	2.33E-07	2.36E-07	4.04E-07	3.32E-06	3.92E-06	6.65E-06	1.19E-05
	5 th percentile	4.69E-98	1.13E-15	3.68E-15	1.06E-10	1.09E-10	2.06E-10	1.45E-09	1.30E-09	1.15E-09	1.20E-08

Dec-16	Max	2.01E-09	2.54E-09	3.36E-09	1.53E-06	1.40E-06	2.85E-06	1.94E-05	2.55E-05	4.10E-05	5.16E-05
	95 th percentile	1.02E-09	1.90E-09	2.54E-09	1.39E-06	1.33E-06	2.41E-06	1.15E-05	1.68E-05	2.77E-05	3.79E-05
	Median	6.23E-11	1.94E-10	2.77E-10	1.00E-07	8.57E-08	8.37E-08	1.16E-06	2.27E-06	3.50E-06	7.43E-06
	5 th percentile	2.62E-164	2.70E-15	6.59E-15	1.91E-13	1.85E-13	2.24E-13	1.81E-09	8.54E-10	1.35E-10	3.30E-11

Table A2.17. Summary of predicted concentration (mg/L) of the total TiO₂ ENPs in the sediment per month (from July to December 2016) and per RS. The monthly maximum (Max), median, 95th and 5th percentile for each RS are reported.

		Ouse_1	Ouse_2	Ouse_3	Ouse_4	Ouse_5	Ouse_6	Foss_1	Foss_2	Foss_3	Foss_4
Jul-16	Max	3.29E-04	3.45E-04	4.41E-04	3.42E-04	3.52E-04	4.75E-04	5.52E-04	1.03E-03	2.06E-03	2.52E-03
	95 th percentile	6.48E-05	7.47E-05	9.75E-05	9.37E-05	9.37E-05	9.88E-05	1.23E-05	1.41E-04	3.19E-04	5.29E-04
	Median	1.86E-06	2.67E-06	3.56E-06	2.76E-06	2.88E-06	3.56E-06	4.32E-10	2.01E-06	2.78E-05	6.73E-05
	5 th percentile	3.09E-19	3.76E-10	4.43E-10	1.29E-08	1.28E-08	1.38E-08	1.58E-15	2.16E-11	3.71E-07	1.46E-06
Aug-16	Max	3.29E-04	3.45E-04	4.41E-04	3.42E-04	3.52E-04	4.75E-04	8.91E-04	1.03E-03	2.06E-03	2.52E-03
	95 th percentile	8.16E-05	9.64E-05	1.19E-04	1.21E-04	1.25E-04	1.91E-04	1.92E-04	2.44E-04	3.50E-04	5.49E-04
	Median	1.78E-06	2.48E-06	3.32E-06	2.85E-06	2.97E-06	3.45E-06	3.55E-07	6.60E-06	3.19E-05	7.27E-05
	5 th percentile	1.26E-19	2.49E-10	3.05E-10	8.57E-08	8.68E-08	9.44E-08	1.42E-14	9.36E-10	8.12E-07	2.74E-06
Sep-16	Max	3.29E-04	3.45E-04	4.41E-04	3.42E-04	3.52E-04	4.75E-04	8.91E-04	1.03E-03	2.06E-03	2.52E-03
	95 th percentile	5.89E-05	7.09E-05	9.24E-05	8.76E-05	9.12E-05	1.08E-04	1.65E-04	2.17E-04	3.05E-04	4.91E-04
	Median	2.72E-06	3.52E-06	4.63E-06	3.84E-06	4.06E-06	4.90E-06	9.34E-07	1.42E-05	4.32E-05	8.69E-05
	5 th percentile	5.25E-17	3.75E-10	4.51E-10	1.52E-07	1.51E-07	1.57E-07	7.15E-14	6.21E-09	1.50E-06	4.95E-06
Oct-16	Max	3.29E-04	3.45E-04	4.41E-04	3.42E-04	3.52E-04	4.75E-04	1.11E-03	1.03E-03	2.06E-03	2.52E-03
	95 th percentile	5.41E-05	6.40E-05	8.25E-05	7.77E-05	8.05E-05	1.02E-04	1.67E-04	2.16E-04	2.79E-04	4.62E-04
	Median	2.91E-06	3.86E-06	5.10E-06	4.61E-06	4.86E-06	5.73E-06	1.34E-06	1.80E-05	4.09E-05	9.47E-05
	5 th percentile	4.75E-16	3.78E-10	4.66E-10	1.58E-07	1.58E-07	1.65E-07	4.03E-13	2.41E-08	1.03E-06	6.61E-06
Nov-16	Max	3.29E-04	3.45E-04	4.41E-04	3.42E-04	3.52E-04	6.60E-04	1.11E-03	1.03E-03	2.06E-03	2.52E-03
	95 th percentile	5.26E-05	6.16E-05	7.93E-05	7.41E-05	7.69E-05	9.81E-05	1.62E-04	2.08E-04	2.64E-04	4.30E-04

	Median	2.71E-06	3.64E-06	4.80E-06	4.23E-06	4.64E-06	6.30E-06	1.75E-06	1.72E-05	3.78E-05	8.44E-05
	5th percentile	3.22E-20	2.40E-10	2.96E-10	8.06E-08	7.83E-08	8.37E-08	1.35E-12	5.64E-09	4.68E-07	2.69E-06
Dec-16	Max	3.29E-04	3.45E-04	4.41E-04	3.42E-04	3.52E-04	6.60E-04	1.11E-03	1.03E-03	2.06E-03	2.52E-03
	95th percentile	4.99E-05	5.81E-05	7.50E-05	6.81E-05	7.20E-05	9.13E-05	1.47E-04	2.00E-04	2.51E-04	4.14E-04
	Median	2.64E-06	3.53E-06	4.66E-06	3.88E-06	4.28E-06	5.72E-06	1.83E-06	1.57E-05	3.38E-05	7.66E-05
	5th percentile	5.39E-23	1.53E-10	1.81E-10	3.04E-08	3.81E-08	5.26E-08	3.01E-12	1.73E-09	2.64E-07	1.43E-06

Abbreviations

AF = Assessment factor

ANOVA = Analysis of variance

CB = Carbon black

CDF = Cumulative distribution function

CLP = Classification, Labelling and Packaging

CNT = Carbon nanotube

CPI = Nanotechnology Consumer products inventory

DLVO = Derjaguin and Landau, and Verwey and Overbeck

DMT = Digital elevation map

DO = Dissolved oxygen

DOM = Dissolved organic matter

DRA = Dose response assessment

EC = Electric conductivity

EC10 = 10% effect concentration

EC50 = 50% effect concentration

EDL = Electric double layer forces

EEM = Emissions estimation model

EFM = Environmental fate model

ENM = Engineered nanomaterial

ENP = Engineered nanoparticle

EPs = Emerging pollutants

ERA = Environmental risk assessment

GIS = Geographical information system

HC5 = 5th percentile of the fitted distribution

HZ = hydrological zone

IS = Ionic strength

LC10 = 10% lethal concentration

LC50 = 50% lethal concentration

MFA = Material flow analysis

MPs = Microplastics

MWCNT = Multiwalled carbon nanotube

NOEC = no-observed-effect concentration

NOM = Natural organic matter

NPI = Nano product inventory

NZVI = Zero valent iron

PCP = Personal care products

PEC = predicted environmental concentration

PFA = Particle flow analysis

PNEC = Predicted no effect concentration

PZC = Point zero charge

QDs = Quantum dots

REACH = Registration, Evaluation, Authorization, and Restriction of Chemicals

RIVM = Netherlands National Institute for Public Health and the Environment

ROS = Reactive oxygen species

RQ = Risk quotient

RS = River section

SA = Surface area

SCENIHR = Scientific Committee on Emerging and Newly Identified Health Risks

spICP-MS = Single particle inductively coupled plasma–mass spectrometry

SPM = Suspended particle matter

SSD = Species sensitivity analysis

SWCNT = Single walled carbon nanotube

SWFM = Surface water fate model

SWO = Storm water outlet

T= Temperature

TKTD = Toxicokinetic-toxicodynamic

TSS = Total suspended solids

WWTP = Waste water treatment plant

References

- Akaighe, N., Depner, S. W., Banerjee, S., Sharma, V. K., & Sohn, M. (2012). The effects of monovalent and divalent cations on the stability of silver nanoparticles formed from direct reduction of silver ions by Suwannee River humic acid/natural organic matter. *Science of The Total Environment*, *441*, 277–289. <https://doi.org/10.1016/J.SCITOTENV.2012.09.055>
- Al-Kattan, Ahmed; Wichser, Adrian; Vonbank, Roger; Brunner, Samuel; Ulrich, Andrea; Zuin, Stefano; Nowack, B. (2013). Release of TiO₂ from paints containing pigment-TiO₂ or nano-TiO₂ by weathering. *Environ. Sci. Processes Impacts*, (207890). <https://doi.org/10.1016/j.jpcs.2007.07.118>
- Al-Kattan, A., Wichser, A., Vonbank, R., & &- ... Science: Processes. (2013). Release of TiO₂ from paints containing pigment-TiO₂ or nano-TiO₂ by weathering.
- Allen, B. L., Kichambare, P. D., Gou, P., Vlasova, I. I., Kapralov, A. A., Konduru, N., ... Star, A. (2008). Biodegradation of Single-Walled Carbon Nanotubes through Enzymatic Catalysis. *Nano Letters*, *8*(11), 3899–3903. <https://doi.org/10.1021/nl802315h>
- Amenta, V., Aschberger, K., A., M., B., H., Moniz, F. B., Brandhoff, P., ... Rauscher, H. (2015). Regulatory aspects of nanotechnology in the agri/feed/food sector in EU and non-EU countries. *Regulatory Toxicology and Pharmacology: RTP*, *73*(1), 463–476.
- ANSES. (2013). *Elements issus des déclarations des substances à l'état nanoparticulaire. RAPPORT d'étude.*
- Arnold, J. G., Moriasi, D. N., Gassman, P. W., Abbaspour, K. C., White, M. J., Griensven, V., & Liew, V. (2012). SWAT: Model use, calibration, and validation. *Transactions of the ASABE*, *55*(4), 1491–1508.
- Arvidsson, R., Molander, S., & Sanden, B. A. (2012). Particle Flow Analysis: Exploring Potential Use Phase Emissions of Titanium Dioxide Nanoparticles from Sunscreen, Paint, and Cement. *Journal of Industrial Ecology*, *16*(3), 343–351. <https://doi.org/10.1111/j.1530-9290.2011.00429.x>
- Ashauer, R., & Brown, C. D. (2013). Highly time-variable exposure to chemicals-toward

- an assessment strategy. *Integrated Environmental Assessment and Management*, 9(3), e27–e33. <https://doi.org/10.1002/ieam.1421>
- Auffan, M., Rose, J., Bottero, J. Y., Lowry, G. V., Jolivet, J. P., & Wiesner, M. R. (2009). Towards a definition of inorganic nanoparticles from an environmental, health and safety perspective. *Nature Nanotechnology*. <https://doi.org/10.1038/nnano.2009.242>
- Baalousha, M. (2009). Aggregation and disaggregation of iron oxide nanoparticles: Influence of particle concentration, pH and natural organic matter. *Science of The Total Environment*, 407(6), 2093–2101. <https://doi.org/10.1016/J.SCITOTENV.2008.11.022>
- Baalousha, M., Yang, Y., Vance, M. E., Colman, B. P., McNeal, S., Xu, J., ... Hochella, M. F. (2016). Outdoor urban nanomaterials: The emergence of a new, integrated, and critical field of study. *Science of the Total Environment*, 557–558, 740–753. <https://doi.org/10.1016/j.scitotenv.2016.03.132>
- Batley, G. E., Halliburton, B., Kirby, J. K., Doolette, C. L., Navarro, D., McLaughlin, M. J., & Veitch, C. (2013). Characterization and Ecological Risk Assessment Of Nanoparticulate CeO₂ as a Diesel Fuel Catalyst. *Environmental Toxicology and Chemistry*, 32(8), 1896–1905. <https://doi.org/10.1002/etc.2246>
- Benn, T., Cavanagh, B., Hristovski, K., Posner, J. D., & Westerhoff, P. (2010). The release of nanosilver from consumer products used in the home. *Journal of Environmental Quality*, 39(6), 1875–1882. <https://doi.org/10.2134/jeq2009.0363>
- Bennett, S. W., Adeleye, A., Ji, Z., & Keller, A. A. (2013). Stability, metal leaching, photoactivity and toxicity in freshwater systems of commercial single wall carbon nanotubes. *Water Research*, 47(12), 4074–4085. <https://doi.org/10.1016/J.WATRES.2012.12.039>
- Bian, S.-W., Mudunkotuwa, I. A., Rupasinghe, T., & Grassian, V. H. (2011). Aggregation and Dissolution of 4 nm ZnO Nanoparticles in Aqueous Environments: Influence of pH, Ionic Strength, Size, and Adsorption of Humic Acid, 27, 6059–6068. <https://doi.org/10.1021/la200570n>
- Biesterbos, J. W. H., Dudzina, T., Delmaar, C. J. E., Bakker, M. I., Russel, F. G. M., von Goetz, N., ... Roeleveld, N. (2013). Usage patterns of personal care products: Important factors for exposure assessment. *Food and Chemical Toxicology*, 55, 8–

17. <https://doi.org/10.1016/J.FCT.2012.11.014>
- Boholm, M., & Arvidsson, R. (2016). A Definition Framework for the Terms Nanomaterial and Nanoparticle. *NanoEthics*, *10*(1), 25–40. <https://doi.org/10.1007/s11569-015-0249-7>
- Bossa, N., Chaurand, P., Levard, C., Borschneck, D., Miche, H., Vicente, J., ... Rose, J. (2017). Environmental exposure to TiO₂ nanomaterials incorporated in building material. *Environmental Pollution*, *220*, 1160–1170. <https://doi.org/10.1016/j.envpol.2016.11.019>
- Bowman, D. M., van Calster, G., & Friedrichs, S. (2010). Nanomaterials and regulation of cosmetics. *Nature Nanotechnology*, *5*(2), 92. <https://doi.org/10.1038/nnano.2010.12>
- Boxall, A. B., Chaudhry, Q., Sinclair, C., Jones, A., Aitken, R., B., J., & Watts, C. (2007). Current and Future Predicted Environmental Exposure To Engineered Nanoparticles. *Central Science Laboratory, Department of the Environment and Rural Affairs, London, UK*, 89. <https://doi.org/196111>
- Bradley, E. L., Castle, L., & Chaudhry, Q. (2011). Applications of nanomaterials in food packaging with a consideration of opportunities for developing countries. *Trends in Food Science & Technology*, *22*(11), 604–610. <https://doi.org/10.1016/J.TIFS.2011.01.002>
- Brausch, J. M., & Rand, G. M. (2011). A review of personal care products in the aquatic environment: Environmental concentrations and toxicity. *Chemosphere*. <https://doi.org/10.1016/j.chemosphere.2010.11.018>
- Bundschuh, M., Filser, J., Lüderwald, S., McKee, M. S., Metreveli, G., Schaumann, G. E., ... Wagner, S. (2018, December 8). Nanoparticles in the environment: where do we come from, where do we go to? *Environmental Sciences Europe*. SpringerOpen. <https://doi.org/10.1186/s12302-018-0132-6>
- Caballero-Guzman, A., & Nowack, B. (2016). A critical review of engineered nanomaterial release data: Are current data useful for material flow modeling? *Environmental Pollution*, *213*, 502–517. <https://doi.org/10.1016/j.envpol.2016.02.028>
- Chen, G., Peijnenburg, W. J. G. M., Xiao, Y., & Vijver, M. G. (2018). Developing species

- sensitivity distributions for metallic nanomaterials considering the characteristics of nanomaterials, experimental conditions, and different types of endpoints. *Food and Chemical Toxicology*, *112*, 563–570. <https://doi.org/10.1016/J.FCT.2017.04.003>
- Chen, J., Xiu, Z., Lowry, G. V., & Alvarez, P. J. J. (2011). Effect of natural organic matter on toxicity and reactivity of nano-scale zero-valent iron. *Water Research*, *45*(5), 1995–2001. <https://doi.org/10.1016/J.WATRES.2010.11.036>
- Chowdhury, I., Cwiertny, D. M., & Walker, S. L. (2012). Combined Factors Influencing the Aggregation and Deposition of nano-TiO₂ in the Presence of Humic Acid and Bacteria. *Environmental Science & Technology*, *46*(13), 6968–6976. <https://doi.org/10.1021/es2034747>
- Clavier, A., Praetorius, A., & Stoll, S. (2019). Determination of nanoparticle heteroaggregation attachment efficiencies and rates in presence of natural organic matter monomers. Monte Carlo modelling. *Science of The Total Environment*, *650*, 530–540. <https://doi.org/10.1016/J.SCITOTENV.2018.09.017>
- Coelho, M. C., Torrão, G., Emami, N., & Gr'cio, J. (2012). Nanotechnology in Automotive Industry: Research Strategy and Trends for the Future—Small Objects, Big Impacts. *Journal of Nanoscience and Nanotechnology*, *12*(8), 6621–6630. <https://doi.org/10.1166/jnn.2012.4573>
- Colvin, V. L. (2003). The potential environmental impact of engineered nanomaterials. *Nature Biotechnology*, *21*(10), 1166–1170. <https://doi.org/10.1038/nbt875>
- Dale, A. L., Casman, E. A., Lowry, G. V., Lead, J. R., Viparelli, E., & Baalousha, M. (2015). Modeling nanomaterial environmental fate in aquatic systems. *Environmental Science and Technology*, *49*(5), 2587–2593. <https://doi.org/10.1021/es505076w>
- Dale, A. L., Lowry, G. V., & Casman, E. A. (2015). Stream Dynamics and Chemical Transformations Control the Environmental Fate of Silver and Zinc Oxide Nanoparticles in a Watershed-Scale Model. *Environmental Science and Technology*, *49*(12), 7285–7293. <https://doi.org/10.1021/acs.est.5b01205>
- Dastjerdi, R., & Montazer, M. (2010). A review on the application of inorganic nano-structured materials in the modification of textiles: Focus on anti-microbial properties. *Colloids and Surfaces B: Biointerfaces*, *79*(1), 5–18.

<https://doi.org/10.1016/J.COLSURFB.2010.03.029>

- de Zwart, D., Adams, W., Galay Burgos, M., Hollender, J., Junghans, M., Merrington, G., ... Williams, R. (2018). Aquatic exposures of chemical mixtures in urban environments: Approaches to impact assessment. *Environmental Toxicology and Chemistry*, 37(3), 703–714. <https://doi.org/10.1002/etc.3975>
- Department for Communities and Local Government. (2013). *Housing Standards Review*.
- Derjaguin, B., & Landau, L. (1993). Theory of the stability of strongly charged lyophobic sols and of the adhesion of strongly charged particles in solutions of electrolytes. *Progress in Surface Science*, 43(1–4), 30–59. [https://doi.org/10.1016/0079-6816\(93\)90013-L](https://doi.org/10.1016/0079-6816(93)90013-L)
- Dimitroulopoulou, C., Lucica, E., Johnson, A., Ashmore, M. R., Sakellaris, I., Stranger, M., & Goelen, E. (2015). EPHECT I: European household survey on domestic use of consumer products and development of worst-case scenarios for daily use. *Science of the Total Environment*, 536, 880–889. <https://doi.org/10.1016/j.scitotenv.2015.05.036>
- Dobias, J., & Bernier-Latmani, R. (2013). Silver Release from Silver Nanoparticles in Natural Waters. *Environmental Science & Technology*, 47(9), 4140–4146. <https://doi.org/10.1021/es304023p>
- Domingos, R. F., Tufenkji, N., & Wilkinson, K. J. (2009). Aggregation of Titanium Dioxide Nanoparticles: Role of a Fulvic Acid. *Environmental Science & Technology*, 43(5), 1282–1286. <https://doi.org/10.1021/es8023594>
- Donovan, A. R., Adams, C. D., Ma, Y., Stephan, C., Eichholz, T., & Shi, H. (2016). Single particle ICP-MS characterization of titanium dioxide, silver, and gold nanoparticles during drinking water treatment. *Chemosphere*, 144, 148–153. <https://doi.org/10.1016/J.CHEMOSPHERE.2015.07.081>
- Douglas-Mankin, K. R., Srinivasan, R., & Arnold, J. G. (2010). Soil and water assessment tool (SWAT) model: Current developments and applications. *Transactions of the ASABE*, 53(5), 1423–1431.
- Duester, L., Burkhardt, M., Gutleb, A. C., Kaegi, R., Macken, A., Meermann, B., & von der Kammer, F. (2014). Toward a comprehensive and realistic risk evaluation of engineered nanomaterials in the urban water system. *Frontiers in Chemistry*, 2, 39.

<https://doi.org/10.3389/fchem.2014.00039>

- Dumont, E., Johnson, A. C., Keller, V. D. J. J., & Williams, R. J. (2015). Nano silver and nano zinc-oxide in surface waters ??? Exposure estimation for Europe at high spatial and temporal resolution. *Environmental Pollution*, *196*, 341–349. <https://doi.org/10.1016/j.envpol.2014.10.022>
- Dwivedi, A. D., Dubey, S. P., Sillanpää, M., Kwon, Y.-N., Lee, C., & Varma, R. S. (2015). Fate of engineered nanoparticles: Implications in the environment. *Coordination Chemistry Reviews*, *287*, 64–78. <https://doi.org/10.1016/J.CCR.2014.12.014>
- El Badawy, A. M., Scheckel, K. G., Suidan, M., & Tolaymat, T. (2012). The impact of stabilization mechanism on the aggregation kinetics of silver nanoparticles. *Science of The Total Environment*, *429*, 325–331. <https://doi.org/10.1016/J.SCITOTENV.2012.03.041>
- EPA. (2018). Species sensitivity distribution generator V1. Retrieved February 6, 2019, from https://www3.epa.gov/caddis/da_software_ssdmacro.html
- European Chemicals Agency. (2008). *Guidance on information requirements and chemical safety assessment. Chapter R.15: Consumer exposure estimation. Guidance for the implementation of REACH. Version: 2.1.*
- European Commission. (2008). Nanomaterials in REACH.
- Foss Hansen, S., Roverskov Heggelund, L., Revilla Besora, P., Mackevica, A., Boldrin, A., & Baun, A. (2016). Nanoproducts – what is actually available to European consumers? *Environ. Sci.: Nano*, *3*(1), 169–180. <https://doi.org/10.1039/C5EN00182J>
- Franco, A., Price, O. R., Marshall, S., Jolliet, O., Van den Brink, P. J., Rico, A., ... Ashauer, R. (2017). Toward refined environmental scenarios for ecological risk assessment of down-the-drain chemicals in freshwater environments. *Integrated Environmental Assessment and Management*, *13*(2), 233–248. <https://doi.org/10.1002/ieam.1801>
- Gajewicz, A., Rasulev, B., Dinadayalane, T. C., Urbaszek, P., Puzyn, T., Leszczynska, D., & Leszczynski, J. (2012). Advancing risk assessment of engineered nanomaterials: Application of computational approaches. *Advanced Drug Delivery*

- Reviews*, 64(15), 1663–1693. <https://doi.org/10.1016/J.ADDR.2012.05.014>
- Gao, J., Powers, K., Wang, Y., Zhou, H., Roberts, S. M., Moudgil, B. M., ... Barber, D. S. (2012). Influence of Suwannee River humic acid on particle properties and toxicity of silver nanoparticles. *Chemosphere*, 89(1), 96–101. <https://doi.org/10.1016/J.CHEMOSPHERE.2012.04.024>
- García-Alonso, J., Rodríguez-Sánchez, N., Misra, S. K., Valsami-Jones, E., Croteau, M.-N., Luoma, S. N., & Rainbow, P. S. (2014). Toxicity and accumulation of silver nanoparticles during development of the marine polychaete *Platynereis dumerilii*. *Science of The Total Environment*, 476–477, 688–695. <https://doi.org/10.1016/J.SCITOTENV.2014.01.039>
- Garner, K. L., & Keller, A. A. (2014). Emerging patterns for engineered nanomaterials in the environment: A review of fate and toxicity studies. *Journal of Nanoparticle Research*. <https://doi.org/10.1007/s11051-014-2503-2>
- Garner, K. L., Suh, S., Lenihan, H. S., & Keller, A. A. (2015). Species Sensitivity Distributions for Engineered Nanomaterials. *Environmental Science & Technology*, 49(9), 5753–5759. <https://doi.org/10.1021/acs.est.5b00081>
- Geissen, V., Mol, H., Klumpp, E., Umlauf, G., Nadal, M., van der Ploeg, M., ... Ritsema, C. J. (2015). Emerging pollutants in the environment: A challenge for water resource management. *International Soil and Water Conservation Research*, 3(1), 57–65. <https://doi.org/10.1016/j.iswcr.2015.03.002>
- Giese, B., Klaessig, F., Park, B., Kaegi, R., Steinfeldt, M., Wigger, H., ... Gottschalk, F. (2018). Risks, Release and Concentrations of Engineered Nanomaterial in the Environment. *Scientific Reports*, 8(1), 1565. <https://doi.org/10.1038/s41598-018-19275-4>
- Goldberg, E., Scheringer, M., Bucheli, T. D., & Hungerbühler, K. (2014). Critical assessment of models for transport of engineered nanoparticles in saturated porous media. *Environmental Science and Technology*, 48(21), 12732–12741. <https://doi.org/10.1021/es502044k>
- Gondikas, A. P., Von Der Kammer, F., Reed, R. B., Wagner, S., Ranville, J. F., & Hofmann, T. (2014). Release of TiO₂ nanoparticles from sunscreens into surface waters: A one-year survey at the old danube recreational lake. *Environmental*

- Science and Technology*, 48(10), 5415–5422. <https://doi.org/10.1021/es405596y>
- Gondikas, A., von der Kammer, F., Kaegi, R., Borovinskaya, O., Neubauer, E., Navratilova, J., ... Hofmann, T. (2018). Where is the nano? Analytical approaches for the detection and quantification of TiO₂ engineered nanoparticles in surface waters. *Environmental Science: Nano*, 5(2), 313–326. <https://doi.org/10.1039/C7EN00952F>
- Good, K. D., Bergman, L. E., Klara, S. S., Leitch, M. E., & VanBriesen, J. M. (2016). Implications of Engineered Nanomaterials in Drinking Water Sources. *Journal - American Water Works Association*, 108(1), E1–E17. <https://doi.org/10.5942/jawwa.2016.108.0013>
- Gosling, S. N., & Arnell, N. W. (2016). A global assessment of the impact of climate change on water scarcity. *Climatic Change*, 134(3), 371–385. <https://doi.org/10.1007/s10584-013-0853-x>
- Gottschalk, F., Lassen, C., Kjoelholt, J., Christensen, F., & Nowack, B. (2015). Modeling flows and concentrations of nine engineered nanomaterials in the Danish environment. *International Journal of Environmental Research and Public Health*, 12(5), 5581–602. <https://doi.org/10.3390/ijerph120505581>
- Gottschalk, F., & Nowack, B. (2011). The release of engineered nanomaterials to the environment. *Journal of Environmental Monitoring: JEM*, 13(5), 1145–55. <https://doi.org/10.1039/c0em00547a>
- Gottschalk, F., & Nowack, B. (2013). A probabilistic method for species sensitivity distributions taking into account the inherent uncertainty and variability of effects to estimate environmental risk. *Integrated Environmental Assessment and Management*, 9(1), 79–86. <https://doi.org/10.1002/ieam.1334>
- Gottschalk, F., Ort, C., Scholz, R. W., & Nowack, B. (2011). Engineered nanomaterials in rivers - Exposure scenarios for Switzerland at high spatial and temporal resolution. *Environmental Pollution*, 159(12), 3439–3445. <https://doi.org/10.1016/j.envpol.2011.08.023>
- Gottschalk, F., Scholz, R. W., & Nowack, B. (2010). Probabilistic material flow modeling for assessing the environmental exposure to compounds: Methodology and an application to engineered nano-TiO₂ particles. *Environmental Modelling &*

- Software*, 25(3), 320–332.
- Gottschalk, F., Sonderer, T., Scholz, R. W., & Nowack, B. (2009). Modeled Environmental Concentrations of Engineered Nanomaterials (TiO₂, ZnO, Ag, CNT, Fullerenes) for Different Regions. *Environmental Science & Technology*, 43(24), 9216–9222. <https://doi.org/10.1021/es9015553>
- Gottschalk, F., Sun, T., & Nowack, B. (2013). Environmental concentrations of engineered nanomaterials: Review of modeling and analytical studies. *Environmental Pollution*, 181, 287–300. <https://doi.org/10.1016/j.envpol.2013.06.003>
- Grill, G., Khan, U., Lehner, B., Nicell, J., & Ariwi, J. (2016). Risk assessment of down-the-drain chemicals at large spatial scales: Model development and application to contaminants originating from urban areas in the Saint Lawrence River Basin. *Science of The Total Environment*, 541, 825–838. <https://doi.org/10.1016/J.SCITOTENV.2015.09.100>
- Handy, R. D., Owen, R., & Valsami-Jones, E. (2008). The ecotoxicology of nanoparticles and nanomaterials: Current status, knowledge gaps, challenges, and future needs. *Ecotoxicology*. Springer US. <https://doi.org/10.1007/s10646-008-0206-0>
- Hannon, J. C., Kerry, J., Cruz-Romero, M., Morris, M., & Cummins, E. (2015). Advances and challenges for the use of engineered nanoparticles in food contact materials. *Trends in Food Science & Technology*, 43(1), 43–62. <https://doi.org/10.1016/J.TIFS.2015.01.008>
- Hansen, S. F., Baun, A., Michelson, E. S., Kamper, A., Borling, P., & Stuer-Lauridsen, F. (2009). Nanomaterials in Consumer Products. In *Nanomaterials: Risks and Benefits* (pp. 359–367). Dordrecht: Springer Netherlands. https://doi.org/10.1007/978-1-4020-9491-0_28
- Hansen, S. F., Michelson, E. S., Kamper, A., Borling, P., Stuer-Lauridsen, F., & Baun, A. (2008). Categorization framework to aid exposure assessment of nanomaterials in consumer products. *Ecotoxicology*, 17(5), 438–447. <https://doi.org/10.1007/s10646-008-0210-4>
- Hartmann, N. B., Skjolding, L. M., Hansen, S. F., Kjølholt, J., Gottschalk, F., & Baun, A. (2014). *Environmental fate and behaviour of nanomaterials - New knowledge on*

- important transformation processes. Danish Environmental Protection Agency, 2014* (Vol. 55). APA. <https://doi.org/10.13140/2.1.1943.4240>
- Heberer, T., Reddersen, K., & Mechlinski, A. (2002). From municipal sewage to drinking water: Fate and removal of pharmaceutical residues in the aquatic environment in urban areas. In *Water Science and Technology* (Vol. 46, pp. 81–88).
- Hegde, K., Brar, S. K., Verma, M., & Surampalli, R. Y. (2016). Current understandings of toxicity, risks and regulations of engineered nanoparticles with respect to environmental microorganisms. *Nanotechnology for Environmental Engineering*, 1(1), 5. <https://doi.org/10.1007/s41204-016-0005-4>
- Hendren, C. O., Mesnard, X., Dröge, J., & Wiesner, M. R. (2011). Estimating Production Data for Five Engineered Nanomaterials As a Basis for Exposure Assessment. *Environmental Science & Technology*, 45(7), 2562–2569. <https://doi.org/10.1021/es103300g>
- Hennebert, P., Avellan, A., Yan, J., & Aguerre-Chariol, O. (2013). Experimental evidence of colloids and nanoparticles presence from 25 waste leachates. *Waste Management*, 33(9), 1870–1881. <https://doi.org/10.1016/J.WASMAN.2013.04.014>
- Hischier, R., Nowack, B., Gottschalk, F., Hincapie, I., Steinfeldt, M., & Som, C. (2015). Life cycle assessment of fa??ade coating systems containing manufactured nanomaterials. *Journal of Nanoparticle Research*, 17(2). <https://doi.org/10.1007/s11051-015-2881-0>
- Hotze, E. M., Phenrat, T., & Lowry, G. V. (2010). Nanoparticle Aggregation: Challenges to Understanding Transport and Reactivity in the Environment. *Journal of Environment Quality*, 39(6), 1909. <https://doi.org/10.2134/jeq2009.0462>
- Howard, A. G., Duffus, J. H., Nordberg, M., Templeton, D. M., Klaine, S. J., Alvarez, P. J. J., ... Bettmer, J. (2010). On the challenge of quantifying man-made nanoparticles in the aquatic environment. *J. Environ. Monit.*, 12(1), 135–142. <https://doi.org/10.1039/B913681A>
- Hristozov, D., Malsch, I., Hristozov, D., & Malsch, I. (2009). Hazards and Risks of Engineered Nanoparticles for the Environment and Human Health. *Sustainability*, 1(4), 1161–1194. <https://doi.org/10.3390/su1041161>
- HTF Market Report. (2018). *Global Nanotechnology Market (by Component and*

- Applications), Funding & Investment, Patent Analysis and 27 Companies Profile & Recent Developments - Forecast to 2024.*
- Hussein, A. K. (2015). Applications of nanotechnology in renewable energies—A comprehensive overview and understanding. *Renewable and Sustainable Energy Reviews*, 42, 460–476. <https://doi.org/10.1016/J.RSER.2014.10.027>
- Ibrahim, R. K., Hayyan, M., AlSaadi, M. A., Hayyan, A., & Ibrahim, S. (2016). Environmental application of nanotechnology: air, soil, and water. *Environmental Science and Pollution Research*, 23(14), 13754–13788. <https://doi.org/10.1007/s11356-016-6457-z>
- Jacobs, R., Meesters, J. A. J., ter Braak, C. J. F., van de Meent, D., & van der Voet, H. (2016). Combining exposure and effect modeling into an integrated probabilistic environmental risk assessment for nanoparticles. *Environmental Toxicology and Chemistry*, 35(12), 2958–2967. <https://doi.org/10.1002/etc.3476>
- Jacques Buffle, *, Kevin J. Wilkinson, Serge Stoll, Montserrat Filella, and, & Zhang†, J. (1998). A Generalized Description of Aquatic Colloidal Interactions: The Three-colloidal Component Approach. <https://doi.org/10.1021/ES980217H>
- Jager, T. (2016). Predicting environmental risk: A road map for the future. *Journal of Toxicology and Environmental Health, Part A*, 79(13–15), 572–584. <https://doi.org/10.1080/15287394.2016.1171986>
- Jager, T., & Ashauer, R. (2018). How to Evaluate the Quality of Toxicokinetic-Toxicodynamic Models in the Context of Environmental Risk Assessment. *Integrated Environmental Assessment and Management*, 14(5), 604–614. <https://doi.org/10.1002/ieam.2026>
- Jiang, J., Oberdörster, G., & Biswas, P. (2009). Characterization of size, surface charge, and agglomeration state of nanoparticle dispersions for toxicological studies. *Journal of Nanoparticle Research*, 11(1), 77–89. <https://doi.org/10.1007/s11051-008-9446-4>
- Johnson, A. C., & Park, B. (2012). Predicting contamination by the fuel additive cerium oxide engineered nanoparticles within the United Kingdom and the associated risks. *Environmental Toxicology and Chemistry*, 31(11), 2582–2587. <https://doi.org/10.1002/etc.1983>

- Johnson, A., Cisowska, I., Jurgens, M., ... V. K.-C. for E., & 2011, undefined. (2011). Exposure assessment for engineered silver nanoparticles throughout the rivers of England and Wales. *Lwecext.Rl.Ac.Uk*.
- Kaegi, R., Sinnet, B., Zuleeg, S., Hagendorfer, H., Mueller, E., Vonbank, R., ... Burkhardt, M. (2010). Release of silver nanoparticles from outdoor facades. *Environmental Pollution*, *158*(9), 2900–2905. <https://doi.org/10.1016/J.ENVPOL.2010.06.009>
- Kaegi, R., Ulrich, A., Sinnet, B., Vonbank, R., Wichser, A., Zuleeg, S., ... Boller, M. (2008). Synthetic TiO₂ nanoparticle emission from exterior facades into the aquatic environment. *Environmental Pollution*, *156*(2), 233–239. <https://doi.org/10.1016/j.envpol.2008.08.004>
- Kaegi, R., Voegelin, A., Sinnet, B., Zuleeg, S., Hagendorfer, H., Burkhardt, M., & Siegrist, H. (2011). Behavior of metallic silver nanoparticles in a pilot wastewater treatment plant. *Environmental Science & Technology*, *45*(9), 3902–3908.
- Karn, S. K., & Harada, H. (2001). Surface water pollution in three urban territories of Nepal, India, and Bangladesh. *Environmental Management*, *28*(4), 483–496. <https://doi.org/10.1007/s002670010238>
- Keller, A. A., & Lazareva, A. (2014). Predicted Releases of Engineered Nanomaterials: From Global to Regional to Local. *Environmental Science and Technology Letters*, *1*(1), 65–70. <https://doi.org/10.1021/ez400106t>
- Keller, A. A., McFerran, S., Lazareva, A., & Suh, S. (2013). Global life cycle releases of engineered nanomaterials. *Journal of Nanoparticle Research*, *15*(6), 1692. <https://doi.org/10.1007/s11051-013-1692-4>
- Keller, A. A., Vosti, W., Wang, H., & Lazareva, A. (2014). Release of engineered nanomaterials from personal care products throughout their life cycle. *Journal of Nanoparticle Research*, *16*(7), 2489. <https://doi.org/10.1007/s11051-014-2489-9>
- Khanna, A. S. (2008). Nanotechnology in High Performance Paint Coatings. *Asian Journal of Experimental Science*, *21*(2), 25–32.
- Khin, M. M., Nair, A. S., Babu, V. J., Murugan, R., & Ramakrishna, S. (2012). A review on nanomaterials for environmental remediation. *Energy & Environmental Science*, *5*(8), 8075. <https://doi.org/10.1039/c2ee21818f>

- Khot, L. R., Sankaran, S., Maja, J. M., Ehsani, R., & Schuster, E. W. (2012). Applications of nanomaterials in agricultural production and crop protection: A review. *Crop Protection*, *35*, 64–70. <https://doi.org/10.1016/J.CROPRO.2012.01.007>
- Kirschling, T. L., Golas, P. L., Unrine, J. M., Matyjaszewski, K., Gregory, K. B., Lowry, G. V., & Tilton, D. (2011). Microbial Bioavailability of Covalently Bound Polymer Coatings on Model Engineered Nanomaterials. *Environ. Sci. Technol*, *45*, 5253–5259. <https://doi.org/10.1021/es200770z>
- Klaine, S. J., Alvarez, P. J. J., Batley, G. E., Fernandes, T. F., Handy, R. D., Lyon, D. Y., ... Lead, J. R. (2008). NANOMATERIALS IN THE ENVIRONMENT: BEHAVIOR, FATE, BIOAVAILABILITY, AND EFFECTS. *Environmental Toxicology and Chemistry*, *27*(9), 1825. <https://doi.org/10.1897/08-090.1>
- Klein, J. J. M. de, Quik, J. T. K., Bäuerlein, P. S., & Koelmans, A. A. (2016). Towards validation of the NanoDUFLOW nanoparticle fate model for the river Dommel, The Netherlands. *Environ. Sci.: Nano*, *3*(2), 434–441. <https://doi.org/10.1039/C5EN00270B>
- Kreyling, W. G., Semmler-Behnke, M., & Chaudhry, Q. (2010). A complementary definition of nanomaterial. *Nano Today*, *5*(3), 165–168. <https://doi.org/10.1016/J.NANTOD.2010.03.004>
- Kumar, P., Ketzler, M., Vardoulakis, S., Pirjola, L., & Britter, R. (2011). Dynamics and dispersion modelling of nanoparticles from road traffic in the urban atmospheric environment-A review. *Journal of Aerosol Science*, *42*(9), 580–603. <https://doi.org/10.1016/j.jaerosci.2011.06.001>
- Kumar, P., Pirjola, L., Ketzler, M., & Harrison, R. M. (2013). Nanoparticle emissions from 11 non-vehicle exhaust sources - A review. *Atmospheric Environment*. <https://doi.org/10.1016/j.atmosenv.2012.11.011>
- Lee, S., Kim, K., Shon, H. K., Kim, S. D., & Cho, J. (2011). Biototoxicity of nanoparticles: effect of natural organic matter. *Journal of Nanoparticle Research*, *13*(7), 3051–3061. <https://doi.org/10.1007/s11051-010-0204-z>
- Levard, C., Hotze, E. M., Colman, B. P., Dale, A. L., Truong, L., Yang, X. Y., ... Lowry, G. V. (2013). Sulfidation of Silver Nanoparticles: Natural Antidote to Their Toxicity. *Environmental Science & Technology*, *47*(23), 13440–13448.

<https://doi.org/10.1021/es403527n>

- Levard, C., Hotze, E. M., Lowry, G. V., & Brown, G. E. (2012). Environmental Transformations of Silver Nanoparticles: Impact on Stability and Toxicity. *Environmental Science & Technology*, 46(13), 6900–6914. <https://doi.org/10.1021/es2037405>
- Lewicka, Z. A., Benedetto, A. F., Benoit, D. N., Yu, W. W., Fortner, J. D., & Colvin, V. L. (2011). The structure, composition, and dimensions of TiO₂ and ZnO nanomaterials in commercial sunscreens. *Journal of Nanoparticle Research*, 13(9), 3607–3617. <https://doi.org/10.1007/s11051-011-0438-4>
- Li, C., Liu, M., Hu, Y., Shi, T., Zong, M., & Walter, M. T. (2018). Assessing the Impact of Urbanization on Direct Runoff Using Improved Composite CN Method in a Large Urban Area. *International Journal of Environmental Research and Public Health*, 15(4). <https://doi.org/10.3390/ijerph15040775>
- Li, K., & Chen, Y. (2012). Effect of natural organic matter on the aggregation kinetics of CeO₂ nanoparticles in KCl and CaCl₂ solutions: Measurements and modeling. *Journal of Hazardous Materials*, 209–210, 264–270. <https://doi.org/10.1016/J.JHAZMAT.2012.01.013>
- Li, M., & Huang, C. P. (2010). Stability of oxidized single-walled carbon nanotubes in the presence of simple electrolytes and humic acid. *Carbon*, 48(15), 4527–4534. <https://doi.org/10.1016/J.CARBON.2010.08.032>
- Limbach, L. K., Bereiter, R., Muller, E., Krebs, R., Galli, R., & Srtark, W. J. (2008). Removal of Oxide Nanoparticles in a Model Wastewater Treatment Plant: Influence of Agglomeration and Surfactants on Clearing Efficiency. *Environmental Science and Technology*, 42(15), 5828–5833.
- Lin, D., Tian, X., Wu, F., & Xing, B. (2009). Fate and Transport of Engineered Nanomaterials in the Environment. *Nowack and Bucheli*. <https://doi.org/10.2134/jeq2009.0423>
- Liu, H. H., Bilal, M., Lazareva, A., Keller, A., & Cohen, Y. (2015). Simulation tool for assessing the release and environmental distribution of nanomaterials. *Beilstein Journal of Nanotechnology*, 6(1), 938–951. <https://doi.org/10.3762/bjnano.6.97>
- Liu, J., & Hurt, R. H. (2010). Ion Release Kinetics and Particle Persistence in Aqueous

- Nano-Silver Colloids. *Environmental Science & Technology*, 44(6), 2169–2175. <https://doi.org/10.1021/es9035557>
- Lok, C.-N., Ho, C.-M., Chen, R., He, Q.-Y., Yu, W.-Y., Sun, H., ... Che, C.-M. (2007). Silver nanoparticles: partial oxidation and antibacterial activities. *JBIC Journal of Biological Inorganic Chemistry*, 12(4), 527–534. <https://doi.org/10.1007/s00775-007-0208-z>
- Loosli, F., Le Coustumer, P., & Stoll, S. (2014). Effect of natural organic matter on the disagglomeration of manufactured TiO₂ nanoparticles. *Environmental Science: Nano*, 1(2), 154. <https://doi.org/10.1039/c3en00061c>
- Lorenz, C., Windler, L., von Goetz, N., Lehmann, R. P., Schuppler, M., Hungerbühler, K., ... Nowack, B. (2012). Characterization of silver release from commercially available functional (nano)textiles. *Chemosphere*, 89(7), 817–824. <https://doi.org/10.1016/J.CHEMOSPHERE.2012.04.063>
- Lowry, G. V., Gregory, K. B., Apte, S. C., & Lead, J. R. (2012). Transformations of Nanomaterials in the Environment. *Environmental Science & Technology*, 46(13), 6893–6899. <https://doi.org/10.1021/es300839e>
- Lynch, I., & Dawson, K. A. (2008). Protein-nanoparticle interactions. *Nano Today*, 3(1–2), 40–47. [https://doi.org/10.1016/S1748-0132\(08\)70014-8](https://doi.org/10.1016/S1748-0132(08)70014-8)
- Mangematin, V., & Walsh, S. (2012). The future of nanotechnologies. *Technovation*, 32(3–4), 157–160. <https://doi.org/10.1016/J.TECHNOVATION.2012.01.003>
- Markets, R. and. (2015). *Global Nanotechnology Market Outlook 2022*. RNCOS E-Services Private (Vol. 175). <https://doi.org/10.1177/1357633X12474964>
- Meesters, J. A. J., Koelmans, A. A., Quik, J. T. K., Hendriks, A. J., & van de Meent, D. (2014). Multimedia Modeling of Engineered Nanoparticles with SimpleBox4nano: Model Definition and Evaluation. *Environmental Science & Technology*, 48(10), 5726–5736. <https://doi.org/10.1021/es500548h>
- Meesters, J. A. J., Quik, J. T. K., Koelmans, A. A., Hendriks, A. J., & van de Meent, D. (2016). Multimedia environmental fate and speciation of engineered nanoparticles: a probabilistic modeling approach. *Environ. Sci.: Nano*, 3(4), 715–727. <https://doi.org/10.1039/C6EN00081A>
- Meesters, J. A., Veltman, K., Hendriks, A. J., & van de Meent, D. (2013). Environmental

- exposure assessment of engineered nanoparticles: Why REACH needs adjustment. *Integrated Environmental Assessment and Management*, 9(3), e15–e26. <https://doi.org/10.1002/ieam.1446>
- Micheli, L., Sarmah, N., Luo, X., Reddy, K. S., & Mallick, T. K. (2013). Opportunities and challenges in micro- and nano-technologies for concentrating photovoltaic cooling: A review. *Renewable and Sustainable Energy Reviews*, 20, 595–610. <https://doi.org/10.1016/J.RSER.2012.11.051>
- Mihranyan, A., Ferraz, N., & Strømme, M. (2012). Current status and future prospects of nanotechnology in cosmetics. *Progress in Materials Science*, 57(5), 875–910. <https://doi.org/10.1016/J.PMATSCI.2011.10.001>
- Misra, S. K., Dybowska, A., Berhanu, D., Croteau, M. N., Luoma, S. N., Boccaccini, A. R., & Valsami-Jones, E. (2012). Isotopically Modified Nanoparticles for Enhanced Detection in Bioaccumulation Studies. *Environmental Science & Technology*, 46(2), 1216–1222. <https://doi.org/10.1021/es2039757>
- Misra, S. K., Dybowska, A., Berhanu, D., Luoma, S. N., & Valsami-Jones, E. (2012). The complexity of nanoparticle dissolution and its importance in nanotoxicological studies. *Science of The Total Environment*, 438, 225–232. <https://doi.org/10.1016/J.SCITOTENV.2012.08.066>
- Mitrano, D. M., Mehrabi, K., Dasilva, Y. A. R., Nowack, B., Hering, A. S., Higgins, C., ... Prikopsky, K. (2017). Mobility of metallic (nano)particles in leachates from landfills containing waste incineration residues. *Environ. Sci.: Nano*, 4(2), 480–492. <https://doi.org/10.1039/C6EN00565A>
- Mitrano, D. M., Motellier, S., Clavaguera, S., & Nowack, B. (2015). Review of nanomaterial aging and transformations through the life cycle of nano-enhanced products. *Environment International*, 77, 132–147. <https://doi.org/10.1016/J.ENVINT.2015.01.013>
- Mitrano, D. M., Rimmele, E., Wichser, A., Erni, R., Height, M., & Nowack, B. (2014). Presence of nanoparticles in wash water from conventional silver and nano-silver textiles. *ACS Nano*, 8(7), 7208–7219. <https://doi.org/10.1021/nn502228w>
- Modaresi, R., Westerlund, C., & Viklander, M. (2010). *Estimation of pollutant loads transported by runoff by using a GIS model Case study: Luleå city centre Estimation*

de la charge polluante des eaux de ruissellement à l'aide d'un SIG : étude de cas au centre ville de Luleå (Suède).

- Montoro Bustos, A. R., Purushotham, K. P., Possolo, A., Farkas, N., Vladár, A. E., Murphy, K. E., & Winchester, M. R. (2018). Validation of Single Particle ICP-MS for Routine Measurements of Nanoparticle Size and Number Size Distribution. *Analytical Chemistry*, 90(24), 14376–14386. <https://doi.org/10.1021/acs.analchem.8b03871>
- Mueller, N. C., & Nowack, B. (2008). Exposure Modeling of Engineered Nanoparticles in the Environment. *Environmental Science & Technology*, 42(12), 4447–4453. <https://doi.org/10.1021/es7029637>
- Musee, N. (2011). Simulated environmental risk estimation of engineered nanomaterials: A case of cosmetics in Johannesburg City. *Human & Experimental Toxicology*, 30(9), 1181–1195. <https://doi.org/10.1177/09603271110391387>
- Nations, United. (2014). *World Urbanization Prospects. The 2014 Revision*.
- Neal, C., Jarvie, H., Rowland, P., Lawler, A., Sleep, D., & Scholefield, P. (2011). Titanium in UK rural, agricultural and urban/industrial rivers: Geogenic and anthropogenic colloidal/sub-colloidal sources and the significance of within-river retention. *Science of the Total Environment*, 409, 1843–1853. <https://doi.org/10.1016/j.scitotenv.2010.12.021>
- Nikalje, A. P. (2015). Nanotechnology and its Applications in Medicine. *Nanotechnology and Its Applications in Medicine. Med Chem*, 5(2), 81-089. <https://doi.org/10.4172/2161-0444.1000247>
- Nowack, B. (2017). Evaluation of environmental exposure models for engineered nanomaterials in a regulatory context. *NanoImpact*. <https://doi.org/10.1016/j.impact.2017.06.005>
- Nowack, B., Boldrin, A., Caballero, A., Hansen, S. F., Gottschalk, F., Heggelund, L., ... Hristozov, D. (2016). Meeting the Needs for Released Nanomaterials Required for Further Testing—The SUN Approach. *Environmental Science & Technology*, 50(6), 2747–2753. <https://doi.org/10.1021/acs.est.5b04472>
- Nowack, B., Bornhöft, N., Ding, Y., & Riediker, M. (2015). The flows of engineered nanomaterials from production, use, and disposal to the environment.

- Nowack, B., Ranville, J. F., Diamond, S., Gallego-Urrea, J. A., Metcalfe, C., Rose, J., ... Klaine, S. J. (2012). Potential scenarios for nanomaterial release and subsequent alteration in the environment. *Environmental Toxicology and Chemistry*. John Wiley & Sons, Inc. <https://doi.org/10.1002/etc.726>
- O'Brien, N., & Cummins, E. (2010). Ranking initial environmental and human health risk resulting from environmentally relevant nanomaterials. *Journal of Environmental Science and Health. Part A, Toxic/Hazardous Substances & Environmental Engineering*, 45(8), 992–1007. <https://doi.org/10.1080/10934521003772410>
- Ordnance Survey (GB), U. E. D. O. S. S. (n.d.). OS MasterMap Water Network Layer [GML3 geospatial data], Scale 1:2500, Tiles: se54sw, se54nw, se55sw, se55nw, se56sw, se54se, se54ne, se55se, se55ne, se56se, se64sw, se64nw, se65sw, se65nw, se66sw, se64se, se64ne, se65se, se65ne, se66se, Updated: 24 July.
- OS MasterMap. (n.d.). OS MasterMap Building Heights Layer [Shape geospatial data], Tile(s): SE55, SE65, SE54, SE64 , Updated: October 2017 , Ordnance Survey, Using: EDINA Digimap Ordnance Survey Service, <https://digimap.edina.ac.uk/roam/download/os>, Downloaded: February 2018).
- Pacheco-Torgal, F., & Jalali, S. (2011, February 1). Nanotechnology: Advantages and drawbacks in the field of construction and building materials. *Construction and Building Materials*. Elsevier. <https://doi.org/10.1016/j.conbuildmat.2010.07.009>
- Pal, A., He, Y., Jekel, M., Reinhard, M., & Gin, K. Y. H. (2014, October). Emerging contaminants of public health significance as water quality indicator compounds in the urban water cycle. *Environment International*. <https://doi.org/10.1016/j.envint.2014.05.025>
- Parkin, I. P., & Palgrave, R. G. (2005). Self-cleaning coatings. *Journal of Materials Chemistry*, 15(17), 1689. <https://doi.org/10.1039/b412803f>
- Pauleit, S., & Duhme, F. (2000). Assessing the environmental performance of land cover types for urban planning. *Landscape and Urban Planning*, 52(1), 1–20. [https://doi.org/10.1016/S0169-2046\(00\)00109-2](https://doi.org/10.1016/S0169-2046(00)00109-2)
- Peng, X., Yu, Y., Tang, C., Tan, J., Huang, Q., & Wang, Z. (2008). Occurrence of steroid estrogens, endocrine-disrupting phenols, and acid pharmaceutical residues in urban riverine water of the Pearl River Delta, South China. *Science of the Total*

- Environment*, 397(1–3), 158–166. <https://doi.org/10.1016/j.scitotenv.2008.02.059>
- Peters, R. J. B., van Bommel, G., Milani, N. B. L., den Hertog, G. C. T., Undas, A. K., van der Lee, M., & Bouwmeester, H. (2018). Detection of nanoparticles in Dutch surface waters. *Science of The Total Environment*, 621, 210–218. <https://doi.org/10.1016/J.SCITOTENV.2017.11.238>
- Petosa, A. R., Jaisi, D. P., Quevedo, I. R., Elimelech, M., & Tufenkji, N. (2010). Aggregation and deposition of engineered nanomaterials in aquatic environments: Role of physicochemical interactions. *Environmental Science and Technology*, 44(17), 6532–6549. <https://doi.org/10.1021/es100598h>
- Piccinno, F., Gottschalk, F., Seeger, S., & Nowack, B. (2012). Industrial production quantities and uses of ten engineered nanomaterials in Europe and the world. *Journal of Nanoparticle Research*, 14(9), 1109. <https://doi.org/10.1007/s11051-012-1109-9>
- Praetorius, A. (2014). *Development of environmental fate models for engineered nanoparticles*.
- Praetorius, A., Arvidsson, R., Molander, S., & Scheringer, M. (2013). Facing complexity through informed simplifications: A research agenda for aquatic exposure assessment of nanoparticles. *Environmental Sciences: Processes and Impacts*, 15(1), 161–168. <https://doi.org/10.1039/c2em30677h>
- Praetorius, A., Labille, J., Scheringer, M., Thill, A., Hungerbühler, K., & Bottero, J.-Y. (2014). Heteroaggregation of Titanium Dioxide Nanoparticles with Model Natural Colloids under Environmentally Relevant Conditions. *Environmental Science & Technology*, 48(18), 10690–10698. <https://doi.org/10.1021/es501655v>
- Praetorius, A., Scheringer, M., & Hungerbühler, K. (2012). Development of Environmental Fate Models for Engineered Nanoparticles—A Case Study of TiO₂ Nanoparticles in the Rhine River. <https://doi.org/10.1021/es204530n>
- Praetorius, A., Tufenkji, N., Goss, K.-U., Scheringer, M., von der Kammer, F., & Elimelech, M. (2014). The road to nowhere: equilibrium partition coefficients for nanoparticles. *Environ. Sci.: Nano*, 1(4), 317–323. <https://doi.org/10.1039/C4EN00043A>
- Quik, J. T. K., Lynch, I., Hoecke, K. Van, Miermans, C. J. H., Schamphelaere, K. A. C. De, Janssen, C. R., ... Meent, D. Van De. (2010). Effect of natural organic matter

- on cerium dioxide nanoparticles settling in model fresh water. *Chemosphere*, 81(6), 711–715. <https://doi.org/10.1016/J.CHEMOSPHERE.2010.07.062>
- Quik, J. T. K., Velzeboer, I., Wouterse, M., Koelmans, A. A., & van de Meent, D. (2014). Heteroaggregation and sedimentation rates for nanomaterials in natural waters. *Water Research*, 48, 269–279. <https://doi.org/10.1016/J.WATRES.2013.09.036>
- Rauscher, H., Rasmussen, K., & Sokull-Klüttgen, B. (2017). Regulatory Aspects of Nanomaterials in the EU. *Chemie-Ingenieur-Technik*, 89(3), 224–231. <https://doi.org/10.1002/cite.201600076>
- Risks, S. C. on E. and N. I. H. (2013). *Scientific Committee on Emerging and Newly Identified Health Risks SCENIHR Scientific Committee on Consumer Safety Addressing the New Challenges for Risk Assessment*. <https://doi.org/10.2772/XXXXXXXX>
- Royston, J. P. (1982). An Extension of Shapiro and Wilk's W Test for Normality to Large Samples. *Applied Statistics*, 31(2), 115. <https://doi.org/10.2307/2347973>
- Sani-Kast, N., Scheringer, M., Slomberg, D., Labille, J., Praetorius, A., Ollivier, P., & Hungerbühler, K. (2015). Addressing the complexity of water chemistry in environmental fate modeling for engineered nanoparticles. *Science of the Total Environment*, 535, 150–159. <https://doi.org/10.1016/j.scitotenv.2014.12.025>
- Santamouris, M. (2013). Using cool pavements as a mitigation strategy to fight urban heat island—A review of the actual developments. *Renewable and Sustainable Energy Reviews*, 26, 224–240. <https://doi.org/10.1016/J.RSER.2013.05.047>
- Schmid, K., & Riediker, M. (2008). Use of Nanoparticles in Swiss Industry: A Targeted Survey. *Environmental Science & Technology*, 42(7), 2253–2260. <https://doi.org/10.1021/es071818o>
- Schneider, C. A., Rasband, W. S., & Eliceiri, K. W. (2012). NIH Image to ImageJ: 25 years of image analysis. *Nature Methods*, 9(7), 671–675. <https://doi.org/10.1038/nmeth.2089>
- Schwirn, K., Tietjen, L., & Beer, I. (2014). Why are nanomaterials different and how can they be appropriately regulated under REACH? *Environmental Sciences Europe*, 26(1), 4. <https://doi.org/10.1186/2190-4715-26-4>
- Selvan, V. A. M., Anand, R. B., & Udayakumar, M. (2009). Effects of cerium oxide

- nanoparticle addition in diesel and diesel-biodiesel-ethanol blends on the performance and emission characteristics of a CI engine. *Journal of Engineering and Applied Sciences*.
- Sharma, V. K., Siskova, K. M., Zboril, R., & Gardea-Torresdey, J. L. (2014). Organic-coated silver nanoparticles in biological and environmental conditions: Fate, stability and toxicity. *Advances in Colloid and Interface Science*, *204*, 15–34. <https://doi.org/10.1016/J.CIS.2013.12.002>
- Silva, B. F. da, Pérez, S., Gardinalli, P., Singhal, R. K., & Mozeto, A. A. (2011). Analytical chemistry of metallic nanoparticles in natural environments. *TrAC Trends in Analytical Chemistry*, *30*(3), 528–540. <https://doi.org/10.1016/J.TRAC.2011.01.008>
- Stark, W. J., Stoessel, P. R., Wohlleben, W., & Hafner, A. (2015). Industrial applications of nanoparticles. *Chemical Society Reviews*, *44*(16), 5793–5805. <https://doi.org/10.1039/C4CS00362D>
- Stone, V., Nowack, B., Baun, A., van den Brink, N., von der Kammer, F., Dusinska, M., ... Fernandes, T. F. (2010). Nanomaterials for environmental studies: Classification, reference material issues, and strategies for physico-chemical characterisation. *Science of The Total Environment*, *408*(7), 1745–1754. <https://doi.org/10.1016/J.SCITOTENV.2009.10.035>
- Sun, T. Y., Bornhöft, N. A., Hungerbühler, K., & Nowack, B. (2016). Dynamic probabilistic modeling of environmental emissions of engineered nanomaterials. *Environmental Science & Technology*, *41*, 8–11. <https://doi.org/10.1038/nature>
- Sun, T. Y., Conroy, G., Donner, E., Hungerbühler, K., Lombi, E., & Nowack, B. (2015). Probabilistic modelling of engineered nanomaterial emissions to the environment: A spatio-temporal approach. *Environmental Science: Nano*, *2*(4), 340–351. <https://doi.org/10.1039/c5en00004a>
- Sun, T. Y., Gottschalk, F., Hungerbühler, K., & Nowack, B. (2014). Comprehensive probabilistic modelling of environmental emissions of engineered nanomaterials. *Environmental Pollution*, *185*, 69–76. <https://doi.org/10.1016/J.ENVPOL.2013.10.004>
- Sun, T. Y., Mitrano, D. M., Bornhöft, N. A., Scheringer, M., Hungerbühler, K., &

- Nowack, B. (2017). Envisioning Nano Release Dynamics in a Changing World: Using Dynamic Probabilistic Modeling to Assess Future Environmental Emissions of Engineered Nanomaterials. *Environmental Science and Technology*, 51(5), 2854–2863. <https://doi.org/10.1021/acs.est.6b05702>
- Taebi, A., & Droste, R. (2004). Pollution loads in urban runoff and sanitary wastewater. *Science of the Total Environment*.
- TGD. (2003). *Technical Guidance Document on Risk Assessment*.
- Thio, B. J. R., Zhou, D., & Keller, A. A. (2011). Influence of natural organic matter on the aggregation and deposition of titanium dioxide nanoparticles. *Journal of Hazardous Materials*, 189(1–2), 556–563. <https://doi.org/10.1016/J.JHAZMAT.2011.02.072>
- Tiede, K., Foss Hanssen, S., Westerhoff, P., Fern, G. J., Hankin, S. M., Aitken, R. J., ... Boxall, A. B. A. (2016). How important is drinking water exposure for the risks of engineered nanoparticles to consumers? *Nanotoxicology*, 10(1), 1743–5390. <https://doi.org/10.3109/17435390.2015.1022888>
- Tijani, J. O., Fatoba, O. O., & Petrik, L. F. (2013). A review of pharmaceuticals and endocrine-disrupting compounds: Sources, effects, removal, and detections. *Water, Air, and Soil Pollution*, 224(11), 1770. <https://doi.org/10.1007/s11270-013-1770-3>
- Tripathi, D. K., Tripathi, A., Shweta, Singh, S., Singh, Y., Vishwakarma, K., ... Chauhan, D. K. (2017). Uptake, Accumulation and Toxicity of Silver Nanoparticle in Autotrophic Plants, and Heterotrophic Microbes: A Concentric Review. *Frontiers in Microbiology*, 08, 7. <https://doi.org/10.3389/fmicb.2017.00007>
- Tsuzuki, T., & Tsuzuki, T. (2009). Commercial scale production of inorganic nanoparticles. *Article in International Journal of Nanotechnology*, 6(6), 567–578. <https://doi.org/10.1504/IJNT.2009.024647>
- Tukey, J. W. (1949). Comparing Individual Means in the Analysis of Variance. *Biometrics*, 5(2), 99. <https://doi.org/10.2307/3001913>
- Tulve, N. S., Stefaniak, A. B., Vance, M. E., Rogers, K., Mwilu, S., LeBouf, R. F., ... Marr, L. C. (2015). Characterization of silver nanoparticles in selected consumer products and its relevance for predicting children's potential exposures. *International Journal of Hygiene and Environmental Health*, 218(3), 345–357.

<https://doi.org/10.1016/j.ijheh.2015.02.002>

- Uskoković, V. (2013). Entering the era of nanoscience: time to be so small. *Journal of Biomedical Nanotechnology*, 9(9), 1441–70.
- Valsami-Jones, E., & Lynch, I. (2015). How safe are nanomaterials? *Science*, 350(6259), 388–389.
- Vance, M. E., Kuiken, T., Vejerano, E. P., McGinnis, S. P., Hochella, M. F., & Hull, D. R. (2015). Nanotechnology in the real world: Redeveloping the nanomaterial consumer products inventory. *Beilstein Journal of Nanotechnology*, 6(1), 1769–1780. <https://doi.org/10.3762/bjnano.6.181>
- Verwey, E., & Overbeek, J. T. G. (1955). Theory of the stability of lyophobic colloids : Letters to the Editor. *The Journal of Colloid Science*, 10(2), 224–225.
- Wagner, S., Gondikas, A., Neubauer, E., Hofmann, T., & von der Kammer, F. (2014). Spot the Difference: Engineered and Natural Nanoparticles in the Environment-Release, Behavior, and Fate. *Angewandte Chemie International Edition*, 53(46), n/a-n/a. <https://doi.org/10.1002/anie.201405050>
- Walczyk, D., Bombelli, F. B., Monopoli, M. P., Lynch, I., & Dawson, K. A. (2010). What the Cell “Sees” in Bionanoscience. *Journal of the American Chemical Society*, 132(16), 5761–5768. <https://doi.org/10.1021/ja910675v>
- Walser, T., Limbach, L. K., Brogioli, R., Erismann, E., Flamigni, L., Hattendorf, B., ... Stark, W. J. (2012). Persistence of engineered nanoparticles in a municipal solid-waste incineration plant. *Nature Nanotechnology*, 7(8), 520–524. <https://doi.org/10.1038/nnano.2012.64>
- Wang, H., Ho, K. T., Scheckel, K. G., Wu, F., Cantwell, M. G., Katz, D. R., ... Burgess, R. M. (2014). Toxicity, Bioaccumulation, and Biotransformation of Silver Nanoparticles in Marine Organisms. *Environmental Science & Technology*, 48(23), 13711–13717. <https://doi.org/10.1021/es502976y>
- Warheit, D. B. (2018). Hazard and risk assessment strategies for nanoparticle exposures: how far have we come in the past 10 years? *F1000Research*, 7, 376. <https://doi.org/10.12688/f1000research.12691.1>
- Warren, C., Mackay, D., Whelan, M., & Fox, K. (2005). Mass balance modelling of contaminants in river basins: A flexible matrix approach. *Chemosphere*, 61(10),

- 1458–1467. <https://doi.org/10.1016/J.CHEMOSPHERE.2005.04.118>
- Weather Pages, Department of Electronics, University of York. (n.d.). Retrieved September 2, 2019, from <https://weather.elec.york.ac.uk/archive.html>
- Weir, A., Westerhoff, P., Fabricius, L., Hristovski, K., & von Goetz, N. (2012). Titanium Dioxide Nanoparticles in Food and Personal Care Products. *Environmental Science & Technology*, *46*(4), 2242–2250. <https://doi.org/10.1021/es204168d>
- Whiteley, C. M., Valle, M. D., Jones, K. C., & Sweetman, A. J. (2013). Challenges in assessing release, exposure and fate of silver nanoparticles within the UK environment. *Environmental Science: Processes & Impacts*, *15*(11), 2050. <https://doi.org/10.1039/c3em00226h>
- Wiek, A., Guston, D., van der Leeuw, S., Selin, C., & Shapira, P. (2013). Nanotechnology in the City: Sustainability Challenges and Anticipatory Governance. *Journal of Urban Technology*, *20*(2), 45–62. <https://doi.org/10.1080/10630732.2012.735415>
- Wiesner, M. R., Lowry, G. V., Jones, K. L., Hochella, Jr., M. F., Di Giulio, R. T., Casman, E., & Bernhardt, E. S. (2009). Decreasing Uncertainties in Assessing Environmental Exposure, Risk, and Ecological Implications of Nanomaterials † ‡. *Environmental Science & Technology*, *43*(17), 6458–6462. <https://doi.org/10.1021/es803621k>
- Wijnhoven, P., Dekkers, S., & Hagens, W. I. (2009). *Exposure to nanomaterials in consumer products Exposure to nanomaterials in consumer products. Public Health.*
- Williams, R. J., Harrison, S., Keller, V., Kuenen, J., Lofts, S., Praetorius, A., ... van Wijnen, J. (2019). Models for assessing engineered nanomaterial fate and behaviour in the aquatic environment. *Current Opinion in Environmental Sustainability*, *36*, 105–115. <https://doi.org/10.1016/J.COSUST.2018.11.002>
- Xia, Q., Hwang, H.-M., Ray, P. C., & Yu, H. (2014). Mechanisms of nanotoxicity: Generation of reactive oxygen species. *Journal of Food and Drug Analysis*, *22*(1), 64–75. <https://doi.org/10.1016/J.JFDA.2014.01.005>
- Yang, Y., Vance, M., Tou, F., Tiwari, A., Liu, M., & Hochella., M. F. (2014). Nanoparticles in road dust from impervious urban surfaces: distribution, identification, and environmental implications. *Atmospheric Environment*, *2*(1), 534–544. <https://doi.org/10.1039/C6EN00056H>
- Yin, Y., Yang, X., Zhou, X., Wang, W., Yu, S., Liu, J., & Jiang, G. (2015). Water

- chemistry controlled aggregation and photo-transformation of silver nanoparticles in environmental waters. *Journal of Environmental Sciences*, 34, 116–125. <https://doi.org/10.1016/J.JES.2015.04.005>
- Zhang, S., Jiang, Y., Chen, C.-S., Spurgin, J., Schwehr, K. A., Quigg, A., ... Santschi, P. H. (2012). Aggregation, Dissolution, and Stability of Quantum Dots in Marine Environments: Importance of Extracellular Polymeric Substances. *Environmental Science & Technology*, 46(16), 8764–8772. <https://doi.org/10.1021/es301000m>
- Zhang, Y., Leu, Y. R., Aitken, R. J., & Riediker, M. (2015). Inventory of engineered nanoparticle-containing consumer products available in the singapore retail market and likelihood of release into the aquatic environment. *International Journal of Environmental Research and Public Health*, 12(8), 8717–8743. <https://doi.org/10.3390/ijerph120808717>
- Zhang, Z., Zhang, S., Huang, X., & Liang, L. (2013). A pilot trial of the iPad tablet computer as a portable device for visual acuity testing. *Journal of Telemedicine and Telecare*, 19(December 2012), 55–9. <https://doi.org/10.1177/1357633X12474964>
- Zhu, H., Jiang, S., Chen, H., & Roco, M. C. (2017). International perspective on nanotechnology papers, patents, and NSF awards (2000–2016). *Journal of Nanoparticle Research*, 19(11), 370. <https://doi.org/10.1007/s11051-017-4056-7>
- Zoppou, C. (2001). Review of urban storm water models. *Environmental Modelling & Software*, 16(3), 195–231. [https://doi.org/10.1016/S1364-8152\(00\)00084-0](https://doi.org/10.1016/S1364-8152(00)00084-0)
- Zuin, S., Gaiani, M., Ferrari, A., & Golanski, L. (2014). Leaching of nanoparticles from experimental water-borne paints under laboratory test conditions. *Journal of Nanoparticle Research*, 16(1), 2185. <https://doi.org/10.1007/s11051-013-2185-1>